UC Santa Barbara
UC Santa Barbara Electronic Theses and Dissertations

Title

An Analysis of Landslide Risk and Vulnerability in Distinct Realities: Low- Income Communities in Brazil and a Wealthy Community in the United States

Permalink

https://escholarship.org/uc/item/1pd3w8k3

Author

Goto, Erica Akemi

Publication Date

2020

Peer reviewed|Thesis/dissertation

UNIVERSITY OF CALIFORNIA

Santa Barbara

An Analysis of Landslide Risk and Vulnerability in Distinct Realities: Low-Income

Communities in Brazil and a Wealthy Community in the United States

A dissertation submitted in partial satisfaction of the

requirements for the degree Doctor of Philosophy

in Geography

by

Erica Akemi Goto

Committee in charge:

Professor Keith Clarke, Committee Co-Chair

Professor Edward Keller, Committee Co-Chair

Professor Hugo Loáiciga

Professor Summer Gray

March 2021

The dissertation of Erica Akemi Goto is approved.

_____

Hugo Loáiciga

_____

Summer Gray

_____

Keith Clarke, Committee Co-Chair

_____

Edward Keller, Committee Co-Chair

February 2021

An Analysis of Landslide Risk and Vulnerability in Distinct Realities: Low-Income
Communities in Brazil and a Wealthy Community in the United States

iii

ACKNOWLEDGMENTS

VITA OF ERICA AKEMI GOTO
December 2020

EDUCATION

Bachelor of Social Communication, University of Sao Paulo, Sao Paulo, 2006
Bachelor of Teaching Geoscience and Environmental Education, University of Sao Paulo, Sao Paulo, 2013
Master of Geoscience, University of Campinas, Campinas, 2014
Doctor in Geography, University of California, Santa Barbara, June 2020 (expected)

PROFESSIONAL EMPLOYMENT

Summer 2020: Research Assistant, Department of East Asian Language & Cultural Studies, University of California, Santa Barbara
Summer 2000, 2019, 2018: Graduate Student Research, Earth Research Institute – University of California, Santa Barbara
2019-2020: Teaching Assistant, Department of Environmental Studies, University of California, Santa Barbara
2020: Instructor, Department of Environmental Studies, University of California, Santa Barbara
2015-2018: Teaching Assistant, Department of Geographyt, University of California, Santa Barbara

PUBLICATIONS

"Ordinal Logistic Regression to automatic classify shallow landslide risk level in Sao Paulo city, Brazil," *Landslide inventory mapping and vulnerability assessment* (2020)

"A mixed-methods approach to understanding debris flow vulnerability in Montecito, CA. Landslide inventory mapping and vulnerability assessment," *Landslide inventory mapping and vulnerability assessment* (2020)

"Using Expert's Knowledge based on the Analytical Hierarchical Process (AHP) and the Brazilian Government Methodology (BGM) to map and compute the level of risk for shallow landslides in Brazil.," submitted (2019)

"A tool to compute the landslide degree of risk using R-Studio and R-Shiny," *Proceedings of the 4th ACM SIGSPATIAL International Workshop on Safety and Resilienc*e (2018), ACM, New York.

AWARDS

WLF5 Travel and Registration Support, 2019

Conference Grant - Dangermond Travel Funds Award, University of California, Santa Barbara, 2018, 2019

Student best paper - 4th ACM SIGSPATIAL International Workshop on Safety and Resilience, 2018

Conference Grant - UCSB GSA,2018

Summer fellowship – Earth Research Institute (ERI), 2016, 2017

Field Work Grant - Leal Anne Kerry Mertes Scholarship Award, 2016-2017

Ph.D. fellowship - Science Without Borders, CAPES, Brazilian Government, 2014-2018

FIELDS OF STUDY

Major Field: Geography

ABSTRACT

by

Erica Akemi Goto

Landslides are natural events that occur in many parts of the world in both developed and developing countries. They can be triggered by rainfall, earthquakes, volcanos, and a combination of post-fire and rainfall. However, the impact they cause in a community can be very different, based on how the community can anticipate and respond. They can cause material losses and some minor property damage, but also, they can become natural disasters, resulting in significant material and human losses.

One way to avoid and mitigate landslide disasters is by implementing Disaster Risk Reduction measures, such as risk mapping or developing an evacuation plan. These measures help municipalities plan before an event occurs, thereby protecting their communities and being proactive. In this doctoral dissertation, the focus is on two of these Disaster Risk Reduction measures: risk and vulnerability assessments.

In the first part, the study is conducted in the Metropolitan Area of Sao Paulo, Brazil. In these urban areas, shallow landslides are frequent in low-income neighborhoods on hillslopes, especially during summer months, when intense rainfall frequently occurs. Chapters 2 and 3 propose two distinct methodologies to quantify an inventory-based shallow landslide risk mapping. The quantification is intended to reduce bias and standardize risk mapping methodology. In chapter 2, experts' knowledge and the Analytical Hierarchical Process (AHP) method is applied to compute weights for variables, and application is developed and used to calculate the risk level automatically. In this study, variables that

illustrate instability in the terrain were the ones with the highest contribution for a higher risk. In chapter 3, a large dataset from a previous mapping of Sao Paulo city and Ordinal Logistic Regression (OLR) was used to select essential variables and to compute their weights. The equation calculated can be used in the developed application to compute the risk level automatically. In chapter 4, a spatial analysis of the slope stability using SHALSTAB and Factor of Safety and saturated hydraulic conductivity was computed in two hillslopes of São Bernardo do Campo, in the Metropolitan area of Sao Paulo. In one of these sites, the hillslope is disturbed by human activities (previous homes, cut and filling, landfill), and in the second site, the hillslope is undisturbed. The saturated hydraulic conductivity and the slope stability analysis illustrate that the disturbed site has less homogeneous soil than does the undisturbed site. Additionally, based on the soil characteristics and results from SHALSTAB and Factor of Safety analysis, the undisturbed hillslope is more stable than the disturbed hillslope.

The second part of the study was conducted in Montecito, California. The study was proposed after the 2018 Montecito debris flows that killed 23 people and damaged more than 400 homes. In this study, I used a parallel mixed-methods approach and a temporal-spatial analysis to understand the main factors that made the community vulnerable to debris-flows and to determine who were the most vulnerable people. The study concludes that the most vulnerable people were informal workers (gardens, housekeepers, caretakers, nannies), renters, and residents of areas that were in the voluntary evacuation zone. Lack of education about debris-flows and previous debris-flows in the region by the community increased the vulnerability of the entire community. Moreover, the institutional vulnerability was high for the entire community, but county measures in the aftermath contributed to the community

resilience.

TABLE OF CONTENTS

ABBREVIATIONS

ABNT: Associação Brasileira de Normas Técnicas
AHP: Analytical Hierarchical Process
app: application
BGM: Brazilian Government Methodology
BP: bad proportion
BPMSG: Business Performance Management Singapore
CR: consistency ratio
DEM: Digital Elevation Model
DRM: Departamento de Recursos Minerais
DRR: Disaster Risk Reduction
FS: Factor of Safety
GP: good proportion
GPS: Global Positioning System
IBGE: Instituto Brasileiro de Geografia e Estatistica
IPT: Instituto de Pesquisas Tecnológicas
JICA: Japan Internacional Cooperation Agency
LMS: *Laboratório de Mecânica dos Solos*
KPa: kilo Pascal
MCDM: Multi-Criteria Decision-Making
MOF: moderate ordinal fashion
NOF: non-ordinal fashion
OLR: Ordinal Logistic Regression
OF: ordinal fashion
OR: odds ratio
PTSD: Post-traumatic stress disorder
R1: low risk
R2: moderate risk
R3: high risk
R4: very high risk
Regea: Regea Geologia, Engenharia e Estudos Ambientais Ltda
RI: Random Index
RMSP: Região Metropolitana de São Paulo
SBC: São Bernardo do Campo
SHALSTAB: Shallow Landsliding Stability
SD: standard diviation
UCSB: University California, Santa Barbara
UFABC: Universidade Federal do ABC
UAV: unmanned aerial vehicle
USP: University of Sao Paulo

EQUATION SYMBOLS

a: drainage area
b: ring radius
$b:$ outflow boundary
C: cohesion
C1: Constant 1
C2: Constant 2
$D:$ depth (part of the bottomless bucket that is inside the soil).
D: depth of ponding
D_0: initial depth of ponding
D_p: density of the soil particles
D_{water}: water density
g: gravitational acceleration
h: height between the slip plane and the top of the soil
L_G : ring-installation scaling
K_{sat}: saturated hydraulic conductivity
$M_{dry\ soil}$: mass of the dry soil
M_p: mass of the particles
$Q:$ effective precipitation
$t:$ time from the initial depth to the depth of the ponding
θ: hillslope angle
ρ_w: water density
ϕ: angle of internal friction
τ: shear stress
u: pore pressure
ρ_s: soil bulk density
z: height of the water column

LIST OF EQUATIONS

LIST OF TABLES

LIST OF FIGURES

CHAPTER 1: INTRODUCTION

Landslides are natural events that occur in many parts of the world in both developed and developing countries. They can be triggered by rainfall, earthquakes, volcanos, and a combination of post-fire and rainfall. However, the impact they cause in a community can be very different, depending on how the community can anticipate and respond. They can cause material losses and damage, but they can also become natural disasters, resulting in extreme material and human losses.

One way to avoid and mitigate landslide disasters is to be proactive rather than reactive. For instance, through landslide risk assessment, it is possible to identify areas that require regular monitoring or where inhabitants must be relocated due to the high risk of landslides. Such assessments must consider the landslide hazard and the exposure of people and property to the hazard and their vulnerability, as well as its aftermath. In this dissertation, risk is seen as a combination of a natural hazard and vulnerability (Maskrey, 1989; Wisner et al., 2003) for a specific type of natural hazard. Hazardous events are natural events that can threaten human lives and the things that are important for them (Keller, 2011), and vulnerability consists of the characteristics and circumstances of a community, system, or asset that make them more or less susceptible to damage due to hazardous events (UNISDR, 2009).

In the past, natural disaster studies would prioritize the assessment of natural hazards over vulnerability, and, if they do include vulnerability, it was only the vulnerability of infrastructure and the number of people and not the community's socioeconomic characteristics (i.e., Mejianavarro et al., 1994). Recently, more risk and vulnerability studies

have included the socioeconomic aspects of the community (e.g., Maskrey, 1989; Flanagan et al., 2011; Cutter et al., 2003; Cardozo and Monteiro, 2019; Frigerio et al., 2018). However, most of these studies assess vulnerability as the same for all types of natural hazards. This assumption is problematic since natural hazards have singular characteristics, as do their impacts in the community. Their impact can be local or regional. A shallow landslide usually has a local impact, but a hurricane can impact larger areas (regional impact). Their impact characteristics are also different. Earthquakes can destroy huge buildings, roads, and damage infrastructure, and floods can impact the lower areas in which the water is concentrated.

Natural hazards and vulnerability are interconnected. They occur at the same spatial location, and the impact in the community depends on the natural hazard and the vulnerability of the community. Therefore, understanding their interconnection or studying them together can enrich the assessment and avoid overlooking relevant characteristics of one of the parts.

In the studies included in this dissertation, I worked on two main projects: shallow landslides in the Metropolitan Area of Sao Paulo and the debris flows vulnerability of the community of Montecito, California.

The Metropolitan Area of Sao Paulo (Região Metropolitana de São Paulo or RMSP) is the largest metropolitan area of Brazil, with around 22 million residents (EMPLASA, 2019). This urban area has many people living in at-risk areas, especially shallow-landslides, riverbank erosion, and floods. These areas are mainly concentrated in low-income neighborhoods, the *favelas*. In these areas, *favelas* developed due to the rapid urbanization and lack of infrastructure (Fischer, 2014). Residents from different parts of Brazil migrate to RMSP for better job and life opportunities (Maricato, 2008). However, the city was not

2

prepared to receive all these new residents and did not have enough jobs, housing, and infrastructure to incorporate all these new incoming residents (Maricato, 2008). Consequently, many residents occupied and self-built their homes in available public lands, usually located on hillslopes and in floodplain areas (Maricato, 2008). These changes in the terrain by residents in these already hazardous areas resulted in a considerable number of risk areas.

The Brazilian government has been using inventory-based landslide and riverbank erosion mapping to map risk areas. In this study, the methodology is referred to as the Brazilian Government Methodology (BGM). In the BGM, pairs of technicians do a field inventory and map the risk areas by observing local characteristics and using a checklist. Based on their evaluation and expertise and the BGM recommendations, they decide upon the overall risk level. The methodology is not standardized and does not apply mathematical computation to the risk level classification, allowing for classification variability and subjectivity. In chapters 2 and 3, I proposed two different methodologies to quantify the BGM. In chapter 2, I used the fieldwork evaluation form of the BGM, experts' knowledge, and the Analytical Hierarchical Process (AHP) to compute weights for variables and automatically compute the risk level. In the first phase, I designed a pairwise questionnaire, using the information in the fieldwork evaluation form of the BGM, and I delivered the survey to experts that have been working in the disaster risk field for some years. Using their answers, I could compute the weight for each of the variables. Moreover, an application (app) using ShinyApp (R) was developed to collect data in the field and to automatically generate a table with data collected and the level of risk. Therefore, the technicians would not be able to subjectively decide the risk level.

In chapter 3, I used the São Paulo city risk mapping from 2010 and Ordinal Logistic Regression (OLR) to select essential variables and compute their weights. In this study, an equation that calculates the risk level automatically was developed. The equation also can be plugged into the application and used by field technicians to compute risk levels based on the data they collect in the field. Both studies contribute to quantifying the BGM, using different methodologies, helping to reduce the bias and standardizing the computation of the risk level.

In chapter 4, the study areas are two sites in the city of São Bernardo do Campo, also in the RMSP. In this study, I selected one site that had anthropogenic activities (people previously lived in the site), also called the disturbed site, and another site with no anthropogenic activities, the undisturbed site. In urban risk areas, it is common for residents to change the land by cutting and filling the terrain, throwing garbage and sewage onto the slope, or even having municipality or companies throw unused and used construction material and waste onto slopes. Therefore, in this study, the goal was to conduct a geospatial analysis of the slope stability and the saturated-hydraulic conductivity in these two sites and to observe if there was a significant difference due to the anthropogenic activities. Fieldwork was conducted to collect a digital elevation model (DEM) and to compute saturated-hydraulic conductivity, using the bottomless bucket methodology, and soil was collected to be analyzed in the laboratory. In the laboratory, three main tests were conducted: soil texture analysis, wet soil bulk density, and a shear stress test. These tests were essential to perform the slope analysis using SHALSTAB and to compute the Factor of Safety.

These three studies, conducted in Brazil, aimed to contribute to Disaster Risk Reduction by quantifying, standardizing, and reducing the bias of the BGM, and to conduct and

compare landslide susceptibility analysis and saturated-hydraulic conductivity in disturbed and undisturbed sites.

The second part of the dissertation took place after the 2018 debris flows in Montecito, CA. They occurred as a result of wildfire (Thomas Fire) followed by intense rainfall in the catchments of the Santa Ynez Mountains (Kean et al., 2019). Montecito is in Santa Barbara County, and the distance between the University California, Santa Barbara (UCSB), and Montecito is around 24 km or 20 minutes' drive. The debris flows were a surprise for the local community, and it killed 23 people, injured at least 167, and damaged more than 400 homes (Kean et al., 2019). The main highway 101 was closed for ten days since the debris flows brought mud, boulders, and debris from the mountains towards the ocean; water was not considered safe for drinking; and utilities (gas and electricity) were shut down in parts of Montecito.

In chapter 4, I focus on the debris flows and the vulnerability of the community. I used a parallel mixed-methods approach by conducting personal interviews with members of the community and sending surveys to residents. Individual interviews complemented the surveys, and both, together, tell a better story of who are the most vulnerable people and what are the main factors that made the community vulnerable. In this study, I took a spatial and temporal approach to vulnerability. The spatial part considers the local community affected by the debris flows, and the temporal part accounts for the different phases of the disaster (before, during, and after). The main contribution of this study is to conduct a more inclusive and sophisticated discussion of variables that account for debris flows vulnerability in Montecito, such as revealing hidden elements that a traditional assessment would not consider.

CHAPTER 2: A Heuristic Approach to Map Risk Level of Shallow Landslides in Urban Areas in Brazil

ABSTRACT

Shallow landslides are common in Brazil's urban areas. Geomorphology and land use are contributing factors, and rainfall is the triggering factor. In these urban areas, anthropogenic activities that contribute to increase the level of landslide risk are common, such as cutting and filling or discharging wastewater and garbage onto the slopes. The Brazilian government has developed a methodology to map the level of risk in landslide-prone areas. The methodology is based on field observation and divides the risk into four main categories: low, moderate, high, and very high (R1, R2, R3, and R4). Technicians in the field decide a landslide sector's level of risk without mathematical calculations or using specific weights for the contributing factors. This study proposes a method for automatically computing the level of risk, thereby reducing the subjectivity in the selection of the final level of risk. A methodology was implemented that involves specific weights for classifiers and automatically computes a sector's level of landslide risk. The weights were computed using the Analytical Hierarchical Process (AHP), based on experts' knowledge. The thresholds of the risk levels were quantified by using a field-inventory dataset. Finally, an application (app) that can be used on a tablet, computer, or smartphone was created to facilitate data collection during field work and to automatically compute the level of risk.

Key-words: AHP, risk assessment, Brazil, expert knowledge, landslide, application, Analytical Hierarchical Process

1. Introduction

Landslides are common events in Brazil due to both geomorphology and land use. In the South and Southeast of Brazil, they are frequently triggered by intense rainfall during the summer (Tominaga et al., 2009). The region has experienced many landslide disasters and catastrophes, such as a 2011 event that killed 947 people in the Rio de Janeiro Mountainous Area (Dourado et al., 2012).

In Brazil, the development of landslide risk areas is directly related to irregular and unplanned urbanization. Today, many of these areas are in former or current favelas.[1] During the urbanization of major cities, such as São Paulo, inhabitants moved from rural areas towards the city for better jobs opportunities and to improve their quality of life (Maricato, 2008). However, the city lacked the capacity to accommodate this new population, and many inhabitants ended up occupying and building informal housing in public areas unsuitable for dwellings (e.g., floodplains and steep slopes) (Maricato, 2008). These areas became favelas, and they usually have low-quality buildings and lack basic infrastructure. Frequently, inhabitants engage in activities that increase the landslide risk, such as cutting and filling slopes and throwing garbage and wastewater onto the slope (see Figures 2.1A and 2.1B).

---

[1] favela – the Portuguese name for slum and shanty town. According to the IBGE, the Brazilian Institute of Geography and Statistics, favela or 'aglomeramento subnormal' means a "set with at least 51 dweller units with no property title and at least one of the following characteristics: irregular paths and size and shape of the allotment and/or lack of basic public service (official garbage collection, sewage network, water network, energy network and street lighting)."

Figure 2.1. 1A and 1B. Fig. 2.1A illustrates a mixed-material building in a favela in São Paulo city (Source: Goto, 2012). Fig. 2.1B illustrates brick buildings in one of São Paulo's favelas. Both brick and mixed-material buildings are precarious, but mixed-material ones are less resistant than brick buildings and can be easily destroyed (Source: Goto, 2012)

Today, many urban residents in Brazil are living in areas at risk to landslides, floods, and riverbank-erosion. Major cities such as São Paulo, Rio de Janeiro, and Belo Horizonte have 6%, 7%, and 16% of their population living in at-risk areas, respectively (IBGE, 2018). For instance, in São Paulo city, there were 1,179 risk sectors and 105,427 houses in these sectors (IPT, 2010), and 27% of these houses were in high or very high risk level categories (see Table 2.1).

Table 2.2. Number of sectors and houses for each level of risk in São Paulo city

Risk Degree	Number of Sectors	Number of houses
R1 (low)	153	13,778
R2 (moderate)	420	62,923
R3 (high)	445	20,513
R4 (very high)	161	8,213

Municipalities that mapped landslide risk areas know their sectors' risk levels and locations. Still, they do not always have initiatives in place to relocate all of the residents or to implement infrastructure measures (modification of slope geometry, drainage, retaining structure, or internal slope reinforcement), and when they do, it requires time (to build new

dwellings) and financial resources. Besides, these risk areas are dynamic, requiring constant updating in mapping since informal urbanization is constantly happening. This current situation will not change in the short term. In this context, proactive preventive measures can help manage the risk, i.e., outreach courses for residents and keeping municipalities' risk mapping up to date.

The Brazilian government has developed a methodology to map the level of risk of landslides and riverbank erosion-prone areas. In this study, we called this methodology the Brazilian Government Methodology (BGM). In the BGM, the mapping is done in the field by two technicians who fill out a paper evaluation form and decide the level of risk. The decision is based on the field perception of the technicians and does not involve any mathematical computation or weighting of classifier, and it can result in subjective choices of the risk level.

This study proposes to reduce the subjective element and standardize landslide risk mapping by using mathematical equations to compute the risk level automatically, based on specific classifier weights. The weights are based on expert knowledge and computed using the AHP (Analytical Hierarchical Process). Moreover, an application (app) was developed to facilitate the data collection and automatically and simultaneously compute the level of risk.

2. Background

2.1 The Brazilian Government Methodology for Landslide Risk Mapping

The Brazilian Government, through the Ministério das Cidades (Ministry of Cities), together with the IPT (Instituto de Pesquisas Tecnológicas or Institute for Technological Research), developed a methodology to map the risk level of sectors that are prone to landslides and river bank erosion (Carvalho, Macedo, & Ogura, 2007). First, the methodology decides which landslide-prone areas should be mapped, based on municipality knowledge. After that, two technicians go into the field and map the level of risk of sectors by gathering information to fill out previously prepared forms and taking photos as proof.

The prepared evaluation form has eight sections: (1) general information, (2) characterization, (3) determinants, (4) water, (5) vegetation, (6) signs of destabilization/movement, (7) type of destabilization process expected or in the past, and (8) level of risk (Table 2.2).

Table 2.3. Sections of the prepared evaluation form

Sector	Description/Aspects
(1) General Information	Name of the city District Neighborhood Sector Team members Date Type of unit: slope or riverbank erosion
(2) Characterization	Location (address – as reference) Name of inhabitant (as reference) Access to the area Type of housing: brick, wood, or mixed material
(3) Determinants	Natural slope, cut slope, rock formation, boulders and rock blocks, natural drainage, riverbank slope, deposit onto the slope Slope angle Distance house to the base or top of the slope Maximum height Presence of material: landfill, garbage, and construction dumped material
(4) Water	Concentration of superficial water (rainfall accumulation) Wastewater onto the terrain Pipe leak Septic tank Spring Superficial drainage system: none, precarious, or adequate
(5) Vegetation	Trees Short vegetation (grass, shrubs, etc.) Deforestation Plantation
(6) Signs of Destabilization/Movement	Cracks in the house Cracks in the terrain Floor drawback Wall with a slump or "belly" Tilted trees, poles or walls Riverbank erosion Landslide scars Fracture in the rock
(7) Destabilization process (expected or occurred in the past)	Natural slide Cut slope slide Slope of material (landfill, garbage, or construction dumped material) Topple Block slides Rockfall Mudflow Erosion River bank erosion
(8) Level of risk	R1 R2 R3 R4 Number of houses in the sector

11

2.2 The Analytical Hierarchical Process (AHP)

The Analytical Hierarchical Process (AHP) is a Multi-Criteria Decision-Making method (MCDM) that relies on experts' knowledge, using pairwise comparison (Kousalya et al., 2012; Saaty, 1980, 2008). Each pairwise comparison is evaluated by a ranking scale comparing one criterion to another (Table 2.3). For instance, considering criteria *a* and *b*, first the expert chooses which criterion is more important for very high risk level and then how much more important it is. The pairwise comparison attempts to capture the subjective and objective elements inherent in the decision-making process (Saaty, 2008).

Table 2.4. Table of ranking scale for criteria and alternatives (Source: adapted from Saaty 1980)

Value of *a*	Interpretation
1	*a* and *b* are equally important
3	*a* is slightly more important than *b*
5	*a* is more important than *b*
7	*a* is strongly more important than *b*
9	*a* is absolutely more important than *b*
2,4,6, 8	intermediate values

AHP can be used with different hierarchy structures or no hierarchy structure (Saaty, 1980; Malczewski & Rinner, 2015). The specific classifier weight is computed, based on the pairwise comparison. The higher the weight, the more important is the criterion (Saaty, 2008). The last level of the priority hierarchy is related with the final priority. For instance, in terms of satisfaction with school, the last level could be school A, B, and C, and the second level of the hierarchy could be criteria related with satisfaction with school (i.e., learning, friends, school life, etc.) (Saaty, 1980).

AHP assumes experts are rational, and that their choices for the criteria are consistent. However, experts can be inconsistent, and the methodology uses a consistency ratio (CR) to

check for their consistency in pairwise comparison (Saaty, 1980). CR is computed to check for consistency for each criterion comparison (Saaty, 1980, 1984, 2008), and if greater than 0.1, the pairwise comparison is not consistent and close to random (Saaty, 1980, 1984, 2008; Sedan & Suv, 2013). For instance, if an expert chooses *A* as heavier than *B* and *B* as heavier than *C*, they also should choose *A* as heavier than *C;* otherwise, the choices are inconsistent.

3 Methodology

In this study, we were interested in quantifying the qualitative methodology by using more experts than the field-inventory methodology to reduce the subjective element in the current methodology. We chose to use the AHP methodology because of its ability to achieve our goal of computing a specific weight for the classifiers. We used an inventory-dataset with our computed classifiers weights to define the risk level thresholds. In this section, we discuss the (1) hierarchical structure used and the parameters and classifiers, (2) questionnaire development, (3) experts involved, and (4) the application.

3.1 Developing AHP for the Brazilian Government Methodology (BGM)

The AHP approach has been used for landslide risk assessment in multiple studies (Kayastha *et al.*, 2013; Barredo *et al.*, 2000; Ayalew *et al.*, 2004; Gorvevski *et al.*, 2006; Wu & Chen, 2009; Akgun & Türk, 2010; Rozos *et al.*, 2011; Akgun, 2012; Hasekiog˘ulları & Ercanoglue, 2012; Mondal & Maiti, 2012; Yalcin, 2008; Yalcin *et al.*, 2011; Mezughi *et al.*,

2012; Phukon *et al.*, 2012; Pourghasemi *et al.*, 2012; Long & De Smedt, 2012). Some studies compared AHP with another methodology (Akgun & Turk, 2010; Rozos *et al.*, 2011, Pourghasemi *et al.*, 2012) and other studies combined AHP with another methodology (Ayalew *et al.*, 2004; Yalcin, 2008; Mondal & Maiti, 2012). Information regarding the experts consulted is usually not included in these studies (except for Wu & Chen, 2009).

First, we defined the parameters and classifiers (see Figure 2.2). Parameters and classifiers are also called criteria in the AHP methodology. We called the choices users can make when mapping the landslide risk area classifiers. For instance, in the category of instability, the classifiers are *(i) leaning wall*; *(ii) house crack*; *(iii) wall crack*; *(iv) floor downward sloping*; *(v) tilted trees, poles, walls*; and *(vi) landslide scars*. The IPT/Ministério das Cidades evaluation form (Table 2.2) was used to build a hierarchical structure and decide which classifiers we would include (see Figure 2.3). Unlike the original AHP methodology, we didn't include a final level in the hierarchical structure that represents the possible options since we are just interested in the criteria that contribute to a higher risk level.
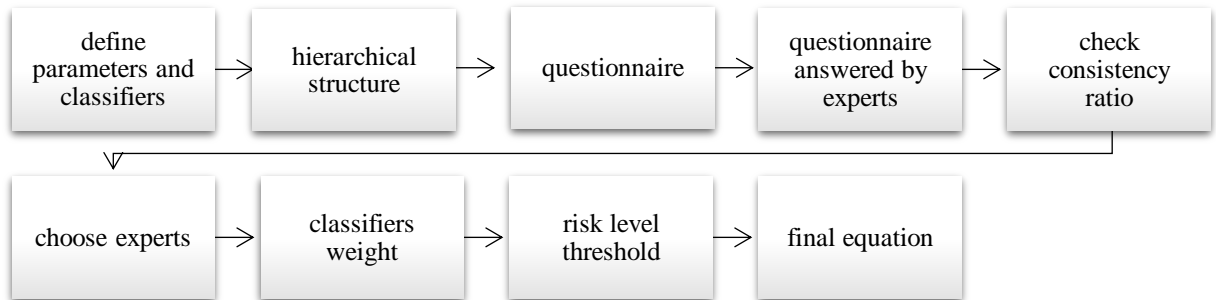
Figure 2.2. Flowchart of the Methodology
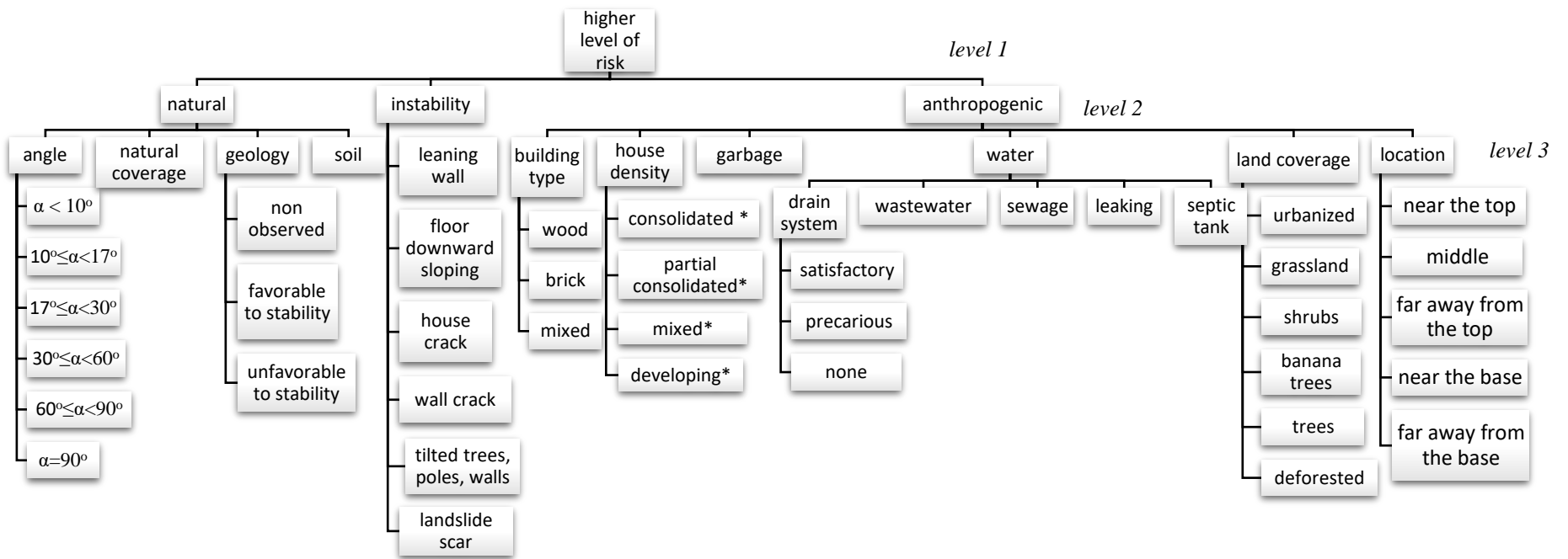
Figure 2.3. AHP hierarchy structure, based on BGM

3.2 Questionnaire design and the experts involved

We used the hierarchical structure (Figure 2.3) to design the questionnaire. The elements of each branch of the hierarchical structure were compared with each other. For instance, in the branch *natural*, we pairwise compared the *angle*, *natural coverage*, *geology*, and *soil*. The entire questionnaire is included as *Appendix 2.1*.

The questionnaire was delivered in person (paper survey) and by email, with a link to an online survey created by using Google Forms. The paper survey was delivered and collected at two events: i) Workshop of the Brazilian Committee of Geotechnical Cartography and Geoenvironment in São Bernardo do Campo – 2017 and ii) a visit to IPT. The workshop and visit to IPT targeted experts in the field of landslide risk assessment, and the online questionnaires were sent to researchers who preferred to answer the survey at another time. Table 2.4 reports the number of experts and their gender, institution, and discipline. Detailed information about the experts can be found in *Appendix 2.2*.

Table 2.5. Summary of experts involved in the study

Number of Experts	23
Female	9
Male	14
Mean years working with landslide assessment	16
Institutions	Cemaden, IPT, JICA (Japan Internacional Cooperation Agency), Civil Protections and Habitation Ministry from different Municipalities (Santana do Parnaíba - SP, Castelo - ES, Jundiaí – SP, São Bernardo do Campo – SP, São Paulo – SP), DRM (Departamento de Recursos Minerais) -RJ, UFABC (Universidade Federal do ABC), Regea (Regea Geologia, Engenharia e Estudos Ambientais Ltda)
Discipline	Geography, Civil Engineering, Chemistry, Geoscience, Environmental Studies

The total number of experts involved was 23, but due to the CR, the number of experts for

each classifier weight value involved between 7 and 13 experts (MEAN=9.77, SD=2.17).

3.3 Classifiers Weight Value and Consistency Ratio

Using an Excel spreadsheet developed by Business Performance Management Singapore (BPMSG), we computed classifier weight and checked their CR for each expert and collectively. See *Appendix 2.3* for a detailed explanation with an example.

Equation 2.1 computes each value $(\bar{a}_{jk})$ of the pairwise comparison, and Equation 2.2, the weight for each criterion.

$$\bar{a}_{jk} = \frac{a_{jk}}{\sum_{l=1}^{n} a_{lk}} \tag{2.1}$$

$$W_j = \frac{\sum_{i=0}^{n} \bar{a}_{jk}}{n} \tag{2.2}$$

Where *n* is the number of criteria, $\bar{a}_{jk}$ is the normalized value of a_{jk} and W_j is the specific weight of each criterion.

We checked the CR of the experts using Equation 2.3 (see *Appendix 2.3* for detailed explanation). Pairwise comparisons from experts with CR > 0.1 were not used, as previous studies consider CR> 0.1 to be random and not consistent (Saaty, 1980, 1984, 1990, 2008; Sedan & Suv, 2013).

$$CR = CI/RI \tag{3}$$

CI stands for critical index and *RI* for random index. The values of *RI* were computed in previous studies, and Table 2.5 illustrates these values (Saaty, 1980).

Table 2.6. Random Index Values (RI)

n	2	3	4	5	6	7	8	9	10
RI	0	0.58	0.90	1.12	1.24	1.32	1.41	1.45	1.51

3.4 Classifiers rules

Using the AHP methodology, we computed the specific weight of classifiers. Additionally, we created rules to account for the singularity of each classifier. Some branches of the hierarchical structure (3), such as water, can have more than one classifier chosen; other branches, such as type of building, can have just one classifier chosen. Rules of the classifiers are illustrated in Figure 2.4.
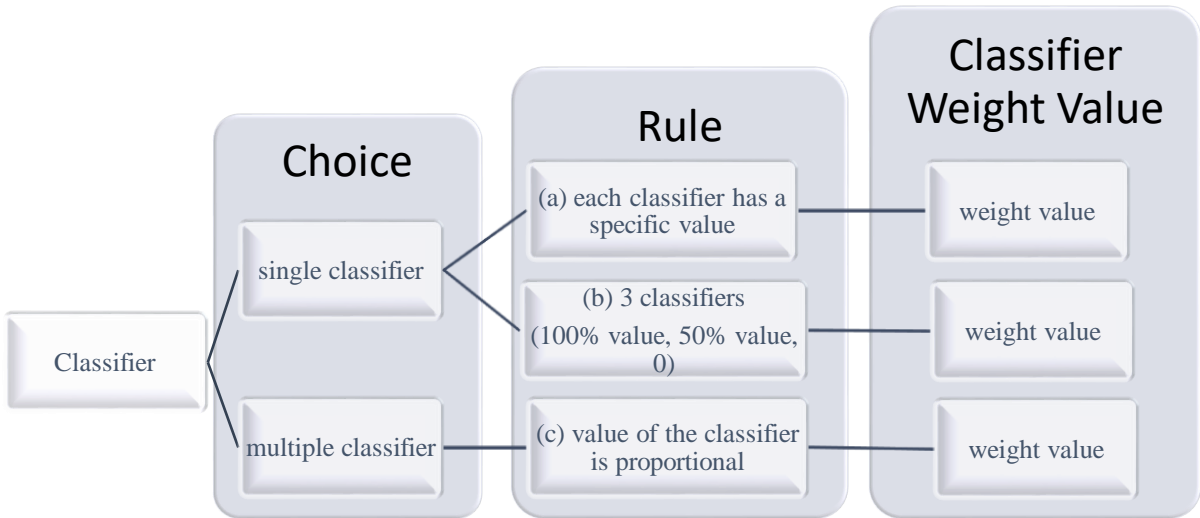
Figure 2.4. Rules for classifiers. Classifier weight value is computed, based on these rules.

3.5 Threshold for Risk Level

The BGM has four level of risk: low, moderate, high, and very high. However, the final value of risk computed with AHP is numerical. In this section, we go through the steps necessary to categorize the risk into these four levels.

We used a field-inventory dataset of 2010 São Paulo landslide risk and riverbank erosion to define the risk level thresholds. A total of 503 risk sectors from the field-inventory were used, in which 60 were mapped as R1, 194 as R2, 188 as R3, and 61 as R4. Numbers of R1 and R4 sectors are lower since there are fewer sectors at these risk levels when compared to R2 and R3. We plotted the dataset in a density histogram and used kernel density estimation in *RStudio* as it allows visual identification of the thresholds.

3.6 The Application

The application (app) has the same inputs as the prepared paper evaluation form and was developed to compute the level of risk of shallow landslides automatically. It has a simple interface, in which users select classifiers observed in the field and type their observations in one tab (Diagnóstico), and in the other tab (Respostas), a table with the data collected and the level of risk are displayed.

The app was built using RStudio, and I used two main libraries, Shiny and Rmarkdown. The app runs on a tablet, smartphone, and computers with internet access or with RStudio installed. Also, the data can be easily collected and stored, both centrally and locally. Direct digital encoding of the form also reduces errors and misinterpretations on the written forms. The app is in Portuguese and has two main tabs: (i) Diagnostic (Diagnóstico): input dataset (Figure 2.5A); (ii) Data Collected and Degree of Risk (Respostas): display dataset collected in a table and computes the level of risk (Figure 2.5B). In the second tab, the user can export the data file in PDF, HTML, and CSV formats.

19
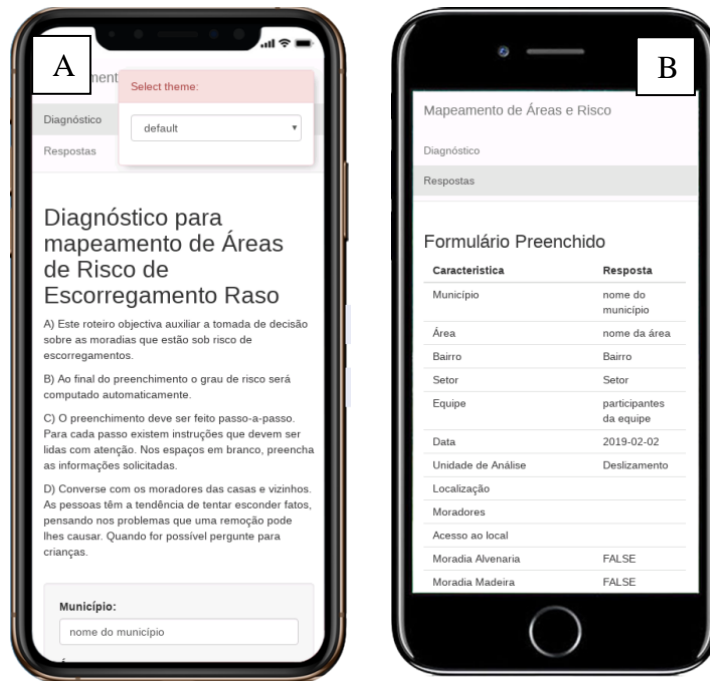
Figure 2.5. 5A and 5B. Fig. 2.5A illustrates the Diagnostic Tab in a Smartphone. Fig. 2.5B illustrates the Answer Tab in a Smartphone

4 Results

4.1 Classifier Specific Weight

Instability is the category that contributes the most to very high risk level of shallow landslides (Figure 2.6). Experts consider the instability category (59.6) more than two times more important than the natural category (23.3) and 3.5 times more important than the anthropogenic category (17.1). This pairwise comparison, at level two of the hierarchical structure (Figure 2.3), impacts the overall weight of the classifiers (Figure 2.7).
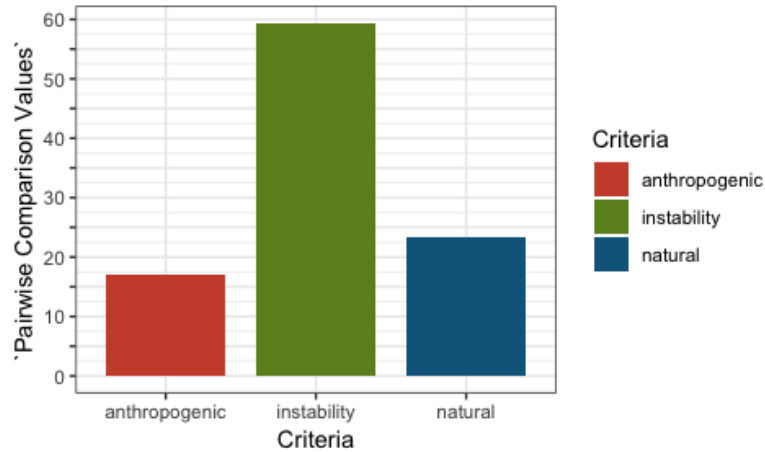
Figure 2.6. Values of Pairwise Comparison

Classifiers from the instability category have a higher specific weight value when compared with classifiers from anthropogenic and natural categories (Figure 2.7). Overall, anthropogenic classifiers represent the lowest specific weights, such as good drainage system (0.10), building far away from the top of the slope (0.29), and impermeabilization/urban coverage (0.34). Yet, natural category classifiers, like geology, soil, and natural coverage favorable to slope stability have a specific weight value equal to zero due to rule *b* (Methods section).
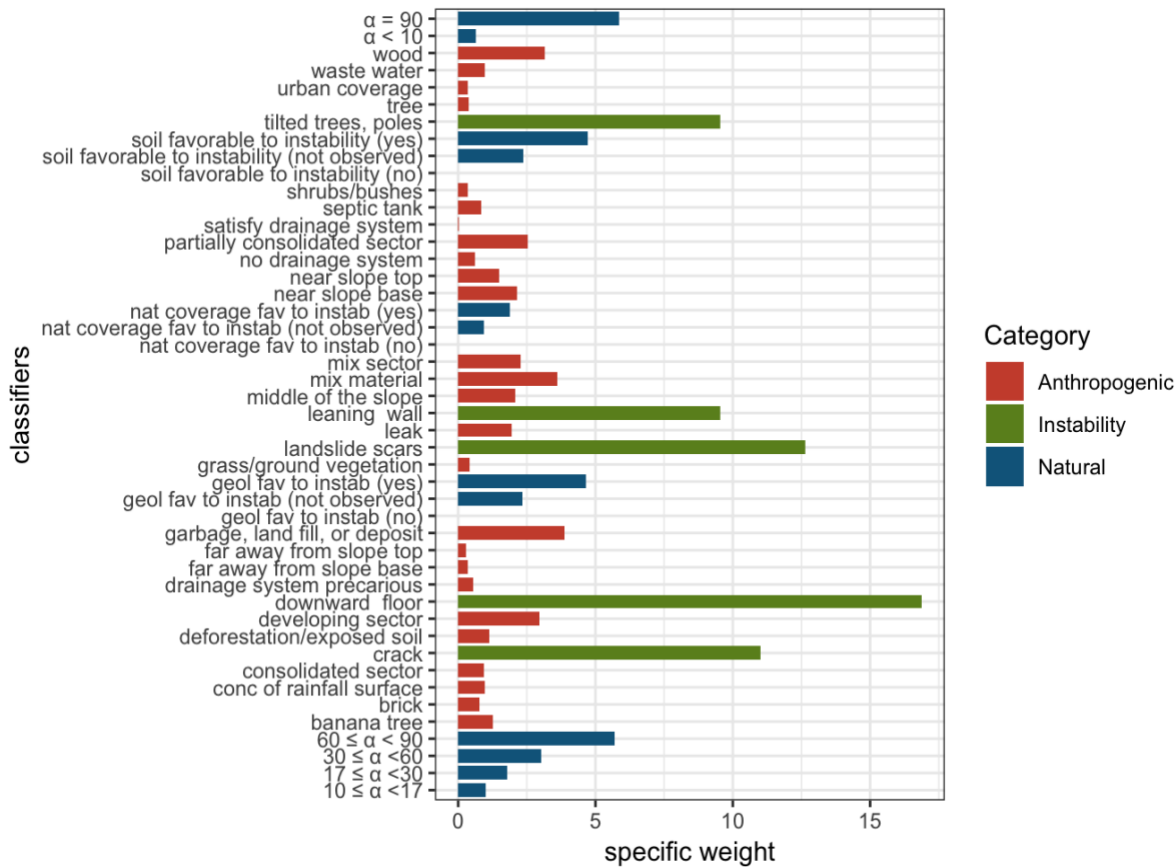
Figure 2.7. Classifiers Specific Weight Value Computed with AHP

The instability category includes alternatives that represent past and present movement in the terrain, and the classifiers of this category have the highest specific weight, such as downward sloping floor (16.88), landslide scars (12.64), cracks (11.02), leaning wall (9.53), and tilted trees or poles (9.53). It is expected that these classifiers have higher weight values since their presence in the site contribute to a higher level of risk (Carvalho et al, 2007).

The natural category, in the experts' pairwise comparison, is the second most influential category. Slope angle classifiers $\alpha = 90$ and $60 \leq \alpha < 90$ have the highest specific weight in this category (5.85 and 5.69, respectively). Other classifiers with high specific values are soil and geology favorable to slope instability with specific weigh values of 4.72 and 4.65, respectively. Nevertheless, if these classifiers are contributing to slope instability, they are expected to have a

high weight value. However, we notice they are at least 3 times less important than downward sloping floor.

Experts considered anthropogenic as the least important category to contribute to a very high-risk level of shallow landslide. Garbage classifier (3.88) has the highest weight value in this category, followed by houses built with mixed materials (3.60) and wood (3.15) classifiers. However, in the anthropogenic category, water is the category with the highest weight value (5.52), followed by garbage (3.88), and land use (3.85). Water represents increase of water content on the terrain. In these risk sectors, it is common to find precarious buildings with no sewage system that discharge wastewater onto the terrain, and water leaks through their self-engineered pipelines. An increase of water in the terrain can decrease cohesion in soil and increase weight and pore water pressure in granular material, decreasing the shear strength (De Blasio, 2011); in the shallow landslides sites in Brazil, this is the most important trigger component (Carvalho et al., 2007). If the soil is almost saturated, even a light rainfall could trigger a shallow landslide. The garbage classifier has a higher weight value than classifiers from the water category because more than one classifier of the water category can occur at the same time, and they add up. For instance, a sector can have a pipe leak (1.94), wastewater on the terrain (0.96), and no drainage system (0.62). The total for the water classifiers in the sector is 3.5. The mixed material houses classifier (3.60) has the highest weight value of the building material category, followed by wood (3.15), and brick (0.77). Houses made of brick are more resistant and less prone to be destroyed during a shallow landslide when compared with wood and mixed material houses.

More information about classifiers weight values and pairwise comparison values are given in *Appendix 2.4*.

4.2 Risk level classification

We plotted a density histogram with the 503 risk sectors and used kernel density estimation to display a normal distribution in *RStudio*, where each normal distribution represents one risk level (R1 < 26, 26 ≤ R2 <42, 42 ≤ R3 < 67, R4 <67).

R1 has the larger number of sectors (N=128), followed by R3 (N=63), R4 (N=25), and R2 (N=34).
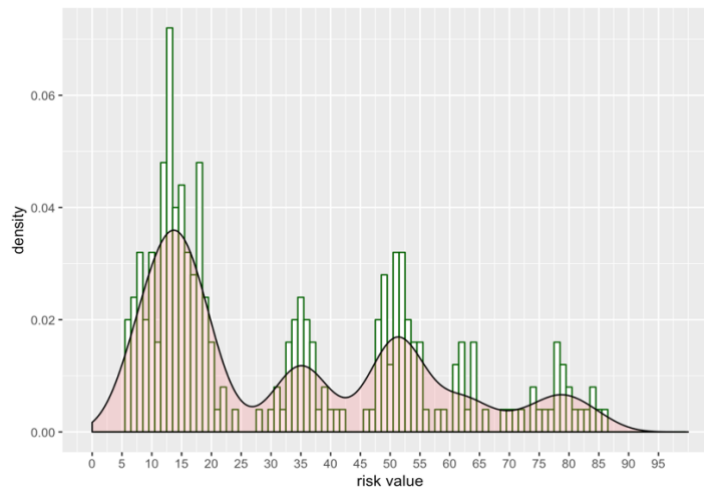
Figure 2.8. Density Histogram of risk value computed with AHP. Plot visualization and the four normal distributions were used to define the thresholds between risk levels (26, 42, and 67)

5   Discussion

The instability category was expected to have a higher weight value since classifiers of this category describe features of landslides that have already happened (landslide scars) in the sector or have already been initiated (crack, downward sloping floor, tilted poles and trees, leaning wall). There is a high probability of shallow landslides occurring in an area where they occurred in the

past (Highland & Bobrowsky, 2008). Therefore, we expect the landslide scars classifier to have a high weight value. Classifiers that demonstrate signs of landslide initiation are also expected to have high weight values since the sector has a very high risk of a landslide.

Slope stability is expressed by the relationship between the driving and resisting forces (Keller, 2011). These forces are determined by the relationship between some variables, such as type of earth materials, slope angle, climate, vegetation, water, and time (Keller, 2011). Experts considered slope angle the most important classifier in the natural category for a high level of risk. It is expected that shallow landslides occur more frequently on slopes with high angles than with a small angle; but in natural slopes, they don't occur with $\alpha = 90^o$. On the other hand, in these informal urban areas, it is common for residents to cut the slopes at a vertical angle (equal or close to 90°). The self-engineering cuts in the slope change the stability of the slope and increase the landslide risk (Carvalho *et al,*. 2007; Nogueira, 2002). Based on field inventory by technicians and the field inventory form, the line that divides natural slope and slope angle changed by anthropogenic activity is a narrow one. Some field inventory had both angles collected, some didn't have any, and others have one of them.

The most important classifiers for high risk level in the anthropogenic category are garbage, landfill, and construction deposits. In the favelas, the presence of garbage, landfill, and construction deposits onto the slope is visible and very common (Figures 9A and 9B), and these materials commonly move downwards with soil (Carvalho *et al.,* 2007). In this matter, experts point this out as being the most important anthropogenic classifier matches what have been observed in the field. Experts considered type of building the second most important classifier for a higher risk level, and this is related with the structure vulnerability of the dwellings. Mixed material and wood dwellings are more likely to be destroyed during a landslide than brick dwellings (see Figures 2.1A and 2.1B).

Figure 2.9. 2.9A and 2.9B. Fig. 2.9A illustrates slope with garbage and construction material mixed with soil in landslide risk area in Sao Paulo (Source: Goto, 2012). Fig. 2.9B is detailed photo of the material mixed with soil (Source: Goto, 2012)

Shallow landslides or translational landslides move the mass material above the surface of rupture out or down and outward (Highland & Bobrowsky, 2008). Mass material moved on the surface of a rupture accumulates at the base of the landslide. Therefore, experts' opinion on the level of impact based on the position of a dwelling aligns with the landslide literature and with what is observed in the field. Dwellings near the slope base (2.15) have higher risk since the mass material is moving down and outward and might damage or destroy the dwellings suddenly, while dwellings far away from the slope have lower risk (0.35). However, based on the Sao Paulo city mapping dataset, these classifiers are not that relevant since most of the sectors consider the whole slope as one entire risk sector and don't divide it up by base, middle, and top.

Experts' knowledge considers brick houses (0.77) less influential for a high level of risk than mixed material (3.60) and wood houses (3.15). Brick dwellings (Figure 1B) are more structured and resistant and less susceptible to being destroyed if a landslide is triggered, when compared with mixed material dwellings (Figure 2.1A) or wood. Less affluent residents in these underprivileged neighborhoods build their dwellings initially with very precarious materials, particularly with materials they find at the site, such as plastic, pieces of wood, and cardboard boxes (Figure 2.1A).

As their financial situation improves, residents also upgrade their dwellings by using better materials (first wood, then brick).

To complement the sectors that did not have a slope angle recorded, we looked at the photos in the sector and manually classified them into one of the six slope angle sub-parameters ($\alpha < 10$, $10 \leq \alpha < 17$, $17 \leq \alpha < 30$, $30 \leq \alpha < 60$, $60 \leq \alpha < 90$, and $\alpha = 90$). This could result in misinterpretation since photos are an interpretation of the reality and not necessarily the reality. Other aspects noticed when inputting the slope angle was the number of sectors with more than one slope; also, many sectors have more than one angle and different numbers of slopes with human interference (cut slope). Another aspect to point out is the diversity in area size of the risk sectors and number of dwellings in each sector (ranging from one to 97 dwellings). This diversity in sectors can likewise impact the landslide risk mapping.

6   Conclusion

This study improves the BGM mapping for shallow landslide risk by using the AHP methodology since it removes some of the subjective elements of the original methodology and standardizes the values for choosing the risk level. The AHP makes it less dependent on the personal experience of the two technicians in the field. A contribution of this study is diminishing the subjectivity by becoming less dependent on the personal experience of the technicians, but some subjectivity still exists since AHP is built based on expert knowledge. Nevertheless, the subjectivity is smaller since the methodology involves more experts, provides objective weights for parameters and sub-parameters, and automatically classifies the risk level. Besides, the application makes the field data collection easier and less error-prone, and, as soon as data is entered, the sector can be

classified by its risk level. For future improvement of the application, researchers can use the *tmap* package to display Google Maps to allow the technicians to locate and draw in the map the sector being mapped. Also, a downloaded report in PDF and HTML generated by *Shiny* and *RMarkdown* packages in interactive documents is not visually simple, so more studies of how to generate displays from these downloaded documents should be explored by further researchers.

This study quantifies only shallow landslides for the BGM. Therefore, similar studies could be done for other types of risk mapping of the BGM, such as riverbank erosion and other types of landslides. For future studies, different methodologies of landslide assessment for shallow landslides in urban areas, such as statistically and mathematically based ones, should be conducted to compare and validate the AHP results.

CHAPTER 3: Landslide Risk Assessment Using Ordinal Logistic Regression for Sao Paulo city, Brazil

ABSTRACT

Landslides are natural events that can cause disasters and catastrophes and threaten human lives and assets. Catastrophic landslides are more common in developing countries than developed countries. In Brazil, many people live within landslide risk zones, which amplifies the human impact and increases the number of disasters and catastrophes. Landslide risk mapping is one way to help prevent landslides and reduce the losses they bring. The mapping provides information about location and risk level, allowing better monitoring and the relocation of dwellings when possible. The Brazilian Government has developed an inventory-based assessment to map these risk areas. Pairs of technicians do field inventory and decide on the risk level, based on their personal and technical experience. However, the risk areas need to be constantly updated, and the inventory-based assessments are not standardized and so carry the technicians' subjectivity. In this study, we quantify the assessment methodology for shallow landslides by developing corresponding mathematical equations and automatically classifying the risk level regardless of the technicians' decisions. Using a dataset from Sao Paulo city, risk mapping, and Ordinal Logistic Regression (OLR), we quantify the field methodology by assigning weights for classifiers and thresholds for risk levels. The mapping can be done using an application on a tablet or smartphone in the field. The application computes the risk level and creates and stores a table with the data collected in the field. In conclusion, this methodology, by more rapidly updating the sector risk levels, standardizes the methodology and diminishes the subjectivity of the mapping and so can contribute to the prevention of future landslides and the mitigation of their human impacts.

Key-words: ordinal logistic regression, Sao Paulo, landslide, risk, landslide assessment

1. Introduction

Landslides are natural events that threaten human lives and assets. Landslide disasters and catastrophes are more common in developing countries, as are deaths and loss of property (Alcántara-Ayala, 2002). For example, in 1987, 1,000 people were killed due to the *Reventador landslides* in Ecuador, and in 1994, 271 people were killed and 1,700 were missing due to the *Paez landslides* in Colombia (USGS, 2019). In these countries, a large number of people live in at-risk areas due to the rapid increase of population, unplanned urbanization, and poverty.

Brazil is a developing country that has faced many landslide catastrophes. In the Southeastern states, these landslide events frequently occur during the rainy season (summer) and past landslides have resulted in major disasters, like those in Rio de Janeiro state in 2011 with 947 people killed (Dourado et al., 2012). Rio de Janeiro's landslide risk areas are a combination of the geography of the hazard events (landslides) and the vulnerability of the local residents. As a consequence of the residents' financial situation, they often occupy public lands, commonly in flood-plain or hillslope areas, and self-engineer the construction of their homes (Maricato, 2008).

Neither the local nor the federal government can remove all the residents that live in at-risk areas in the short term. As a preventative measure, it is important to monitor these areas to anticipate and prevent human casualties. By mapping the landslide-prone areas and their risk levels, local governments can closely monitor the risk conditions and allocate resources or prioritize removals of residents living in high and very high-risk level sectors. Moreover, these risk sectors need continuous updates since they are constantly changing.

The Brazilian government has developed an inventory-based landslide risk mapping methodology to map landslide and river-bank erosion (Carvalho, Macedo, & Ogura, 2007). In this

study, we call this method the Brazilian Government Methodology (BGM). In the BGM, pairs of technicians do a field inventory and map the risk areas by observing local characteristics. Based on their evaluation and expertise, and the BGM recommendations, they decide upon the overall risk level. The methodology is not standardized and does not apply mathematical computation to the risk level classification, allowing for classification variability and subjectivity.

In this study, we propose using ordinal logistic regression (OLR) to quantify the BGM for shallow landslides. The methodology allows the mathematical computation of classifier weights and standardization of the risk level classification, diminishing the subjectivity of field technician decisions. The developed application can help municipalities update and validate their mapped risk areas.

2. Background

2.1 Risk Areas in Brazil

In Brazil, many people live in at-risk areas (IBGE, 2018). In the southeast, major cities like Sao Paulo and Rio de Janeiro have 6% and 7% of the population living in these risk areas, respectively (IBGE, 2018). Smaller cities also have a large number of people living in at-risk areas, such as Ribeirão das Neves (60.5%) and São João de Meriti (18.8%) (IGBE, 2018). Knowing the location, the type of risk, and the level of risk is important to preventing landslide disasters. By mapping these areas, local municipalities can manage and monitor the risk sectors. Also, they can allocate financial resources for removal or prioritize reallocation of residents in the very high-risk sectors.

Risk, in this study, is a combination of hazard and vulnerability (Maskrey, 1989; Wisner et al., 2003). In developing countries, such as Brazil, the vulnerability of the residents contributes to the large number of people living in at-risk areas. Vulnerability, in the field of disaster reduction,

31

consists of "the conditions determined by physical, social, economic and environmental factors or processes which increase the susceptibility of an individual, a community, assets or systems to the impacts of hazards" (United Nations, 2015). These vulnerability conditions are related to the root causes of these communities, such as dynamic pressures, fragile livelihoods, and unsafe locations (Marchezini and Wisner, 2017).

Disaster risk reduction (DRR) plays an important role to prevent and mitigate disasters. Mapping landslide risk areas is part of DRR, and it contributes to knowledge of the type, location, and level of risk, which is fundamental to closely monitoring risk and to helping local governments make decisions, such as dwelling removal or building infrastructure to reduce the risk.

2.2 Landslide Assessment Methodologies

We can assess landslides with four main types of methodologies: (i) inventory-based; (ii) deterministic; (iii) heuristic; and (iv) statistical (Das, 2011; Van Westen *et al.,* 2006). The assessment can rely on one methodology or combine more than one. Decisions about which type of methodology to use is related to the data available, time, and the site scale. In our study, we are using a type of statistical methodology (ordinal logistic regression), that was chosen based on the data available (landslide risk mapping by risk level in Sao Paulo city).

2.3 Ordinal Logistic Regression

Ordinal Logistic Regression (OLR) is a statistical methodology that is frequently used in psychological, medical, and educational studies, in which the response variable (y or dependent variable) has an order, and the explanatory variables (x or independent variables) can be discrete (categorical, numerical, or ordinal) and/or contiguous. Examples of ordinal response variables are

32

restaurant satisfaction (low, moderate, high) or academic grades (F, E, D, C, B, A). OLR is not

frequently used to assess landslides since the response variable commonly is not ordinal. However,

the BGM classifies the landslide risk areas in an ordinal fashion with four risk levels (low,

moderate, high, and very high), which makes OLR the most appropriate methodology for this study.

We used the MASS package in the open source R statistical software and the polr equation

to estimate the ordinal logistic regression model. The method is also called the ordered logistic

regression model, proportional odds model, cumulative link model, ordered logit model, and

ordered probit model (Christensen, 2018). Equation 3.1 represents how *polr()* computes the ordinal

logistic regression.

$$logit[P(y \leq j)] = \propto_j - \beta_1 \chi_1 - \dots - \beta_n \chi_n , \qquad j = 1, 2, \dots, c - 1 \qquad (3.1)$$

(Agresti and Finlay, 2009; UCLA, 2019)

In which, *y* is the outcome with c categories and $y \leq j$ is the cumulative probability of y

being less than equal to a specific category *j*.

3. Method

The flowchart in Figure 3.1 illustrates the steps of the methods used in this study. We used RStudio

to do all the analysis in this section.
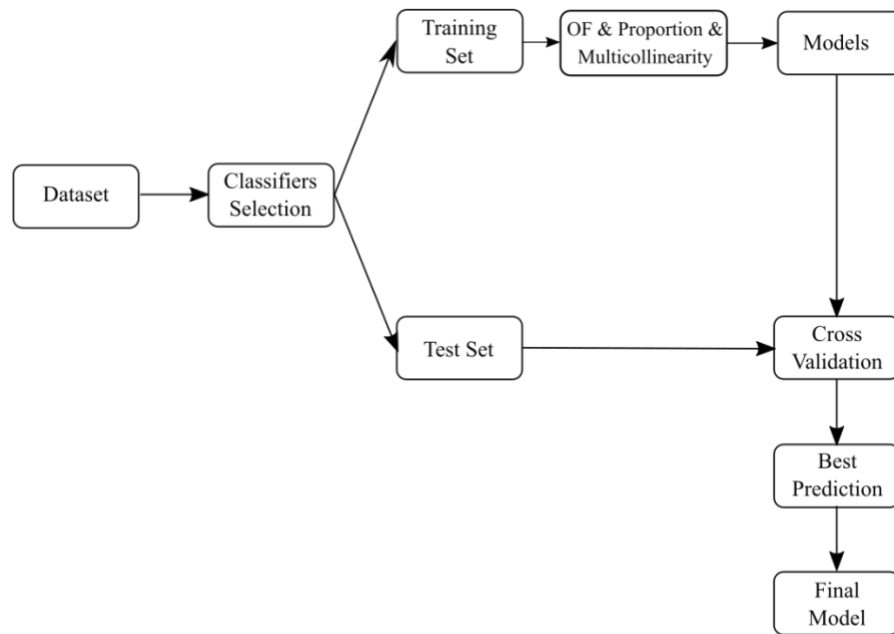
Figure 3.1. Flowchart of the steps in this study to find best OLR model

3.1 Dataset

The dataset for this study is from a 2010 Sao Paulo landslide and riverbank erosion mapping in which the BGM was used. The mapping was done by the Technological Institute of Research (IPT) and Sao Paulo Municipality during 2009 and 2010 and covered the entire city of Sao Paulo, including the risk level of sectors with any type of landslides and/or riverbank erosion.

We selected those sectors with shallow landslides and excluded the sectors with other type of landslides or riverbank erosion. The original dataset has 1,789 risk sectors, and it was reduced to 754 sectors. The new dataset was divided into two: 70 % training (N=530) and 30% test (N=224) sets. We used the training set to create the OLR models and the test set to predict the models. Figure 3.2A and 3.2B illustrate the spatial distribution of training and test sets in Sao Paulo city.
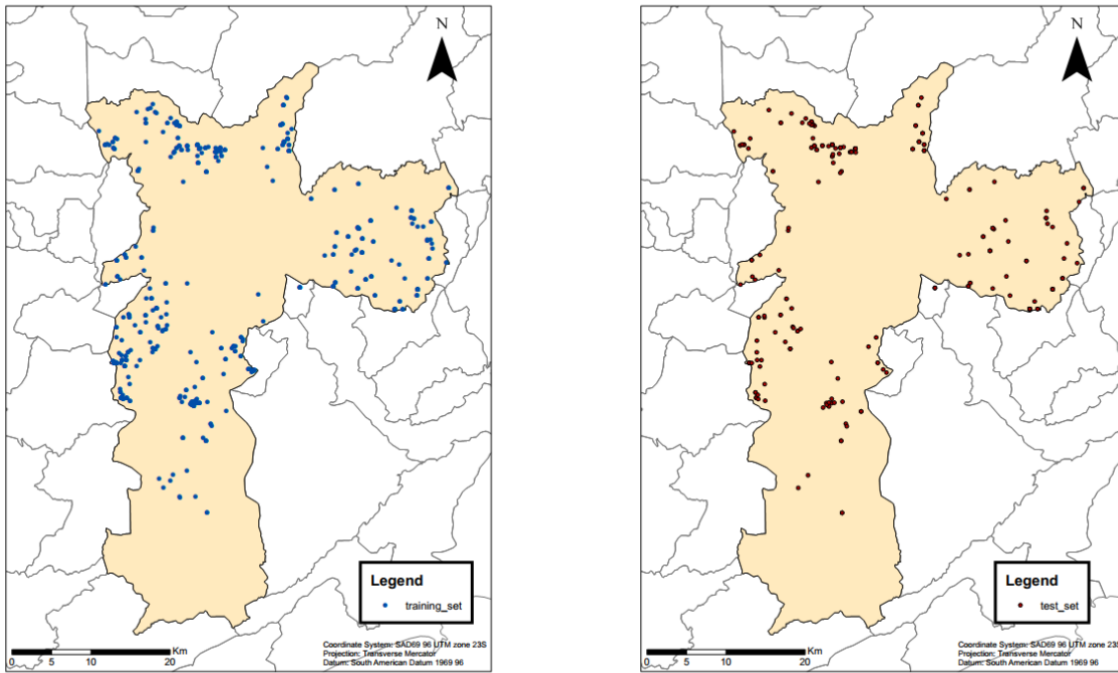
Figure 3.2. 3.2A and 3.2B. Fig. 3.2A. Spatial distribution of location of training sets. Fig. 3.2B. Spatial distribution of location of test sets

3.2 Classifiers Selection and Models

We select the classifiers by looking into the dataset and selecting the ones related with shallow landslides. We divided the classifiers into four categories: not relevant, relevant but inconsistent, relevant, and outcome.

a) Not relevant: spring, riverbank erosion, rockfall, earth slide, block slide, erosion, number of houses.

b) Relevant but not consistent: maximum height, distance from the base, distance from the top.

c) Relevant: type of building (brick, mix material, wood), landfill, garbage, construction deposit, landslide scars, drawback steps, tilted pole, fractures, crack (terrain/houses), belly wall, water in the terrain (concentration of rainfall water, leak, septic tank, type of drainage (none, precarious, good)), vegetation (trees, grassland, deforestation, banana trees), density (1, 2, 3, 4), natural slope, cut slope, slope with landfill, type of soil, geology.

d) Outcome: level of risk (low, moderate, high, very high)

Initially, we had 97 classifier variables and we excluded those not related to shallow landslide risk (i.e., riverbank erosion or other landslide types) and the classifiers that were inconsistent (i.e., many had unavailable data).

We tested the selected classifiers (N=32) for their ordinal fashion. In this test, a plot of each response variable with the predictor variable illustrates the ordinal fashion of the variable. Figure 3.3 shows eight classifiers tested for their ordinal fashion (check *Appendix 3.1* for all classifiers). The continuous line is how the response variable behaved, and the dashed line is how it was expected to behave. Based on this test, we divided the classifiers into three groups: ordinal fashion (OF), moderate ordinal fashion (MOF), and non-ordinal fashion (NOF). An example of OF is conc_rainfall, for MOF is ground_veg, and for NOF is deforestation (check Figure 3.3 for the example and Table 3.1 for the classification of all classifiers).
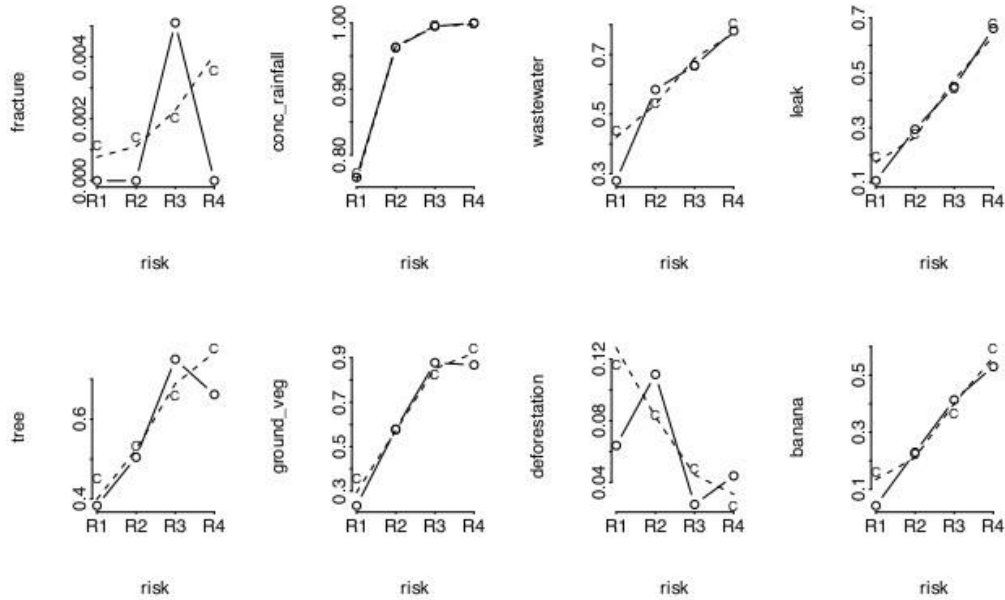
Figure 3.3. Test for Ordinal Fashion (OF). Continuous lines connect circles of the computed values, and dashed lines connect the estimated expected values. Variables conc_rainfall, wastewater, leak, and banana are in the OF category. Variables tree and ground_veg are in the MOF category. Variables fracture and deforestation are in the NOF category.

The second test was to check for the proportion of the dataset across the predictor variables. Based on the representativeness of the predictor variables for one classifier, we divide them into two categories: good proportion (GP) and bad proportion (BP). Choices (i.e., True or False) of explanatory predictors with less than 5% of what is expected by each choice (i.e., 2 categories, expected N = 265; 3 categories, expected N= 177) in at least half of the choices are classified as BP. GP, on the other hand, has at least 5% of what is expected by each choice. Tables with the frequency of each classifier choice and percentage are listed in *Appendix 3.2*.

Based on the proportion and ordinal fashion of the predictor variables, we selected the predictor variables for Equations 3.1 and 3.2. Categories (OF, MOF, NOF, GP, and BP), and respective predictor variables are illustrated in Table 3.1.

Table 3.1. Category and respective predictor variables

Category	Predictor Variables
OF (Ordinal Fashion) (*N=21*)	angle (slope angle), brick, wood, mixed, EN, TC_mature_soil (slope cut with soil), TC_saprolite_soil (cut slope with saprolite), spring, landifll,

	construction (slope with contruction material), garbage, crack, leaning_wall, scars, downward_floor, tilted, conc_rainfall (concentration of rainfall water), wastewater, leak, septic_tank, banana
MOF (Moderate Ordinal Fashion) (*N=6*)	density, TC (slope cut), TC_unstable_structure (slope cut unstable structure), tree, ground_veg, drainage
NOF (Non-Ordinal Fashion) (*N=3*)	TC_weath_rock (cut slope with weathering rock), deforestation, fracture
GP (Good Proportion) (*N=27*)	all classifiers minus BP classifiers
BP (Bad Proportion) (*N=3*)	TC_weath_rock (*True N=13 , False N=529*), fracture (*True N=1 , False N=529*), septic_tank (*True N=4 , False N=526*)

To test if a simple model would be better than more complex models for our dataset, we reduced the number of predictor variables while tracking the *p*-value. The *p*-value can explain if the predictor variable is statistically significant as a predictor of the response variable. A significance level (α) of 0.05 is usually used, but for this study, we were more concerned with reducing the number of predictor variables while still keeping the important ones. Therefore, being conservative, we first used a *p*-value < 0.10, then, we accounted for a *p*-value < 0.5. We did these steps on our base models (Equation 3.1 and Equation 3.2), creating Equations 3.3 and 3.4 from Equation 3.2 and creating Equations 3.5 and 3.6 from Equation 3.1.

Regression equations should consider multicollinearity. Multicollinearity occurs when more than two predictor variables influence the response variable equally by inflating it. For instance, no drainage, density 3, and wastewater are correlated. Risk sectors classified as density 3 don't have a drainage system; consequently, the dwelling wastewater is thrown onto the terrain. Therefore, no drainage, density 3, and wastewater predictor variables seem to have a similar influence in the response variable. When accounting for multicollinearity, we need to exclude predictor variables that can inflate the response variable. Model 7 was created by taking into consideration the multicollinearity. Table 3.2 has information for all the equations compared in this study.

Table 3.2. Equations, number of predictor variables, and aspects considered to choose predictor variables

Equation	Number of Predictors Variable	Aspects Considered to Choose Predictors Variable	Predictors Variable
Model 1	20	OF, GP	angle, brick, wood, mixed, EN, TC_mature_soil, TC_saprolite_soil, spring, landfill, construction, garbage, crack, leaning_wall, scars, downward_floor, tilted, conc_rainfall, wastewater, leak, banana
Model 2	26	OF, MOF, GP	angle, brick, wood, mixed, EN, TC_mature_soil, leak, TC_saprolite_soil, construction, spring, landfill, garbage, crack, leaning_wall, scars, downward_floor, tilted, conc_rainfall, wastewater, banana, density, TC, TC_unstable_structure, tree, drainage, ground_veg
Model 3	16	OF, MOF, GP, p-value ≤ 0.10 from Equation 2	brick, wood, EN, TC_mature_soil, construction, crack, leaning_wall, scars, downward_floor, drainage, conc_rainfall, wastewater, leak, ground_veg, tilted, TC_unstable_structure
Model 4	13	OF, MOF, GP, p-value ≤ 0.05 from Equation 3	brick, wood, TC_mature_soil , construction, crack, leaning_wall, scars, downward_floor, tilted, conc_rainfall , leak, ground_veg, drainage
Model 5	20	OF, GP, p-value $\leq$ 0.10 from Equation 1	angle, brick, wood, mixed, EN, TC_mature_soil, TC_saprolite_soil, spring, landfill, construction, garbage, crack, leaning_wall, scars, downward_floor, tilted, conc_rainfall, wastewater, leak, banana
Model 6	13	OF, GP, p-value $\leq$ 0.10 from Equation 5	brick, wood, EN, TC_mature_soil, crack, wastewater, leaning_wall, scars, downward_floor, tilted, banana, conc_rainfall, leak
Model 7	19	OF, MOF, GP, multicollinearity	angle, brick, wood, EN, TC_mature_soil, tree, TC_saprolite_soil, TC_unstable_structure, landfill, garbage, crack, leaning_wall, tilted, scars, banana, conc_rainfall, leak, wastewater, ground_veg

3.3 Comparison of Models by Cross Validation

To choose the model that best represents our dataset, we compared the seven models by cross validation. We used the test set to predict and compare the models created with the training set. We predicted the models ten times and compared the means, standard deviations, and ranges. Based on that, we chose the model with the best overall predictive power.

3.4 The application (app)

We developed an application (app) that automatically computes the risk level of shallow landslides. The application was coded in RStudio software, and the two main packages used were Shiny and Rmarkdown. The app mimics the BGM field evaluation paper form on a digital device. It can be accessed with a smartphone, computer, or tablet with internet access and RStudio installed. The manipulation is simple, and the user simply checks the boxes with the preset classifiers observed in the field. The application has two main tabs: i) Diagnostic (Diagnóstico): input dataset (Figure 3.4A) and ii) Answer (Respostas): display dataset collected in a table to compute and classify risk level (Figure 3.4B). In the second tab, the user can export the data file in PDF, HTML, and CSV formats.

Figure 3.4. 3.4A and 3.4B. Fig. 3.4A. Display Diagnostic Tab in a smartphone. Fig. 3.4B. Display Answer tab in a smartphone.

4. Results and Discussion

We computed the coefficient value of the classifiers using the MASS package in the RStudio environment (Table 3.1). In our study, the majority of classifiers are binary (classifierTRUE and classifierFALSE). ClassifierTRUE is the one displayed in Table 1; classifierFALSE is the dummy variable with value equal to zero. The name of the classifiers starts with the predictor variable followed by options (i.e., brick is the predictor variable and TRUE and FALSE are the options, or angle is the predictor variable and A, B, C, D, and E are the options). Detailed information on the models is included as *Appendix 3.3*.

Table 3.3. Classifiers and their specific weight (coef) and odds ratio (OR) for each model. OR is interpreted as the same within risk levels and it is computed by exponentiating the coef. For instance, in Model 1, OR =2.77 for woodTRUE. The odds of having higher level of risk is 2.77 times for sectors with wood houses (woodTRUE) when compared with sectors without wood houses (woodFALSE) if all other variables in the model are held constant.

Classifier	Model 1		Model 2		Model 3		Model 4		Model 5		Model 6		Model 7	
	coef	OR	coef	OR	coef	OR	coef	OR	coef	OR	coef	OR	coef	OR
brick	-1.7	0.18	-1.48	0.23	-1.6	0.20	-1.6	0.20	-1.7	0.18	-1.8	0.17	-1.7	0.19
wood	1.02	2.77	0.79	2.20	0.84	2.32	0.94	2.56	1.02	2.77	1.04	2.83	1.04	2.83
mixed	0.09	1.09	0.07	1.07					0.09	1.09				
EN	0.7	2.01	0.63	1.88	0.39	1.48			0.7	2.01	0.65	1.92	0.69	1.99
TC			-0.12	0.89										
TC_mature_soil	0.58	1.79	0.58	1.79	0.54	1.72			0.58	1.79	0.65	1.92	0.78	2.18
TC_saprolite_soil	0.25	1.28	0.24	1.27					0.25	1.28			0.13	1.14
spring	-0.2	0.80	-0.08	0.92					0.22	0.80				
landfill	0.1	1.11	0.03	1.03					0.1	1.11			0.4	1.49
garbage	0.03	1.03	0.08	1.08					0.03	1.03			0.3	1.35
construction	0.46	1.58	0.54	1.72	0.61	1.84	0.69	1.99	0.46	1.58				
leak	-0.4	0.66	-0.62	0.54	-0.6	0.54	-0.6	0.57	-0.4	0.66	-0.4	0.68	-0.4	0.68
conc_rainfall_water	1.63	5.10	1	2.72	1.01	2.75			1.63	5.10	1.75	5.75	1.66	5.26
wastewater	0.6	1.82	0.39	1.48	0.39	1.48			0.6	1.82	0.64	1.90	0.57	1.77
drainage.L[2]			1.31	3.71	1.31	3.71	1.4	4.06						
drainage.Q[3]			-0.03	0.97	-0.03	0.97	-0.1	0.95				1.00		
crack	2.18	8.85	2.28	9.78	2.27	9.68	2.26	9.58	2.18	8.85	2.23	9.30	2.14	8.50
leaning_wall	2.03	7.61	2.26	9.58	2.21	9.12	2.26	9.58	2.03	7.61	2.06	7.85	2.14	8.50
scars	4.25	70.11	4.25	70.11	4.2	66.7	4.21	67.4	4.25	70.11	4.31	74.4	4.29	73
downward_floor	1.28	3.60	1.1	3.00	1.1	3.00	1.07	2.92	1.28	3.60	1.26	3.53		
tilted	0.85	2.34	0.73	2.08	0.75	2.12			0.85	2.34	0.87	2.39		
angleD	0.24	1.27	0.15	1.16					0.24	1.27			0.4	1.49
angleE	0.32	1.38	0.47	1.60					0.32	1.38			0.54	1.72
tree			-0.27	0.76									-0.3	0.76
banana	0.39	1.48	0.22	1.25					0.39	1.48	0.48	1.62	0.27	1.31
ground_veg							0.92	2.51					1.13	3.10
TC_unstable_structure			-1.1	0.33	-0.9	0.41							-0.7	0.50
densityd2			0.07	1.07										
densityd3			0.21	1.23										
R1/ R2	*-0.7*	0.49	*-1.07*	0.34	*-1.5*	0.21	*-1.6*	0.19	*-0.7*	0.49	*-1.1*	0.33	*-0.1*	0.94
R2/ R3	*3.56*	35.2	*3.72*	41.3	*3.23*	25.3	*3.03*	20.7	*3.56*	35.16	*3.08*	21.8	*4.36*	78.3
R3/ R4	*9.02*	8267	*9.3*	10938	*8.77*	6438	*8.59*	5378	*9.02*	8267	*8.5*	4915	*9.78*	17677

[2] drainage.L refers to precarious drainage system

[3] drainage.Q refers to no drainage system

ScarsTRUE is the classifier, in all the models, with the highest coefficient value, and it does not differ much between models (see Table 3.1). It represents the presence of prior landslide scars in the sector, which means that in the past a landslide occurred in the sector. Past landslide indicates the possibility of reactivation of the same landslide (Highland & Brobrowsky, 2008). Classifiers that represent signs of instability have positive coefficient values (see crackTRUE, leaning_wallTRUE, downward_floorTRUE, and tiltedTRUE). Signs of instability specify movement on the terrain and suggest that a landslide could be initiated (Carvalho, 2007). Therefore, the classifier coefficient value should be positive since its presence in the sector contributes to a high-risk level.

Classifiers brickTRUE, woodTRUE, and mixedTRUE represent the type of dwelling. Mixed material dwellings are more precarious than wood since they combine pieces of cardboard boxes, plastic, wood, and any other material available, and mixed material and wood dwellings are more precarious than brick (see Figure 3.5A and 3.5B). Risk areas are usually located in impoverished neighborhoods, and residents commonly build their initial dwellings with any materials available on site (mixed material dwellings), later upgrading to wood dwellings and eventually to brick as their financial situation improves. One of the reasons mixed material dwellings have lower coefficient values than wood dwellings could be related to the fact that usually there are less mixed material dwellings in a sector or mixed material could be misclassified as wood (since it usually has some pieces of wood). Combining wood and mixed material would be one way to solve this problem and should yield a more consistent coefficient value for this classifier.

Figure 3.5. 3.5A and 3.5B. Fig. 3.5A. Brick dwellings are the ones with most of the dwellings made with bricks. They are more resistant than wood and mixed material dwellings. Fig. 3.5B . Mixed material dwellings combine different materials and the dwellings are very precarious

Landfill (landfillTRUE), garbage (garbageTRUE), and construction material (construction_TRUE) can be found in the risk sectors, and they contribute to increase the level of risk. Garbage and construction material on the slope (see Figure 3.6A) can move downslope, and dwellings built on top of landfills or disturbed soil are less stable (Carvalho, 2007). The quantity and composition of the materials in each sector are different (see Figure 3.6A and 3.6B). They have positive coefficient values in the models, contributing to an increase of the risk level. However, *p*-values for these coefficient values were higher than 0.05 (*Appendix 3.3*). Since garbage and construction material are usually found in the same site, combining both into one single classifier could improve models. Another aspect to consider is that in the field inventory form, the option is to choose if there are garbage, landfill, and construction materials on the sector, but whether the amount is small, moderate, or high, the choice is the same. A Likert scale for this factor could improve the data collection and contribute to better models.

Figure 3.6. 3.6A and 3.6B. Fig. 3.6A. Slope with garbage and construction material. Notice the difference in amount of material in each part of the hill. Fig. 3.6B. Detail of the material on the slope. Notice the presence of garbage but also construction material.

Shallow landslides in these urban risk sectors in Brazil are triggered by rainfall (Tominaga et al., 2009). Increase of the soil water content in the slope can contribute to shallow landslide initiation. In these risk sectors, self-engineered dwellings have precarious pipelines that can leak, and sewage is left to flow onto the slope (see Figures 3.7A and 3.7B). Some sectors have dwellings with a septic tank. Overtime, as these informal sectors become more formal, municipalities attempt improvements in public utilities, like drainage systems and electricity. However, these improvements take time and depend on the municipality's financial resources and priorities. Classifiers that contribute to increasing the water content on the terrain should have a positive correlation coefficient since they contribute to increasing the risk level. WastewarTRUE and conc_rainfall_waterTRUE have positive coefficient values. LeakTRUE has negative coefficient value in all the models, but it would be expected to be positive. A negative coefficient value of the classifier could be related to the difficulty of quantifying the leakage in the sector because on the field evaluation form you have just the options of presence or absence of leakages in the sector. For

instance, a sector with just one dwelling with a leakage has the same weight as a sector with all dwellings with leakages.

Figure 3.7. 7A and 3.7B. Fig. 3.7A. Precarious wastewater pipes and pipes to conduct water. Fig. 3.7B. Self built pipelines. Note black tape to help keep pipes connected.

Vegetation classifiers in all the models have coefficient values as would be expected. Banana trees (bananaTRUE) and ground vegetation (ground_vegTRUE) have positive classifiers values, and tree (treeTRUE) has a negative value. Banana trees are known to increase water content in the soil, which can increase the risk level since the soil is more saturated (Carvalho et al., 2007). Ground vegetation can increase risk level since the soil has less coverage protection than with the original vegetation. However, it would be expected that banana trees in the terrain would contribute more for a high-risk level than ground vegetation, but in the models, ground vegetation contributes more toward a high-risk level than banana trees. Aspects that are difficult to account for the classifiers related to vegetation are the quantity of vegetation, its location (near the dwellings or not), and the combination of one or more classifiers.

We ran the models ten times to compare the predictive power of each of them (Table 3.2). Model 4 has the best prediction (Mean = 0.729, SD =0.024, Range = 0.071). Still, the mean prediction power of model 3, 6, and 7 is very similar (0.0720, 0.0721, 0.724, respectively). Based

on our results, models with smaller numbers of predictor variables performed better than those with larger number of classifiers.

Table 3.4 - Comparison of Models Prediction (Mean, SD, and Range). Predictive power was tested ten times and mean of these tests were computed and compared. Model 4 (M4) has the highest overall predictor power of all the models.

Model	Test1	Test2	Test3	Test4	Test5	Test6	Test7	Test8	Test9	Test10	Mean	SD	Range
M1	0.714	0.763	0.690	0.719	0.688	0.696	0.701	0.696	0.777	0.728	*0.717*	*0.031*	*0.089*
M2	0.714	0.723	0.696	0.710	0.701	0.688	0.714	0.696	0.768	0.737	*0.715*	*0.027*	*0.080*
M3	0.710	0.732	0.696	0.741	0.710	0.696	0.701	0.705	0.750	0.755	*0.720*	*0.023*	*0.058*
M4	0.705	0.759	0.714	0.746	0.741	0.688	0.723	0.705	0.755	0.755	*0.729*	*0.024*	*0.071*
M5	0.714	0.763	0.692	0.719	0.688	0.696	0.701	0.696	0.777	0.728	*0.717*	*0.028*	*0.089*
M6	0.710	0.746	0.683	0.723	0.714	0.701	0.710	0.705	0.777	0.741	*0.721*	*0.028*	*0.094*
M7	0.710	0.741	0.719	0.737	0.696	0.710	0.719	0.696	0.768	0.741	*0.724*	*0.024*	*0.072*

5. Conclusion

Updating risk level more rapidly can prevent disasters in shallow landslides risk areas, allowing a local municipality to better monitor the area and to relocate financial resources to sectors with high risk levels. Automatically computing shallow landslide risk level using an application (app) allows the standardization of the BGM, rapid updates to the mapped areas, and results in a reduction in human subjectivity in assessing the landslide risks.

In this study, when comparing the models, those with a smaller number of classifiers had better performance and were simpler. Model 4 had the best mean predictive power when compared with six other models. The mean predictive power was 0.73. The total number of predictor variables is 14 and it accounts for OF, MOF, GP, and p-value ≤ 0.05. To improve the model for shallow landslides, we recommend that the BGM field evaluation form adopt a Likert scale for some classifiers, like leaks, presence of garbage, and construction material. This would allow the differentiation of sectors with small, moderate, and high leak or garbage and not treat the small and

high amounts as the same. Combining classifiers that are similar and found in the same sector, like wood and mixed material dwellings, or classifiers that are found in same site, like garbage and construction material, could improve the model as well.

CHAPTER 4: Shallow Landslide Susceptibility in Disturbed and Undisturbed Sites, São Bernardo do Campo, Brazil

ABSTRACT

Many people live in shallow landslide risk areas in São Bernardo do Campo, Brazil. These risk areas are a result of the natural geomorphology, the intense rainfall during summer months, and human activities that disturb the terrain, such as cut and filling or discharging sewage onto the hillslope. Ideally, people should not be living in high and very high-risk areas. However, relocating all residents that live in these areas is not feasible in the short term since the measure would require the availability of financial resources coupled with political motivation. Therefore, actions that can mitigate and manage the risk, such as slope stability studies, can prevent human and material losses. In this study, the main goal is to measure and compare the slope stability and the saturated-hydraulic conductivity of disturbed and undisturbed sites. The study was conducted at two sites: one disturbed and one undisturbed. First, soil tests were conducted to identify soil texture and to compute wet soil buck density, soil cohesion, and soil angle of internal friction. Using these values, a spatial analysis of the slope stability using SHALSTAB and the Factor of Safety was conducted. Additionally, in situ-saturated hydraulic conductivity was measured at each location in each site. The undisturbed site had a soil cohesion of 2.88 kPa, an angle of internal friction of 18.19º, and a wet soil bulk density of 1720 kg/m^3, and the disturbed site had a soil cohesion of 2.04 kPa, an angle of internal friction of 22.90º, and a wet soil bulk density of 1534 kg/m^3. Considering the soil characteristics, the disturbed soil is more stable with the slope stable in dry and wet conditions at an angle of 17º, which is not the case for the undisturbed site, in which it becomes unstable when 76% saturated. The saturated hydraulic conductivity had greater variability at the disturbed site

(Mean=138.15 mm/h, SD=266.94 mm/h, and Range= 675.16 mm/h) than at the undisturbed site

(Mean=19.80 mm/h, SD=12.12 mm/h, and Range=28.44 mm/h).

1. Introduction

Shallow landslides are common in urban areas in the Metropolitan Region of Sao Paulo, Brazil. Over the last 30 years, many shallow landslides have resulted in material or human losses at São Bernardo do Campo (SBC) (Folha de São Paulo, 2005; SãoBernardo.Info, 2019; Diário do Transporte, 2020).

The shallow landslides in SBC are a result of the geomorphology, including the slope angle and soil characteristics, and the intense rainfall of the region, but also due to the urbanization and consequent anthropogenic activities on the terrain. Part of SBC has hillslopes with medium to high slope angle in the *Morraria do Embu* and medium to high slope angle in the *Serra do Mar* (Regino et al, 2014), and intense and continuous rainfall are common during the summer months (December to March). In addition, Brazilian urbanization was fast and disorganized (Maricato, 2008), resulting in informal settlements built on hillslopes and in flood plain areas (Fischer, 2014). Residents in these informal settlements built themselves their own houses and these homes are not always safe. These houses are built on terrain that is cut and filled with soil and/or landfill, there is commonly wastewater disposal onto the hillslopes, garbage is thrown onto the hillslopes, and the houses are built with non-durable materials (wood, cardboard boxes, and any other material available on site).

Therefore, the combination of the geomorphology and the pressures on people to live in these areas has resulted in many residents living in at-risk locations.

Ideally, people should not be living in high and very high-risk areas. However, relocating all people that live in these at-risk areas is not feasible in the near future since the measure would require the availability of financial resources coupled with political motivation. Therefore, actions that can mitigate and manage the risk, such as Disaster Risk Reduction (DRR) measures, can be used to prevent natural disasters. For instance, DRR measures include mapping of areas susceptible to shallow landslides and sending out early warnings. In this study, we aim to answer the following research questions: i) what is the susceptibility to shallow landslides in a disturbed hillslope when compared to an undisturbed hillslope in SBC?, and ii) how are these undisturbed and disturbed sites similar and different in terms of slope stability and saturated hydraulic conductivity?

2. Background

2.1 Study Area

The study area is located in São Bernardo do Campo and on the boundary between SBC and Santo André (see Figure 4.1). Both cities are part of the São Paulo Metropolitan Area, São Paulo state, in Southeastern Brazil. The estimated population for SBC in 2019 was 838,936 (IBGE, 2020), and the population density was 1,869 people/km^2 (IBGE, 2020).
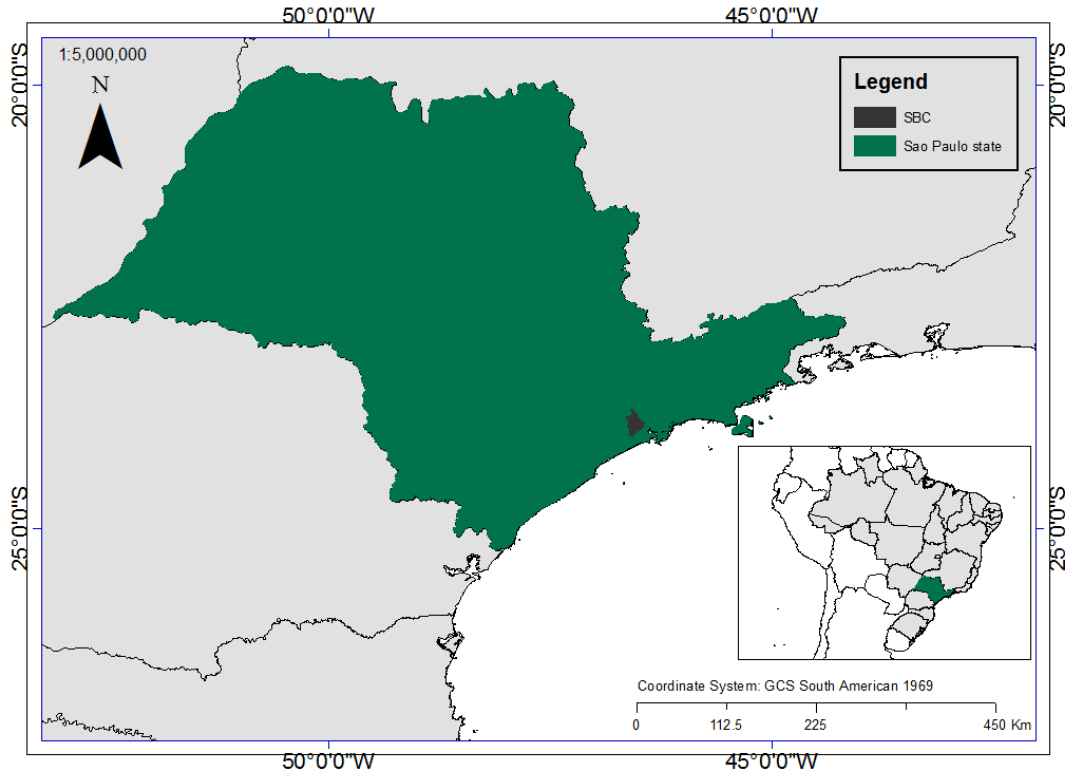
Figure 4.2. The location of the city of São Bernardo do Campo (SBC), São Paulo state, Brazil. SBC is shown in black, and São Paulo state in green. (Source: Author)

The city of SBC was chosen for this study due to its past shallow landslide history, researcher familiarity with the area, and support of the local municipality to conduct the field work. These risk areas are commonly located in favelas (slums) and are similar to other urban shallow landslide risk areas observed in Southeastern Brazil. Since 1996, at least 21 people have died due to previous landslides in SBC (UOL, 2017).

Two main sites were selected (see Figure 4. 2) in which to conduct the study, using the following characteristics to define these locations: safety, previous landslides, geological formation, and variability (disturbed and undisturbed). Landslide risk areas are commonly located in favelas in São Bernardo do Campo, and some of these favelas are not safe for fieldwork due to drug cartels. Therefore, finding a favela that was safe was an important factor in choosing the disturbed site. The

choice of the location was made together with the local Civil Protection staff. To guarantee the safety of the fieldwork, the Civil Protection and the Social Work Secretary contacted residents and community leaders, asking for their local support. For the undisturbed site, we chose the location based on the municipality technicians' knowledge. For the disturbed site, a hillslope in the Jardim Silvina (Figure 4.3) was selected, and for the undisturbed site, a hillslope at Monte Sião (Figure 4.4).
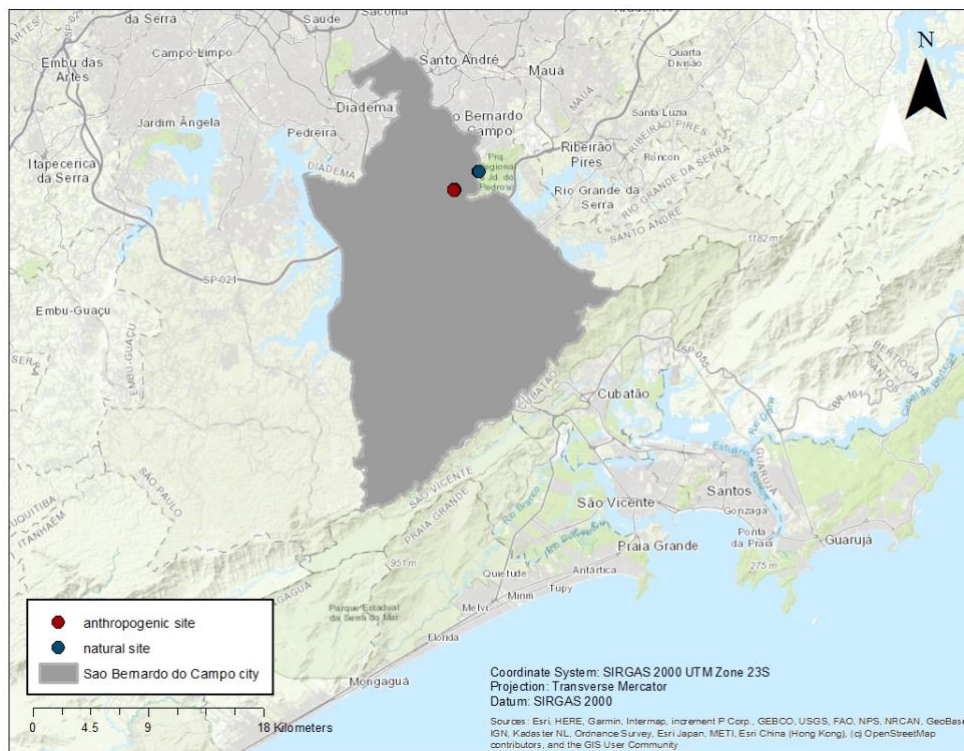
Figure 4.3. The location of São Bernardo do Campo city and the location where fieldwork was conducted. The red dot is the disturbed site (anthropogenic site) and the blue one is the undisturbed site (undisturbed site). (Source: Author)

Figure 4.4. Disturbed site. Red dots indicate locations at which soil was collected and hydraulic conductivity test was conducted in situ. (Source: Author)
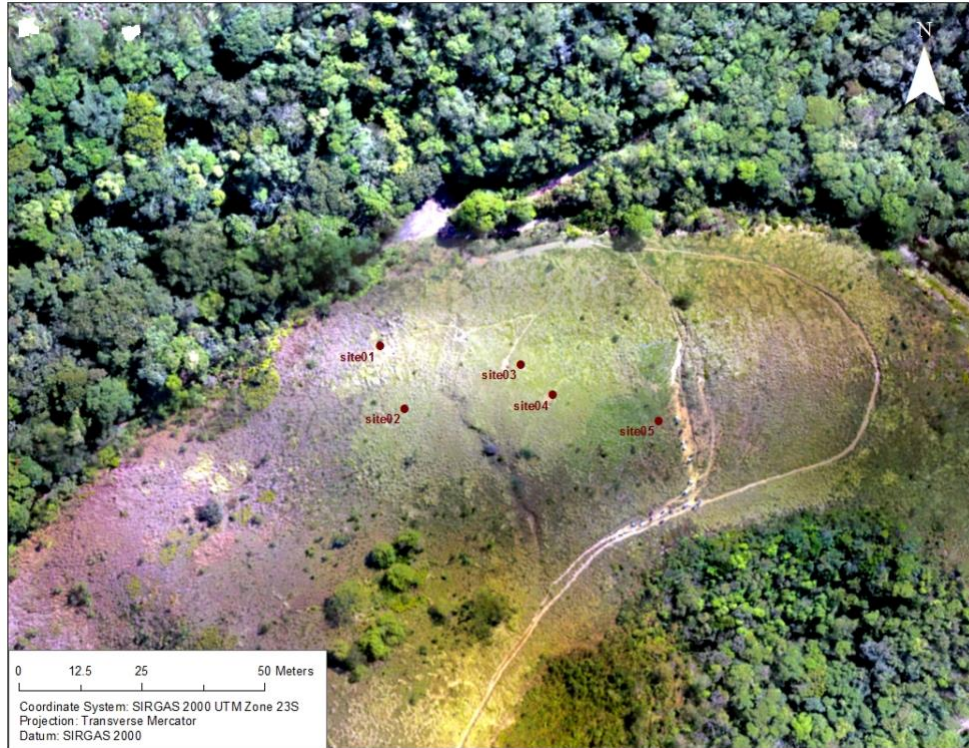
Figure 4.5. Undisturbed Site. Red dots indicate locations where hydraulic conductivity was conducted in the site and soil samples were collected to be analyzed in the lab (Source: Author)

At both sites we conducted field work. The red dots in Figs. 4.3 and 4.4 represent locations at which soil samples were collected to be analyzed in the lab, tests for saturated hydraulic conductivity were conducted *in situ*, and drone flights were made to collect imagery to produce DEM. In the laboratory, we conducted tests of granulometry, soil bulk density, and direct shear stress.

2.2 Physical Characteristics

The city of SBC has an area of 408.45 km^2, which is divided into urban (118.21 km^2), rural (214.42 km^2), and Billings Reservoir (75.82 km^2); 53.7% of the total area of the city is located in the Spring Protection Area (Proteção aos Mananciais) (Município de São Bernardo do Campo, 2020).

The geomorphology is divided into three main zones: *Colinas de São Paulo*, *Morraria do Embu*, and *Serra do Mar* (Regino et al, 2014). The *Colinas de São Paulo* has gentle hill landforms and floodplain areas, the *Morraria do Embu* has primarily gentle hills with medium to high slope angle, and *Serra do Mar* has steep terrain (Regino et al, 2014). The majority of the city is located on a crystalline base of pre-Cambrian bedrock with shale, gneiss, and migmatites. In the northern part of the city and in some areas near the Billings Reservoir, the geological formations are originally from the *São Paulo Sedimentary Basin* of the Cenozoic Era (Regino et al, 2014).

The weather is warm and temperate with an average annual temperature of 17.8°C (64.04°F). Rainfall season is concentrated during the summer months (December-March), with January being the month with highest average total precipitation (see Figure 4.5) (Município de São Bernardo do Campo, n.d.).
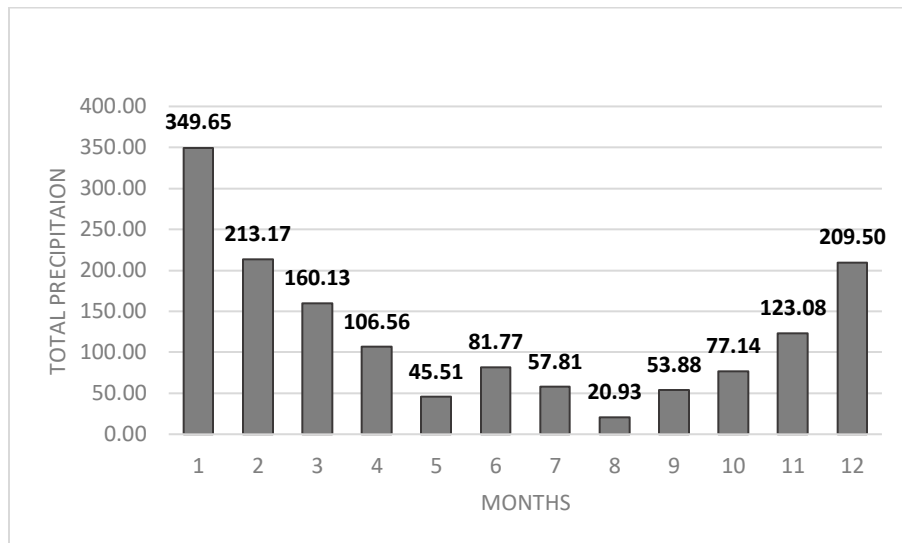
Figure 4.*6*. Average by Month of total precipitation by month from 2010 to 2014, in millimeters, in which 1 is January and 12 is December (Source: Município de São Bernardo do Campo, n.d.)

2.3 Rainfall Threshold and Saturated Hydraulic Conductivity

Shallow landslides in SBC are triggered by heavy rainfall. Therefore, knowledge of the rainfall threshold allows the local Civil Protection to monitor the rainfall and to send early warnings to residents so they can evacuate their homes. In this way, natural disasters can be prevented, and lives saved.

In this study, the field-saturated hydraulic conductivity was computed in situ using the Bottomless Bucket Methodology (Nimmo et al., 2009), and it was then used to calculate the slope factor of safety (FS) and level of soil saturation necessary for a shallow landslide to be initiated.

2.4 Slope Stability

The slope stability can be simplified as the forces acting on a slope (Keller, 2011). The main forces are the driving and the resisting forces. The driving forces are those acting to move the materials downhill, and the resisting forces are those acting to keep the materials stable and prevent them from falling.

In this study, the landslides are translational slides, and they can be analyzed by the infinite slope method (Selby, 1993). The infinite slope method is a two-dimensional analysis of a slice of the slope (see Figure 4.6), and it assumes that the slope has an infinite extent, rests on a constant angle slope, and that the thickness of the mobile slice is uniform (Selby, 1993). For a spatial analysis of the stability of the slope, we used the infinite slope methods: SHALSTAB and Factor of Safety.
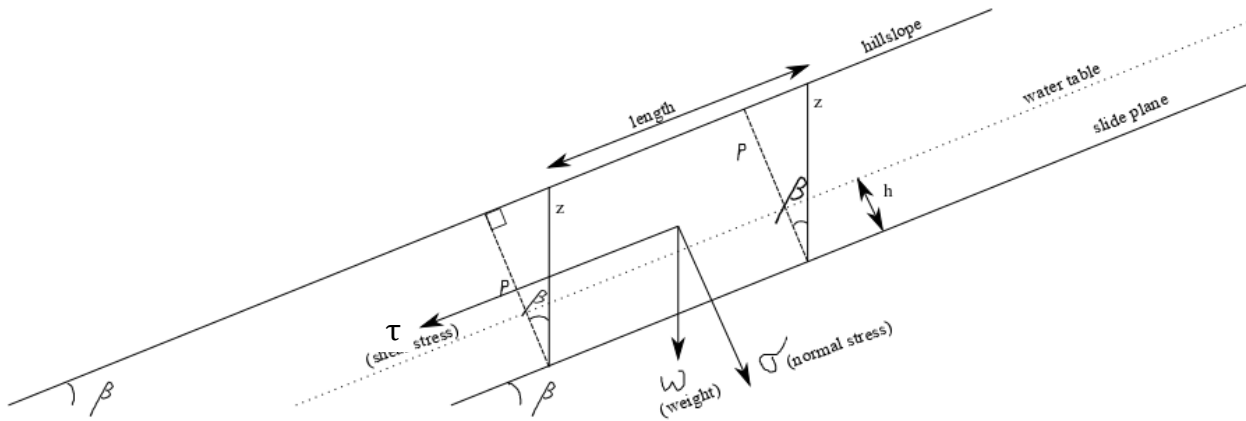
Figure 4.7. Slope stability on an infinite slope. The angle of slope is represented by β, p is the height between the hillslope and the slide plain, h is the height of the water table, W is the weight, σ is the normal stress, and **τ** is the shear stress.
(Source: adapted from Selby, 1993).

3. Methods

3.1 Saturated Hydraulic Conductivity

The saturated hydraulic conductivity (K_{sat}) was computed using the bottomless bucket methodology (Nimmo et al., 2009). For the disturbed site, six locations were chosen (see Figure 4.3), and for the undisturbed site, four locations were chosen (see Figure 4.4).

In the field, we measured the time that the water took to infiltrate into the soil. In each site, we first cleared the vegetation off from a small area (~ 0.4 m by 0.4 m) and leveled the soil using a shovel so we could perform the measurements (see Figure 4.7). Then, we dug a small trench (~ 1 to 3 cm deep) and placed the bottomless bucket on top of it. On the outer side of the bucket, we used clay to seal the edges of the bucket to the ground to prevent lateral water leakage. Inside the bucket we placed a ruler in a horizontal position to measure the height of the water. As we poured the water, we placed a small plastic bag to reduce the water impact. Then, we placed the water inside the bucket and used a stopwatch to measure the time that the water took to completely infiltrate the

58

soil from the initial height. We also used a GPS (Global Positioning System) device to get the

GeoReference of each individual site.

Figure 4.8. One of the sites in which the field-saturated hydraulic conductivity was measured. The area was first cleared with the shovel and the paintbrush to place the bottomless bucket. Between the outer part of the bucket and the soil, clay was spread to avoid lateral water leakage. Water was placed inside the bucket and the time that the water took to infiltrate the soil was measured.

Measurements of the top and bottom diameters of the bottomless bucket were taken to

compute the K_{sat}. At each site, we measured the height of the bucket in four locations (90° apart

from each other) and averaged the values. The following two main equations (Eqs. 4.1 and 4.2)

were used to compute K_{sat}.

$$K_{sat} = \frac{L_G}{t} * \ln\frac{L_G + \lambda + D_0}{L_G + \lambda + D} \tag{4.1}$$

$$L_G = C_1 * d + C_2 * b \qquad (4.2)$$

where L_G is the ring-installation scaling, D is the depth of ponding, D_0 is the initial depth of ponding, λ is the macroscopic capillarity of the length of the soil and is equal to 0.8 cm, K_{sat} is the field-saturated hydraulic conductivity, t is the time from the initial depth to the depth of the ponding, C_1 is Constant 1 and equal to 0.993, C_2 is Constant 2 and is equal to 0.578, b is the ring radius, and d is the depth (part of the bottomless bucket that is inside the soil).

3.2. Digital Elevation Model (DEM)

The spatial analysis of the slope stability requires a Digital Elevation Model (DEM) of the terrain. Moreover, a high-resolution DEM increases the quality of the spatial analysis. However, the highest resolution DEM available for SBC was 30m, which is too coarse for the proposed analyses. Therefore, the solution employed was to collect imagery with an unmanned aerial vehicle (UAV: DJI Phantom 4 quadcopter) and then to produce the DEM by processing the imagery collected using PhotoScan and Structure from Motion processing. To conduct the UAV flights, the application (app) Drone Deploy was used. The app can plan a flight and take photos at a constant interval, which is very difficult to do when the user is controlling the UAV.

After processing the imagery, we manually removed trees, houses, and cars from the data. Figures 4.8A and 4.8B illustrate the original drone flight for the disturbed site and the one with the objects removed, respectively. Other raster grids used in the models (slope and flow accumulation) are included in *Appendix 4.1*.
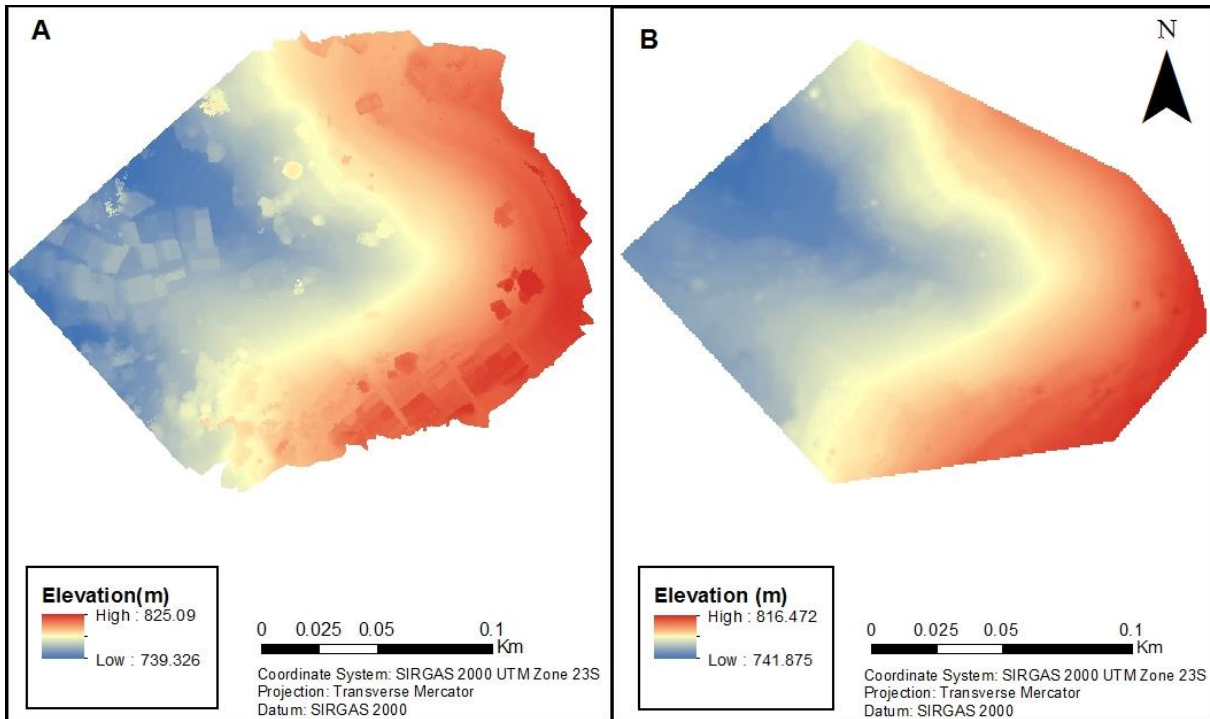
Figure 4.9. 4.8A and 4.8B. Fig. 4.8A illustrates the original high-resolution DEM produced from imagery from the drone flight with houses and trees not removed. Fig 4.8B illustrates the DEM used in the model corrected by exclusion of houses and trees.

Figures 4.9A and 4.9B illustrate the original DEM (0.046m by 0.046m pixel resolution) and the one used in the models (0.50m by 0.50m pixel resolution) for the undisturbed site, in which trees were excluded. Notice that Fig. 4.9B incorporates just a small portion of the raster grid and the hillslope and contains very few trees. Comparing the original grids produced by the drone flight (Fig. 4.8A and Fig. 4.9A), the hillslope used in the analysis in the disturbed site (Fig. 4.8A) had more noise than the hillslope used in the undisturbed site, and the cleaning process was more complicated and took longer. First, the original DEM was converted into contour lines, and objects were removed by changing the value of the contour lines and retaining the natural tendency of the hillslope manually.
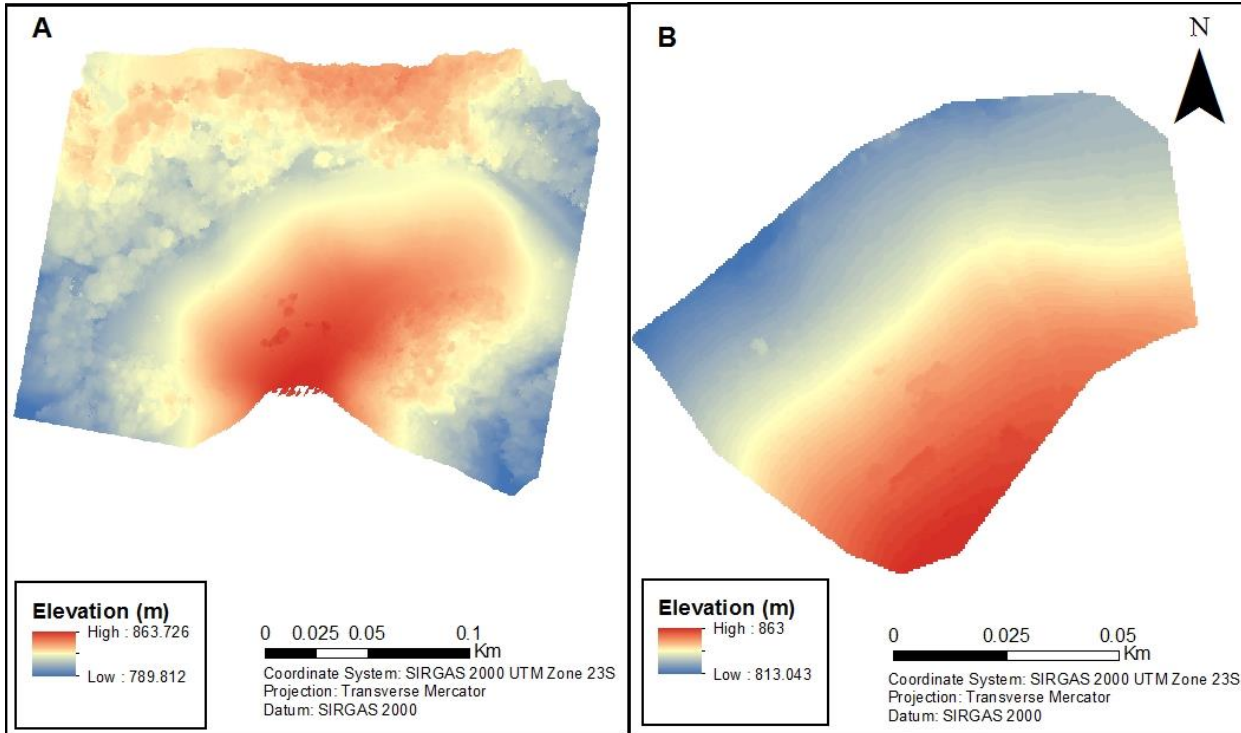
Figure 4.10. 4.9 A and 4.9B. Fig. 4.9A illustrates the original raster grid produced from the drone flights. In the North and parts of the East and West, it is possible to observe many trees. Fig. 4.9B illustrates the DEM used in the model. This DEM is a small part of the original raster.

The original resolution of the grids from both the Disturbed and Undisturbed Sites were not used in the models. We tested the models at three raster sizes (0.046 m, 0.5 m, and 1 m) (see Figure 4.10), and contrary to what would be expected, the high-resolution raster (4.10A) did not perform the best. The ability to capture an area of around $25cm^2$ made the analysis less smooth, capturing unnecessary small objects. We found the 0.5 m raster to have a better performance in this spatial analysis.
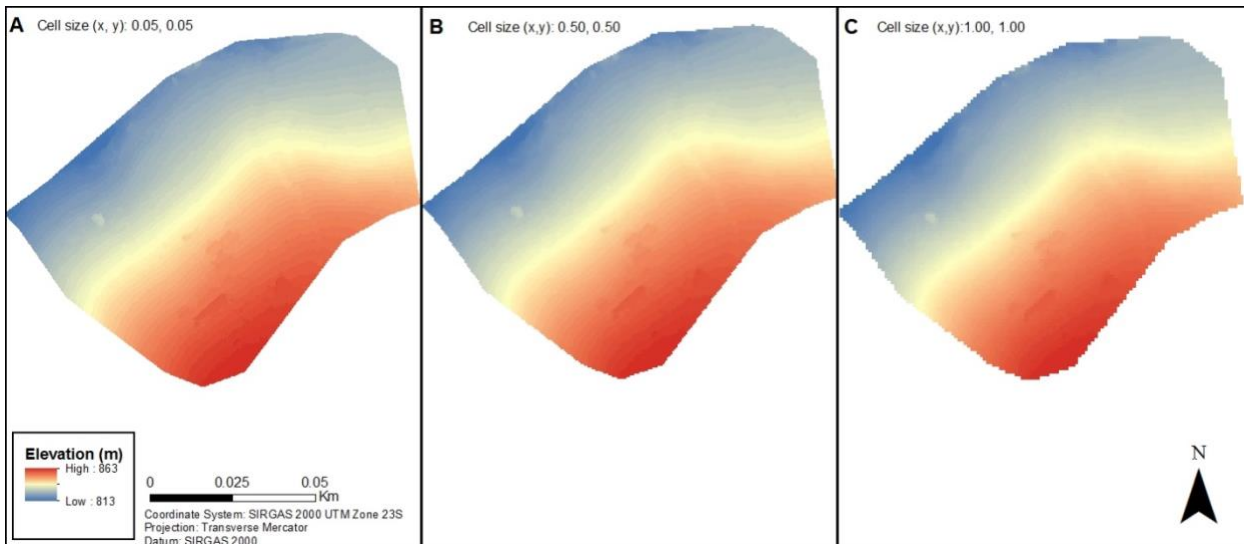
Figure 4.11. 4.10A, 4.10B, and 4.10C. Fig. 4.10A DEM at the original resolution with cell size 0.050m. Fig. 10B raster with cell size 0.5m. 10C raster with a coarser resolution of 1.0 m. Looking at the boundary of the three grids it is possible to notice that 4.10C has a sharper boundary than 4.10A and 4.10B, and 4.10B has a sharper boundary than 10A.

3.3 Soil Analysis

The analysis of the soil collected in the field aimed to identify the type of soil and find the value of wet and dry bulk density, soil cohesion, and angle of internal friction of the soil. To compute these values and identify the type of soil, we conducted three analyses: granulometry, bulk density, and direct shear stress. The direct shear stress test allows us to compute the values of soil cohesion and the angle of internal friction of the soil. These soil analyses were conducted at the *Laboratório de Mecânica dos Solos*[4] (LMS) at the University of Sao Paulo (USP) as would not be the best option to travel from Brazil to the United States carrying a bunch of soil samples.

3.3.1 Granulometric Structure of Soil, Soil Texture Classification, and Bulk Density

---

[4] Laboratório de Mecânica dos Solos – LMS: Soil Mechanics Laboratory

We used the ABNT [5] NBR 6457 and ABNT NBR 7181 to prepare the soil and conduct the granular

analysis of the soil, and, consequently, to classify the texture of the soil, based on the triangular

classification system. The NBR 6457 is a standard test method to prepare for the soil samples, and

the NBR 71781 is a standard test method to conduct the soil texture classification analysis. We used

these standard test methods since they were the standard methods used in the Brazil and by LMS.

3.3.1.1 Granulometric Structure of Soil and Soil Texture Classification

The granulometric structure of the soil test finds the percentage of each grain size in the soil by

shifting the soil or by combining soil sedimentation and soil shifting (ABNT, 1984).

The soil samples were dried naturally in individual containers until the samples reached the

hygroscopic humidity. Then, the soil samples were carefully broken apart, so their soil texture was

more homogeneous to sift with a sieve #10 (2 mm). The material that was sifted was saved for the

soil texture classification, and the sifted and unsifted materials were weighed. Two samples of the

fine grains (sifted soil), each 40g, were placed in small metal containers. The coarse material

(unsifted) was washed with distilled water in the sieve #10. The coarse material that did not sift was

placed in a small metal container. These three containers were placed inside a greenhouse with a

temperature between 105°C and 110°C for 12 hours to completely dry.

To sift the coarse grain sample (larger than 2mm), we used sieves on top of each other and a

machine that shook the material (see Figures 4.11A and 4.11B). We shook each sample of the

coarse soil for 15 minutes using a machine (Fig. 4.11 A) so the grains would be separated by their

grain size. Based on the weight of the soil in the fine and coarse sieves, we are able to compute the

percentage of each grain size. Therefore, we can identify the soil texture.

---

[5] ABNT: Associação Brasileira de Normas Técnicas (Brazilian Association of Technical Standards)

Figure 4.12. 4. 11A and 4.11B. Fig. 4.11A illustrates the machine with the sieves to sift the soil grain and separate them based on their grain size. Fig. 4.11B illustrates the coarse soil on top of the sieves ready to be placed in the machine.

We used one of the samples of the fine grains that was dried in the greenhouse to conduct a sedimentation test. We mixed the fine soil sample with sodium hexametaphosphate (125 ml) and let it rest for 12h. After that, we put the mixed material in the dispersion machine and, using distilled water, we included the remaining soil grains. We mixed the material with the dispersion machine (Figure 4.12A) for 15 minutes. Then, we put the mixed material in a 1000 ml graduated cylinder and completed the mixed material with distilled water until it reached 1000 ml (Figure 4.12B). Covering the opening of the graduated cylinder with a hand, we used a rotational cycle, in which we switched the graduated cylinder from upside down to upright for 30s. We measured the temperature with a thermometer and the density of the mixed material with a hydrometer in a process that took 24h and 12 measurements. After 24h, the mixed material was sifted with a sieve

#200 (0.075mm) and the grains left in the sieve were put in a metal container to dry in the

greenhouse.

Figure 4.13. 4.12A and 4.12B. Fig. 4.12A illustrates the soil dispenser machine that mixed the dry sample soil, sodium hexametaphosphate, and distilled water. Fig. 4.12B illustrates mixed material (muddy color) in the graduated cylinder to measure the density and temperature over 24h.

3.3.1.2 Density

We used one of the dried samples of the fine grains to compute the soil grain density. Using the soil

dispenser machine (Fig. 4.12A), we mixed the soil sample with distilled water for 15 min and put

the mixed material in a Florence flask and plugged it into a vacuum pump (Fig. 4.13A). After the

air was removed, more distilled water was carefully added until it reached 1000 ml. The sample was

weighed (Fig. 4.13B), and the temperature measured. The density of the soil particles was

computed with Equation 4.3.

$$D_p = \frac{M_{dry\ soil}}{[(M_p + water) + (M_{dry\ soil})] - (M_p + water + dry\ soil)} * \frac{1}{D_{water}} \qquad (4.3)$$

66

In which D_p is the density of the soil particles, $M_{dry\ soil}$ is the mass of the dry soil, M_p is the mass of the particles, and D_{water} is the water density.

Figure 4.14. 4.13A and 4.13B. Fig. 4.13A illustrates the air being removed from the mixed material with a vacuum pump. Fig. 4.13B illustrates mixed material being weighed to compute the particle soil density

3.3.2 Shear Stress Test

A shear stress test was performed to compute the values of soil cohesion and angle of internal friction. We collected soil without disturbance from both sites using a hole digger and piece of PVC pipe (see Figs. 4.14A and 4.14B).

Figure 4.15. 4.14A and 4.14B. Fig. 4.14A illustrates the use of the hole digger to take the soil sample using PVC pipe. Fig. 4.14B illustrates soil collected with the PVC pipe.

Each soil sample collected was molded inside the pipe with a square metal box (see Figure 4.15A). After the soil was molded, the squared metal mold was removed, and the soil sample was ready for use (Figure 4.15B). The square metal molds the soil sample (see Figure 4.15B) so it can fit perfectly into the mold for the shear stress test (see Figures 4.16A and 4.16B). For each PVC pipe or soil sample location, three samples were necessary to do the test, applying three different normal stresses. We applied 50 KPa, 100 KPa, and 200 KPa for all four locations. In one of the locations, we were able to do one more soil mold, therefore, we applied an additional normal stress (150 KPa). With the measurement of the shear stress rupture with at least three normal stresses, we can compute the soil cohesion and angle of internal friction.

Figure 4.16. 4.15A, 4.15B, and 4.15C. Fig. 4.15A illustrates soil being molded inside the PVC pipe. Fig. 15B soil molded and ready to be used in the shear stress test. Fig. 4.15C shows the sample after its rupture.

Figure 4.17. Fig. 4.16A and 4.16B. Fig. 4.16A shows location in which the molded soil sample was placed to do the shear stress test. Fig. 4.16B illustrates the shear stress test machine used in this study.

3.4 SHALSTAB

We used SHALSTAB (Shallow Landsliding Stability) model to compute landslide susceptibility, based on the slope stability and hydrological factors (Dietrich & Montgomery, 1998). For the slope stability part, SHALSTAB uses the infinite slope of the Mohr-Coulomb failure law, and for the hydrological part, the steady-state shallow subsurface flow proposed by O'Loughlin in 1986 (Dietrich & Montgomery, 1998). The methodology was developed in 1998 by Dietrich and Montgomery and has been used in several studies with some variation to map shallow landslides (Michel, 2014; Listo & Vieira, 2012; Safaei et al., 2013; Dietrich et al., 2001; Reginatto et al, 2012; Dietrich et al, 1998; Montgomery & Dietrich, 1994; Witt, 2005; Vieira & Ramos, 2015; Zaidan & Fernandes, 2009; Reginatto, 2013; Hare, 2003).

SHALSTAB requires some parameters to run the model, such as wet soil bulk density, soil cohesion, slope angle, flow accumulation, and angle of internal friction. The wet soil bulk density, soil cohesion, and angle of internal friction were obtained from the soil sample collected in the field. Slope angle and flow accumulation were computed using the high-resolution DEM produced with imagery from the UAV flights. The direction of flow accumulation was computed in ArcMap using the high-resolution DEM.

To compute the final map, we coded the equations in R. We used Equations 4.4, 4.5, 4.6, and 4.7. The possible values of Equation 4.5 and the condition of the slope are presented in Table 4.1. The two extreme values in Table 4.1 are represented by Equations 4.6 and 4.7. Equation 4.6 represents $h/z = 0$ (absence of water column), and if the condition in Equation 4.6 is true, the slope is unconditionally unstable (Michel et al., 2014). Equation 4.7 represents the condition in which h/z is equal to one (totally saturated), and if the condition of Equation 4.7 is true, the slope is unconditionally stable (Michel et al., 2014).

$$\frac{Q}{T} = \frac{b}{a} * \sin\theta \left\{ \frac{\rho_s}{\rho_w} * \left(1 - \frac{\tan\theta}{\tan\phi}\right) + \frac{C}{\cos^2\theta * \tan\phi * \rho_w * g * z} \right\} \qquad (4.4)$$

$$\log\left(\frac{Q}{T}\right) \qquad (4.5)$$

$$\tan\theta \ge \tan\phi + \frac{C}{\cos^2\theta * \rho_s * g * z} \qquad (4.6)$$

$$\tan\theta \le \tan\phi * \left(1 - \frac{\rho_w}{\rho_s}\right) + \frac{C}{\cos^2\theta * \rho_s * g * z} \qquad (4.7)$$

These equations use: drainage area (a) [m^2], outflow boundary (b) [m], hillslope angle (θ), wet soil bulk density (ρ_s) [kgm^{-3}], water density (ρ_w) [kgm^{-3}], angle of internal friction (ϕ), soil transmissivity (T) [m^2/day], and the effective precipitation (Q) [m/day], cohesion (C) [kPa] , and gravitational acceleration (g) [m/s^2] (Dietrich & Montgomery, 1998).

Table 4.7. SHALSTAB classes (Source: adapted from Reginatto *et al*., 2012; Michel et al., 2014)

Condition	Stability
$\tan\theta \ge \tan\phi + \dfrac{C}{\cos^2\theta * \rho_s * g * z}$	Unconditionally unstable
$\log\left(\dfrac{Q}{T}\right) < -3.1$	Unconditionally unstable and saturated
$-3.1 < \log\left(\dfrac{Q}{T}\right) < -2.8$	Unstable and saturated
$-2.8 < \log\left(\dfrac{Q}{T}\right) < -2.5$	Unstable and unsaturated
$-2.5 < \log\left(\dfrac{Q}{T}\right) < -2.2$	Stable and unsaturated
$\log\left(\dfrac{Q}{T}\right) < -2.2$	Unconditionally stable and unsaturated
$\tan\theta \le \tan\phi * \left(1 - \dfrac{\rho_w}{\rho_s}\right) + \dfrac{C}{\cos^2\theta * \rho_s * g * z}$	Unconditionally stable

3.5 Factor of Safety

Slope stability can be measured by the factor of safety (FS), which can be computed as the ratio of resisting forces to driving forces illustrated by Equation 4.8 (Selby, 1993; Keller, 2011). The slope is stable when the FS is greater than one (the resisting forces exceed the driving forces). The greater the FS, the greater the stability of the slope. Changes in the local conditions can change the forces, and consequently change the FS (Keller, 2011). For instance, an intense rainfall might change the stability of a stable slope since it can saturate the soil, increasing the pore water pressure, increasing the slope weight, decreasing the resisting force, and decreasing the FS. However, the destabilizing effect of rainfall can be reduced by placing drains into the slope to remove surface and subsurface water and increasing the FS.

$$FS = \frac{sum\ of\ resisting\ forces}{sum\ of\ driving\ forces} \tag{4.8}$$

The factor of safety was computed using Equation 4.8 (Selby, 1993). Equation 4.11 was derived from Equations 4.9 and 4.10, in which Eq. 4.9 is based on the Mohr-Coulomb law, in which, at the moment of failure, the shear stress is equal to the resistance strength caused by cohesion and by the frictional resistance due to the effective normal stress on the failure plane.

$$\tau = C + (\sigma - u)\tan\phi \tag{4.9}$$

$$\rho_s * g * z * \sin\theta * \cos\theta = C + (\rho_s * g * z * \cos^2\theta - \rho_w * g * h * \cos^2\theta) * \tan\phi \tag{4.10}$$

$$FS = \frac{C + (\rho_s * g * z * \cos^2\theta - \rho_w * g * h * \cos^2\theta) * \tan\phi}{\rho_s * g * z * \sin\theta * \cos\theta} \tag{4.11}$$

Here τ is the shear stress (N/m²), C is the cohesion (N/m²), σ is the normal stress (N/m²), u is the pore pressure opposed to the normal load (N/m²), ϕ is the angle of internal friction of the soil

(degree), ρ_s is the soil bulk density (kg/m^3), g is the gravity force (m/s^2), θ is the slope angle, h is the height between the slip plane and the top of the soil, and z is the height of the water column.

Using Equation 11, FS=1 is at balance state; when FS<1, slope failure occurs, and when FS>1, the slope is stable (Michel et al., 2014).

3. Results

3.1 Saturated Hydraulic Conductivity

The saturated hydraulic conductivity was computed to understand the behavior of rainfall in the study sites. All the values measured in the field to compute in situ saturated hydraulic conductivity (K_{sat}) can be found in *Appendix 4.2*.

Both undisturbed and disturbed sites have similar geological formations from *Complexo Embu* (CPRM, 2019). Therefore, some similarities in the K_{sat} would be expected in natural conditions. Table 4.2 illustrates values of K_{sat} computed in each of the locations for the undisturbed site (see Figure 4.4). The mean K_{sat} is 19.80 mm/h (SD=12.12 mm/h). The location N5 has a higher K_{sat} value than at all other locations, and can be considered an outlier since all the other locations are in the range between 10 to 20 mm/h. Therefore, K_{sat} in the undisturbed site is overall spatially homogeneous.

Table 4.8. K_{sat} computed for each of the specific locations of the undisturbed site

Location	K_{sat} (mm/h)
N1	12.47
N2	18.14
N3	16.15
N4	11.30
N5	40.91
Site Mean	*19.80*
Site SD	*12.12*
Sites Mean without outlier N5	*14.52*
Sites SD without outlier N5	*3.18*

Table 4.3 illustrates K_{sat} at each location from the disturbed site (see Fig. 4.3). The mean K_{sat} is 138.15 mm/h (SD=266.94 mm/h). In this site, A5 has an extremely high K_{sat} (679.95 mm/h), and it is an outlier. Still, the mean K_{sat} without outlier A5 is six times smaller than the lowest value at location A1 and 2.5 times higher than the highest K_{sat} value at location A3. Therefore, K_{sat} is very heterogeneous, having very low to very high values in this site.

Table 4.9. K_{sat} computed for each location for the Disturbed Site

Location	K_{sat} (mm/h)
A1	4.79
A2	8.47
A3	76.40
A4	49.19
A5	679.95
A6	10.11
Site Mean	*138.15*
Site SD	*266.94*
Site Mean without outlier A5	*29.79*
Site SD without outlier A5	*31.68*

3.2 Soil Analysis

3.2.1 Granulometric Structure of Soil and Soil Texture Classification

Soil texture classification correlates with values found for K_{sat}, cohesion and angle of internal friction. Therefore, particle size analysis was performed on the soil samples collected in the field to identify the texture class of the soils (see Tables 4.4 and 4.5). *Appendix 4.3* contains the details of the percentage of each particle size in each location of the study sites. In the undisturbed site, all locations are clay loam, but N3 is a sandy clay loam. Moreover, N3 is also clay loam. In the disturbed site, there is more variability in the soil texture since five locations are some type of loam (silt loam, loam, or clay loam), and one location is sandy clay.

A1 and A4 are loam, A2 and A5 are silt loam, A3 is sandy clay, and A6 is clay loam. Therefore, soil texture classes for the undisturbed site are more homogeneous than in the disturbed site.

Table 4.10. Soil texture for each location at the undisturbed site

Location	Clay (%)	Silt (%)	Fine sand (%)	Medium sand (%)	Coarse sand (%)	Soil Texture
N1	18.26	20.35	16.75	1.40	22.57	sandy clay loam
N2	23.25	18.87	17.68	1.51	21.18	sandy clay loam
N3	33.45	25.03	21.46	1.59	13.33	clay loam
N4	33.65	14.52	24.45	5.05	15.63	sandy clay loam
N5	24.32	13.10	13.35	1.72	24.90	sandy clay loam

Table 4.11. Soil texture for each location at the disturbed site

Location	Clay (%)	Silt (%)	Fine sand (%)	Medium sand (%)	Coarse sand (%)	Soil Texture
A1	18.03	49.70	27.49	1.65	2.64	loam
A2	14.36	55.59	24.36	1.68	3.74	silt loam
A3	35.53	11.59	15.91	0.60	36.12	sandy clay
A4	13.60	36.12	23.29	0.08	10.67	loam
A5	7.15	47.47	19.71	1.05	7.50	silt loam
A6	37.60	31.70	21.72	0.75	5.13	clay loam

3.2.2 Shear Stress Test

75

The Shear Stress Test was conducted to compute values of soil cohesion (C) and angle of internal friction (ϕ). These two variables are essential for the spatial distribution of the slope stability using SHALSTAB and Factor of Safety. The procedure requires at least three undisturbed soil samples from each location. In each of these samples, a different normal stress force is applied (usually 50, 100, and 200 kPa) to find the shear peak for each of the normal stresses. These values are used to plot a best fit line to find the linear equation that computes C and ϕ. We collected two random samples in the locations in which we conducted the in situ-hydraulic saturated conductivity. These locations were the ones in which the soil collected in the field was enough to get three undisturbed samples. Additionally, samples collected in the undisturbed sites were classified as NA and NB since we cannot match these locations with the locations of the saturated-hydraulic conductivity. After collecting the sample, GPS information of these two locations was lost due to mechanical failure of the GPS device.

Figure 4.17 plots shear stress peaks versus normal stress. In the plot, the best fit line was adjusted to intersect x and y at the origin (0, 0), so the equation resulting from the line would have cohesion be zero and not negative, since negative soil cohesion is not possible. The Equation for A3 is $y = 1.41x$ ($R^2=0.81$). Therefore, C is equal to zero and ϕ is equal to 54.68°.
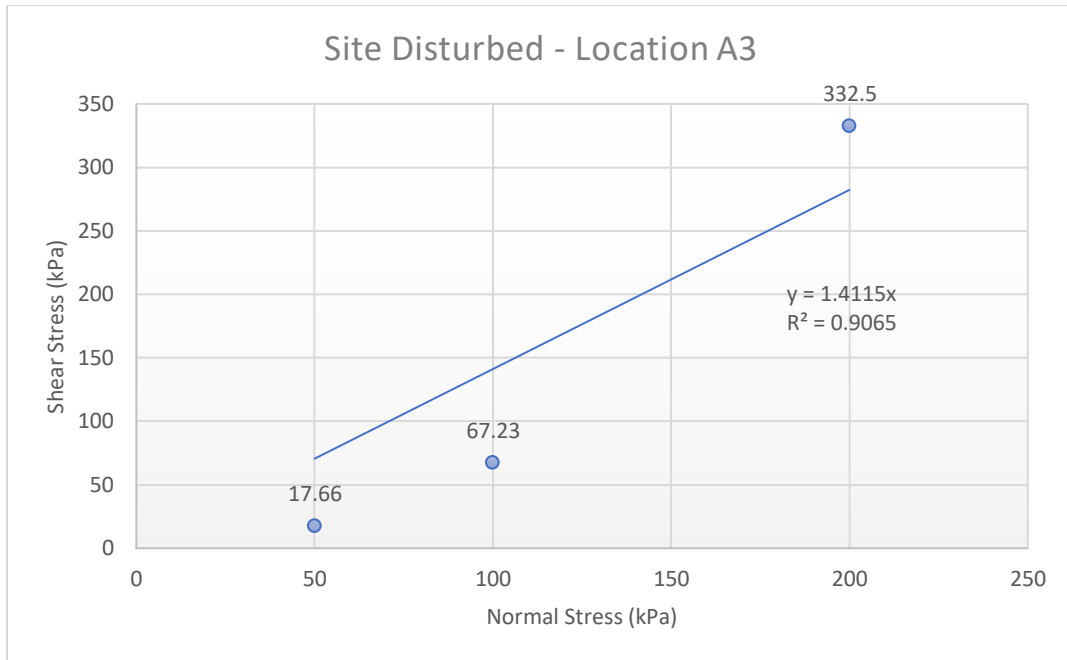
Figure 4.18. Shear Stress Peak versus Normal Stress for location 3 at the disturbed site. In this plot, the line to build linear equation was adjusted to cross x, y at the origin (0,0), so soil cohesion would not be negative, which is not possible.

The values to compute *C* and ϕ for location A6 in the disturbed site were computed with the linear equation from the best fit line of the shear peaks (see Figure 4.18). Since *C* was positive, the best fit line did not have to be adjusted to cross the intersection. Using the equation *y = 0.33x+ 2.88* (R^2=0.95), we found the value of *C*= 2.88 kPa and ϕ = 18.19º.
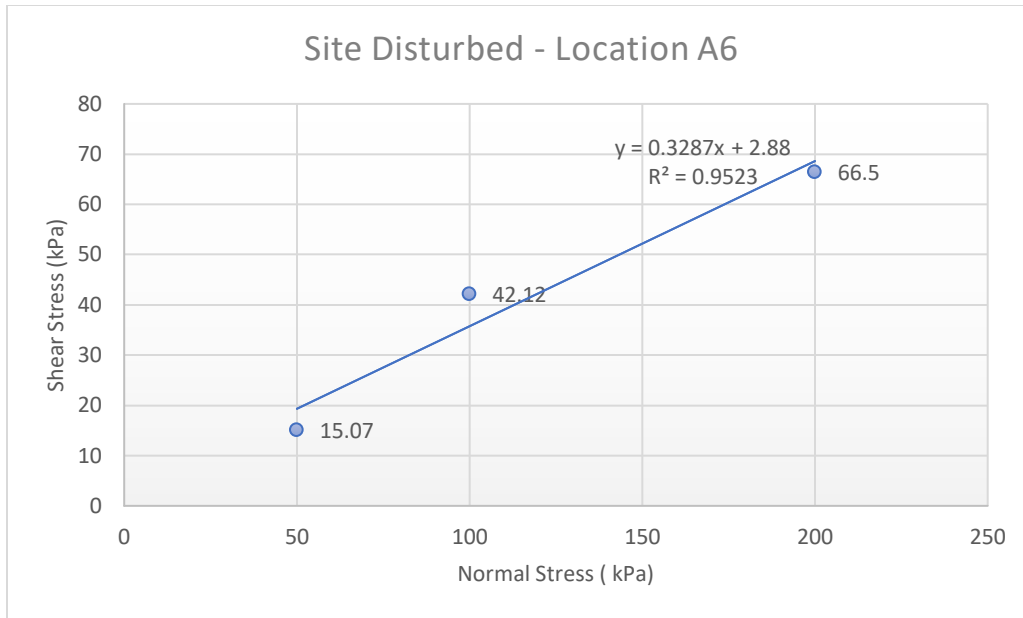
Figure 4.19. Shear Stress Peak versus Normal Stress for location A6 at the disturbed site.

The angles of internal friction at locations A3 and A6 are very different from each other, which could be related to the variability of composition of the soil in this site. The variability of composition is a result of a previous landslide and landfill dumping in at least two different periods as described by local resident who lives near the hillslope. Moreover, a very high ϕ, such as 54.68º, is not an expected value for ϕ.

Figures 4.19 and 4.20 illustrate plots to compute C and ϕ at the undisturbed site. The best fit line of the plot from Figure 4.19 had to be adjusted slightly to intercept the origin; however, R^2 was still very high (R^2=0.97). The linear equation computed with the shear stress peaks for each normal stress force is y = 0.6253x. In this location (NA), the computed C is equal to zero and ϕ is equal to 32.02 º. For location NB, the line of best fit for the plot in Figure 4.20 resulted in the equation y = 0.23x + 4.07 (R^2=0.99). Therefore, C is equal to 4.07 kPa, and ϕ is equal to 13.02 º.
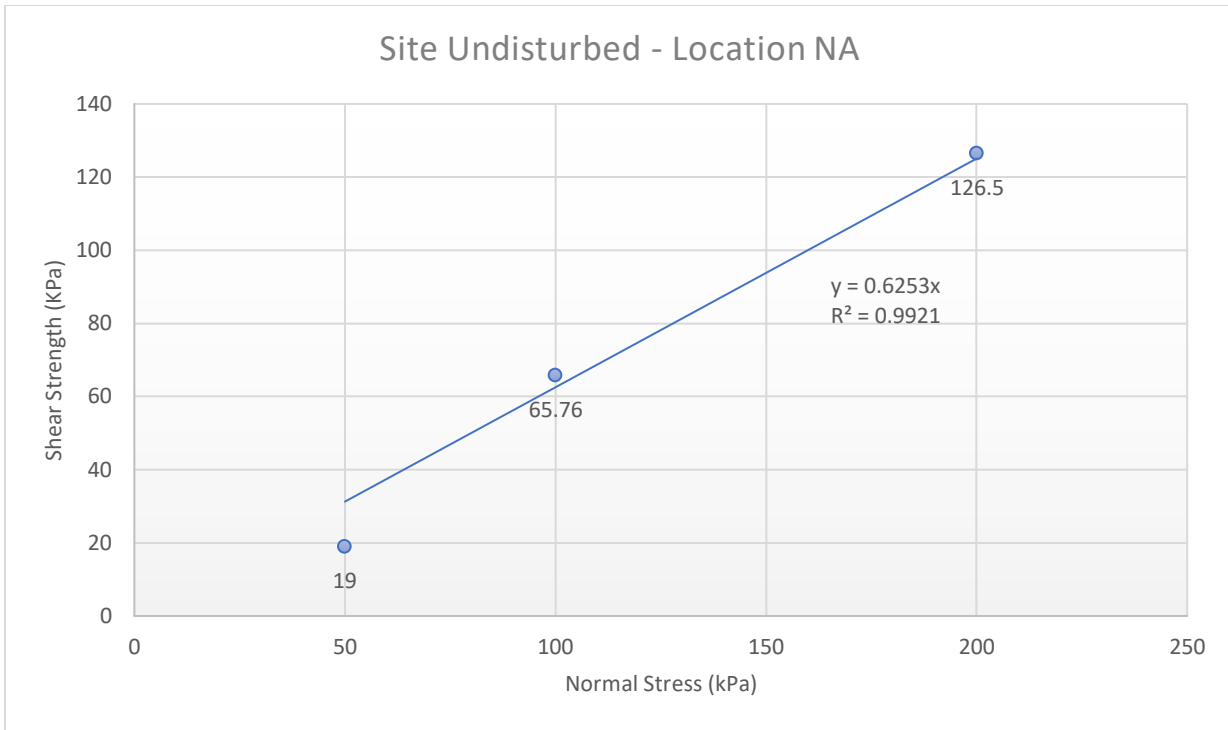
Figure 4.20. Shear Stress Peak versus Normal Stress for location NA at the undisturbed site. In this plot, the line to build equation was slightly adjusted to cross x,y at the origin (0,0), so soil cohesion would not be negative.
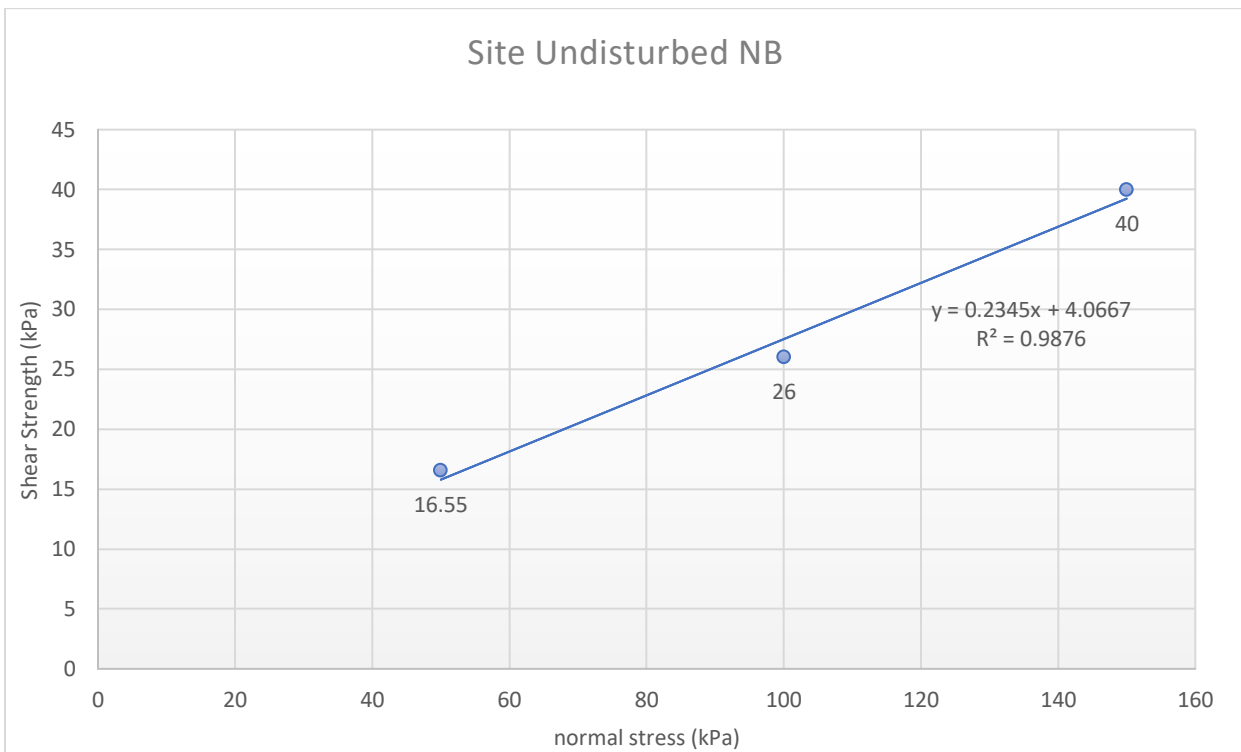
Figure 4.21. Shear Stress Peak versus Normal Stress for location NB at the undisturbed site.

3.3 SHALSTAB

The susceptibility to landslide in the disturbed and undisturbed sites was analyzed using

SHALSTAB. Areas more susceptible to landslides have slopes that are less stable, and slopes that

are more stable are less likely to trigger landslides. The SHALSTAB function was run in R, with

the dataset collected in the field and computed in the lab. We used the drone flight DEM, the wet

bulk density, C, and the ϕ computed in the lab (see values in Table 4.6).

Table 4.12. Values of variables computed by lab analysis necessary to run SHALSTAB

Location	A3	A6	NA	NB	Average Undisturbed
Soil Cohesion (kNm^2)	0	2.88	0	4.07	2.04
Angle of Internal Friction (degree)	54.68	18.19	32.60	13.20	22.90
Wet Soil Bulk Density (kg/m^3)	1720	1720	1534	1534	1534

The slope stability distribution in the undisturbed site using different soil cohesion and angle of

internal friction did not present great variability. We used the C and ϕ from location NA, NB, and

Average Undisturbed (see Table 4.6) to plot three different maps with the spatial distribution of the

slope stability (see Fig. 4.21A, 4.21B, and 4.21C). Figure 4.21A is the more stable map of the three

(less dark green areas). However, the spatial distribution of the slope stability does not change that

much between the three spatial analyses. Figure 4.21B is slightly less stable than Figure 4.21A, and

Figure 4.21C is slightly less stable than Figures 4.21A and 4.21B.
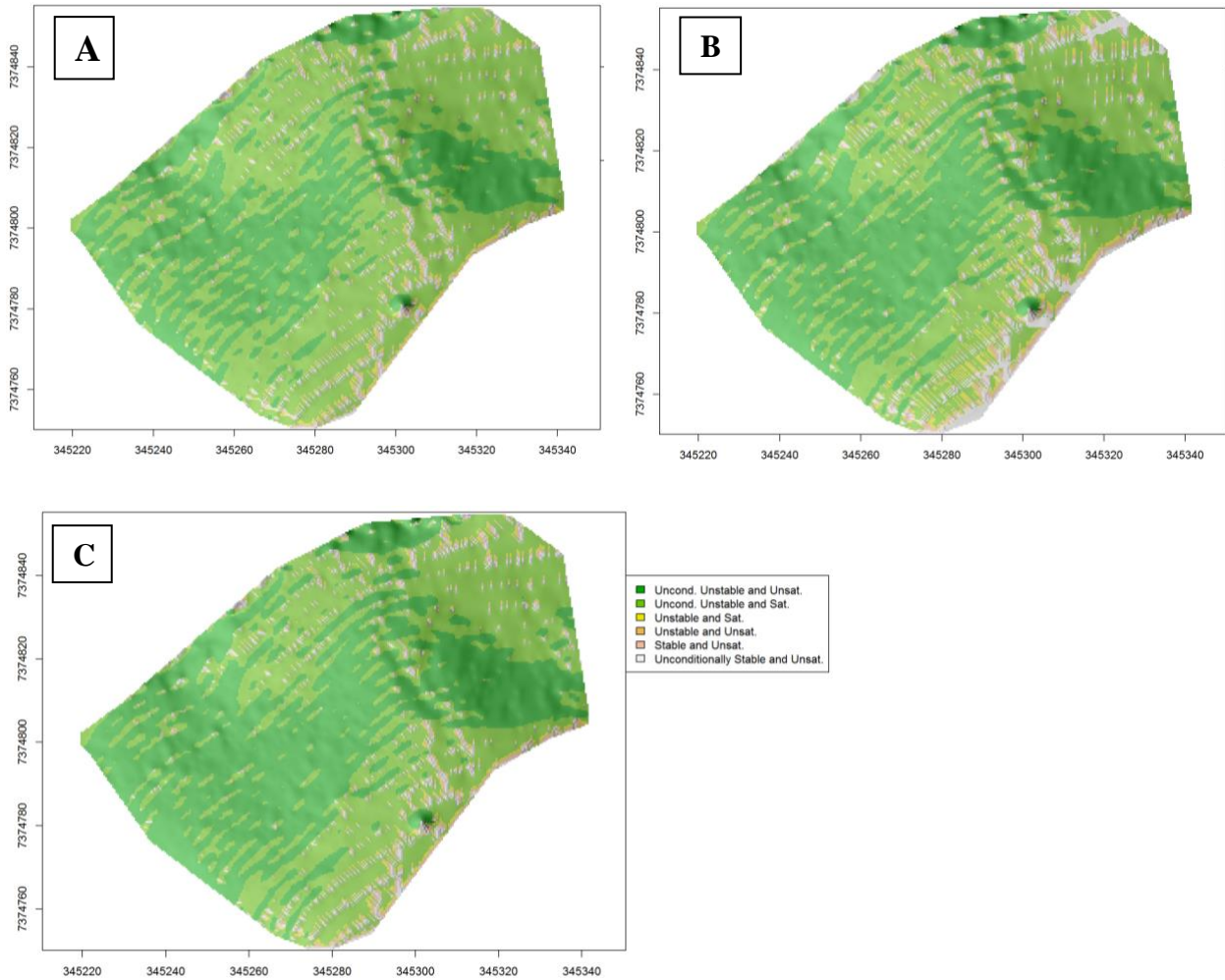
Figure 4.21. 4.21A, 4.21B, and 4.21C. Spatial analysis of slope stability using SHALSTAB from the undisturbed site. Fig. 4.21A computed with C=0, and ϕ=32.60. Fig. 4.21B computed with C=4, and ϕ=13.2. Fig. 4.21C computed with average values of the undisturbed site (C=2.04, and ϕ=22.9). The dark green in the plots are fewer stable areas, and the pink and white areas are the more stable ones.

Variation in the value of cohesion and angle of internal friction can cause great variability in the spatial distribution of the slope stability using SHALSTAB. We notice this variability in Fig. 4.22A and 4.22B. The slope stability distribution of Fig. 4.22A illustrates a more stable hillslope (mainly white, pink, and light green ramifications). The map from Fig. 4.22A was produced using cohesion and angle of internal friction from location A3 (see Table 4.6). However, when using

81

values of location A6, we observed a less stable hillslope (Fig. 4.22B) with more dark green areas (unconditionally unstable and unsaturated) and fewer white and pink areas when compared with Fig. 4.22A.
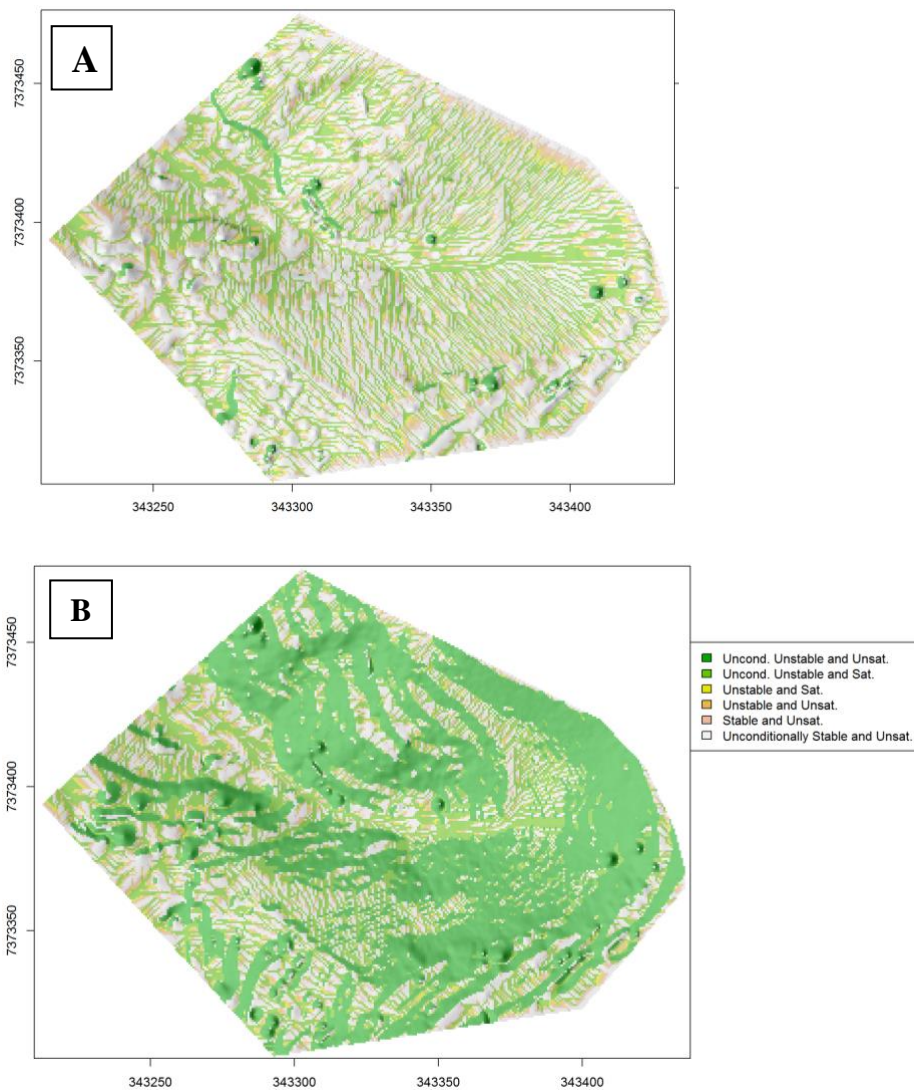
Figure 4.22. 4.22A and 4.22B. Spatial Analysis from disturbed site. Fig. 4.22A computed with C=0, and ϕ=54.68. Fig. 4.22B computed with C=3.5, and ϕ=17.37. The light green in both plots shows areas that are Unconditionally Unstable and Saturated, and the pink and white areas illustrate more stable areas. There is a clear difference between areas that are Uncond. Unstable and Sat. and Uncond. Stable and Unsat. in both plots. Based on the spatial analysis, Fig. 4.22B is less stable than Fig. 4.22A.

Observing both spatial analyses from the disturbed and undisturbed sites, we can conclude that both C and ϕ play an important role in determining the stability of the slope. In addition, the

changes in the terrain, such as cut and fillings, seems to result in a less continuous hillslope, as can

be observed by the small ramifications in the undisturbed site and not present in the disturbed site.

Moreover, variability in these parameters can produce distinct slope stability distribution (as

observed in the undisturbed site).

3.4 Factor of safety

The Factor of Safety (FS) uses a combination of parameters (see Eq. 4.11) to indicate if a slope is

stable (FS >1), unstable (FS<1), or at balance state (FS=1). In this section, using parameters from

undisturbed and disturbed sites, we illustrate, by plotting the FS, the height of water column

necessary to make the slope angle unstable in each of the sites.

Hillslopes have an average slope angle, but they present spatial variability in the slope angle

(see Fig. 4.23A and B). Therefore, the slope stability also will present slope variability in the same

hillslope. Additionally, slope angles in the undisturbed site are more homogeneous and clustered

than in the disturbed site. In the undisturbed and the disturbed sites, the angle categories between

17.01° and 30°, and between 30.01° and 60° are predominant in the hillslope (see Table 4.7).
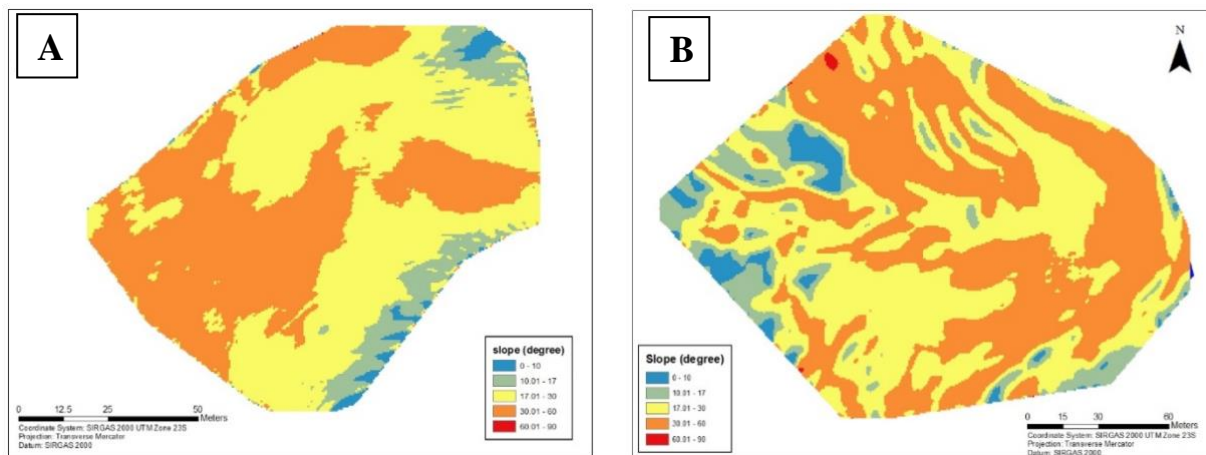
Figure 4.23. 4.23A and 4.23B. Slope angle categories. Fig. 4.23A illustrates the slope angle categories in the undisturbed site, and Fig. 23B illustrates the slope angle categories the disturbed site. Both Fig. 4.23A and 4.23B, the angle categories 17.01°-30°(orange) and 30.01°-60° (yellow) categories are the most common in the hillslope.

Table 4.13. Percentage of each slope angle category in the undisturbed and disturbed sites. In both disturbed and disturbed sites more than 40% of the hillslope has angle higher than 30 degrees.

Slope angle (degree)	Undisturbed site (%)	Disturbed site (%)
0-10	1.69	3.28
10.01-17	7.76	9.07
17.01-30	48.21	42.02
30.01-60	42.32	45.49
60.01-90	0	0

The slope angle plays an important role in the SF in both sites. In the undisturbed site, slope angles higher than 30.01° are unstable. However, slopes start to become unstable at lower angles, like the example of 17°. Figures 4.24 A, B, and C illustrate different slope angles (10°, 17°, and 30°) and how FS changes with the water column. Important to notice is that the maximum water column for the undisturbed site is 1 m, but in the plots, there are values higher than 1 m and negative values for the water column. These values are input in the plots to illustrate continuity, but they do not represent what would be observed in the site. In the slope angle equal to 17°, the threshold at which the slope becomes unstable is 0.76 m (or 76%). At that height, FS is equal to 1, and when the water column is higher than 0.76, the slope is unstable. For 10°, slope is stable for all heights of the water column, and for 30°, slope is unstable even when the soil is nearly dry.

84
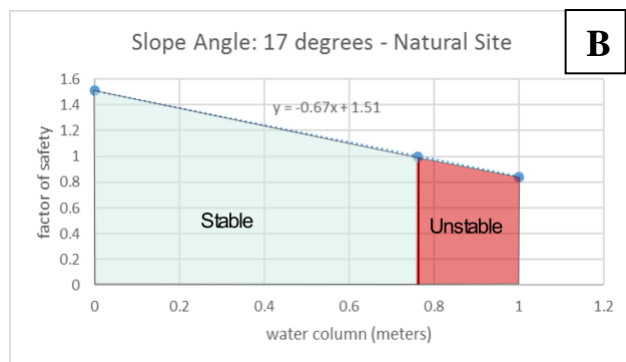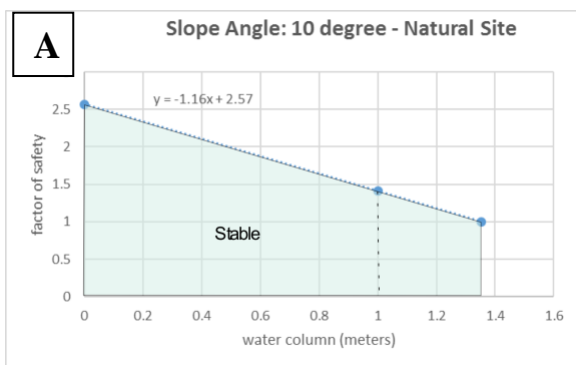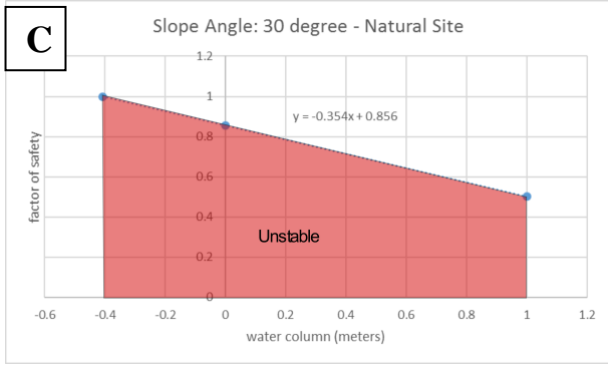
Figure 4.24. 4.24A, 4.24B, 4.24C. Factor of Safety illustrated by different slope angle and water column height at the undisturbed site. Figure 4.24A illustrates the factor of safety for slope angle of 10°. For that angle, slope is stable for all heights of the water column. Figure 4.24B illustrates the factor of safety for slope angle of 17°. For that angle, slope is stable until 0.76m and after that it becomes unstable. Figure 4.24C illustrates the factor of safety for slope angle of 30°. For that angle, slope is unstable for all height of the water column.

In the disturbed site, a slope angle equal to 30.01° is unstable when the water column is higher than 0.06 m. Figures 4.25 A, B, and C illustrate different slope angles (10°, 17°, and 20°) and how FS changes with the water column. For slope angles equal to 10° and 17°, the slope is stable for all heights of the water column. Therefore, when keeping the slope angle constant, the undisturbed site is less stable than the disturbed site. Thus, C and ϕ are the variables responsible for the undisturbed site being less stable than the disturbed site.
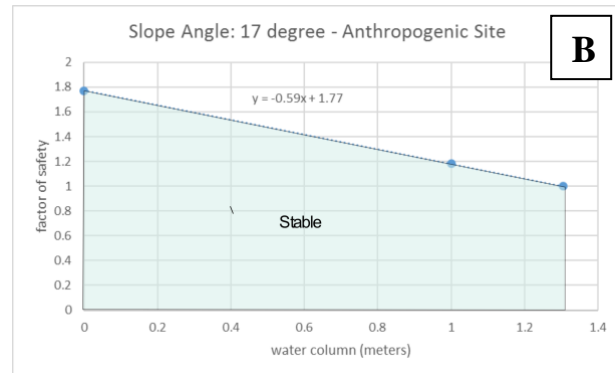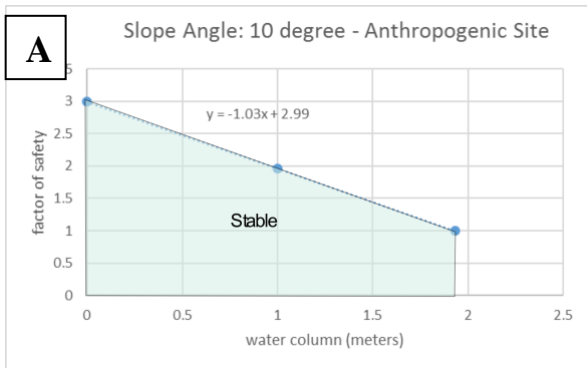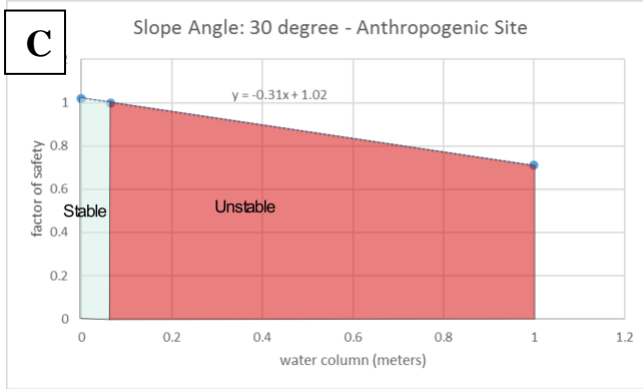
Figure 4.25. 4.25A, 4.25B, 4.25C. Factor of safety illustrated by different slope angle and height of water column at the disturbed site. Figure 4.25A illustrates the factor of safety for slope angle of 10°. For that angle, slope is stable for all heights of the water column. Figure 4.25B illustrates the factor of safety for slope angle of 17°. For that angle, slope is stable for all heights of the water column. Figure 4.25C illustrates the factor of safety for slope angle of 30°. For that angle, slope is unstable for water column higher than 0.06m.

3.5 Sensitivity

Soil sensitivity can illustrate the loss of strength and structure of a soil that has being disturbed. Therefore, soil with less internal strength would be more susceptible to landslides. Therefore, testing for soil sensitivity can illustrate the change in strength between the undisturbed and disturbed sites.

Soil sensitivity is the ratio between the shear stress peak of the undisturbed soil by the disturbed (Terzaghi et al., 1996; Abuhajar et al., 2010), and it can be illustrated by the following equation (Eq. 4.12). Soil sensitivity is normal for values between 1-4, sensitive for values between 4-8, extra-sensitive for values between 9-15, and quick for values higher than 15.

$$Soil\ Sensitivity = \frac{\tau_{peak_{undisturbed}}}{\tau_{peak_{disturbed}}} \tag{4.12}$$

Table 4.14. Soil Sensitivity Computed with Shear Peak of Disturbed and Undisturbed Sites

Normal Stress	Shear Peak Undisturbed		Shear Peak Disturbed	Soil Sensitivity

kPa	kPa		kPa	
50	18.01		15.07	1.20
100	46.105		42.12	1.09
200	148.815		66.5	2.24

Using shear peak of the undisturbed and disturbed sites, we computed the soil sensitivity for each normal stress, using the shear peak obtained in the Shear Stress Test. We observed that, contrary from what would be expected, soil sensitivity is normal for all normal stresses since all values computed are between 1 and 4 (see Table 4.8).

5. Discussion

Previous studies in landslide susceptibility focused on slopes with natural hillslopes (Van Westen et al., 2003; Marjanović et al., 2011; Thiery et al., 2007; Ermini & Casagli, 2005) or larger areas with a combination of urban and natural areas (Feizizadeh & Blaschke, 2013; Süzen & Doyuran, 2004; Jäger & Wieczorek, 1994), and some studies discuss human actions (Xu et al., 2019; Jaboyedoff et al., 2016). Less common are landslide susceptibility studies on informal settlements (*favelas*, also known as slums) or studies comparing disturbed with undisturbed sites. By comparing the saturated-hydraulic conductivity of both sites, it is clear that the soil behavior of these disturbed sites is not predictable or homogeneous, which makes it harder to predict their safety and future behavior. In addition, these disturbed sites are frequently changing as new loads of construction materials and soil are dumped in the terrain. Therefore, this study contributes to the broad field of landslide susceptibility, addressing an urban environment that is common in many of the larger cities in developing countries, the *favelas* (slums). Moreover, it gives clues to the impact of these

informal settlements on the slope stability and provides evidence of the importance of

municipalities to manage these areas and relocate residents to safer areas whenever possible.

5.1 Saturated Hydraulic Conductivity

Even though both disturbed and undisturbed sites have similar geological formations with schist

and locally migmatite schist from Complexo Embu (CPRM, 2019) and similar soil texture (see

Tables 4.4 and 4.5), the values of K_{sat} computed for the disturbed site have more variability than

those at the undisturbed site (see Tables 4.2 and 4.3). This extreme variability can be explained by

the anthropogenic interference and variability of material input in the terrain. Over time, different

materials were input into the site artificially by humans, such as pieces of construction material and

the remains of garbage, and the soil was cut and filled for building construction. In the hillslope of

the disturbed site, houses were built previously and later removed due to a shallow landslide.

Therefore, the soil has a mix of soil with other materials and can be classified as a Technosol (FAO,

2006). This variability in the K_{sat} demonstrates how the hydraulic conductivity behavior of soil in

these disturbed sites is challenging to predict, which makes the slope stability harder to measure

since each part of the slope has its own behavior, based on material inputted over time.

In the disturbed site, there is no correlation between K_{sat} and soil texture. For instance,

locations A2 and A5 are both silt-loam soils, and their K_{sat} values are not similar at all (8.47 mm/h

and 679.95 mm/h, respectively); or, A1 and A4 are both sand-loam soils but also have high K_{sat}

variability (4.79 mm/h and 49.19 mm/h). Moreover, a sand-loam soil texture would be expected to

have higher K_{sat} than a silt-loam soil texture since it has a higher proportion of sand, but this

behavior is not observed in site A5. However, A5 might be an outlier since K_{sat} is extremely high

when compared with all other values of K_{sat} for the same site. The variability of K_{sat} in the disturbed

site can be explained by the variability of the material input by human activities over time in each location. Materials input are different, and they were input at different times; therefore, the Technosols are not the same in the locations of the disturbed site.

The mean K_{sat} of the disturbed and undisturbed sites are not similar, which would be expected, based on the presence of the Technosols in the disturbed site. In the disturbed site, mean K_{sat} was almost seven times higher than the undisturbed site (138.15 mm/h and 19.80 mm/h, respectively). Thus, the rainfall percolates the soil faster in the disturbed site since the soil is more permeable. However, even though the mean K_{sat} in the disturbed site is 138.15 mm/h, there is great variability between locations (SD=266.94 mm/h and Range=675.16 mm/h).

5.2 Soil Analysis

The variability in the disturbed site also was observed in the values computed in the lab for ϕ (54.68° and 18.19°), which again illustrates how variable are the soils in the same slope. In addition to the variability, when we computed the slope stability using SHALSTAB and Factor of Safety, we concluded that the disturbed site is a more stable slope than the undisturbed site. In this matter, for future research it would be relevant to compute stability with a model that accounts for saturated-hydraulic conductivity to compare the results.

5.3 SHALSTAB

The accessibility of high-resolution data has become easier, but studies should consider the scale of their study area to define which raster resolution is most appropriate for the analysis. The analysis of slope stability using SHALSTAB was done at a large scale and choosing the correct resolution to conduct the analysis was essential for presenting the results in the final map. When running the

analyses, contrary to expectations, the very fine raster (4 cm) did not present a good visual map and

showed discontinuities, which made it harder to interpret the map (see Fig. 4.26A). Also, using a

coarser raster (1 m) would not be the best representation of the area. In this map, the pixels are

visible, which resulted in a less smooth map (Fig. 4.26C), and a very coarse raster (30 m) resulted

in a map with no data (Fig. 4.26D) since flow accumulation was equal to zero (see *Appendix 4.5* for

the DEM and Flow Accumulation raster used in the four analyses). Based on the visual information

of these maps, we concluded that a raster with a pixel resolution between 0.5m - 0.6m would

produce a better visual map (Fig. 4.26 B).
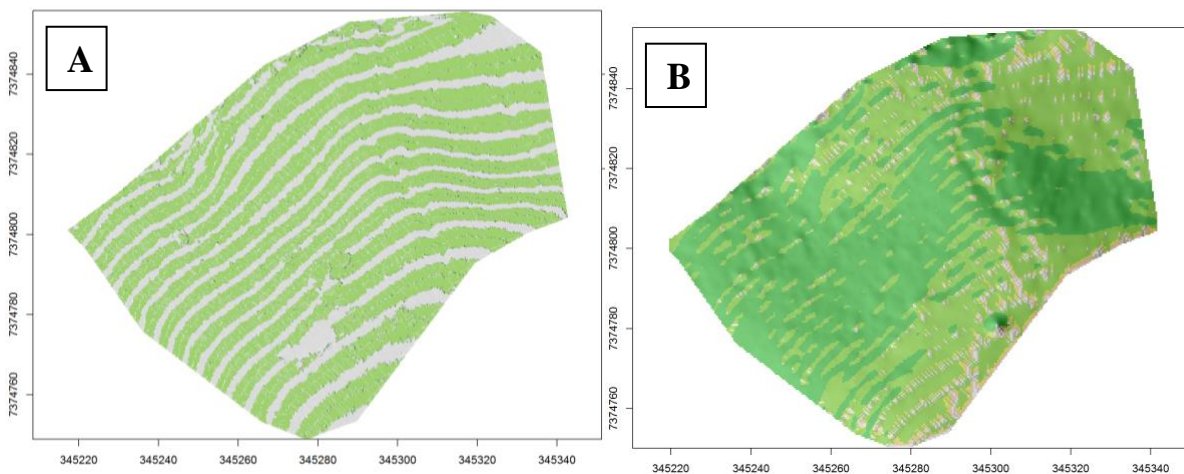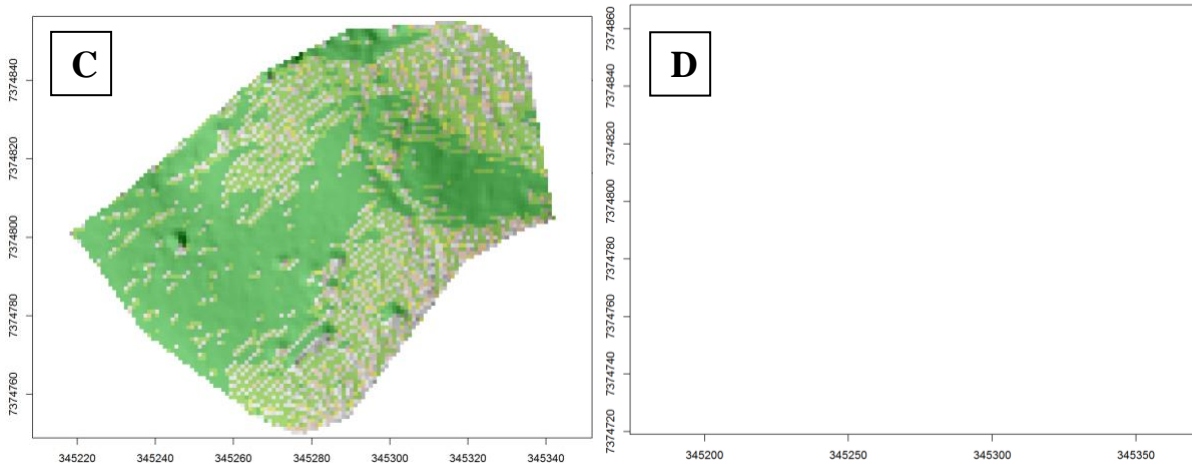
Figure 4.26. 4.26A, 4.26B, 4.26C, and 4.26D. Slope stability computed with different pixel resolution. Fig. 4.26A was computed with the original data collected from the drone with 4cm pixel resolution. Fig. 4.26B was computed with a 0.5m pixel resolution. Fig. 4.26C was computed with 1m pixel resolution. Fig. 4.26D was computed with 30m pixel resolution. Notice how Fig. 4.26A seems to follow the elevation contour line and Fig. 4.26C is coarse when compared with Fig. 4.26A and Fig. 4.26B. Fig. 4.26D pixels were so coarse that could not produce a map that would represent the study area. Therefore, Fig. 4.26B illustrates the study area better.

In accordance with the saturated-hydraulic conductivity results, the values of soil cohesion and angle internal friction computed in the lab for the disturbed and undisturbed illustrate the variability of the soil behavior in the disturbed site when compared with the undisturbed site. In each site, two soil samples were collected in two locations. For each location, soil cohesion and angle of internal friction were computed. The two maps produced using the values of each location in the disturbed site produced very distinct slope stability maps (see Figs. 4.21A and B), but this was not observed in the slope stability maps of the undisturbed site (see Figs. 4.20A and 4.20B).

5.5 Factor of Safety

Contrary to what would be expected, in the same slope angle, the disturbed site is more stable (see Figs. 4.22B and 4.23B and Figs. 4.22C and 4.23C). The Factor of Safety was computed with Eq. 4.11, and the equation does not include saturated-hydraulic conductivity. Therefore, for future

91

studies in disturbed sites, it would be interesting to use an equation that uses the saturated-hydrologic conductivity to understand its impact on the stability of the slope.

5.6 Sensitivity

Values computed for soil sensitivity are normal, which indicates that the loss of strength and structure of the soil in the disturbed site is not a significant factor in their landslide risk.

6. Conclusion

The undisturbed site is overall less stable than the disturbed site when using SHALSTAB and Factory of Safety. However, the soil in the disturbed site is less homogeneous than the undisturbed site, and it can be classified as Technosol. The variability in the soil of the disturbed site was observed by the variability in the saturated-hydraulic conductivity and in the values computed for the angle of internal friction. Moreover, saturated-hydraulic conductivity in the disturbed site shows great variability between locations (Mean= 138.15 mm/h, SD=266.94 mm/h, and Range=675.16 mm/h). In contrast, the undisturbed site has more homogeneous saturated-hydraulic conductivity (Mean= 19.80 mm/h, SD=12.12 mm/h, and Range=29.61 mm/h). Even though the disturbed and undisturbed sites have similar geological formations, we observed the saturated-hydraulic conductivity in the disturbed site to be almost seven times higher than in the undisturbed site. Therefore, saturated-hydraulic conductivity in the disturbed and undisturbed sites are not similar.

While by using SHALSTAB and Factor of Safety, the undisturbed site seems to be more susceptible to shallow landslides than the disturbed site, we would recommend additional studies, using models that take into consideration saturated-hydraulic conductivity in order to compare the results. Moreover, the variability presented in the disturbed site makes monitoring the shallow

landslide risk harder, since each area of the same hillslope does not present the same soil characteristics. Furthermore, informal areas in the urban areas of Brazil have similar urban settings as the one observed in the disturbed site, and this type of soil is very unstable and heterogenous, not being the best location for people to build their houses. As people build, relocate, and rebuild, the soil keeps being altered. Therefore, to prevent natural disasters in these urban hillslopes, municipalities should monitor these areas, not allow new informal buildings, and educate residents about the negative consequences of human activities in these hillslopes, such as discarding garbage and sewage or cut and filling.

CHAPTER 5: The Importance of space, time, and type of natural hazard in assessing vulnerability: Lessons from the 2018 Montecito Debris Flows, CA

Abstract

More communities around the world are living in natural hazard risk-prone areas. These risk-prone areas are susceptible to natural disasters, which can be prevented by adopting Disaster Risk Reduction (DRR) measures. Understanding what makes the community vulnerable and who are the most vulnerable people in the community is one of the DRR measures. However, vulnerability assessments have historically failed to incorporate the spatial and temporal dimensions of vulnerability by type of natural hazard. In 2018, the Montecito community in Southern California was heavily impacted by debris flows, resulting in material and human losses. In this study, we use the case of Montecito and a mixed-methods approach to highlight the importance of the spatial and temporal dimensions of vulnerability. Our results showed that informal workers and residents of voluntary areas were the most vulnerable people in the community. The main aspect that made the community vulnerable was the lack of understanding of their risk and the lack of proactive action, like education the community, by the local authorities. Local authorities failed to use historical and local data to educate the community of their risk and by using problematic evacuation map based on previous wildfire.

1. Introduction

> *"Even when they said the rains were coming, you don't expect a mountain to come down." (Respondent 04)*

Natural hazard events impact communities negatively around the world. For instance, hurricanes in the United States and Central America or landslides in South America. The increase in negative impacts in these communities is linked to the increase of population and, consequently, more people living in at-risk areas.

There are multiple ways to assess risk. The framework we are using to understand risk is a combination of the hazardous events and vulnerability (Maskrey, 1989; Wisner et al., 2003). Hazardous events will continue to be hazardous, but a better assessment of the vulnerability can prevent disasters by building stronger and more resilient communities. In that matter, local governments have an essential role in their communities in preventing and reducing negative impacts of possible hazardous events by adopting Disaster Risk Reduction (DRR) measures.

Vulnerability assessment is part of DRR measures. A good vulnerability assessment should consider all members of the community, the local particularities, and the local dynamics. Broad quantitative assessments of vulnerability consider the spatial extent of the community but do not take into consideration the local heterogeneity as they use same variables in their regional or national assessments. Using the same variables to assess vulnerability nationwide or even at a county-level can help understand general vulnerability patterns but not specific aspects of the community, which can be influenced by cultural and local dynamics. Therefore, quantitative and qualitative assessments targeting the local community can tell a better story about a community's vulnerability. Furthermore, broad vulnerability assessments, especially those in the developed countries, commonly have no tools with which to include the marginalized population within the community, and these are usually the most vulnerable people (Wisner, 1998), for instance, the homeless during the Tokyo earthquake (Wisner, 1998) or informal workers during a wildfire (Thomas fire) in Ventura and Santa Barbara Counties, California. Not including the marginalized

populations keeps the cycle in which the marginalized people continue to be marginalized; even if they survive the natural disaster, they do not recover their livelihoods (Wisner & Luce, 1993) and become even more vulnerable.

In this study, we used lessons learned from the 2018 Montecito debris flows to illustrate the importance of using qualitative and quantitative data to explore the spatial, temporal, and type of natural hazards to understand the vulnerability of a community. In this study, we do not aim to assess the vulnerability, but we aim to point out how a mixed-methods approach can enhance the understanding of local characteristics that contribute to increasing the community vulnerability. Considering Montecito and the 2018 debris flows, we want to answer the following research questions: 1) Who are the most vulnerable people in the community? 2) What are the characteristics of the community that made it more vulnerable? We used a parallel mixed-method approach to explore in-depth the particularities of the local community and to develop a case study by using a survey, one-on-one interviews, local news, and records of community meetings.

2. Background

2.1 Natural hazard, vulnerability, and risk

Natural hazards referred to natural events that threaten things that are important for human (Keller & DeVecchio, 2016; Hyndaman & Hyndman, 2012). Therefore, if a landslide occurs, but it does not affect things that are important for human, it is a natural event, not a natural hazard (Keller & DeVecchio, 2016). The vulnerability is defined as the condition of a community that makes it more susceptible to the impacts of a natural hazard (UNDRR, 2017). The combination of both natural hazards and vulnerability creates the risk (Maskrey, 1989; Wisner et al., 2003).

Figure 5.22. Risk as a combination of hazard and vulnerability of the community

Disaster studies, in the past, have prioritized the assessment of natural hazards over vulnerability, and if they do include vulnerability, it was only the vulnerability of infrastructure and number of people and not the community socioeconomic characteristics (i.e., Mejianavarro et al., 1994). Recently, more risk and vulnerability studies have included the socioeconomic aspects of the community (e.g., Maskrey, 1989; Flanagan et al., 2011; Cutter et al., 2003; Cardozo et al., 2019; Frigerio et al., 2018). However, most of these studies have considered vulnerability as the same for all types of natural hazards. This assumption is problematic since natural hazards have singular characteristics, as well as their impact in the community. They vary in size and how they impact. For instance, a shallow landslide is usually local, while a hurricane is regional. In terms of impact, floods impact low and flat areas and, frequently, can damage but not destroy buildings, but debris flows are faster and typically less predictable and can easily destroy buildings in the path of the flow.

Natural hazards and vulnerability are interconnected. They occur in the same spatial location, and the impact in the community will depend on the intensity and type of natural hazard and the vulnerability of the community. Therefore, understanding their interconnection or studying them together can enrich the assessment and avoid overlooking relevant characteristics of one of the parts.

2.2 The dissemination of information

Small disasters caused by natural hazards do not get the same attention as catastrophes[6] or large disasters[7]. Catastrophes and disasters are headlines in newspapers and get TV coverage for days to months, like Hurricane Katrina or the Camp Fire. But small disasters, with no deaths and some property lost, do not get the same coverage. However, these events are also important, and recognizing that can prevent future catastrophes and large disasters.

The 2018 Montecito debris flow was a large disaster and a rare event. It killed 23 people, impacted at least 400 homes, and many people were injured. The disaster received headline coverage in the local news for days and was covered by regional and national news. Yet, other debris flows have occurred in the past in Montecito and Santa Barbara County with varying magnitudes in 1926, 1964, 1971, 1990, 2009, and 2016 (Kean et al., 2019). These debris flows did not get the same attention due to their small impact, or they were forgotten over time (i.e., 1926 and 1964). Unsurprisingly, most Montecito residents did not know what a debris flow was before the disaster and were astonished by the impact on their community. The fact that media dominates the

---

[6] Catastrophe has a larger impact in a community than disasters. Most or all community infrastructure is heavily impacted and community functions are almost all or fully interrupted; local officials are not able to do their usual work, so their work extends into the recovery period; help from nearby communities cannot be provided (Quarantelli, 2000)
[7] A serious disruption of the functioning of a community or a society due to hazardous events interacting with conditions of exposure, vulnerability and capacity, leading to one or more of the following: human, material, economic and environmental losses and impacts (UNDRR, 2016)

dissemination of information and selects what to broadcast can create a misunderstanding of the local environment. In this context, local governments have an important role. They should make sure that previous events and natural disasters and possible impacts on the community are communicated to the community, thus educating the community, and making it less vulnerable, and, consequently, protecting lives and assets.

2.3 Vulnerability assessment

Around the late 70s and early 80s, the discussion of vulnerability in disaster research emerged, and it was influenced by the field of geographic development and poverty (Birkmann, 2013). At the same time, in different parts of the world, the idea of risk as a cultural and socioeconomic phenomenon, and highlighting the importance of vulnerability, was happening (Birkmann, 2013).

The focus of vulnerability assessment varies in the disaster research. These main foci (or dimensions) are social, economic, environmental, and institutional (Birkmann, 2013). The social dimension of vulnerability includes aspects of justice, social characteristics, and societal organization (Birkmann, 2013). The economic dimension includes economic aspects of households or their place within the economic system and how these economics aspects are part of the community (Birkmann, 2013). The environmental dimension includes the environmental system and how the impact of the natural hazard on the environmental system would affect the community, and the institutional dimension refers to the modes and constraints of governmental organizations and their capacity to include DRR measures (Birkmann, 2013).

The fragmentation of vulnerability into these dimensions might help its assessment but also might favor one dimension over another. For example, when the focus is just on the social

dimension, it might wrongly imply that vulnerability is synonymous with poverty, but they are not the same thing (Chambers, 1989). In addition, it is important to recognize the difficulty of assessing vulnerability and the fact that none of the indicators/variables used in each dimension will perfectly explain the vulnerability of the community (Dwyer et al., 2014).

2.3.1 Spatial Component of Vulnerability

Vulnerability assessments use local, regional (e.g., Cardozo *et al*., 2019), or national scales (Cutter *et a*l. 2003) and can assess one type of natural hazard (e.g., Kaynie *et al.*, 2008; Cardozo *et al*., 2019) or many (Cutter *et al.* 2003; Flanagan *et al.,* 2011; Hummell *et al.,* 2016; Frigerio *et al*., 2018). In this study, we consider the spatial dimension of the vulnerability as a local scale so that we can have a complex understanding of the community and its vulnerability towards a specific natural hazard (in this study, debris flows). Moreover, the impact of a natural hazard in a community is not dependent just on the magnitude of the event but also on the damage caused by the conditions and dynamics to the different social groups inside of the community (Birkmann, 2013). Communities are unique, and generalization of the vulnerability assessment can exclude important variables or exclude the most vulnerable people. Other than that, vulnerability assessment should consider the type of natural hazard. For instance, preparedness and education measures are unique for each type of natural hazard. Earthquake education is not the same as for tsunamis or landslides; preparedness and mitigation measures for floods are not the same as for earthquakes; safe homes for landslides are not the same as for earthquakes. Furthermore, vulnerability is not static; it can change over time, and a community can become more or less vulnerable. Maybe more elderly people are living in the community because a retirement

community was built in the prior year, or perhaps the municipality has trained residents for a specific natural hazard, and they became more prepared to deal with future natural hazards.

For example, consider communities A and B located in risk-prone areas for the same landslide in Time 1 (Figure 5.2). Both communities have similar socioeconomic characteristics and infrastructure. During Time 1, Community A has been working with DRR measures, and Community B has not. As a result, in Time 2, Community A is more educated about their local hazard, they know their risk, and they are more likely to evacuate when the local government issues an evacuation order. Therefore, Community A, in Time 2, is less vulnerable than B, even though their socioeconomic characteristics and infrastructure are the same.
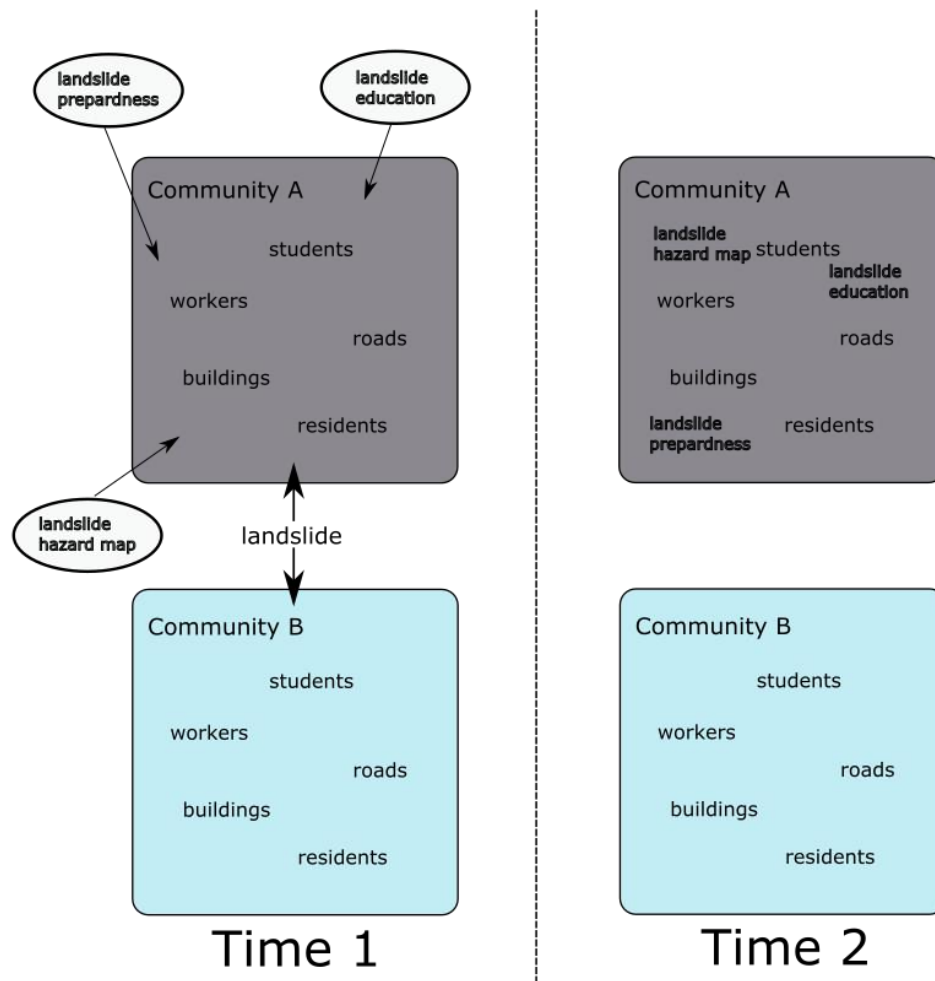
Figure 5.23. Two communities at risk for the same landslide in Time 1. Community A has been working with education, preparedness and mapped the landslide hazard areas. Community B, on the other hand, has not adopted any DRR measures. Therefore, in Time 2, Community A is less vulnerable than Community B to landslides.

2.3.2   Temporal Component of Vulnerability

Natural disasters have three main phases: before, during, and after. Vulnerability assessment should be done in the before phase and take into consideration the conditions of the community before the disaster that can contribute to negative impacts in the during and after phases. The after phase (Figure 5.3) has three main phases: short-term, intermediate, and long term (Homeland Security, 2016).
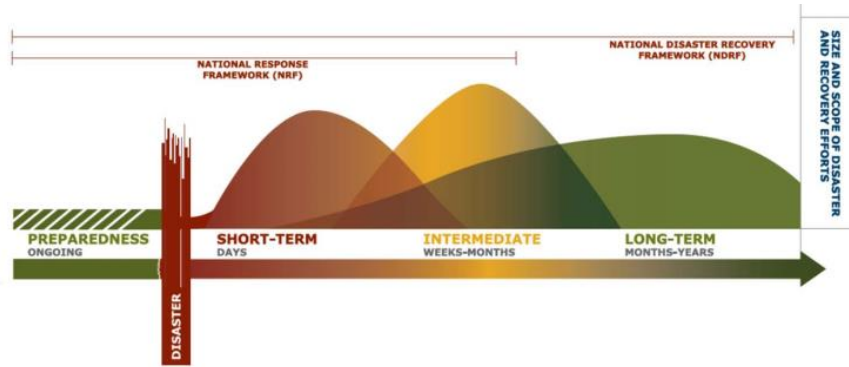
Figure 5.24. Phases of disaster used by FEMA as part of the National Disaster Recovery Framework. During the After phase, you see the short-term, intermediate, and long-term periods (Source: Homeland Security, 2016)

This temporal assessment of vulnerability helps to identify the people that are part of the community and how a negative impact would affect differently their members considering short-term, intermediate, and long term period.

3. Methods
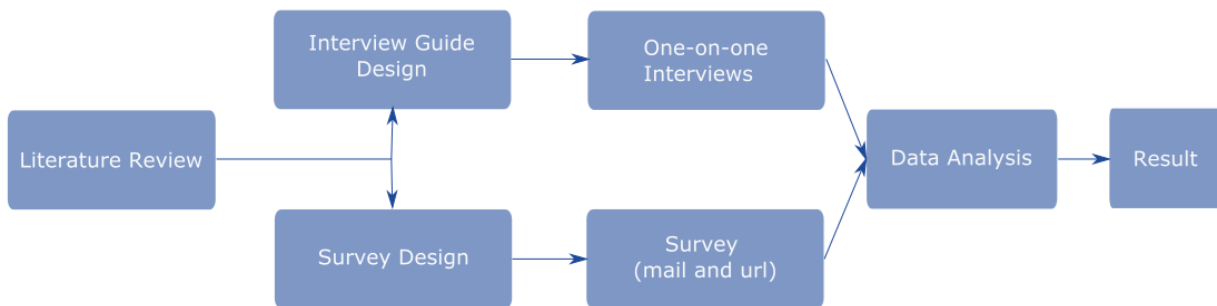
Figure 5.25. Method workflow. Parallel mixed methods were used in this study. The first phase is the literature review to design the survey and semi-structured interview guide. The data were collected from people that answered the surveys and by interviewers, and we analyzed both datasets. Based on our analysis, we came to our result (who were the most vulnerable people in the community and the variables to be considered)

3.1 Literature Review

A literature review was fundamental to define the research question and to design survey questions and the semi-structured one-on-one interview guideline. We divided our research into five main topics: demographics, risk perception, evacuation, education, and climate change. In this study, we are most interested in the questions that explain the vulnerability of the community (demographics, risk perception, evacuation, and education).

3.2 Quantitative Survey Design

Quantitative surveys are a useful tool for collecting particular information from a large population. The information collected is based on a set of questions designed to collect responses to the questions by the population. In our study, we asked target questions that would provide information about community vulnerability, which includes demographic, evacuation behavior, and risk perception questions.

Quantitative surveys also can target a larger group of people in a shorter time when compared with qualitative interviews. We had 529 surveys answered, and interviewing and transcribing the same number of people would take longer, and did not match the financial and human resources we had available.

We targeted residents of Montecito by including all buildings in the postal zip code 93108 (Figure 5.5). First, we sent postcards with a survey hyperlink, and two weeks later, we sent a paper survey by mail with a pre-paid envelope. The online survey was developed using Qualtrics software, which facilitated data collection and analyses. Considering that 32% of Montecito's residents are more than 60 years old (Census, 2010), we choose to use both online and paper surveys. The paper survey gave options for respondents that did not want to use a digital platform to answer the survey and increased the response rate. We sent 4,798 postcards and paper surveys, and

we got a response rate of 11%. Since questions were voluntary, some questions had fewer answers than others. Therefore, the total number of answers varies from one question to another.
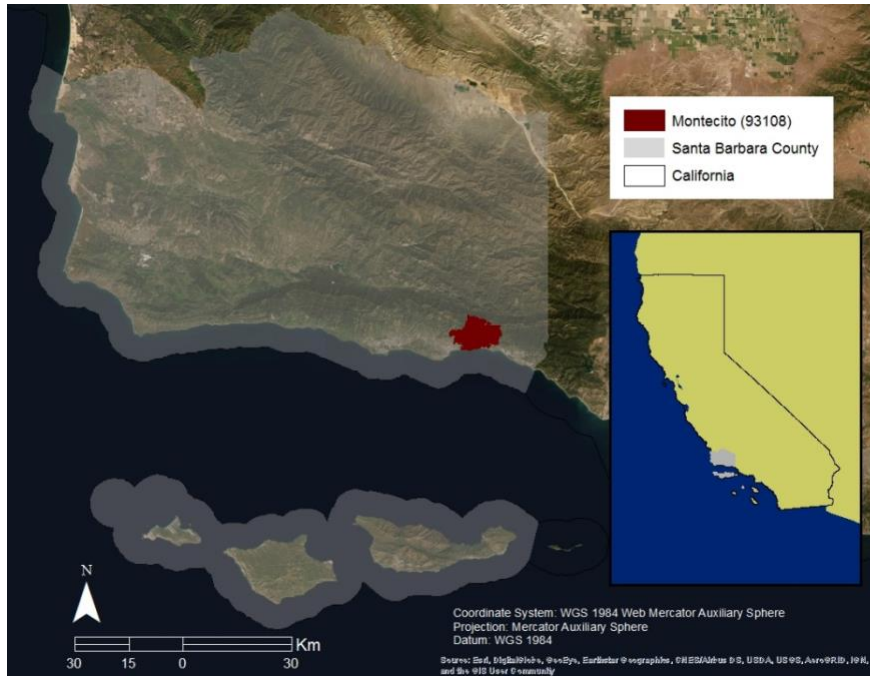
Figure 5.26. Zip code 93108 (Montecito) in red is the location to which the survey was sent by mail. Light gray in both maps represents Santa Barbara County.

3.3 Qualitative Interview Design

One-on-one interviews give a richer understanding of the vulnerability of the community. They allow the interviewee to tell their own story, since interviews are not as rigid as surveys. We used a semi-structured technique, which included a guideline with our main topics of interest, but we allowed some flexibility for interviewers to talk about their reasoning, opinions, feelings, values, and any topic they thought was relevant. We did 25 one-on-one interviews, starting three months after the disaster. These interviews included residents and residents' relatives, members of grassroots organizations, workers, and officers of government organizations that were directly affected by or worked with people affected by the debris flows.

The first interviewees were residents that had their property impacted by the event. A local

community organization, the Montecito Community Center, reached out by email and invited

individuals to contact us if they were interested in giving an interview about their experience with

the debris flows. After these first interviewees, we reached out to more interviewees by snowball

sampling. As we began receiving surveys, we contacted more residents who said they were

interested in participating in an individual interview.

We audio-recorded the interviews and transcribed and edited the transcriptions. Interviews took

around one hour, but some were shorter (around 20 minutes) and others longer (more than 120

minutes).

3.4 Data Analysis

We applied descriptive statistics in the survey data to summarize and describe our sample of the

Montecito population, and we used inferential statistics to draw conclusions, using R software.

Moreover, to use a phenomenological approach by exploring the meaning of people involved with

the debris flows, we coded the interviews and used themes in NVivo software. Themes emerged

from our semi-structured survey, together with recurring topics brought up by different

interviewees. Based on the themes and statistical analysis, we focused on developing a case study

of the 2018 debris flow vulnerability in Montecito.

4. Study Area: Montecito, CA

In January 2018, debris flows heavily impacted the community of Montecito, Santa Barbara

County, CA. They occurred as a result of wildfire (the Thomas Fire) followed by intense rainfall in

the catchments of the Santa Ynez Mountains (Kean et al., 2019). These catchments are steep and short and combine as they reach the Pacific Ocean. The debris flows killed 23 people, injured at least 167, and damaged at least 400 homes (Kean et al., 2019). Residents, workers, and businesses in the community were impacted. The area was covered by mud and debris for at least two weeks, the main highway (101) was closed for ten days, water was considered not safe for drinking, and utilities (electricity and gas) were shut down. Beyond these direct impacts, there were many indirect impacts. For instance, emotional and psychological issues caused by the loss of family members and/or loss of income due to closure of the highway, making it impossible to go to work.
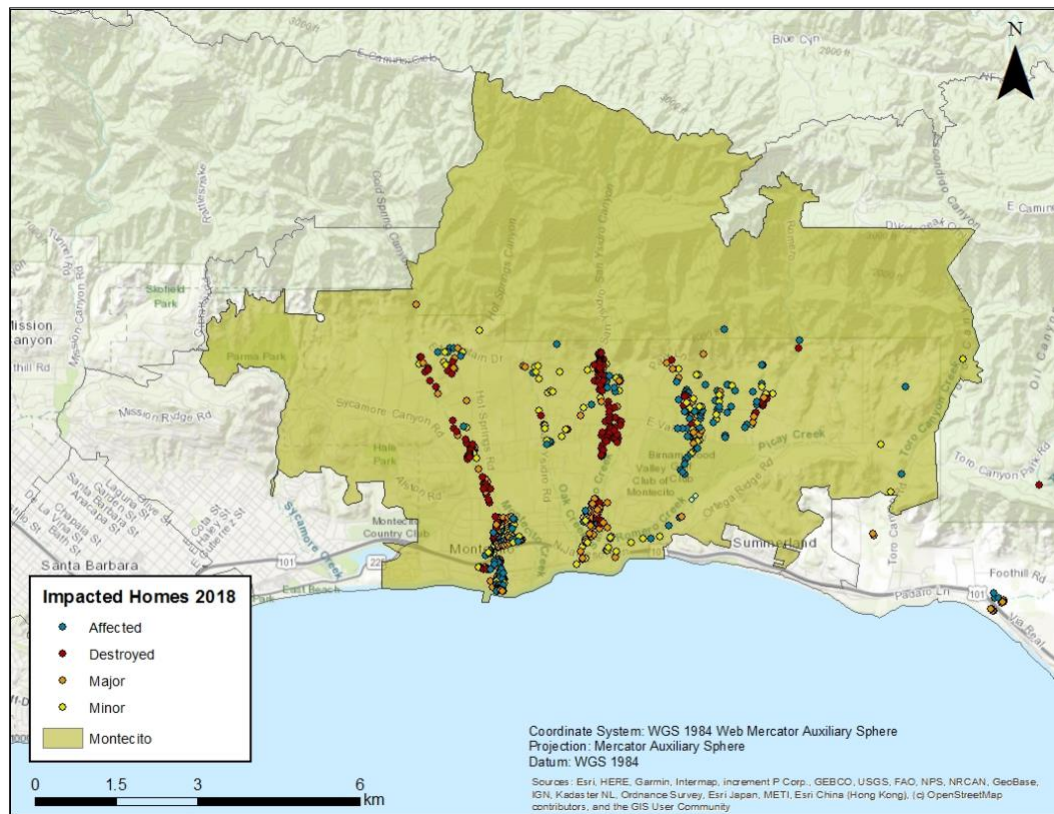
Figure 5.27 – Buildings impacted by the Montecito 2018 debris flows. Different colors show the building impact level.

The disaster was a surprise for residents and the local community. During the prior month (December), Montecito had been subjected to several mandatory evacuations because of the Thomas Fire. Montecito residents had been observing the impacts of the Thomas Fire since it started in the neighbor county (Ventura County) and made its way to Santa Barbara County. The ashes were a real problem impacting the air and homes, and when the Thomas Fire burned Summerland and Montecito, it could be seen when driving on Highway 101. Moreover, wildfires had been occurring all over California, had good media coverage, and you could see them progressing and causing destruction from one region to another (i.e., the Thomas Fire started in Ventura County and spread to Santa Barbara County). Debris flows, on the other hand, got less media coverage as they were rare events, and it was harder to predict where they were going to occur. However, because of previous natural disasters, local, state, and federal agencies were well aware of potential debris flows in the area (Kean et al., 2019). The day before the event, voluntary and mandatory evacuation orders for Montecito were issued by the county. Debris flows and floods have occurred in the past in Montecito, and several debris flows have occurred post-wildfires in Santa Barbara County with diverse magnitudes, such as the ones in 1926, 1964, 1971, 1990, 2009, and 2016 (Kean et al., 2019). Moreover, Southern California, in general, has a history of debris flow disaster post-wildfire, like Camarillo Springs in 2014 and La Crescenta in 2010 (Kean et al., 2019).

5. Results and Discussion

5.1 Spatial Dimension of Vulnerability

The Montecito community is a combination of residents, workers, and businesses. There are no industries. Overall, Montecito residents are wealthy, have little ethnic diversity, and are old (Table

108

5.1). The majority of residents live alone or with one other person (78.0%). The majority of residents make more than $150,000/year in income (66%), but in the same community, some residents make less than $25,000/year (4%). Furthermore, the majority of residents (63%) hire at least one worker at their property. These workers are gardeners, housekeepers, caretakers, babysitters, and home cares for the elderly. These workers are commonly immigrants, both documented and undocumented. Considering that one-third of the human losses during debris flows were from immigrant families and that only 9% of the Montecito residents are non-white, it is clear that people of color and workers were more vulnerable than white residents. Moreover, after the debris flows, workers were financially impacted because they could not work in the community for around two to four weeks. Part of the community and access to the community was closed due to debris and mud on the roads, and houses had no electricity. Indeed, some of these homes remain uninhabited almost two years after the event.

Table 5.15. Descriptive statistics from the survey and 2010 Census

		Survey	2010 Census
Number		529	8,965
Ownership	Owner	91.0%	76%
	Renter	9.0%	24%
Age	19 to 39	3%	21%
	40 to 59	24%	31%
	60 to 70	28%	18%
	70 or more	45%	30%
Number Household (Mean)		2.5	2.5
Race/Ethnicity	White	91.0%	90.8%
	American Indian or Alaskan Native	2.0%	0.2%
	Asian or Pacific Island	2.0%	3.7%
	others	5.0%	5.3 %
Education	High school graduate or higher	99.5%	97.8%
	Bachelor's degree or higher	87.3%	71.8%
Years living in Montecito	Less than two	4 %	NA
	Between 2 and 5	9 %	NA
	Between 5 and 10	16 %	NA
	Between 10 and 20	22 %	NA
	More than 20	49 %	NA
Employed caretaker/caregiver	Yes	63%	NA
	No	37%	NA

About 24% of Montecito residents are renters (Census, 2010). The difference between our survey and the census might be explained by renters who moved out and did not answer the survey. Renters are a vulnerable population since they are a transient population, and they usually do not know about the previous history of debris flows or floods in the area. Commonly, renters in Montecito are families with school-aged children who attend Montecito Union School. These families moved to Montecito so their children could get an excellent public education by attending the Montecito Union School District. The school is known to provide a good education and has a small student/teacher ratio.

5.1.1 Sense of Community

The sense of community differs from resident to resident. Some of the interviewees pointed out that they were close to their neighbors before the natural disasters (strong neighborhood dynamics) , others mentioned how they got even closer to their neighbors after the debris flows, and some mentioned that they do not feel they are part of a community.

Residents that already had a sense of community were more likely to check if neighbors were going to evacuate. Neighbors' decisions influenced their own, or they tried to influence others to evacuate considering their previous experience with floods in the area. They communicated mainly by person, group text messages, or phone calls. During the event, residents tried to communicate with other residents to check in. However, cellphone service was unstable during the debris flows, and messages sometimes would go through and others would not. As mentioned by one of our interviewers:

"I had a fully charged phone, and we were calling to each other across like I can stand on my front porch with a flashlight and other neighbors across the street, and we were just like doing a calling chain. 'Have you heard from so and so?' 'Does everybody know?' Because in ninety-five when we flooded, what we would do is we would go and check on the elderly people because, you know, in those days, you didn't have everybody's phone number." *(Respondent 09)*

Residents were also checking on other neighbors after the disaster, and some relationships became stronger, as this resident describes: "*Oh my gosh, the sense of community that has been created out of this for me- I knew many of my neighbors, but now I know them on a much different level.*" (Respondent 19) After the natural disaster, a group of women in the community started to meet weekly to cook dinner together and chat. These weekly meetings helped these women cope better as they could rely on each other and talk about different aspects of their lives but also disaster-related topics.

The debris flows almost totally destroyed the homes in some neighborhoods. In these neighborhoods, some residents moved out. Residents that decided to rebuild and continue in the community mentioned how difficult it was to come back and have to see nearby homes destroyed and not having their neighbors around.

After the debris flows, organizations and the county groups were actively helping the community to bounce back. These organizations played different roles, from psychological health to cleaning up the mud. The main organizations that had an important role in the aftermath were the Montecito Union School District, Cottage Health with the Post-Disaster Healing Process, the Bucket Brigade, the Montecito Association, Habitat for Humanity, the *Montecito Center for Preparedness, Recovery, and Rebuilding*, and local churches.

Interviewees frequently mentioned the amazing work done by the Bucket Brigade. The organization was created to help residents with the cleanup of mud and debris of their properties in the aftermath. Volunteers would go to impacted homes and cleanup. Moreover, the volunteers created a hopeful environment, as mentioned by one interviewee: *"Not just that they did it, but that they were there, they were comforting, they were happy*." (Respondent 09) The volunteers would come to a home, clean it, and leave.

Santa Barbara County organized community meetings in Montecito to help residents to deal with the aftermath. A center was opened in the community, the *Montecito Center for Preparedness, Recovery, and Rebuilding*, and it offered support to impacted people, especially residents. In the center, information about other organizations helping in the aftermath was available, such as Habitat for Humanity, the Bucket Brigade, the American Institute of Architects, and the Community Wellness Team/805 Hope. Interviewees highlighted the resources Santa Barbara County offered and how helpful the Montecito Center was, especially by locating these aid organizations on the same site. In addition to the Montecito Center, Santa Barbara County organized community meetings to help residents navigate in the aftermath, with topics like maps, insurance, rebuilding, and permitting. The survey showed that 55% of residents attended at least one community meeting planned by the county. These meetings were also broadcast online live and uploaded online, so people did not necessarily need to attend in person the meetings.

Local churches and schools helped residents to deal with the aftermath. Interviewee that was evacuated during the debris flows described the support she got from her church and its members by having a place to stay in the aftermath and helping with the cleanup of her home. The Montecito Union School District played an important role by not cancelling classes even though school was

closed. The school would find places to keep the classes going so parents could deal with the aftermath. The school also hosted non-school related meetings and events to help families deal with insurance, contractors, and rebuilding.

The local businesses gave discounts for people impacted or free products and meals. Cottage Health by their Post-Disaster Healing Process program offered one year free phycological support to people that had personal or material losses during the debris flows. Residents that were part of the program describe how the program has helped them in the aftermath, how they would recommend it, and how grateful they were to be able to participate in the program.

The landscape changed in the aftermath and during the rebuilding process. For most of Montecito, as an interviewee mentioned, you could not tell that something happened after the debris flows, but if you lived in the area and needed to drive around, you could see the closed roads and bridges and the areas being rebuilt. The new landscape brought negative memories for some of the residents. One interviewee was very disturbed by seen "green wall" when she would drive in the neighborhood. These green walls are properties that are rebuilding, and they would bring memories of the natural disaster to this particular interviewee. Another interviewee had her home in a neighborhood where most of the homes were destroyed and while driving in her neighborhood, memories of the natural disaster arose.

5.2 Temporal Dimension of Vulnerability

The temporal dimension of the vulnerability of the 2018 debris flows in Montecito can be divided into before, during, and after.

5.2.1 Before the 2018 Debris flows

Some local aspects of the community contributed to their increase in the debris flow vulnerability before the event. Residents showed evidence of evacuation fatigue from the Thomas Fire. There were multiple evacuations orders for the Thomas Fire the month before the debris flow evacuation order, as described by one of the interviewees: "*we were evacuated six times.*" (Respondent 20). Furthermore, some residents had pets, which made the evacuation even more challenging.

Both the evacuation order (69%) and the evacuation zone map (68%) were clear for residents (*Appendix 5.1*). One problem with the January debris flow evacuation order was that the county used U.S. Route 192 as a dividing line to delineate areas under voluntary and mandatory evacuation orders - the same line used during the Thomas Fire. Debris flows are very different from fire risk, and the impact of the debris flows confirmed that. Many homes in the voluntary zone were destroyed, and 19 of the people that died lived in the voluntary evacuation zone, not in the mandatory evacuation zone (Hayden, 2018).

In addition to the problematic evacuation zones, there was a lack of knowledge about debris flows by residents and workers, as well as a "drought mentality." Due to the weather characteristics of Santa Barbara County, some residents have doubts about possible intense rainfall:

> *And you know they said the rain was supposed to start much earlier in the day. It had sprinkled a little bit but, we were kind of joking because that happens a lot, here in Santa Barbara. "It's gonna come later, it's gonna come later," and then it never comes.* (Respondent 04)

All the interviewees with the exception of one had not heard the term debris flow prior to the event and had no idea that debris flows had happened in the past in Montecito and Santa Barbara County. "… *I don't remember hearing anything about a debris flow those words... I heard about how unstable the mountain was, that flash flooding means lots of water coming down really*

114

fast … I don't if I heard the term debris flow; it wasn't explained so that you would I would you would click in." Another resident that had his/her house destroyed mentioned "*… so first and foremost, we were in a voluntary evacuation zone. And I did not understand the history of Montecito.*" (Respondent 11)

Residents that had lived in the area longer knew that creeks could flood or that La Conchita, in Ventura County, had landslides in the past, but they did not have any knowledge of past debris flows in Montecito or Santa Barbara County. Local, regional, and national public authorities, on the other hand, knew that there was high susceptibility for debris flows. For example, Montecito Union School District decided to close school the day of the debris flow, based on the convincing argument given by public authorities that a debris flow was very likely to occur, and the school could be isolated if the community was impacted.

Some residents stated that their decision not to evacuate was based on being in the voluntary zone and/or on the opinions of their neighbors. "*And the other thing is everybody in our neighborhood was staying, and so my neighbor across the street…*" (Respondent 19) In this matter, the county lacked sufficient communication with which to explain to the community what a debris flow consists of and the damage that past debris flows caused in Montecito and other places in Santa Barbara County and Southern California.

The survey showed that the majority of residents got evacuation information from Santa Barbara County (76%), but other media also were releasing the information about the evacuation order. Some interviewees felt overwhelmed by the amount of information about evacuation and evacuation maps coming from different news sources.

"Well yeah, it was constant, just constant. So we got numb, everybody goes numb to it. I don't think when people describe they had weariness from evacuation, that definitely was part of the problem, but I think… there were too many cries of wolf. You know, it felt like that after a while, so you just you don't hear it anymore…" (Respondent 18)

The cellphone signals in Montecito during the event was weak and unstable, which had a negative impact during the event as it was harder to communicate with other people. Another problem that increased the vulnerability of residents was a lack of maintenance of the local creeks, which were filled with boulders and the channels were not wide enough for the flow of the water that came during the event.

5.2.2 During the 2018 Debris flows

The lack of knowledge about debris flows increased residents' vulnerability during the event. Without previous knowledge about debris flows, some residents decided to leave by car when they realized the mud was coming toward their home or when they saw the light in the sky caused from a gas explosion when boulders hit a gas pipeline during the debris flows. The decision to leave the house during the debris flows increased their risk. The interviewees were safer at their homes (none of those that described driving had much damage on their homes), but their lack of debris flows knowledge made them decide to evacuate during the event. These residents were driving during the storm, without street power, with mud and debris coming downhill. One interviewee mentioned that a family that did not get mud inside the home when trying to escape during the debris flow was swept away inside their car.

During and right after the debris flow, there was no information for residents that got stuck in their homes. The area had no electricity, and cellphone signals were on and off. Some residents

tried to get information from the radio, but they mentioned they felt helpless. No information about what to do was available from the radio.

5.2.2 After 2018 Debris flows

5.2.2.1 Short Term After 2018 Debris Flows

The combination of a lack of information right after the event and no debris flow knowledge increased the risk to residents. A couple of residents that did not have their houses impacted got stuck in the mud the day after the event when they went to the pharmacy to get medication.

> "...And we got caught in the mud and we were up to our waist in mud in that orange grove mountain street and we were screaming for help in the evening and my wife is where you are and I was here in the mud I couldn't even get to her because we couldn't move our legs it was like quicksand it was up this high up to your thigh, middle thigh." (Respondent 20)

Another example was an older woman whose house was not impacted but was one block away from the homes that were. She had no idea what was going on since there was no access to information, and she would go for walks in the neighborhood.

> "They couldn't get my grandmother to leave… I'm like having to stay with my grandmother because we can't get her to leave because the cops can't get her to leave because she's - I mean she was literally walking up and down the streets, and we were like, talking to the first responders … And she thought there was nothing going on. And they're giving her sandwiches…. she was walking up to the village, and wouldn't understand that the bank was closed, and the shops were closed. It was just, you know. My family is following her around…" (Respondent 05)

The local authorities were able to respond quickly to the disaster since they had prepared for a worst-case scenario and had teams ready in case a disaster was to happen (Respondent 11). However, the timing of response by the local authorities was felt differently between interviewees

117

that had distinct experience with the debris flow. Interviewees that were injured or cover with mud felt that the rescue took a long time, and interviewees that were not injured and in their homes during the event did not experience the same timing. "*We were in shock, and I knew that [names omitted] had some injuries, I did not know how severe, but I had looked at [name omitted] shoulder and it was all bruised…*" (Respondent 19)

Workers at Montecito properties were impacted in a different fashion than residents. They were mainly impacted financially for at least two weeks. These workers were already financially vulnerable and going some weeks without a paycheck compromise their basic necessities, like rent. Since workers do not necessarily live in Montecito, attention to their plight and need of financial support from the government was minimal. Some financial resources were put together by an NGOS, CAUSE, by donations and small financial support by the county.

5.2.2.2 Mid and Long Term After the 2018 Debris Flows

In the initial process of the aftermath, there was much attention given to the people that were impacted, but after some time, the impacted people were left by themselves to deal with rebuilding, getting permits, dealing with insurance, contractors, and so on, which can be mentally challenging and can be frustrating, as interviewees brought to our attention. Many homes were totally or partially destroyed by the debris flows. These homeowners had to deal with the insurance and rebuilding process.

Residents relied on their homeowner's insurance to rebuild or fix their properties in the aftermath. Right after the debris-flows, fire insurance companies were refusing to pay insurance for homes impacted by debris-flows. However, on January 29, California's Department of Insurance

released a notice indicating that the debris-flows and floods on January 9th were caused by the Thomas Fire and recommended that homeowners file a claim to their insurance program. Santa Barbara County also offered support to homeowners in that matter. This was an important achievement for homeowners since fire insurance companies were not going to pay insurance to impacted homes. But the fight with insurance companies did not end with the notice. Residents described how challenging their experiences with insurance companies were. Some insurance companies required residents to list every single item damaged to reimburse, which is the least someone wants to deal with immediately after having material or personal losses. Each affected resident has a different story about insurance companies, but, overall, the insurance companies do not seem to have cooperated with the rebuilding and healing process. Based on interviewees, agents can be rude or ageist, and, when things are already stressful and arduous, that is the least thing people want to deal with.

The rebuilding process was different for each resident in terms of time and resources available. Some residents had their homes insured with insurance companies that paid the claims, so they were able to start the rebuilding process right after the disaster, other homeowners had a slower and more stressful process with their insurance companies, and others did not want to rebuild or wanted to wait a couple of winters before starting rebuilding.

Rebuilding in Montecito can involve historic properties, which makes the rebuilding process more complicated and requires the involvement of the planning department, architects, and historians — making the process more expensive and longer. Another problem in the aftermath was defining lines between properties that were destroyed. Some property document surveys were lost during the event, so the lines needed to be redrawn as mentioned by the interviewee "... *no one*

knows where their property lines are anymore, and it's like the wild west out there." (Respondent 14)

The rebuilding also brought some tension between neighbors. To protect themselves from future debris flows, some residents decided to build high walls or rebuild their homes on higher elevation ground. However, these changes in the landscape might impact other homes since they change the pattern of how water flow, so homes that were once safe might not besafe anymore.

In the aftermath, some real estate agencies wanted to buy properties that had homes destroyed and build new homes. These homes are in at-risk areas, and people impacted commonly want to move out and are willing to sell their homes cheaper than the market value. These real estate agencies buy these properties, rebuild them, and sell or rent them to new families who have never experience such a natural disaster. Another resident, when commenting about the rebuilding of their home, stated: "*From an ethical perspective, I don't think that we should be allowed to rebuild. We're in a flood zone, and that's not gonna change.*" (Respondent 19). However, if their home was totally destroyed, they are legally allowed to rebuild, and depending of the insurance, the rebuilding need to be in the property that was destroyed.

Real estate agencies have been offering to buy homes that were severely damaged or totally destroyed by debris flows. Interviewees who had houses destroyed by debris flows had real estate agencies reaching out to buy their properties.

> "*We had someone approach us when we soon after we bought this house [where they are living now] and asked if we were interested in selling [the house that was destroyed], and we had a couple of offers, and they were way people thought they were going to get into a deal …*" (Respondent 18)

120

Post-traumatic stress disorder (PTSD) can be triggered by a traumatic event, like the 2018 Montecito debris-flows. Community Wellness Team/805 Hope offered a free one-year service for people that had personal or material losses during the event. Interviewees mentioned how important and helpful they were for their healing process. Different than the deaths and home destroyed, PTSD does not get the same attention as well as injured people. The natural disaster resulted in many people injured, trapped in the mud, and also people that survived but lost someone they knew.

6. Conclusion

In conclusion, we discussed the spatial and temporal dimensions of vulnerability and why it is important to point out whom the vulnerable people of the community are and the main aspects that made the community more vulnerable. Considering the socio and economic dimensions, homeowners that were in the voluntary evacuation zone and workers were the most vulnerable people in the community. The main characteristic that made the community more vulnerable was the lack of knowledge about debris flows and the fact that they occur in this region. Due to this lack of knowledge, some people increased their risk unnecessarily by driving in an unsafe environment when they were actually safer at home. Moreover, the institutional dimensionality of vulnerability was high for the whole community. Public authorities did not educate the community about past debris flows and also made a poor choice by choosing to use the same evacuation line used during the Thomas Fire. One the other hand, public authorities have been very supportive of residents in the after phase, creating the *Montecito Center for Preparedness, Recovery, and Rebuilding* and hosting many community meetings in the aftermath, which contributed to reducing the negative impact on homeowners.

These findings can help public authorities in their DRR measures and Disaster Risk

Management. Moreover, the present study can provide valuable information for a future assessment

of the spatial distribution of debris flow vulnerability and consequent debris flows risk in

Montecito.

CHAPTER 6: CONCLUSION

Landslides occur in different parts of the world, regardless of whether the country impacted is a developed or a developing country. However, the choice of which disaster risk reduction (DRR) measures to use differs, based on financial resources and political priorities. Some countries choose to invest in risk mapping, reinforcement walls, or maybe evacuation planning and drills. This dissertation has presented two environments in which natural disasters can occur, but which have very distinct realities. The first studies are in poor neighborhoods in urban areas in Brazil that are prone to shallow landslides, and the second study is in a wealthy community in Montecito, CA, prone to debris flows. Despite their differences, both projects suggest that DRR measures can contribute to protect communities and make them better prepared to deal with future natural disasters.

In the Brazilian study, quantifying the Brazilian Government Methodology (BGM) allowed standardization of the methodology and permitted the system to avoid relying on the subjectivity of two technicians in deciding the risk level; therefore, it reduces the bias. In the first study, expert knowledge and the AHP methodology were used to assign specific weights to causal variables. The second study used a large dataset from a previous risk mapping of Sao Paulo city and OLR to select important variables and compute their weights. In conclusion, both methodologies were successful in quantifying the BGM. However, OLR used fewer variables (14) than the AHP methodology (39) an important principle of regression is data reduction. But the AHP methodology did not focus on reducing the variable, instead the goal was to keep all the primary variables that the BGM uses in the field to decide on the risk level. Moreover, results using different OLR models were not that different (*Mean=0.72, SD=0.005*). Future studies using OLR could include mapping datasets from other cities to improve the model.

The challenges encountered in the landslide risk mapping in Brazil were related to anthropogenic activities in the terrain, such as sewage and garbage disposal onto the slope. For instance, one sector can have several houses disposing sewage onto the slope and another sector can have just one home, but they will weigh the same when computing the risk since the original BGM just accounts for presence or absence of an aspect (variable). Other characteristics that make the assessment challenging are signs of movement in the same sector, like cracks in the house or leaning walls. Considering two sectors, one may have signs of movement in a single house, and another sector may have signs of movement found in many homes; if all other variables are kept the same, both sectors will have the same risk level. Therefore, an improvement in the methodology considering these observations would be necessary to improve quantitative methodologies assessing shallow landslides in these urban settings. Complementary to these two studies, an app was developed to compute the risk level automatically. In this app, the weight of both methodologies can be used. The benefit of using the app is that it is a fast way to map these areas and automatically compute the risk level based on the field data and not the personal decision of a technician. The app can be used by municipalities to update their risk mapping rapidly since these sectors change very fast and the mobile app would allow them to monitor these changes without depending of another risk mapping.

Even though the BGM is called a risk assessment, the vulnerability is not fully assessed in the methodology. The BGM includes some variables that partially account for vulnerability, but not for the complexity present in a complete vulnerability assessment. For instance, the type of building (wood, brick, or mixed materials) indicates to some level the economic characteristics of the households. Residents that live in mixed materials homes have the most precarious homes since these houses are a combination of everything found available on the site. As residents become more

financially stable, they improve their homes, initially upgrading to wood and later to brick. However, other aspects that are essential to a more robust vulnerability assessment, such as age group and race/ethnicity, are not accounted for in the BGM. Therefore, the assessment tends to be a hazard assessment accounting for anthropogenic changes in the land, and not a risk assessment.

The variability in these anthropogenic risk sectors can be observed in the variability of saturated hydraulic conductivity found in the disturbed site (Mean= 138.15 mm/h, SD=266.94 mm/h, Range=675.16 mm/h) when compared with the undisturbed site (Mean= 19.80 mm/h, SD=12.12 mm/h, Range=29.61 mm/h). In the undisturbed site, soil texture does not play an important role in the saturated hydraulic conductivity, suggesting that the variability is related to different materials that were placed onto the terrain over time. In the same study, values of soil cohesion, soil angle of internal friction, and soil bulk density computed in the lab were used to compute slope stability by using SHALSTAB and FS (factor of safety). In both studies, the undisturbed slope is more stable than the disturbed slope. However, based on field observation and values of hydraulic conductivity, the soil in the disturbed site is heterogeneous, and even though it seems to be more stable than the undisturbed soil, a study of slope stability that included saturated hydraulic conductivity could arrive at a different outcome. Moreover, shallow landslides in these urban settings are initiated by intense rainfall; therefore, the role of water is fundamental.

In the Montecito study, the main conclusion deals with the importance of assessing vulnerability by considering the type of natural hazard and the temporal and spatial dimensions. The spatial dimension is the area prone to the natural hazard, and the temporal dimension consists of the phases of a natural disaster (before, during, and after). In a natural disaster with a similar magnitude as the one in Montecito, we tend to focus on the material and human losses. These aspects are essential, but it is also important to understand the community dynamic and who are the

members of the community, and not consider just the residents as the members of the community. Moreover, there are side effects that come with material and human losses, such as psychological trauma and injuries, which are given less attention.

In Montecito, resources were offered to residents, such as free counseling, free cleaning of the mud by a local non-profit organization, and community meetings organized by the county to help residents navigate the rebuilding and insurance procedures. These resources helped residents cope with the aftermath and bounce back. But wealthy communities like Montecito have hidden elements that also need to be accounted for. A survey of residents illustrated that 60% of the residents employ at least one worker, such as a gardener, housekeeper, nanny, or caregiver. Regardless of whether or not these workers were in the community daily or spent more time than their employers in the property (such as vacation homes), they were not accounted as a critical people impacted in the community. Some of these workers lost their financial resources in the aftermath and since they were already vulnerable, they were highly financially impacted; some of them had to move to other areas to work since they could not afford to stay without a salary.

Another aspect that made the entire community vulnerable was the institutional dimensionality, which was high for the entire community. On the one hand, public authorities offered informational support to residents in the after phase, creating the *Montecito Center for Preparedness, Recovery, and Rebuilding* and hosting many community meetings, which contributed to reducing the negative impact on homeowners. On the other hand, public authorities did not educate the community about past debris flows in Montecito and Santa Barbara county area, and the county made a poor choice when using the same evacuation zones for the mandatory and voluntary zones used during the Thomas Fire, despite both natural hazards being completely different. This lack of information and education and the problematic evacuation zones resulted in

residents not evacuating, residents driving during the debris flows, trying to escape and putting themselves at higher risk than staying in their home, and residents walking around their neighborhood after the natural disaster and getting stuck in the mud.

These two studies present different realities and ways to deal with natural hazards, but both can use knowledge of DRR to adapt to their reality and protect their community. Both in Brazil and Montecito, public authorities can educate communities so they can understand their risk and make better decisions. Moreover, communities in risk-prone areas would benefit from correct risk mapping and evacuation zones maps, thereby lessening the chance of having members of the community not evacuating because they wrongly think they are safe.

In summary, this dissertation proposes methodologies for both developing and developed countries that contribute to the DRR, considering the local particularities. Future studies in shallow landslide risk in Brazil should include a more complex assessment of the vulnerability to account for the complexity of the vulnerable population. Moreover, before starting a vulnerability assessment in any community, interviews with a variety of members of the community would benefit from the vulnerability assessment. Communities have their own dynamics, and not taking these aspects of vulnerability in consideration limits the quality of the assessment since the most vulnerable people might be left behind, as observed in the case of Montecito.

References:

12.608/2012, L. (2012, April 10). Política Nacional de Proteção e Defesa Civil - PNPDEC. Diário Oficial da União, 70.

ABNT (1984). NBR 7181 – *Solo Análise Granulométrica.*

ADB - Asian Development Bank. (2015, May 12). Schools with Earthquake-proof Technology Survive Nepali Disaster. Retrieved March 12, 2016, from ADB- Asian Development Bank: http://www.adb.org/news/features/schools-earthquake-proof-technology-survive-nepali-disaster

Abuhajar, O., El Naggar, M. H., Newson, T. (2010). Review of available methods for evaluation of soil sensitivity for seismic design. *5th International Conference* on *Recent Advances in Geotechnical Earthquake Engineering and Soil Dynamics and Symposium in Honor of Professor I.M. Idris*, San Diego, California.

Agência Brasil. (2014, June 19). Deslizamento de terra em natal atingem 100 famílias. Retrieved January 05, 2016, from Agencia Brasil: http://agenciabrasil.ebc.com.br/geral/noticia/2014-06/deslizamentos-de-terra-em--al-atingem-100-familias

Agresti, Alan; Finley, Barbara (2009). Statistical methods for social sciences.4 Edition, Upper Saddle River, New Jersey, Pearson Prentice Hall.

Akgun, A., & Türk, N. (2010). Landslide susceptibility mapping for Ayvalik (Western Turkey) and its vicinity by multicriteria decision analysis. Environmental Earth Sciences, 61(3), 595–611. https://doi.org/10.1007/s12665-009-0373-1

Akgun, A. (2012). A comparison of landslide susceptibility maps produced by logistic regression, multi-criteria decision, and likelihood ratio methods: a case study at Izmir, Turkey. Landslides. 9: 93. https://doi.org/10.1007/s10346-011-0283-7

Alcantara-Ayala, I. (2002). Geomorphology, Natural Hazards, Vulnerability and Prevention of Natural Disasters in Developing Countries. Geomorphology, 47 (September 2016), 107–124. https://doi.org/10.1016/S0169-555X(02)00083-1

Alexander, D. (2002). Principles of emergency planning and management. (O. U. Press, Ed.) New York.

Alexander, D. (2004). Vulnerability to landslide. In T. Glade, M. Anderson, & M. J. Crozier, Landslide Hazard and Risk (pp. 175-198). Hoboken, NJ: John Willey & Sons.

Amaral, C., & Furtado, A. (2004). Large-scale quantitative landslide risk mapping at Favela da Formiga, Rio de Janeiro. Landslides: evaluation and stabilization.

Aronica, G. T., Biondi, G., Brigandi, G., Cascone, E., Lanza, S., & Randazzo, G. (2012). Assessment and mapping of debris-flow risk in a small catchment in eastern Sicily through integrated numerical simulations and GIS. Physics and Chemistry of Earth, 49, 52-63.

Ayalew, L., Yamagishi, H., Marui, H., & Kanno, T. (2005). Landslides in Sado Island of Japan: Part II. GIS-

based susceptibility mapping with comparisons of results from two methods and verifications. Engineering Geology, 81(4), 432–445. https://doi.org/10.1016/j.enggeo.2005.08.004

Barbosa, J. L. (2006, 11). Em busca do fio de Ariadne. Retrieved 02 10, 2016, from Observatorio de favelas: http://of.org.br/acervo/em-busca-do-fio-de-ariadne/

Barredo, J., Benavides, A., Hervás, J., & van Westen, C. J. (2000). Comparing heuristic landslide hazard assessment techniques using GIS in the Tirajana basin, Gran Canaria Island, Spain. International Journal of Applied Earth Observation and Geoinformation, 2(1), 9–23. https://doi.org/10.1016/S0303-2434(00)85022-9

BBC. (2014, 08 02). Massive landslide hits river near Nepal capital. Retrieved 08 07, 2016, from BBC News: http://www.bbc.com/news/world-asia-28619288

BBC. (2015, 05 19). Colombian town searches for victims of deadly landslide. Retrieved 08 07, 2016, from BBC: http://www.bbc.com/news/world-latin-america-32785201

Bell, R., & Glade, T. (. (2004). Quantitative risk a-lysis for landslides – Examples from Bildudalur, NW – Iceland. -tural Hazards and Earth System Sciences(4), 117-131.

Birkmann, J. (2013). Measuring vulnerability to promote disaster-resilient societies and to enhance adaptation: Conceptual frameworks and definitions. In: Birkmann, J. *Measuring Vulnerability to Natural Hazards: towards disaster resilient societies*. UNU- EHS: Institute for Environment and Human Security. Retrieved from http://archive.unu.edu/unupress/sample-chapters/1135-MeasuringVulnerabilityToNaturalHazards.pdf

Boston.com. (2011, January 21). Boston.com. Retrieved from Boston.com: http://archive.boston.com/bigpicture/2011/01/landslides_in_brazil.html

Boustain, Leah P.; Yanuas, Maria L.; Kahn, Matthew, Rhode, Paul W. (2017). New data set explores 90 years of natural disaster in the US. *The Conversation*. Retrieved from https://theconversation.com/new-data-set-explores-90-years-of-natural-disasters-in-the-us-78382

BPMSG (Business Performane Management Singapure) (June 2018). New AHP Excel template with multiple inputs. https://bpmsg.com/new-ahp-excel-template-with-multiple-inputs/

Brasil. (2007). Mapeamento de riscos em encostas e margens de rios. Ministério ds Cidades/Instituto de Pesquisas Tecnológicas - IPT. Brasília: Ministério ds Cidades; Instituto de Pesquisas Tecnológicas - IPT.

Brasil. (2015). Carta de suscetibilidade a movimentos gravitacionais de massa e inundações - Município de São Ber-rdo do Campo - SP. 1:50,000. Brasil.

British Geological Survey. (n.d.). How does BGS classify landslides. Retrieved 08 30, 2016, from British Geological Survey: http://www.bgs.ac.uk/landslides/how_does_BGS_classify_landslides.html

Campos, A. (1998). Educacion y prevencion de desastres. La Red na Red de Estudios Sociales en Prevencion de Desatres en America Latina.Cardozo, C. P. & Monteiro, A. M. (2019). Assessing Vulnerability to

Natural Hazards in Nova Friburgo, Rio de Janeiro Mountain Region, Brazil. *Revista de Estudios Latinoamericanos Sobre Reducción Del Riesgo de Desastres REDER*, 3(2), 71–83.

Carvalho, C. S., Macedo, E. S. de, & Ogura, A. T. (2007). *Mapeamento de Riscos em Encostas e Margem de Rios*. Brasilia: Ministério das Cidades & Instituto de Pesquisas Tecnológicas.

Cardona, O. D. (2001). La necesidad de repensar de manera holistica los conceptos de vulnerabilidad y riesgo "Una critica y una Revision necesaria para la gestion". Work-Conference on Vulnerability in Disaster Theory and Practice, (p. 18). Wageningeon.

Cutter, S. L.: Boruff, B. J. & Shirley, W. L. (2003). Social Vulnerability to Environmental Hazards. *Social Science Quarterly,* 84(2), 242–261. https://doi.org/10.1111/1540-6237.8402002

Cardozo, C. P. & Monteiro, A. M. (2019). Assessing Vulnerability to Natural Hazards in Nova Friburgo, Rio de Janeiro Mountain Region, Brazil. *Revista de Estudios Latinoamericanos Sobre Reducción Del Riesgo de Desastres REDER*, 3(2), 71–83.

CENSUS (2010) *DP-1 Profile of General Population and Housing Characteristics: 2010*. https://factfinder.census.gov

CEPED UFSC. (2013). Atlas Brasileiro de Desastres Naturais 1991 a 2012. Florianópolis: CEPED UFSC.

CEPED UFSC. (2013). Atlas Brasileiro de Desastres Naturais: 1991 a 2012. Florianópolis: CEPED UFSC.

CEPED UFSC. (2015, 08 12). 2011 - Inundações e Deslizamentos - Região Serra- do Rio de Janeiro. Retrieved 08 07, 2016, from CEPED UFSC: http://www.ceped.ufsc.br/2011-inundacoes-e-deslizamento-na-regiao-serrana-do-rio-de-janeiro/

Cerri, L. E., & Amaral, C. P. (1998). Riscos geologicos. In A. M. Santos, & S. N. Brito, Geologia de engenharia. Sao Paulo: Associacao Brasileira de Geologia de Engenharia.

Chacon, J., Irigaray, C., Hamdouni, R. E., & Jimenez-Peralvarez, J. (2014). Urban Landslides at the South of Sierra Nevada and Coastal Areas of the Granada Province (Spain) - Springer. In K. S. al., Lanslide Science for a Safer Geoenvironment (Vol. 3, pp. 425-430). Springer International Publishing Switzerland.

Chacón, J., Irigaray, C., Fernández, T. E., & Hamdouni, R. (2006). Engineering geology maps: Landslides and geographical information systems. Bulletin of Engineering Geology and the Environment, 65(4), 341-411.

Chambers, R. (1989) Vulnerability, coping and policy. *Institute of Development Studies Bulletin,,* 2, 20, p. 1-7.

Christensen, R. H. B. (2018). Cumulative Link Models for Ordinal Regression with the R Package ordinal. Journal of Statistical Software, (Christensen 2018), 1–40.

Chung, C., & Fabbri, A. (2003). Validation of spatial prediction models for landslide hazard mapping. Natural Hazards, 30(3), pp. 451-472.

Clark, G; Moser, S; Ratick, S.; Dow, K, Meyer, W.; Jin, W.; Kasperson, J.; Kasperson, R.; Schwarz, H. (1998). Assessing the vulnerability of coastal communities to extreme storms: the case of Reverse, MA, USA. *Mitigation and Adaptation Strategies for Global Change*, 3, 59-82, Kluwer Academic Publishers.

Clarke, K. (2014). Maps & Web Mapping. Pearson College Dv.

CNN. (2015, 05 20). Colombia landslide kills dozen. Retrieved 08 07, 2016, from CNN: http://www.cnn.com/2015/05/18/americas/colombia-salgar-deadly-landslide/

CNN. (2015, 10 10). Guatemala landslide death toll rises to 271. Retrieved 08 07, 2016, from CNN: http://www.cnn.com/2015/10/10/americas/guatemala-landslide-deaths/

Coach, N. K. (1995). Geohazards - Natural and human. New Jersey: Prentice Hall.

Coromi-s, J., van Western, C., Cascini, L., Malet, J. P., Fotopoulou, S., Catani, F., Smith, J. T. (2014, May). Recommendations for the quantitative analysis of landslide risk. Bulletin of Engineering Geology and the Envionment, 73(2), pp. 209-263.

Cozier, M. J., & Glade, T. (2004). Landslide Hazard and Risk Issues, Concepts and Approach. In T. Glade, M. Anderson, & M. J. Crozier, Landslide Hazard and Risk (pp. 1-40). Hoboken, NJ: John Willey & Sons.

CPRM (2019). Mapa Geológico da Região Metropolitana de São Paulo – Escala 1:250.000.

CRED . (2015, 12 22). Retrieved from EM-DAT The International Disaster Database: http://emdat.be/Glossary

Cruden, D. M., & Varnes, D. J. (1996). Landslides: investigation and mitigation. In A. K. Turner, & R. L. Shuster, Landslides: investigation and mitigation. Washington, USA: National Academy of Science.

Cutter, S. L.: Boruff, B. J. & Shirley, W. L. (2003). Social Vulnerability to Environmental Hazards. *Social Science Quarterly,* 84(2), 242–261. https://doi.org/10.1111/1540-6237.8402002

Daily Mail. (2010, April 09). *Daily Mail.* Retrieved from http://www.dailymail.co.uk/news/article-1264601/Brazil-floods-Rio-De-Janeiro-mudslide-kills-200-people.html

Das, F. C., Lee, C. F., & Ngai, Y. Y. (2002). Landslide risk assessment and management – an overview . Engineering Geology, 64, 65-87.Das, I. C. (2011). *Spatial statistical modelling for assessing landslide hazard and vulnerabiity.* Enschede, TheNetherlands: ITC - Faculty of Geo-information science and earth observation - University of Twente.

Das, I. C. (2011). *Spatial statistical modelling for assessing landslide hazard and vulnerability.* Enschede, TheNetherlands: ITC - Faculty of Geo-information science and earth observation - University of Twente.

Davis, J. D., & Sims, S. M. (2013, September 07). Physical and maximum entropy models applied to inventories of hillslope sediments sources. (S.-V. B. 2013, Ed.) *J Soil Sediments*, p. 20 pages.

131

De Blasio, F. V. (2011) Friction, Cohesion, and Slope Stability. In: *Introduction to the Physics of Landslides – lecture notes on the dynamics of mass wasting.* Springer Science + Business Media B.V.

Dazzi, Carmelo & Papa, Giuseppe Lo (2015). Anthropogenic soils: general aspects and features. *Ecocycles,* 1(1), pages 308, DOI: DOI: http://dx.doi.org/10.19040/ecocycles.v1i1.23

Diário do Transporte. (2020, February 10). Deslizamento deixa bairro sem ônibus em São Bernardo do Campo. Retrieved May 22, 2020, from https://diariodotransporte.com.br/2020/02/10/deslizamento-deixa-bairro-sem-onibus-em-sao-bernardo-do-campo/

Dietrich, W. E., Asua, R. R., Orr, J. C., & Trso, M. (1998). *A validation study of the shallow slope stability model, SHALSTAB, in forested lands of Northern California.* Berkley.

Dietrich, W. E., Bellugi, D., & Asua, R. R. (2001). Validation of the Shallow Landslide Model, SHALSTAB, for Forest Management. *Water Science and Application, 2*, 195-227.

Dietrich, W., & Montgomery, D. (1998, November 29). *Shalstab: a digital terrain model for mapping shallow landslide potential*. Retrieved from Geomorph//shalstab: http://calm.geo.berkeley.edu/geomorph//shalstab/

Dourado, F., Arraes, T. C., & Silva, M. F. (2012). O Megadesastre da Região Serrana do Rio de Janeiro - as causas do evento, os mecanismos dos movimentos de massa e a distribuição espacial dos investimentos de reconstrução no pós-desastre . *Anu. Inst. Geocienc., 35*(2), pp. 43-54.

Dunning, S. A., Massey, C. I., & Rosser, N. J. (2009). Structural and geomorphological features of landslides in the Bhutan Himalaya derived from Terrestrial Laser Scanning. *Geomorphology*, 17-29.

Dwyer, A.; Zoppou, C. & Nielsen, O. (2004). Quantifying Social Vulnerability: A methodology for identifying those at risk to natural hazards. *Spatial Information for the Nation*, 101.

EBC. (2014, 06 19). *Deslizamentos de terra em Natal atingem 100 famílias.* Retrieved from EBC Agência Brasil: http://agenciabrasil.ebc.com.br/geral/noticia/2014-06/deslizamentos-de-terra-em-Natal-atingem-100-familias

EM-DAT. (2016, June 13). *EM-DAT Base.* Retrieved from EM-DAT Base: http://www.emdat.be/advanced_search/index.html

EMPLASA (2019). Sobre a RMSP, Retrieved 10 of September 2020, from: https://emplasa.sp.gov.br/RMSP

Ermini, L., Catani, F., & Casagli, N. (2005). Artificial Neural Networks applied to landslide susceptibility assessment. *Geomorphology*, *66*(1-4 SPEC. ISS.), 327–343. https://doi.org/10.1016/j.geomorph.2004.09.025

ESRI. (2016). *ESRI.* Retrieved from ESRI: http://www.esri.com/

Estadão. (2011, 01 13). Catástrofe no Rio de Janeiro. Retrieved 08 07, 2016, from Estadão: http://blogs.estadao.com.br/olhar-sobre-o-mundo/catastrofe-no-rio-de-janeiro/

Fan, D., Cui, X.-m., Yuan, D.-b., Wang, J., Yang, J., & Wang, S. (2011). Weight of Evidence Method and Its Applications and Development. *Procedia Environmental Sciences , 11*, pp. 1412-1418.

FAO, 2006. *World reference base for soil resources, 2006: A framework for international classification, correlation, and communication*. Rome: Food and Agriculture Organization of the United Nations

Feizizadeh, B., & Blaschke, T. (2013). GIS-Multicriteria Decision Analysis for landslide susceptibility mapping: comparing three methods for the Urmia lake basin, Iran. *Natural Hazards*, *65*(3), 2105–2128. https://doi.org/10.1007/s11069-012-0463-3

Fedeski, M., & Gwillian, J. (2007). Urban sustainability in the presence of flood and geological hazards: the development of a GIS-based vulnerability and risk assessment methodology. *Landscape and urban planning, 83*, 50-61.

Fernández, T., Irigaray, C., Hamdount, R. E., & Chacón, J. (2003). Methodology for landslide susceptibility mapping by means of a GIS. Application to the Contraviesa Area (Granada Spain). *Natural Hazards, 30*(3), 297-308.

Ferrier, N., & Haque, C. E. (2003). Hazard risk assessment methodology for emergency managers: a standardized framework for application. *Natural Hazards*(28), 271-290.

Fischer, B. (2014). A Century in the Present Tense: Crisis, Politics, and the Intellectual History of Brazil's Informal Cities. In B. Fischer, B. McCann, & J. Auyero, *Cities from scratch - poverty and informality in urban Latin America* (pp. 9-67). Durham and London: Duke University Press.

Flanagan, B. E.; Gregory, E. W.; Hallisey, E. J.; Heitgerd, J. L.; Lewis (2011). A Social Vulnerability Index for Disaster Management A Social Vulnerability Index for Disaster Management. *Journal of Homeland Security and Emergency Management*, 8(1). https://doi.org/10.2202/1547-7355.1792

Foret, F., Penetta, L., & Strobl, R. O. (2005). Historic records and GIS applications for flood risk analysis in the Salento peninsula (southern Italy). *Natural Hazards and Earth System Science, 5*(6), 833-844.

Folha de São Paulo. (2005, January 12). Deslizamentos de terra deixam 9 mortos e 3 feridos em São Bernardo. *Folha de São Paulo*.

Folha de São Paulo (2005, January 13). Deslizamento matam 9 em São Bernardo. Retrieved May 22, 2020 from https://www1.folha.uol.com.br/fsp/cotidian/ff1301200501.htm

Ford, A., Clarke, K. C., & Raines, G. (2009, July 27). Modeling Settlement Patterns of the Late Classic Maya Civilization with Bayesian Methods and Geographic Information Systems. *An-ls of Association of America Geographers*, pp. 496-520.

Forman, E. H., & Gass, S. I. (n.d.). *The Analytic Hierachy Process - An Exposition.* George Washington University/University of Maryland.

Formetta, G., Capparelli, G., Rigon, R., & Versace, P. (2014). Physically based landslide susceptibility models with different degree of complexity : calibration and verification. *International Environmental Modelling and Software Society (iEMSs).* San Diego, CA.

Frigerio, I.; Carnelli, F.; Cabinio, M. & De Amicis, M. (2018). Spatiotemporal Pattern of Social Vulnerability in Italy. *International Journal of Disaster Risk Science*, *9*(2), 249–262. https://doi.org/10.1007/s13753-018-0168-7

Godfrey, A.; Ciurean, R. L.; van Westen, C. J.; Kingma, N. C. & Glade, T. (2015). Assessing vulnerability of buildings to hydro-meteorological hazards using an expert based approach – An application in Nehoiu Valley, Romania. *International Journal of Disaster Risk Reduction*, 229–241. http://doi.org/10.1016/j.ijdrr.2015.06.001

Guzzetti, F.; Carrara, A.; Cardinali, M. & Reichenbach, P. (1999). Landslide hazard evaluation: A review of current techniques and their application in a multi-scale study, Central Italy. *Geomorphology*, *31*(1–4), 181–216. https://doi.org/10.1016/S0169-555X(99)00078-1

Hare, V. C. (2003). *Evaluation of a Geographic Information System Model of Shallow Landsliding in Redwood Creek, California - master of science thesis.* The Faculty of Humboldt State University.

Hancock, D. R. & Algozzine, B. (2018). *Doing Case Study Research: A practical Guide for Beginning Researchers*. *Dalton Transactions* (Vol. 47). New York and London: Teachers College Press. https://doi.org/10.1039/c8dt02254b Homeland Security. (2016). *National Disaster Recovery Framework*. *National Disaster Recovery Framework*. https://doi.org/10.1002/9780470925805.ch5

Hasekioğulları, G. D., & Ercanoglu, M. (2012). A new approach to use AHP in landslide susceptibility mapping: a case study at Yenice (Karabuk, NW Turkey). Natural Hazards, 63(2), 1157–1179. https://doi.org/10.1007/s11069-012-0218-1

Hayden, Tyler (2018, June 14). Public Survey Exposes Montecito Debris Flow Communication Failures. *Santa Barbara Independent.* Retrieved from https://www.independent.com/2018/06/14/public-survey-exposes-montecito-debris-flow-communication-failures/

Highland, L.M., and Bobrowsky, Peter, 2008, *The landslide handbook—A guide to understanding landslides*: Reston, Virginia, U.S. Geological Survey Circular 1325, 129 p.

Homeland Security (2016). *National Disaster Recovery Framework*, 2nd Edition.

Hummell, B. M. de Loyola; Cutter, S. L. & Emrich, C. T. (2016). Social Vulnerability to Natural Hazards in Brazil. International Journal of Disaster Risk Science, 7(2), 111–122. https://doi.org/10.1007/s13753-016-0090-9

Hyndman, Donald; Hyndman, David (2012). *Natural Hazards & Disasters.* 4th Edition. Brooks/Cole – Cengage Learning.

G1. (2012, January 09). Onze morreram em deslizamentos de terra no Rio e em Minas. Retrieved 01 05, 2016, from G1: http://g1.globo.com/jornal-nacional/noticia/2012/01/onze-morrem-em-deslizamentos-de-terra-no-rio-e-em-minas.html

G1. (2013, December 17). Deslizamento de terra deixa seis mortos em Minas Gerais. Retrieved January 05, 2016, from G1: http://g1.globo.com/jornalnacional/noticia/2013/12/deslizamento-de-terra-deixa-seis-mortos-em-minas-gerais.html

G1. (2015, March 27). Desabamento após chuvas deixam mortos em Salvador. Retrieved January 05, 2016, from G1: http://g1.globo.com/bahia/noticia/2015/04/crianca-morre-apos-desabamento-na-regiao-da-san-martin-em-salvador.html

Geomatic Laboratory. (2016). A model for shallow landslide susceptibility - R.SHALSTAB. Retrieved Nov 19, 2016, from Geomatic Laboratory: http://geomatic.disat.unimib.it/node/36

Goedecke, W. (2013). Efficacy of mathematical models using physical soil factors in determining landslide hazard (master of Science in Geographic Information System). San Francisco State University.

Gorsevski, P. V., Gessler, P. E., & Jankowski, P. (2003). Integrating a fuzzy k-means classification and a Bayesian approach for spatial prediction of landslide hazard. Journal of Geographical System, 223-251.

Gorsevski, P. V. E., & Jankowski, P. , Gessler, P. (2006). An heuristic approach for mapping landslide hazard by integrating fuzzy logic with analytic hierarchy process. *Control ad Cybernetics, 35, 1.*

Granger, K., Jones, T., Leiba, M., & Scott, G. (1999). Community Risk in Cairns: a multi-hazard risk assessment. Australian Geological Survey Organisation, Cites Project. Commonwealth of Australia.

Greele, G., Soriano, M., Revelino, P., Guerriero, L., Anderson, M. G., Diambra, A., Guadagno, F. M. (2014). Space-time prediction of rainfall-induced shallow landslides through a combined probabilistic approach optimized for initial water table conditions. Bulletin of Engineering Geology and the Environment, 73(3), 877-890.

Hamm, N., Hall, J., & Anderson, M. (2006). Variance-based sensitivity analysis of the probability of hydrologically induced slope instability. Computers and Geosciences, 32(6), 803-817.

Hare, V. C. (2003). Evaluation of a Geographic Information System Model of Shallow Landsliding in Redwood Creek, California - master of science thesis. The Faculty of Humboldt State University.

Hasekiog˘ulları, G. D., Ercanoglu, M. (2012) A new approach to use AHP in landslide susceptibility. *Natural Hazards*, 63, 1157-1179.

mapping: a case study at Yenice (Karabuk, NW Turkey).

Harell, F. (2015). Regression Modelling Strategies: With Applications to Linear Models, Logistic and Ordinal Regression, and Survival Analysis, 2nd Edition, Springer International Publishing AG Switzerland.

Highland, L.M., and Bobrowsky, Peter, 2008, The landslide handbook—A guide to understanding landslides: Reston, Virginia, U.S. Geological Survey Circular 1325, 129 p.

Hollenstein, K. (2005). Reconsidering the risk assessment concept: standardizing the impact description as a building block for vulnerability assessment. Natural hazards and earth system sciences(5), 301-307.

Hungr, O., Leroueil, S., & Picarelli, L. (2013). The Varnes classification of landslide types, an update. Landslides, 167-194.

Hussin, H. Y., Zumpano, V., Reichenbach, P., Sterlacchini, S., & Micu, M. v. (2016). Different landslide sampling strategies in a grid-based bi-variate statistical susceptibility model. Geomorphology, 508-523.

Hyndaman, D. & Hyndman, D. (2012). *Natural Hazards and Disasters*, 2nd Edition.

IBGE - Instituto Brasileiro de Geografia e Estatística. (2018). População em áreas de risco no Brasil. Rio de Janeiro: IBGE, 2018. 91 p. ISBN 978-85-240-4468-7

IBGE - Instituto Brasileiro de Geografia e Estatística. (2016). Infocidades. Retrieved November 1, 2016, from IBGE - Instituto Brasileiro de Geografia e Estatística: http://cidades.ibge.gov.br/xtras/perfil.php?codmun=354870

IG. (2012, October 22). Minas é estado com maior número de deslizamento de terra em 2012. Retrieved January 05, 2016, from IG: http://www.em.com.br/app/noticia/gerais/2013/10/22/interna_gerais,462492/minas-e-estado-com-maior-numero-de-deslizamentos-de-terra-em-2012.shtml

INPE. (2011). 7) Como se mede o índice de chuva? Retrieved November 18, 2016, from INPE - Instituto - cio-l de Pesquisas Espaciais: http://www.inpe.br/acessoainformacao/node/402

IBGE - Instituto Brasileiro de Geografia e Estatisitca. (2010). Aglomerados Subnormais Informacoes Territoriais. IBGE.

IBGE - Instituto Brasileiro de Geografia e Estatística. (2020). *Infocidades*. Retrieved May 31, 2020 from http://cidades.ibge.gov.br/xtras/perfil.php?codmun=354870

IPT – Instituto de Pesquisas Tecnológicas (2010). Mapeamento de Áreas de Risco – São Paulo

Irigaray, C., Fernández, T. E., Hamdouni, R., & Chacón, J. (2007). Evaluation and validation of landslide-susceptibility maps obtained by a GIS matrix method: Examples from the Betic Cordillera (southern Spain). *Natural Hazards, 41*(1), 61-79.

Iwai, O. K. (2003). *Mapeamento do uso do solo urbano do município de São Bernardo do Campo, através de imagens de satélites. Dissertação de mestrado.* São Paulo: Escola Politécica da Universidade de São Paulo (USP).

Jaboyedoff, M., Michoud, C., Derron, M. H., Voumard, J., Leibundgut, G., Sudmeier-Rieux, K., … Leroi, E. (2016). Human-Induced Landslides: Toward the analysis of anthropogenic changes of the slope environment. *Landslides and Engineered Slopes. Experience, Theory and Practice*, *1*(June), 217–232. https://doi.org/10.1201/b21520-20

Jäger, S., & Wieczorek, G. F. (1994). Landslide Susceptibility in the Tully Valley Area, Finger Lakes Region, New York. *US Geological Survey*, *615*, 1–15. https://doi.org/10.1111/acer.13536

Jesus, L. B. (2009). *A tecelagem tognato e as transformações do espaço industrial em São Bernardo do Campo.* São Paulo: Programa de Pós-graduação em geografia humana da Universidade de São Paulo (US).

Jiménez-Perálvarez, J. D., Irigaray, C., Hamdouni, R. E., & Chacón, J. (2011). Landslide-susceptibility mapping in a semi-arid mountain environment: An example from the southern slopes of Sierra Nevada (Grada, Spain). *Bulletin of Engineering Geology and the Environment, 70*(2), 265-277.

Jones, F. (1973). Landslides of Rio de Janeiro and the Sierra das Araras Escarpment, Brazil. U.S. Geological Survey Professional Paper.

Kayastatha, P. Dhital, M.R., De Smedt, F. (2013) Application of the analytical hierarchy process (AHP) for landslidesusceptibility mapping: A case study from the Tinau watershed,west Nepal. *Computers & Geosciences*, 52, 398-408.

Kaynia, a. M., Papathoma-Köhle, M., Neuhäuser, B., Ratzinger, K., Wenzel, H., & Medina-Cetina, Z. (2008). Probabilistic assessment of vulnerability to landslide: Application to the village of Lichtenstein, Baden-Württemberg, Germany. Engineering Geology, 101(1–2), 33–48. https://doi.org/10.1016/j.enggeo.2008.03.008

Kean, J. W.; Staley, D. M.; Lancaster, J. T.; Rengers, F. K.; Swanson, B. J.; Coe, J. A.; Hernandez, J.L.; Sigman, A.J.; Allstadt, K.E.; Lindsay, D. N. (2019). Inundation, flow dynamics, and damage in the 9 January 2018 Montecito debris-flow event, California, USA: Opportunities and challenges for post-wildfire risk assessment. *Geosphere*, *15*(4), 1140–1163. https://doi.org/10.1130/ges02048.1

Keller, E. A.; DeVecchio, D. E. (2016). *Earth's Process as Hazards, Disasters, and Catastrophes.* Fourth Edition. Routledge, New York.

Keller, E. (2011). *Environmental Geology* (Vol. 9). Upper Saddle River, New Jersey, United States: Pearson Prentice Hall.

Kemp, L. D., Bonham-Carter, G., & Raines, G. L. (1999). *Arc-WofE: Arcview extension for weights of evidence mapping*. Retrieved from http://www.ige.unicamp.br/wofe/documentation/wofeintr.htm

Kousalya, P., Reddy, G. M., Supraja, S., & Prasad, V. S. (2012). Analytical Hierarchy Process approach – An application of engineering education. *Mathematica Aeterna, 2*(10), pp. 861-878.

Lavell, A. (1999). *Gestion de Riesgos Ambientales Urbanos.* Red de Estudios Sociales en Prevention de Desatres en America Lati-. Retrieved 12 22, 2015, from http://www.desenredando.org/public/articulos/1999/grau/GestionDeRiesgosAmbientalesUrbanos-1.0-sep-12-2001.pdf

Lee, S. (2005). Application of logistic regression model and its validation for landslide susceptibility mapping using GIS and remote sensing data. *International Journal of Remote Sensing, 26*(7), pp. 1477-1491.

Lee, S. (2007). Application and verification of fuzzy algebraic operators to landslide susceptibility mapping. *Environmental Geology*, 615-623.

Lee, S., Chang, B., Choi, W., & Shin, E. (2002). Regional Susceptibility, Possibility and Risk Analyses of Landslide in Ulsan Metropolitan City, Korea. *IEEE*.

Lee, S., Choi, J., & Min, K. (2002). Landslide susceptibility a-lysis and verification using the Bayesian probability model. *Environmental Geology*, 120-131.

Lee, S., Choi, J., Chwae, J., & Chang, B. (2002). Landslide susceptibility a-lysis using weight of evidence. *Geoscience and Remote Sensing Symposium. 5*, pp. 2865-2867. Toronto, Canada: IEEE Inter-tio-l.

Lima, I. F. (2013). *O fluxo de massa do Vieira, Teresopolis-RJ, megadesastre da Serra em 2011: analise das feicoes sedimentologicas e de sua fenomenologia (dissertacao de mestrado).* Rio de Janeiro: UERJ.

Linkov, I., Massey, O., Keisler, J., Rusyn, I., & Hartung, T. (2015). Food for thought... from "weight of evidence" to quantitative data integration using multicriteria decision analysis and bayesian methods. *Altex, 32*(1), pp. 3-8.

Listo, F., & Vieira, B. C. (2012). Mapping of risk and susceptibility of shallow-landslide in the city of São Paulo, Brazil. *Geomorphology*, 30-44.

Liu, X. Y., Tham, L. G., & Lee, C. F. (2002). Empirical assessment of debris flow risk on a Regional Scale in Yun-n Province, Southwestern China. *Environmental Management, 30*(2), 249-264.

Long, N.T., De Smedt, F., 2012. Application of an analytical hierarchical process approach for landslide susceptibility mapping in A Luoi district, Thua Thien Hue Province, Vietnam. Environmental Earth Sciences 66 (7), 1739–1752.

Mahler, C. F., Varnada, E., & Oliveira, L. C. (2012, July). Analytical model of landslide risk using GIS. *Open Journal of Geology*, pp. 182-188.

Malczewski, J., & Rinner, C. (2015). *Multicriteria decision analysis in geographic information science.* Springer-Verlag Berlin Heidelberg.

Maricato, E. (2008). *Brasil, cidades: alternativas para a crise urbana.* Petropolis, RJ: Vozes.

Marchenzini, V. And Wisner, B. (2017) Chlallenges for vulnerability reduction in Brazil: Insights from PAR framework. In: Marchezini et al. *Reduction of vulnerability to disasters: from knowledge to action* . São Carlos, RIMA.

Marjanović, M., Kovačević, M., Bajat, B., & Voženílek, V. (2011). Landslide susceptibility assessment using SVM machine learning algorithm. *Engineering Geology*, *123*(3), 225–234. https://doi.org/10.1016/j.enggeo.2011.09.006

Maskrey, Andrew (1989). Disaster Mitigation: A Community Based Approach. Oxfam Publishing.

Masozera, Michel; Bailey, Melissa; Kerchner, Charles (2007). Distribution of impacts of natural disasters across income groups: A case study of New Orleans. *Ecological Economics,* v. 63, issue 2-3, 299-306

Matos, L. d. (2014). A vulnerabilidade das construções às corridas de detritos - bacia experimental do rio Guaxinduba - município de Caraguatatuba - SP (master dissertation). Faculdade de Filosofia, Letras e Ciências Humanas. São Paulo: Universidade de São PAulo.

Mejianavarro, M.; Wohl, E. E. & Oaks, S. D. (1994). Geological Hazards, Vulnerability, and Risk Assessment Using Gis - Model for Glenwood-Springs, Colorado. *Geomorphology*, *10*(1–4), 331–354. https://doi.org/Doi 10.1016/0169-555x(94)90024-8

Mezughi, T.H., Akhir, J.M., Rafek, A.G., Abdullah, I., 2012. Analytical Hierarchy Process method for mapping landslide susceptibility to an area along the E-W Highway (Gerik-Jeli), Malaysia. Asian Journal of Earth Sciences 5 (1), 13–24

Meyer, V., Scheuer, S., & Haase, D. (2009). A multicriteria approach for flood risk mapping at the Mulde river, Germany. Natural Hazards (48), 17-39.

Michel, G. P., Kobiyama, M., & Goerl, R. F. (2014). Comparative analysis of SHALSTAB and SINMAP for landslide susceptibility mapping in the Cunha River basin, southern Brazil. *Journal of Soils and Sediments*, *14*(7), 1266–1277. https://doi.org/10.1007/s11368-014-0886-4

Michoud, C., Derron, M. NaH., Jaboyedoff, M., Nadim, F., & Leroi, E. (2013). Classification of landslide-inducing anthropogenic activities - Exercise. Oslo: International Center for Geohazards (ICG).Ministério das Cidades (June 2008). *Ministério das Cidades.* Retrieved from Ministério das Cidades: https://www.cidades.gov.br/

Mishra, K. (2013). *Geomorphological studies and flood risk assessment of Kosi River BAsin using remote sensing and GIS techniques (thesis).* (I. I. NAI. Organisation, Ed.)

Mondal, S., & Maiti, R. (2012). Landslide Susceptibility Analysis of Shiv-Khola Watershed, Darjiling: A Remote Sensing & GIS Based Analytical Hierarchy Process (AHP). Journal of the Indian Society of Remote Sensing, 40(3), 483–496. https://doi.org/10.1007/s12524-011-0160-9

Montgomery, D. R., & Dietrich, W. E. (1994, April). A physically based model for the topographic control on shallow landsliding. *Water Resources Research, 30*(4), pp. 1153-1171.

Município de São Bernardo do Campo (2020). Cidades. Retrieved June 12, 2020 from https://www.saobernardo.sp.gov.br/en/cidade

Município de São Bernardo do Campo. (n.d.). TOTAIS MENSAIS (das medições da DCSBC; sem SAISP até dez.2011 e com SAISP após) . São Bernardo do Campo: Prefeitura de São Bernardo do Campo. Retrieved from https://doi.org/10.1029/93WR02979

Nimmo, J. R., Schmidt, K. M., Perkins, K. S., & Stock, J. D. (2009). Rapid Measurement of Field-Saturated Hydraulic Conductivity for Areal Characterization. *Vadose Zone Jornal, 8*(1), 8.

Nogueira, Fernando Rocha (2002). Gerenciamento de riscos ambientais associados a escorregamentos: Contribuição Às Políticas Públicas Municipais (dissertation). Universidade Estadual Paulista, Rio Claro.

Nogueira, F. R., Oliveira, V. E., & Cruz, B. A. (2014). A implementação local de políticas, programas e legislação em nível federal sobre riscos de desastres: o caso de São Bernardo do Campo, SP. *APPURBA- 2014* (pp. 1-16). Belém: UFPA.

Norušis, Marija J. (2012). Ordinal Regression. *IBM SPSS Statistics 19 Advanced Statistical Procedures Companion*. Prentice Hall. Retrieved from https://www.pearson.com/us/higher-education/program/Norusis-IBM-SPSS-Statistics-19-Advanced-Statistical-Procedures-Companion/PGM233179.html

O'Connell, A. A. O. (2011). Introduction. In Logistic Regression Models for Ordinal Response Variables (pp. 2–5). SAGE Publications, LTd. https://doi.org/http://dx.doi.org/10.4135/9781412984812 Print

Oliveira, K. (2013, December 21). Chuvas causam deslizamento de terra no Espírito Santo: 5 pessoas morreram. Retrieved January 05, 2016, from Agência Brasil: http://memoria.ebc.com.br/agenciabrasil/noticia/2013-12-21/chuvas-causam-deslizamentos-de-terra-no-espirito-santo-5-pessoas-morreram

Oliveira, L. C. (2004). *Análise Quantitativa de Risco emprego de Movimentos de Massa com Estatística Bayesia- [Rio de JAneiro] 2004 - tese de doutorado.* Universidade Federal do Rio de Janeiro. Rio de Janeiro: COPPE/UFRJ.

Papathoma-Kohle, M., N. B., Razinger, K., Wenzel, H., & Dominey-Howes, D. (2007, December 5). Elements at risk as a framework for assessing the vulnerability of communities to landslides. *Natural Hazards and Earth System Sciences*, pp. 765-779.

Petrópolis. (2013). *Plano de Contingência de Proteção e Defesa Civil - Plancon 2013/2014.* Petrópolis: Prefeitura de Petrópolis.

Phukon, P., Chetia, D., Das, P., 2012. Landslide susceptibility assessment in the Guwahati City, Assam using Analytic Hierarchy Process (AHP) and Geographic Information System (GIS). International Journal of Computer Applications in Engineering Sciences 2 (1), 1–6.

Pimiento, E. (2010). *Shallow Landslide Susceptibility Modelling and Validation.* Lund, Sweden: Lund University - Department of Earth and Ecosystem Science.

Pourghasemi, H.R., Pradhan, B., Gokceoglu, C., 2012. Application of fuzzy logic and analytical hierarchy process (AHP) to landslide susceptibility mapping at Haraz watershed, Iran. Natural Hazards 63 (2), 965–996.

Pradhan, B., Oh, H.-J., & Buchroithner, M. (2010). Weights-of-evidence model applied to landslide susceptibility mapping in a tropical hilly area. *Geomatics,Natural Hazards and Risk*, 199-223.

Prefeitura de São Ber-rdo do Campo. (n.d.). *TOTAIS MENSAIS (das medições da DCSBC; sem SAISP até dez.2011 e com SAISP após)* . São Bernardo do Campo: Prefeitura de São Bernardo do Campo.

Quarantetlli, E.L. (2000). Emergency, disaster and catastrophes are different phenomena. *Preliminary Paper # 304.* University of Delaware Disaster Research Center.

Rahman, N., Ansary, M. A., & Islam, I. (2015). GIS based mapping of vulnerability to earthquake and fire hazard in Dhaka city, Bangladesh. *International Journal of Disaster Risk Reduction, 13*, 291-300.

Reginatto, G. M. (2013). *Caracterização de movimentos de massa - bacia hidrográfica do Rio Cunha, Rio dos Cedros, SC, com ênfase em escorregamentos translacionais - dissertação de mestrado.* Universidade Ferderal de Santa Catarina, Centro Tecnológico - Programa de Pós-graduação em Engenharia Civil.

Reginatto, G. M., Maccarini, M., Kobiyama, M., Higashi, R. A., Grando, A., Corseuil, C. W., & Caramez, M. L. (2012, May). SHALSTAB application to identify the susceptible areas of shallow landslides in Cunha river watershed, Rio dos Cedros city, SC, Brazil. *4th GEOBIA*, (pp. 108-113). Rio de Janeiro.

Regino, T., Fukumoto, M. M., & Nogueira, F. R. (2014). Estratégia e processo de construção da gestão de risco associados à moradia em São Bernardo do Campo, SP. *Seminário URBFAVELAS 2014.* São Bernardo do Campo: Seminário URBFavelas.

Regmi, N. R., Giardino, J. R., & Vitek, J. D. (2010). Modeling susceptibility to landslides using the weight of evidence approach: Western Colorado, USA. *Geomorphology*, 172-187.

Remondo, J., Bo-chea, J., & Cendrero, A. (2005). A statistical approach to landslide risk modelling at basin scale: From landslide susceptibility to quantitative risk assessment. *Landslides*, 321-328.

Remondo, J., Gonzales-Diez, A., Diaz de Teran, J., & Cendrero, A. (2003). Landslide susceptibility models utilizing spatial data analysis technique. A case study from the Lower Debra Valley, Guipuzcoa (Spain). *Natural Hazards, 30*, 267-279.

Respondent 04. (2018, August). Personal Interview.

Respondent 05. (2018, August). Personal Interview.

Respondent 09. (2018, September). Personal Interview.

Respondent 11. (2018, September). Personal Interview.

Respondent 14. (2018, October). Personal Interview.

Respondent 18. (2018, October). Personal Interview.

Respondent 19. (2018, November). Personal Interview.

Respondent 20. (2018, November). Personal Interview.

Rocha, G. C. (2004). Landslide risk mapping methodology applied to medium size urbanities in Brazil: case study of Juiz de Fora town, Mi-s Gerais state. *Landslides: evaluation and stabilization*.

Rozos, D., Bathrellos, G. D., & Skillodimou, H. D. (2011). Comparison of the implementation of rock engineering system and analytic hierarchy process methods, upon landslide susceptibility mapping, using GIS: A case study from the Eastern Achaia County of Peloponnesus, GREECE. Environmental Earth Sciences, 63(1), 49–63. https://doi.org/10.1007/s12665-010-0687-z

Saaty, T. L. (1980). How to make a decision: the analytic hierarchy process. *European Journal of*

Operational Research, *48*(1), 9–26.

Saaty, T. L. (2008). Decision making with the analytic hierarchy process. *International Journal of Services Sciences*, *1*(1), 83. https://doi.org/10.1504/IJSSCI.2008.017590

Saaty, T. L. (1990). How to make a decision: The Analytic Hierarchy Process. *European Journal of Operational Research*. https://doi.org/10.1016/0377-2217(90)90057-I

Saaty, R. W. (1987). The analytic hierarchy process-what it is and how it is used. *Mathematical Modelling*, *9*(3–5), 161–176. https://doi.org/10.1016/0270-0255(87)90473-8

Saaty, T. L. (1994). How to make a decision: the a-lytic process. *24*(6), pp. 19-43.

Safaei, M., Omar, H., Yousof, Z. B., & Motevalli, A. (2013). Application of a Physically based Model for Terrain Stability Mapping in North of Iran. *Global Journal of Researches in Engineering, 13*(2).

Salciarini, D., Godt, J. W., Savage, W. Z., Conversini, P., Baum, R. L., & Michael, J. A. (2006). Modeling regional initiation of rainfall-induced shallow landslides in the eastern Umbria Region of central Italy . *Landslides*.

Santa Barbara County Fire Department (2018).

SãoBernardo.Info. (2019, March 20). Vídeo: Deslizamento de terra assusta moradores no Ferrazópolis. Retrieved May 22, 2020, from https://saobernardodocampo.info/34343/deslizamento-terra-ferrazopolis/

Scheid, C., Schmitt, T. G., Bischoff, G. H., Krieger, K., Waldhoff, A., & Gunner, C. (2013). GIS-based methodology for pluvial flood risk a-lysis in Hambourg. *Novatech*.

Sedan, A. H., & Suv, C. (2013). Analytic hierarchy process. *PowerPoint Presentation*, 1–22. https://doi.org/10.1002/9781118644898.ch2

Selby, M. J. (1993). Mass Wasting of Soils. *In: Hillslope Materials and Process*, 2nd Edition, New York, Oxford University Press.

Sezer, E. A., Pradhan, B., & Gokceoglu, C. (2011). Manifestation of an adaptive neuro-fuzzy model on landslide susceptibility mapping: Klang valley, Malaysia. *Expert Systems with Applications, 38*(7), 8208-8219.

Sidle, R. C., Pearce, A. J., & O'Loughlin, C. L. (185). *Hillslope Stability and Land Use.* Washington: American Geophysical Union.

Sidle, R. C., Pearce, A. J., & O'Loughlin, C. L. (1985). *Hillslope Stability and Land Use.* Washington D.C.: American Geophysical Union.

SMDU - Secretaria Municipal de Desenvolviment Urbano. (n.d.). *População Recenseada Região Metropolitana de São Paulo e Municípios.* Retrieved 11 01, 2016, from Prefeitura Municipal de São Paulo: http://infocidade.prefeitura.sp.gov.br/htmls/7_populacao_recenseada_1950_10552.html

Souza, F. T. (2004). *Predição de escorregamentos das encostas do município do Rio de Janeiro através de técnicas de mineração de dados (Ph.D. thesis).* Rio de Janeiro: UFRJ.

Souza, L. B., & Zanella, M. E. (2009). *Percepção de Riscos Ambientais: Teoria e Aplicações* . Fortaleza: Coleção Estudos Geográficos – Edições UFC .

Spizzichinno, D., Falconi, L., Delmonaco, G., & Margottini, C. &. (2004). Integrated approach for landslide risk assessment of Craco village (Italy). *Landslides: evaluation and stabilization*.

Srivastava, T. (2016, Febr 19). *Analytics Vidhya*. Retrieved Nov 19, 2016, from 7 Important Model Evaluation Error Metrics Everyone should know: https://www.analyticsvidhya.com/blog/2016/02/7-important-model-evaluation-error-metrics/

Süzen, M. L., & Doyuran, V. (2004). Data driven bivariate landslide susceptibility assessment using geographical information systems: A method and application to Asarsuyu catchment, Turkey. *Engineering Geology*, *71*(3–4), 303–321. https://doi.org/10.1016/S0013-7952(03)00143-1

Sujatha, E. R., Kumaravel, P., & Rajamanickam, G. V. (2014). Assessing landslide susceptibility using Bayesian probability-based weight of evidence model. *B. Eng Geol Environ , 73*, pp. 147-161.

Terra. (2005, January 12). Chuva provoca morte em São Bernardo. *Terra*.

Terra. (2013, January 03). *RJ: chuva provoca deslizamentos e deixa desabrigados em Angra*. Retrieved January 05, 2016, from Terra: http://noticias.terra.com.br/brasil/cidades/rj-chuva-provoca-deslizamentos-e-deixa-desabrigados-em-angra,ced8ffc4daffb310VgnVCM4000009bcceb0aRCRD.html

Terzaghi, K., Peck, R. B., Mesri, G. (1996) *Soil Mechanics in Engineering Practice*, 3rd edition. John Wiley & Sons.

The Guardian. (2014, 08 17). *Nepal flooding and landslides kill scores.* Retrieved 08 07, 2016, from The Guardian: https://www.theguardian.com/world/2014/aug/17/nepal-flooding-landslides-kill-scores

The Guardian. (2015, 10 06). *Guatemala landslide: under the mud dead families found huddled together.* Retrieved 08 07, 2016, from The Guardian: https://www.theguardian.com/world/2015/oct/06/guatemala-landslide-under-the-mud-dead-families-found-huddled-together

Thiery, Y., Malet, J. P., Sterlacchini, S., Puissant, A., & Maquaire, O. (2007). Landslide susceptibility assessment by bivariate methods at large scales: Application to a complex mountainous environment. *Geomorphology*, *92*(1–2), 38–59. https://doi.org/10.1016/j.geomorph.2007.02.020

Tominaga, L. K., Santoro, J., & Amaral, R. (2009). *Desastres naturais: conhecer para prevenir.* São Paulo: Instituto Geologico.

UCLA (2019, July 29). How do I interpret the coefficients in an ordinal logistic regression in R? R FAQ. Retrieved from UCLA Statistical Consulting Group: https://stats.idre.ucla.edu/r/faq/ologit-coefficients/

UCLA (2019, July 29). Ordinal Logistic Regression/R Data analysis examples. Retrieved from UCLA Statistical Consulting Group: https://stats.idre.ucla.edu/r/dae/ordinal-logistic-regression/

UNDRR - UN Office for Disaster Risk Reduction (2017). Terminology. Retrieved from https://www.unisdr.org/we/inform/terminology#letter-v

UNDRR - UN Office for Disaster Risk Reduction (2016). Terminology related to Disaster Risk Reduction – updated technical non-paper. Retrieved from https://www.preventionweb.net/documents/oiewg/Terminology%20related%20to%20Disaster%20Risk%20Reduction%20-%20updated%20technical%20non-paper%2030%20September%202016.pdf

United Nations (2004). Living with Risk – a global review of disaster reduction, volume I, New York and Geneva.

UNISDR. (2009). *Terminology on Disaster Risk Reduction.* Geneva: UNISDR. Retrieved from http://www.unisdr.org/files/7817_UNISDRTerminologyEnglish.pdf

United Nations. (2014, July 10). *Word's population increasingly urban with more than half living in urban areas.* Retrieved November 16, 2016, from United Nations: http://www.un.org/en/development/desa/news/population/world-urbanization-prospects-2014.html

United Nations (2015). Report of the open-ended intergovernmental expert working group on indicators and terminology relating to disaster risk reduction. Retrieved from UNISDR: https://www.preventionweb.net/files/50683_oiewgreportenglish.pdf

United Nations Human Settelements Programe. (2003). *The challenge of slums: global report on human settlements.* Gateshead: Earthscan Publications Ltd.

UN-SPIDER - United Nations Office for Outer Space Affairs (2019, June). Knowledge Portal. Retrieved from UN-SPIDER: http://www.un-spider.org/risks-and-disasters/disaster-risk-ma-gement

U.S. Census. (2015, December 11). *International Programs*. Retrieved from United States Census Bureau: https://www.census.gov/population/inter-tio-l/data/idb/informationGateway.php

UOL (2017, January 31). Deslizamentos de terra mataram 202 pessoas nos últimos 20 anos na Grande SP. Retrieved July 08, 2020 from https://noticias.uol.com.br/cotidiano/ultimas-noticias/2017/01/31/deslizamentos-de-terra-mataram-202-pessoas-nos-ultimos-20-anos-na-grande-sp.htm

USDA - United States Department of Agriculture. (n.d.). Bulk Density Test. Retrieved July 2016, from Natural Resources Conservation Service: http://www.nrcs.usda.gov/Internet/FSE_DOCUMENTS/nrcs142p2_050957.pdf

USDA. (n.d.). Soil Bulk Density/Moisture/Aeration. Retrieved from USDA - United States Department of Agriculture: https://www.nrcs.usda.gov/Internet/FSE_DOCUMENTS/nrcs142p2_053260.pdf

USGS. (2004, July). Landslide Types and Processes. UCGS Science for a Changing world.

USGS. (2016, November 16). USGS Faqs. Retrieved from USGS: https://www2.usgs.gov/faq/node/2613

USGS. (2019, June). Catastrophic Landslides of the 20th Century - Worldwide. Retrieved from USGS: https://www.usgs.gov/-tural-hazards/landslide-hazards/science/catastrophic-landslides-20th-century-worldwide?qt-science_center_objects=0#qt-science_center_objects

van Westen, C. (n.d.). Introduction to landslides Part 4: Use of GIS for landslide mapping. ITC, International Institute for Aerospace Survey and Earth Science.

Van Westen, C. J. (1993). Application of geographic information systems to landslide haazard zonation (thesis). Enschede, The Netherlands: International Institute for Aerospace Survay and Earth Sciences (ITC).

Van Westen, C. J., Rengers, N., & Soeters, R. (2003). Use of geomorphological information in indirect landslide susceptibility assessment. *Natural Hazards*, *30*(3), 399–419. https://doi.org/10.1023/B:NHAZ.0000007097.42735.9e

Van Westen, C. J., Van Asch, T. W., & Soeters, R. (2006). Landslide hazard and risk zonation - why is it still so difficult? Bull. Eng. Geol. Env., 65, 167-184.

Varnes, D. J. (1978). Slope Movement Types and Processes. In R. L. Schuster, & R. J. Krizek, Landslides A-lysis and Control - Special Report 176. Washington: National Academy of Sciences.

Varnes, D. J. (1984). Landslide hazard zonation: a review of principles and practice. Paris: Unesco.

Vaunat, J., & Leroueil, S. (2002). Analysis of post-failure slope movements within the framework of hazard and risk a-lysis. Natural Hazards(26), 83-109.

Vieira, B. C., & Ramos, H. (2015). Aplicação do Modelo SHALSTAB para mapeamento da suscetibilidade a escorregamentos rasos em Caraguatatuba, Serra do Mar (SP). Revista do Departamento de Geografia - USP, 29, 161-1744.

Wahono, B. F. (2010). Applications of statistical and heuristic methods for landslide susceptibility assessments: A case study in Wadas Lintang Sub District, Wonosobo Regency, Central Java Province, Indonesia. (master dissertation). Indonesia: Gadjah Mada university - International Institute for Geo-information and earth observation.

Wallace, M., Holcombe, E. A., Anderson, M. G., & Newbold, D. M. (2012). High-throughput landslide modelling using computatio-l grids. Geophysical Research Abstracts, 14.

Wallemacq, P; House, Rowena (2018). Economic Losses, Poverty & Disasters: 1998-2017. CRED and UNDRR, 31p.

Watts, M. J. & Bohle, H. G. (1993). The space of vulnerability: The causal structure of hunger and famine. *Progress in Human Geography*, *17*(1), 43–67. https://doi.org/10.1177/030913259301700103

Wisner, B. (1998). Marginality and vulnerability. *Applied Geography*, *18*(1), 25–33. https://doi.org/10.1016/s0143-6228(97)00043-x

Wisner, B. & Luce, H. R. (1993). Disaster vulnerability: Scale, power and daily life. *GeoJournal*, *30*(2), 127–140. https://doi.org/10.1007/bf00808129

Wisner, B.; Blaikie, P.; Cannon, T. & Davis, I. (2003). *At Risk: Natural Hazards, People's Vulnerability, and Disasters.* Human Ecology (Second, Vol. 24). https://doi.org/10.4324/9780203428764

Witt, A. C. (2005). Using a GIS (Geographic Information System) to model slope instability and debris flow hazards in the French Broad River Watershed, North Carolina (master of Science - Marine, Earth and Atmospheric Sciences). North Carolina State University.

Wu, C. H., & Chen, S. C. (2009). Determining landslide susceptibility in Central Taiwan from rainfall and six site factors using the analytical hierarchy process method. Geomorphology, 112(3–4), 190–204. https://doi.org/10.1016/j.geomorph.2009.06.002

Wu, Q., Ye, S., Wu, X., & Chen, P. (2004). Risk assessment of earth fractures by constructing an intrinsic vulnerability map, a specific vulnerability map, and a hazard map, using Yuci City, Shanxi, Chi- as an example. Environmental Geology(46), 104-112.

Xu, C., Cui, Y., Xu, X., Bao, P., Fu, G., & Jiang, W. (2019). An anthropogenic landslide dammed the Songmai River, a tributary of the Jinsha River in Southwestern China. *Natural Hazards*, *99*(1), 599–608. https://doi.org/10.1007/s11069-019-03740-y

Yalcin, A. (2008). GIS-based landslide susceptibility mapping using analytical hierarchy process and bivariate statistics in Ardesen (Turkey): Comparisons of results and confirmations. Catena, 72(1), 1–12. https://doi.org/10.1016/j.catena.2007.01.003

Yalcin A, Reis S, Cagdasoglu A, Yomralioglu T (2011) A GIS-based comparative study of frequency ratio, analytical hierarchy process, bivariate statistics and logistics regression methods for landslide susceptibility mapping in Trabzon, NE Turkey. Catena 85:274–287

Zaidan, R. T., & Fernandes, N. F. (2009). Zoneamento de susceptibilidade a escorregamentos em encostas à Bacia de Drenagem Urbana do Córrego do Independência - Juiz de Fora (MG). Revista Brasileira de Geomorfologia, 10(2), pp. 57-76.

APPENDIX

Appendix 2.1

Nome						
Instituição				email		
Formação				Idade		
Tempo de atuação em áreas de risco				Sexo	F	M	outro

AHP para áreas de risco de escorregamento

O AHP (Analytical Hierarchy Process) é um processo desenvolvido por Thomas L. Saaty que calcula pesos para diferente parâmetros baseado no seu grau de influência sobre o processo estudado. O AHP, neste estudo, será usado para computar o peso de cada um dos parâmetros utilizados no mapeamento de áreas de risco de escorregamento raso (translational slide), em áreas urbanas, e desencadeadas por chuvas.

<u>Instrução:</u>

As próximas questões apresentarão fatores naturais e antrópicos que contribuem para o grau de risco de escorregamento raso em áreas urbanas.

Cada questão compara dois parâmetros. Você deve selecionar um dos parâmetros (A ou B) que, em sua opinião, contribui para um maior grau de risco; ou, caso considere os dois parâmetros de igual importância, você deve selecionar a opção (1). Caso tenha selecionado um dos parâmetros (A ou B), você deve apontar qual o seu o grau de importância para um maior grau de risco (valores entre 2 e 9) em relação ao outro parâmetro (o que não foi escolhido). Explicação para os valores 1 a 9 na tabela a seguir.

Valores	1	2	3	4	5	6	7	8	9

	igual importância		moderadamente mais importante		fortemente importante	muito formente importante	extremamente importante

*2, 4, 6, 8: valores intermediários entre seus adjacentes.

Questões:

PARTE A: Aspectos naturais, aspectos antrópicos, e sinais de instabilidade/evidências de movimentação.											
Aspectos naturais (A) ou aspectos antrópicos (B).	A	B	1	2	3	4	5	6	7	8	9
Aspectos naturais (A) ou sinais de instabilidade (B).	A	B	1	2	3	4	5	6	7	8	9
Sinais de instabilidade (A) ou aspectos antrópicos (B).	A	B	1	2	3	4	5	6	7	8	9

PARTE B - Aspectos Naturais											
Ângulo de inclinação (A) ou tipo de solo (B).	A	B	1	2	3	4	5	6	7	8	9
Ângulo de inclinação (A) ou cobertura natural do terreno (B).	A	B	1	2	3	4	5	6	7	8	9
Ângulo de inclinação (A) ou geologia do terreno (B).	A	B	1	2	3	4	5	6	7	8	9
Tipo de solo (A) ou cobertura natural do terreno (B).	A	B	1	2	3	4	5	6	7	8	9
Tipo de solo (A) ou geologia do terreno (B).	A	B	1	2	3	4	5	6	7	8	9
Cobertura natural do terreno (A) ou geologia do terreno (B).	A	B	1	2	3	4	5	6	7	8	9
B1 - Estrutura geológica											
Favorável à estabilidade (A) ou não observada (B).	A	B	1	2	3	4	5	6	7	8	9
Favorável à estabilidade (A) ou desfavorável à estabilidade (B).	A	B	1	2	3	4	5	6	7	8	9
Não observada (A) ou desfavorável à estabilidade (B).	A	B	1	2	3	4	5	6	7	8	9
B2 - Ângulo de Inclinação (θ) em graus *($\theta < 10$, $10 \leq \theta < 17$, $17 \leq \theta < 30$, $30 \leq \theta < 60$, $60 \leq \theta < 90$, $\theta = 90$)*											
$\theta < 10$ (A) OU $10 \leq \theta < 17$ (B).	A	B	1	2	3	4	5	6	7	8	9
$\theta < 10$ (A) OU $17 \leq \theta < 30$ (B)	A	B	1	2	3	4	5	6	7	8	9
$\theta < 10$ (A) OU $30 \leq \theta < 60$ (B)	A	B	1	2	3	4	5	6	7	8	9

$\theta < 10$ (A) OU $60 \leq \theta < 90$ (B)	A	B	1	2	3	4	5	6	7	8	9
$\theta < 10$ (A) OU $\theta = 90$ (B).	A	B	1	2	3	4	5	6	7	8	9
$10 \leq \theta < 17$ (A) ou $17 \leq \theta < 30$ (B).	A	B	1	2	3	4	5	6	7	8	9
$10 \leq \theta < 17$ (A) ou $30 \leq \theta < 60$ (B).	A	B	1	2	3	4	5	6	7	8	9
$10 \leq \theta < 17$ (A) ou $60 \leq \theta < 90$ (B).	A	B	1	2	3	4	5	6	7	8	9
$10 \leq \theta < 17$ (A) ou $\theta = 90$ (B).	A	B	1	2	3	4	5	6	7	8	9
$17 \leq \theta < 30$ (A) ou $30 \leq \theta < 60$ (B).	A	B	1	2	3	4	5	6	7	8	9
$17 \leq \theta < 30$ (A) OU $60 \leq \theta < 90$ (B).	A	B	1	2	3	4	5	6	7	8	9
$17 \leq \theta < 30$ (A) ou $\theta = 90$ (B).	A	B	1	2	3	4	5	6	7	8	9
$30 \leq \theta < 60$ (A) OU $\theta = 90$ (B).	A	B	1	2	3	4	5	6	7	8	9
$30 \leq \theta < 60$ (A) OU $60 \leq \theta < 90$ (B).	A	B	1	2	3	4	5	6	7	8	9
$60 \leq \theta < 90$ (A) OU $\theta = 90$ (B).	A	B	1	2	3	4	5	6	7	8	9

PARTE C: Aspectos antrópicos

(*Tipo de construção:* olhar C1,

Posição da construção: olhar C2,

Densidade da ocupação: olhar C3)

Tipo de construção (A) ou água no terreno (B).	A	B	1	2	3	4	5	6	7	8	9
Tipo de construção (A) ou lixo no terreno (B).	A	B	1	2	3	4	5	6	7	8	9
Tipo de construção (A) ou posição da construção (B).	A	B	1	2	3	4	5	6	7	8	9
Tipo de construção (A) ou densidade da ocupação (B).	A	B	1	2	3	4	5	6	7	8	9
Água no terreno (A) ou posição da construção(B).	A	B	1	2	3	4	5	6	7	8	9
Água no terreno (A) ou lixo no terreno(B).	A	B	1	2	3	4	5	6	7	8	9
Água no terreno (A) ou densidade da ocupação(B).	A	B	1	2	3	4	5	6	7	8	9
Lixo no terreno (A) ou posição da construção(B).	A	B	1	2	3	4	5	6	7	8	9
Lixo no terreno (A) ou densidade da ocupação (B).	A	B	1	2	3	4	5	6	7	8	9
Posição da construção (A) ou densidade da ocupação (B)	A	B	1	2	3	4	5	6	7	8	9

C1 - Tipos de Construção:

Qual tipo de construção contribui para um maior grau de risco? E para o tipo de construção escolhida, qual o seu grau de importância para um maior grau de risco?

Madeira (A) ou alvenaria (B).	A	B	1	2	3	4	5	6	7	8	9
Madeira (A) ou mista (papelão, madeira, e/ou outro material) (B).	A	B	1	2	3	4	5	6	7	8	9
Mista (papelão, madeira, e/ou outro material) OU alvenaria (B)	A	B	1	2	3	4	5	6	7	8	9

C2 - Posição da construção.

(Moradia próxima a base da encosta: localizada em uma distância menor ou igual altura do talude,

moradia distante da base da encosta: localizada numa distância maior do que a altura do talude)

Moradia próxima a base da encosta (A) ou moradia próxima ao topo da encosta (B).	A	B	1	2	3	4	5	6	7	8	9
Moradia próxima a base da encosta (A) ou moradia no meio da encosta (B).	A	B	1	2	3	4	5	6	7	8	9
Moradia próxima a base da encosta (A) ou moradia distante da base da encosta (B).	A	B	1	2	3	4	5	6	7	8	9
Moradia próxima a base da encosta (A) ou moradia distante do topo da encosta (B)	A	B	1	2	3	4	5	6	7	8	9
Moradia no meio da encosta (A) ou moradia próxima do topo da encosta (B).	A	B	1	2	3	4	5	6	7	8	9
Moradia no meio da encosta (A) ou moradia distante da base da encosta (B).	A	B	1	2	3	4	5	6	7	8	9
Moradia no meio da encosta (A) ou moradia distante do topo da encosta (B).	A	B	1	2	3	4	5	6	7	8	9
Moradia próxima do topo da encosta (A) ou moradia distante da base da encosta (B)	A	B	1	2	3	4	5	6	7	8	9
Moradia próxima do topo da encosta (A) ou moradia distante do topo da encosta (B)	A	B	1	2	3	4	5	6	7	8	9
Moradia distante da base da encosta (A) ou moradia distante do topo da encosta (B)	A	B	1	2	3	4	5	6	7	8	9

C3 - Densidade da ocupação

(Área consolidada: áreas densamente ocupadas, com infraestrutura básica.

Área parcialmente consolidada: áreas em processo de ocupação, adjacentes as áreas de ocupação consolidada.

Densidade da ocupação variando de 30% a 90%. Razoável infraestrutura básica.

Área parcelada: áreas de expansão, periféricas e distantes de núcleo urbanizado. Baixa densidade de ocupação (até

30%). Desprovidas de infraestrutura básica.

Área mista: considera-se a área quanto à densidade de ocupação e a implantação de infraestrutura básica.)

Área consolidada (A) ou Área parcialmente consolidada (B).	A	B	1	2	3	4	5	6	7	8	9
Área consolidada (A) ou Área parcelada (B).	A	B	1	2	3	4	5	6	7	8	9
Área consolidada (A) ou Área mista(B).	A	B	1	2	3	4	5	6	7	8	9

Área parcialmente consolidada (A) ou Área parcelada (B).	A	B	1	2	3	4	5	6	7	8	9
Área parcialmente consolidada (A) ou Área mista (B).	A	B	1	2	3	4	5	6	7	8	9
Área parcelada (A) ou Área mista (B).	A	B	1	2	3	4	5	6	7	8	9
C2 - Água no terreno											
Lançamento de água servida em superfície (A) ou concentração de água de chuva em superfície(B)	A	B	1	2	3	4	5	6	7	8	9
Lançamento de água servida em superfície (A) ou vazamento da tubulação (B)	A	B	1	2	3	4	5	6	7	8	9
Lançamento de água servida em superfície (A) ou fossa septica (B)	A	B	1	2	3	4	5	6	7	8	9
Lançamento de água servida em superfície (A) ou tipo de sistema de drenagem (B)	A	B	1	2	3	4	5	6	7	8	9
Concentração de água da chuva em superfície (A) ou vazamento da tubulação (B)	A	B	1	2	3	4	5	6	7	8	9
Concentração de água da chuva em superfície (A) ou fossa séptica (B)	A	B	1	2	3	4	5	6	7	8	9
Concentração de água da chuva em superfície (A) ou tipo de sistema de drenagem (B)	A	B	1	2	3	4	5	6	7	8	9
Vazamento da tubulação (A) ou fossa séptica (B)	A	B	1	2	3	4	5	6	7	8	9
Vazamento da tubulação (A) ou tipo de sistema de drenagem (B)	A	B	1	2	3	4	5	6	7	8	9
Fossa séptica (A) ou tipo de sistema de drenagem (B)	A	B	1	2	3	4	5	6	7	8	9
C3 - Tipo de sistema de drenagem.											
Inexistente (A) OU precário (B).	A	B	1	2	3	4	5	6	7	8	9
Inexistente (A) OU satisfatório (B).	A	B	1	2	3	4	5	6	7	8	9
Precário(A) OU satisfatório (B).	A	B	1	2	3	4	5	6	7	8	9
C4 - Cobertura do terreno.											
Presença de árvores (A) ou vegetação rasteira/arbustiva (B).	A	B	1	2	3	4	5	6	7	8	9
Presença de árvores (A) ou área desmatada/solo exposto (B).	A	B	1	2	3	4	5	6	7	8	9
Presença de árvores (A) ou gramado/campo (B).	A	B	1	2	3	4	5	6	7	8	9
Presença de árvores (A) ou presença de bananeira (B).	A	B	1	2	3	4	5	6	7	8	9
Presença de árvores (A) ou cobertura urbana(B).	A	B	1	2	3	4	5	6	7	8	9

Vegetação rasteira/arbustiva (A) ou área desmatada/solo exposto (B).	A	B	1	2	3	4	5	6	7	8	9
Vegetação rasteira/arbustiva (A) ou gramado/campo (B).	A	B	1	2	3	4	5	6	7	8	9
Vegetação rasteira/arbustiva (A) ou presença de bananeira (B).	A	B	1	2	3	4	5	6	7	8	9
Vegetação rasteira/arbustiva (A ou cobertura urbana(B).	A	B	1	2	3	4	5	6	7	8	9
Área desmatada/solo exposto (A) ou gramado/campo (B).	A	B	1	2	3	4	5	6	7	8	9
Área desmatada/solo exposto (A) ou presença de bananeira (B).	A	B	1	2	3	4	5	6	7	8	9
Área desmatada/solo exposto (A) ou cobertura urbana(B).	A	B	1	2	3	4	5	6	7	8	9
Gramado/campo (A) ou presença de bananeira (B).	A	B	1	2	3	4	5	6	7	8	9
Gramado/campo (A) ou cobertura urbana(B).	A	B	1	2	3	4	5	6	7	8	9
Presença de bananeira (A) ou cobertura urbana(B).	A	B	1	2	3	4	5	6	7	8	9

D - Sinais de instabilidade no terreno

Muro e/ou parede embarrigado (A) ou trinca na moradia (B).	A	B	1	2	3	4	5	6	7	8	9
Muro e/ou parede embarrigado(A) ou árvores, postes, muros inclinados (B).	A	B	1	2	3	4	5	6	7	8	9
Muro e/ou parede embarrigado (A) ou degrau de abatimento (B).	A	B	1	2	3	4	5	6	7	8	9
Muro e/ou parede embarrigado (A) ou cicatriz de escorregamento (B).	A	B	1	2	3	4	5	6	7	8	9
Muro e/ou parede embarrigado (A) ou trinca no terreno(B).	A	B	1	2	3	4	5	6	7	8	9
Trinca na moradia (A) ou árvores, postes, muros inclinados (B).	A	B	1	2	3	4	5	6	7	8	9
Trinca na moradia (A) ou degrau de abatimento (B).	A	B	1	2	3	4	5	6	7	8	9
Trinca na moradia (A) ou cicatriz de escorregamento (B).	A	B	1	2	3	4	5	6	7	8	9
Trinca na moradia (A) ou trinca no terreno (B).	A	B	1	2	3	4	5	6	7	8	9
Árvores, postes, muros inclinados (A) ou degrau de abatimento (B).	A	B	1	2	3	4	5	6	7	8	9
Árvores, postes, muros inclinados (A) ou cicatriz de escorregamento (B).	A	B	1	2	3	4	5	6	7	8	9
Árvores, postes, muros inclinados (A) ou trinca no terreno (B).	A	B	1	2	3	4	5	6	7	8	9
Degrau de abatimento (A) ou cicatriz de escorregamento (B).	A	B	1	2	3	4	5	6	7	8	9
Degrau de abatimento (A) ou trinca no terreno (B).	A	B	1	2	3	4	5	6	7	8	9
Cicatriz de escorregamento (A) ou trinca no terreno (B).	A	B	1	2	3	4	5	6	7	8	9

Appendix 2.2

Respondent	Institution	Field	Time working with landslide assessment (years)	Age (years)	Gender
Respondent 1	JICA[8]	Geology engineering	10	30	Female
Respondent 2	IPT[9]	Geology	10	45	Male
Respondent 3	Civil Protection of City of Jundiai	Geology	3.5	27	Male
Respondent 4	Ministry of Habitation of city of São Bernardo do Campo	Geology	7	43	Female
Respondent 5	COMPDEC[10], Castelo – Espirito Santo State	Geology	8	35	Female
Respondent 6	DRM [11]– Rio de Janeiro State	Geology	10	32	Female
Respondent 7	Cemaden[12]	Geography	9	34	Male
Respondent 8	Regea [13]	Geology	40		Male
Respondent 9	UFABC[14]	Geography		48	Female
Respondent 10	Santana de Parnaiba Municipality	Geology	15	54	Male
Respondent 11	Cemaden	Geology	25	50	Male
Respondent 12	Cemaden	Geography	11		Male
Respondent 13	IPT	Civil technician	25	58	Male
Respondent 14	IPT	Civil engineering	38	63	Male
Respondent 15	IPT	Geology	3	32	Female
Respondent 16	IPT	Civil engineering	3	30	Female
Respondent 17	IPT	Geology	13	46	Female
Respondent 18	IPT	Chemistry	20	54	Male
Respondent 19	IPT	Geology	30	61	Male
Respondent 20	IPT	Civil technician	37	61	Male
Respondent 21	São Paulo Municipality	Geology	25	59	Male
Respondent 22	São Paulo Civil Protection	Geoscience	4	26	Female
Respondent 23	Santos Civil Protection	Geology	4 months	26	Male

---

[8] JICA - Japan International Cooperation Agency

[9] IPT – Instituto de Pesquisas Tecnológicas (Institute for Technological Research)

[10] COMPDEC - Coordenadoria Estadual de Defesa Civil (State Dean of Civil Protection)

[11] DRM - Departamento de Recursos Minerais (Mineral Resource Department)

[12] Cemaden - Centro Nacional de Monitoramento e Alertas de Desastres Naturais (National Center for Natural Disaster Monitoring and Alerts)

[13] Regea – Geologia Engenharia e Estudos Ambientais (Engineering Geology and Environmental Studies)

[14] UFABC - Universidade Federal do ABC (Federal University of ABC)

Appendix 2.3

We used answers from expert 10 and Section A of the survey to explain how AHP computes each

criterion weight and CR of each expert.

Based on the choices made by expert 10, we built the matrix for each level of the hierarchy

structure. Table 6 illustrates expert 10A's choices for the pairwise comparisons on Section A of the

survey. Section A compares three criteria: (i) natural aspects; (ii) anthropogenic aspects; and (iii)

instability signs. For each pairwise comparison, the expert chooses which criterion is more

important (*a* or *b)* and how many times it is more important, based on ranking table (Table 2.7)*.* In

the case of *a* and *b* having the same weight, the choice is 1.

Table 2.6. Answer chosen for Section A - expert 10 A

Pairwise comparison	Choice
(1) Natural aspects (a) or Anthropogenic aspects (b)	1
(2) Natural aspects (a) or Instability signs (c)	B3
(3) Anthropogenic aspects (b) or Instability signs (c)	1

Table 2.7. Table of ranking scale for criteria and alternatives (source: adapted from Saaty, 1980)

Value of a	Interpretation
1	*a* and *b* are equally important
3	*a* is slightly more important than *b*
5	*a* is more important than *b*
7	*a* is strongly more important than *b*
9	*a* is absolutely more important than *b*
2,4,6, 8	intermediate values

The start table is represented by Table 2.8 and illustrates the possible combinations based on the

pairwise comparison. It represents numerical values of a matrix A with n x n, where n is the number

of criteria - in this case, n=3. Each entry of the matrix A is represented by a_{jk}, and it represents the

importance of criterion j relative to the criterion k. If $a_{jk} > 1$, criterion j is more important than

criterion k; if $a_{jk} < 1$ criterion k is more important than criterion j, and if $a_{jk} = 1$, both criteria have the

same importance.

Table 2.8. Combination of possible answers for pairwise comparison of Natural aspects (N), Anthropogenic aspects (A), and Instability signs (I)

	N	A	I
N	1	NA	NI
A	1/NA	1	AI
I	1/NI	1/AI	1

Table 2.9 illustrates Table 2.8 filled with numerical values based on expert 10's choices. The green cells are filled with expert answers, and the yellow cells are filled by the opposite value revealed by the expert's choice. For instance, the pairwise comparison of N and I has a numerical value equal to 1/3 (row N and column I), and the cell that represents the opposite pairwise comparison (row I and column N) is filled with the inverse numerical value (3).

Table 2.9. Numerical values of answer that represents the choices from Table 8

	N	A	I
N	1	1	1/3
A	1	1	1
I	3	1	1

After filling the table with numerical values that represent the pairwise comparisons, we computed the specific weight of the criteria by summing the values on N, A, and I in each column (Table 2.10) and then normalizing the values. Equation 2.4 represents how each value ($\bar{a}_{jk}$) of the normalized matrix A$_{norm}$ is computed, and Equation 2.5 illustrates how the weight for each criterion is computed. Columns in blue from Table 10 represents matrix A$_{norm}$.

$$\bar{a}_{jk} = \frac{a_{jk}}{\sum_{l=1}^{n} a_{lk}} \tag{2.4}$$

$$W_j = \frac{\sum_{i=0}^{n} \bar{a}_{jk}}{n} \tag{2.5}$$

Where n is the number of criteria, $\bar{a}_{jk}$ is the normalized value of a$_{jk}$, and W$_j$ is the specific weight of each criterion.

Table 2.10. Numerical values summed by column

	N	A	I
N	1	1	1/3
A	1	**1**	1
I	3	1	**1**
A$_{sum}$	**5**	**3**	**2.33**

The blue cells on Table 2.11 are the normalized values and the column Priority (W) is the

specific weight of each criterion computed with Equation 2.5.

Table 2.11. Normalized values of main matrix in blue and Priority (W) column is the specific weight of each criterion

	N	A	I	Priority (W)
N	0.20	0.33	0.14	0.23
A	0.20	0.33	0.43	0.32
I	0.60	0.33	0.43	0.45

After computing the specific weight for each criterion of the hierarchy level, based on expert

10, we are interested in computing the CR. The AHP verifies consistency of the pairwise

comparison of each hierarchy level by computing the CR. Values with CR larger or equal to 0.1 are

not used since they are considered random.

To compute CR, we first compute λ_{max} and CI (Consistency Index) with Equations 2.6 and

2.7, respectively.

$$\lambda_{max} = (\sum_{i=1}^{n}(A_{sum\ i} * W_i)) \qquad (2.6)$$

$$CI = ((\lambda_{max}) - n)/(n-1) \qquad (2.7)$$

In our example, $A_{sum} = (5, 3, 2.33)$, and W $= (0.23, 0.32, 0.45)$. Therefore, $\lambda_{max} =$

$(5 * 0.23 + 3 * 0.32 + 2.33 * 0.45) = 3.15$. Computing CI with n=3, the numerical value is 0.074.

Using Table 2.12 and Equation 2.8, we compute the CR of expert 10.

Table 2.12 - Values of Random Index (RI)

n	2	3	4	5	6	7	8	9	10
RI	0	0.58	0.90	1.12	1.24	1.32	1.41	1.45	1.51

$$CR = CI/RI \qquad (8)$$

In our example, *n*=3, so RI is equal to 0.58. Plugging these numbers into Equation 2.8, we find CR equal to 0.128 (around 13%). Since CR is higher than 0.1, pairwise comparision for this hierarchical level is considered random and should not be used.
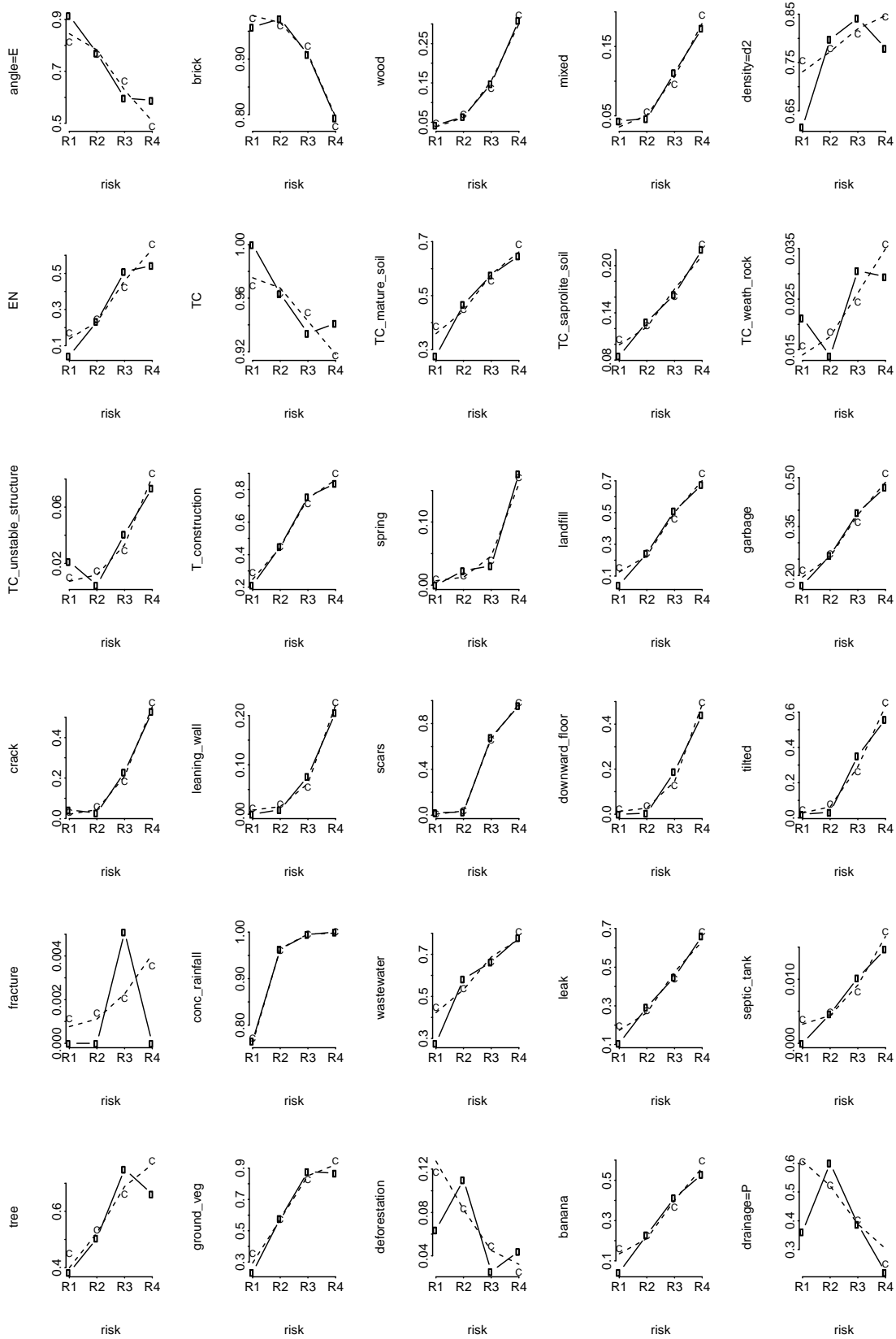
Appendix 2.4

Classifier, Category, and Specific Weight Value

Classifier	Category	Specific Weight
α < 10	N	0.64
10 ≤ α <17	N	1.00
17 ≤ α <30	N	1.798
30 ≤ α <60	N	3.02
60 ≤ α < 90	N	5.69
α = 90	N	5.85
soil favorable to instability (yes)	N	4.72
soil favorable to instability (not observed)	N	2.36
soil favorable to instability (no)	N	0.00
natural coverage favorable to instability (yes)	N	1.88
natural coverage favorable to instability (not observed)	N	0.94
natural coverage favorable to instability (no)	N	0.00
geology favorable to instability (yes)	N	0.00
geology favorable to instability (not observed)	N	2.32
geology favorable to instability (no)	N	4.65
wood	A	3.15
brick	A	0.78
mix material	A	3.60
near slope base	A	2.15
near slope top	A	1.50
far away from slope base	A	0.35
far away from slope top	A	0.29
middle of the slope	A	2.06
consolidated sector	A	0.95
partially consolidated sector	A	2.55
developing sector	A	2.96
mix sector	A	2.27
waste water	A	0.96
concentration of rainfall water (surface)	A	0.98
leak	A	1.95
septic tank	A	0.84
satisfy drainage system	A	0.54
drainage system precarious	A	0.04
no drainage system	A	0.62
tree	A	0.37

shrubs/bushes	A	0.35
deforestation/exposed soil	A	1.14
grass/ground vegetation	A	0.41
banana tree	A	1.25
urban coverage	A	0.34
garbage, land fill, or deposit	A	3.88
leaning wall	I	9.53
crack in the house	I	11.01
crack in the terrain	I	11.01
tilted trees, poles	I	9.53
downward sloping floor	I	16.88
landslide scars	I	12.64

Appendix 3.1

Appendix 3.2

Classifier	Classifier Option	Frequency	Percentage
brick	FALSE	40	15.09
brick	TRUE	490	184.91
wood	FALSE	464	175.09
wood	TRUE	66	24.91
mixed	FALSE	484	182.64
mixed	TRUE	46	17.36
TC_mature_soil	FALSE	257	96.98
TC_mature_soil	TRUE	273	103.02
T_construction	FALSE	216	81.51
T_construction	TRUE	314	118.49
spring	FALSE	507	191.32
spring	TRUE	23	8.68
landfill	FALSE	329	124.15
landfill	TRUE	201	75.85
garbage	FALSE	355	133.96
garbage	TRUE	175	66.04
crack	FALSE	441	166.42
crack	TRUE	89	33.58
leaning_wall	FALSE	499	188.30
leaning_wall	TRUE	31	11.70
DepTaludeAterro	FALSE	325	122.64
DepTaludeAterro	TRUE	205	77.36
scars	FALSE	462	174.34
scars	TRUE	68	25.66
tilted	FALSE	415	156.60
tilted	TRUE	115	43.40
conc_rainfall	FALSE	20	7.55
conc_rainfall	TRUE	510	192.45
wastewater	FALSE	206	77.74
wastewater	TRUE	324	122.26
conc_rainfall_water	FALSE	328	123.77
conc_rainfall_water	TRUE	202	76.23
septic_tank	FALSE	526	198.49
septic_tank	TRUE	4	1.51
angle	C	24	22.64

angle	D	137	129.25
angle	E	369	348.11

Classifier	Classifier Option	Frequency	Percentage
EN	FALSE	340	128.30
EN	TRUE	190	71.70
TC	FALSE	25	9.43
TC	TRUE	505	190.57
TC_saprolite_soil	FALSE	451	170.19
TC_saprolite_soil	TRUE	79	29.81
banana	FALSE	361	136.23
banana	TRUE	169	63.77
drainage	Y	72	40.75
drainage	P	240	135.82
drainage	N	218	123.37
deforestation	FALSE	495	186.79
deforestation	TRUE	35	13.21
TC_unstable_structure	FALSE	515	194.34
TC_unstable_structure	TRUE	15	5.66
tree	FALSE	210	79.25
tree	TRUE	320	120.75
ground_veg	FALSE	161	60.75
ground_veg	TRUE	369	139.25
density	d1	73	55.09
density	d2	422	318.49
density	d3	35	26.42
TC_weath_rock	FALSE	517	195.09
TC_weath_rock	TRUE	13	4.91
fracture	FALSE	529	199.62
fracture	TRUE	1	0.38

Appendix 3.3

Model 1: Table with coefficient value, stander error, t-value and p-value

```
=======================================================
                        Value Std. Error t value p value
-------------------------------------------------------
angleD                   0.49    0.49     0.31
angleE                   0.32    0.56     0.57    0.29
brickTRUE               -1.70    0.53    -3.22    0
woodTRUE                 1.02    0.34     3.01    0
mixedTRUE                0.09    0.51     0.18    0.43
ENTRUE                   0.70    0.39     1.82    0.03
TC_mature_soilTRUE       0.58    0.23     2.53    0.01
TC_saprolite_soilTRUE    0.25    0.29     0.86    0.20
springTRUE              -0.22    0.68    -0.33    0.37
landfillTRUE             0.10    0.33     0.29    0.39
constructionTRUE         0.46    0.37     1.25    0.11
garbageTRUE              0.03    0.31     0.11    0.46
crackTRUE                2.18    0.36     6.11    0
leaning_wallTRUE         2.03    0.57     3.55    0
scarsTRUE                4.25    0.38    11.22    0
downward_floorTRUE       1.28    0.40     3.23    0
tiltedTRUE               0.85    0.34     2.47    0.01
conc_rainfallTRUE        1.63    0.49     3.32    0
wastewaterTRUE           0.60    0.24     2.46    0.01
leakTRUE                -0.41    0.25    -1.65    0.05
bananaTRUE               0.39    0.25     1.55    0.06
R1| R2                  -0.72    0.91    -0.78    0.22
R2| R3                   3.56    0.94     3.78    0
R3| R4                   9.02    1.05     8.60    0
-------------------------------------------------------
```

Model 1: Test to check for ordinal fashion of the classifiers
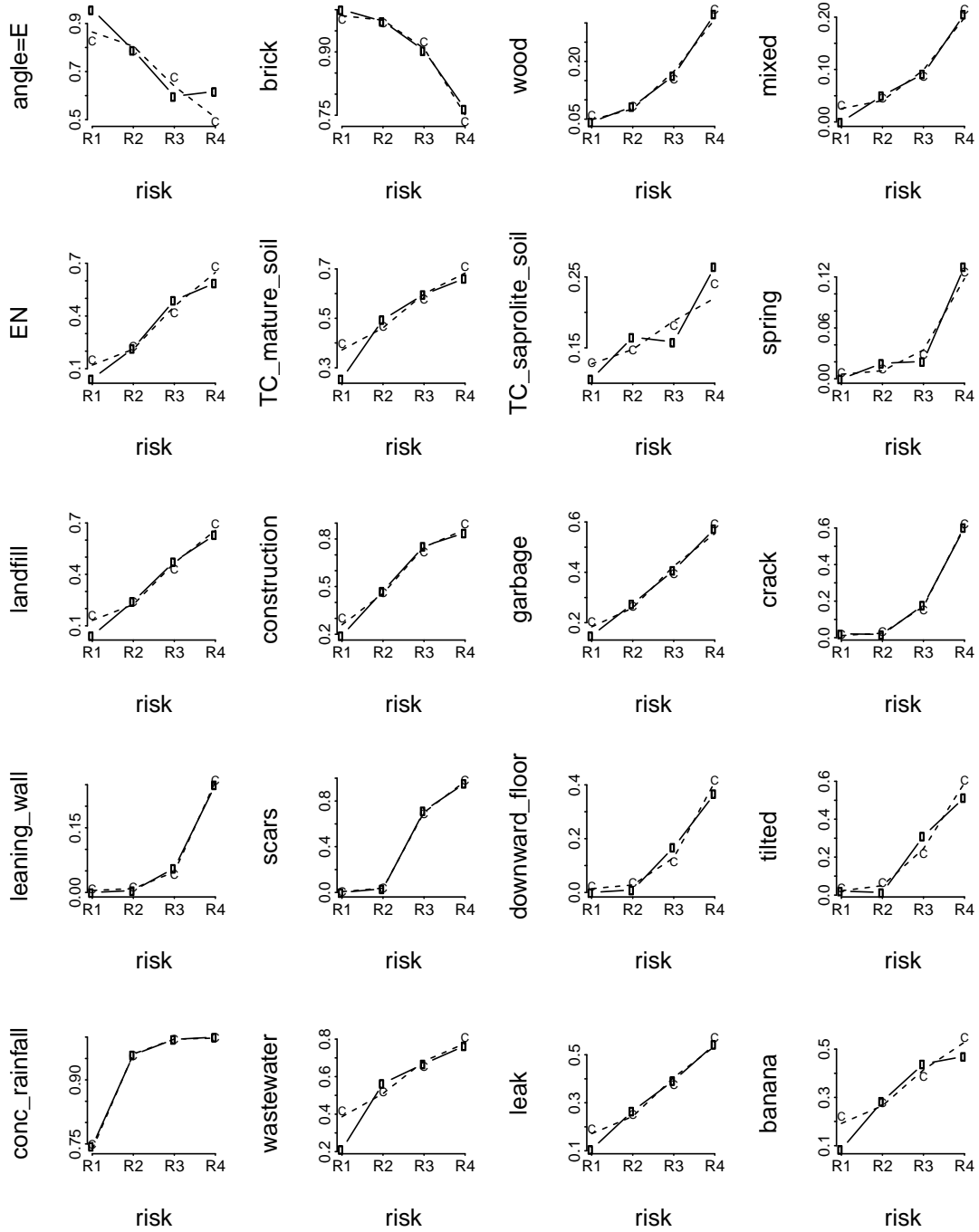
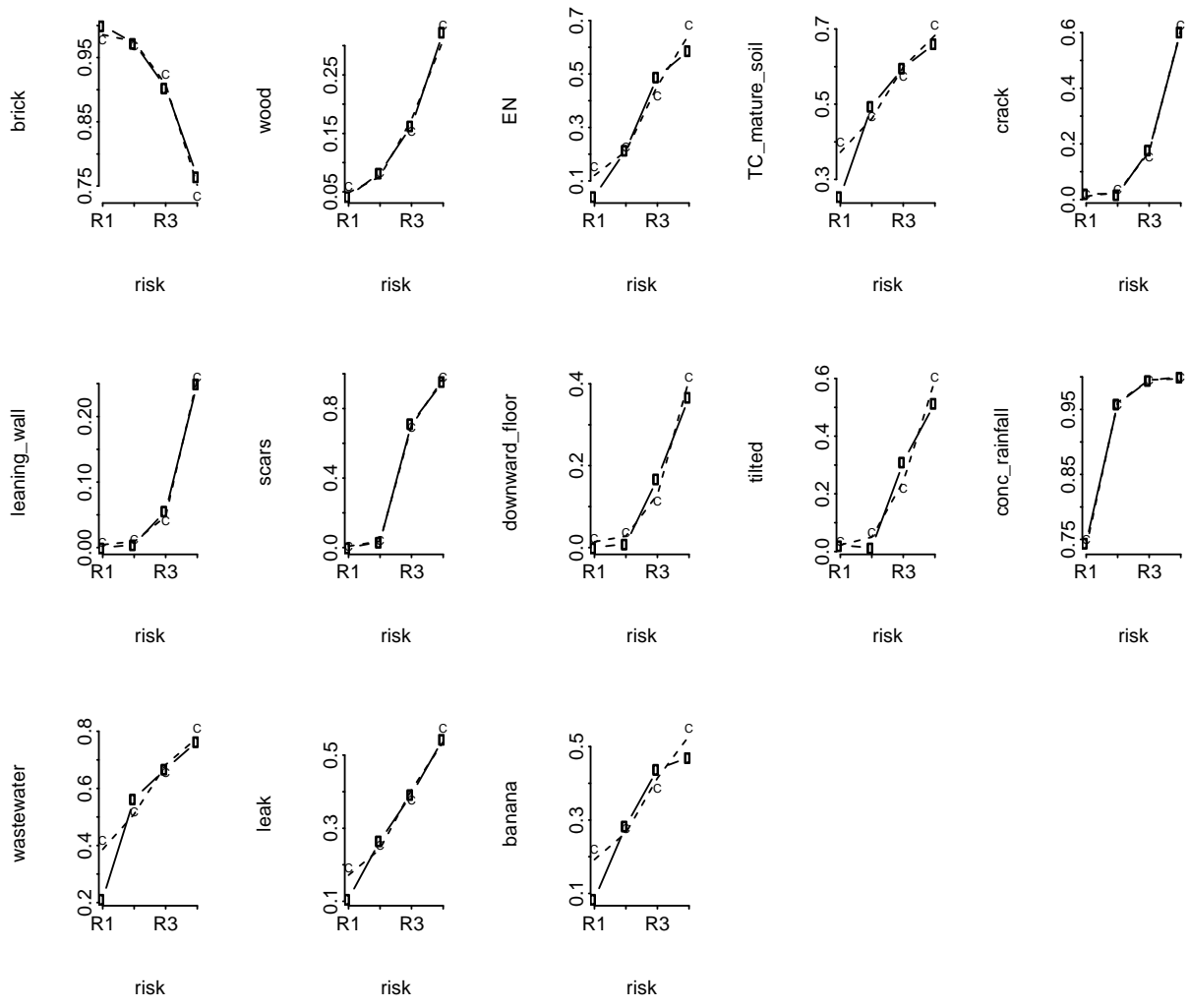## Model 2: Table with coefficient value, stander error, t-value and p-value

```
=========================================================
                          Value Std. Error t value p value
---------------------------------------------------------
angleD                    0.15    0.50      0.31    0.38
angleE                    0.47    0.57      0.82    0.21
brickTRUE                 -1.48   0.55      -2.72   0
woodTRUE                  0.79    0.37      2.14    0.02
mixedTRUE                 0.07    0.53      0.14    0.44
ENTRUE                    0.63    0.42      1.50    0.07
TC_mature_soilTRUE        0.58    0.24      2.38    0.01
TC_saprolite_soilTRUE     0.24    0.31      0.77    0.22
constructionTRUE          0.54    0.38      1.39    0.08
springTRUE                -0.08   0.68      -0.12   0.45
landfillTRUE              0.03    0.35      0.08    0.47
garbageTRUE               0.08    0.32      0.24    0.40
crackTRUE                 2.28    0.37      6.14    0
leaning_wallTRUE          2.26    0.59      3.85    0
scarsTRUE                 4.25    0.39      10.83   0
downward_floorTRUE        1.10    0.39      2.78    0
tiltedTRUE                0.73    0.35      2.12    0.02
conc_rainfallTRUE         1.00    0.55      1.81    0.03
wastewaterTRUE            0.39    0.26      1.51    0.07
leakTRUE                  -0.62   0.26      -2.41   0.01
bananaTRUE                0.22    0.27      0.83    0.20
densityd2                 0.07    0.34      0.21    0.42
densityd3                 0.21    0.59      0.36    0.36
TCTRUE                    -0.12   0.56      -0.21   0.42
TC_unstable_structureTRUE -1.10   0.81      -1.35   0.09
treeTRUE                  -0.27   0.25      -1.08   0.14
ground_vegTRUE            0.88    0.28      3.10    0
drainage.L                1.31    0.29      4.48    0
drainage.Q                -0.03   0.19      -0.17   0.43
R1| R2                    -1.07   1.15      -0.93   0.18
R2| R3                    3.72    1.17      3.19    0.001
R3| R4                    9.30    1.27      7.35    0
---------------------------------------------------------
```

Model 2: Test to check for ordinal fashion of the classifiers
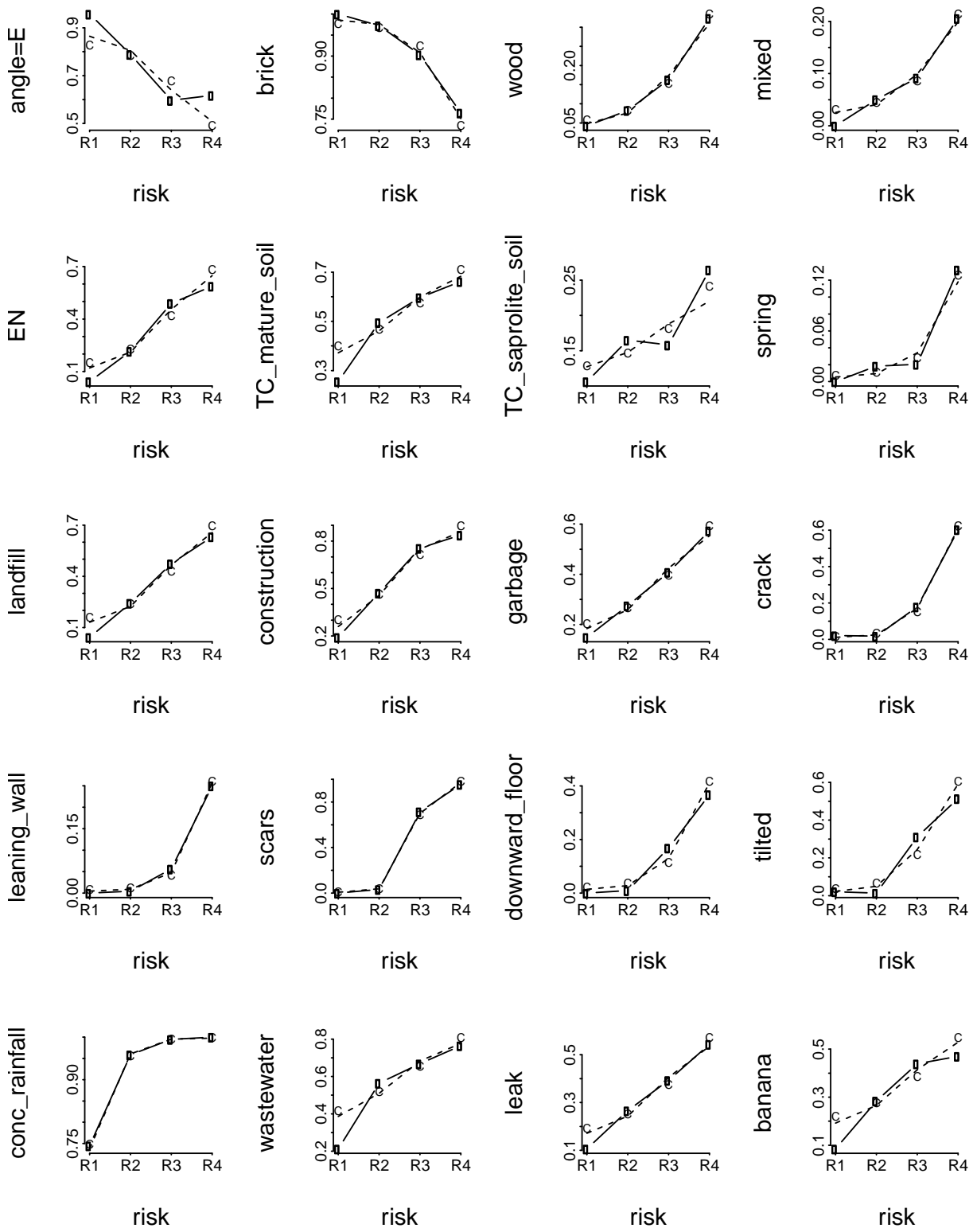
Model 3: Table with coefficient value, stander error, t-value and p-value

```
===========================================================
                             Value Std. Error t value p value
-----------------------------------------------------------
brickTRUE                    -1.60   0.44      -3.65    0
woodTRUE                      0.84   0.34       2.45    0.01
ENTRUE                        0.39   0.26       1.51    0.07
TC_mature_soilTRUE            0.54   0.23       2.33    0.01
constructionTRUE              0.61   0.24       2.49    0.01
crackTRUE                     2.27   0.35       6.46    0
leaning_wallTRUE              2.21   0.56       3.91    0
scarsTRUE                     4.20   0.39      10.88    0
downward_floorTRUE            1.10   0.39       2.79    0
tiltedTRUE                    0.75   0.34       2.22    0.01
conc_rainfallTRUE             1.01   0.52       1.92    0.03
wastewaterTRUE                0.39   0.24       1.59    0.06
leakTRUE                     -0.62   0.25      -2.48    0.01
TC_unstable_structureTRUE    -0.88   0.77      -1.14    0.13
ground_vegTRUE                0.88   0.26       3.32    0
drainage.L                    1.31   0.29       4.52    0
drainage.Q                   -0.03   0.19      -0.18    0.43
R1| R2                       -1.54   0.68      -2.27    0.01
R2| R3                        3.23   0.72       4.47    0
R3| R4                        8.77   0.84      10.47    0
-----------------------------------------------------------
```

Model 3: Test to check for ordinal fashion of the classifiers
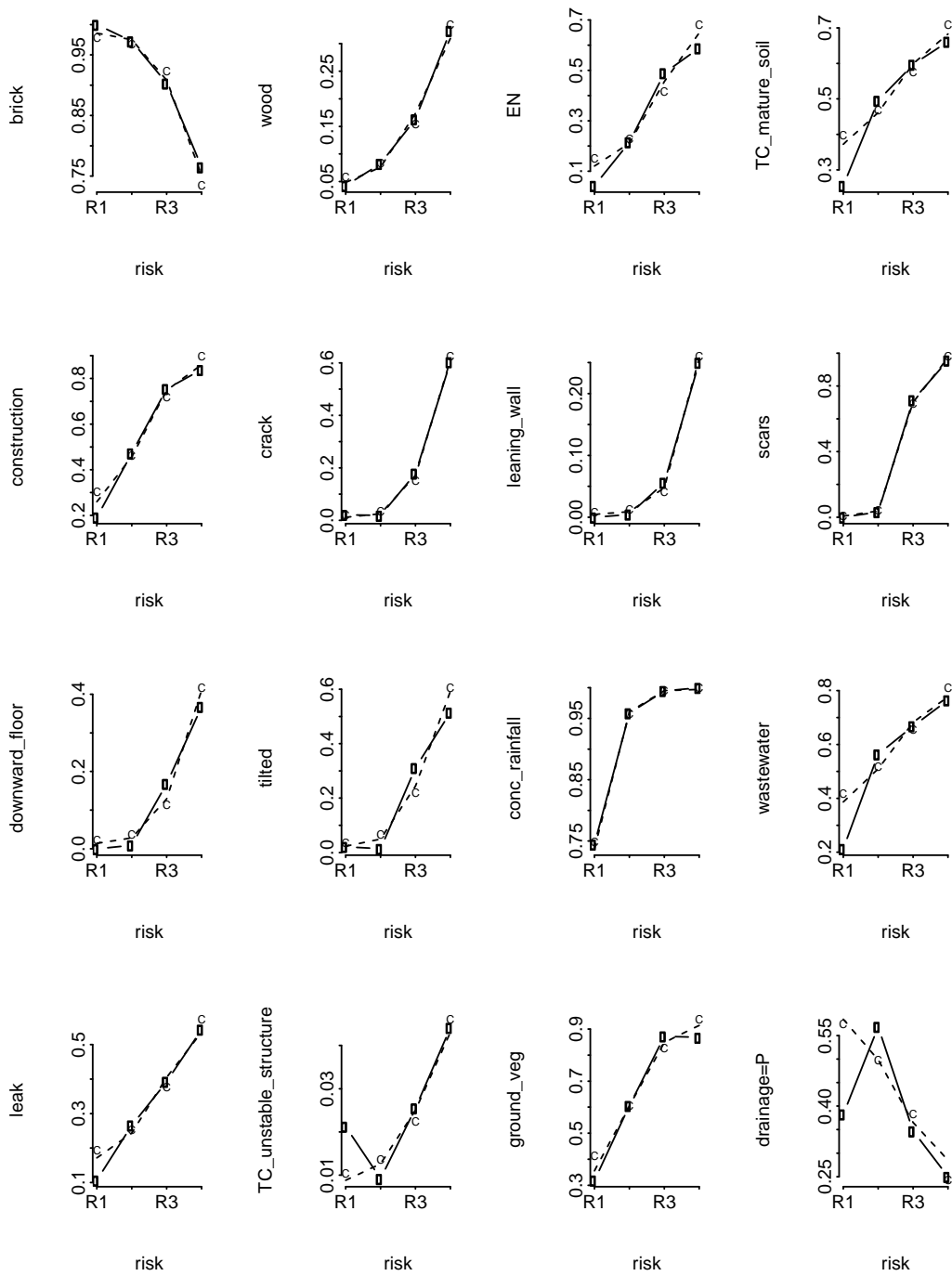
Model 4: Table with coefficient value, stander error, t-value and p-value

```
=====================================================
                     Value Std. Error t value p value
-----------------------------------------------------
brickTRUE            -1.59    0.43    -3.67   0
woodTRUE             0.94     0.34    2.78    0
TC_mature_soilTRUE   0.49     0.23    2.16    0.02
constructionTRUE     0.69     0.24    2.86    0
crackTRUE            2.26     0.35    6.52    0
leaning_wallTRUE     2.26     0.56    4.04    0
scarsTRUE            4.21     0.39    10.90   0
downward_floorTRUE   1.07     0.39    2.78    0
tiltedTRUE           0.86     0.33    2.57    0.01
conc_rainfallTRUE    1.06     0.52    2.03    0.02
leakTRUE             -0.56    0.25    -2.27   0.01
ground_vegTRUE       0.92     0.26    3.57    0
drainage.L           1.40     0.28    4.98    0
drainage.Q           -0.05    0.19    -0.27   0.40
R1| R2               -1.64    0.67    -2.46   0.01
R2| R3               3.03     0.70    4.33    0
R3| R4               8.59     0.83    10.41   0
-----------------------------------------------------
```

Model 4: Test to check for ordinal fashion of the classifiers
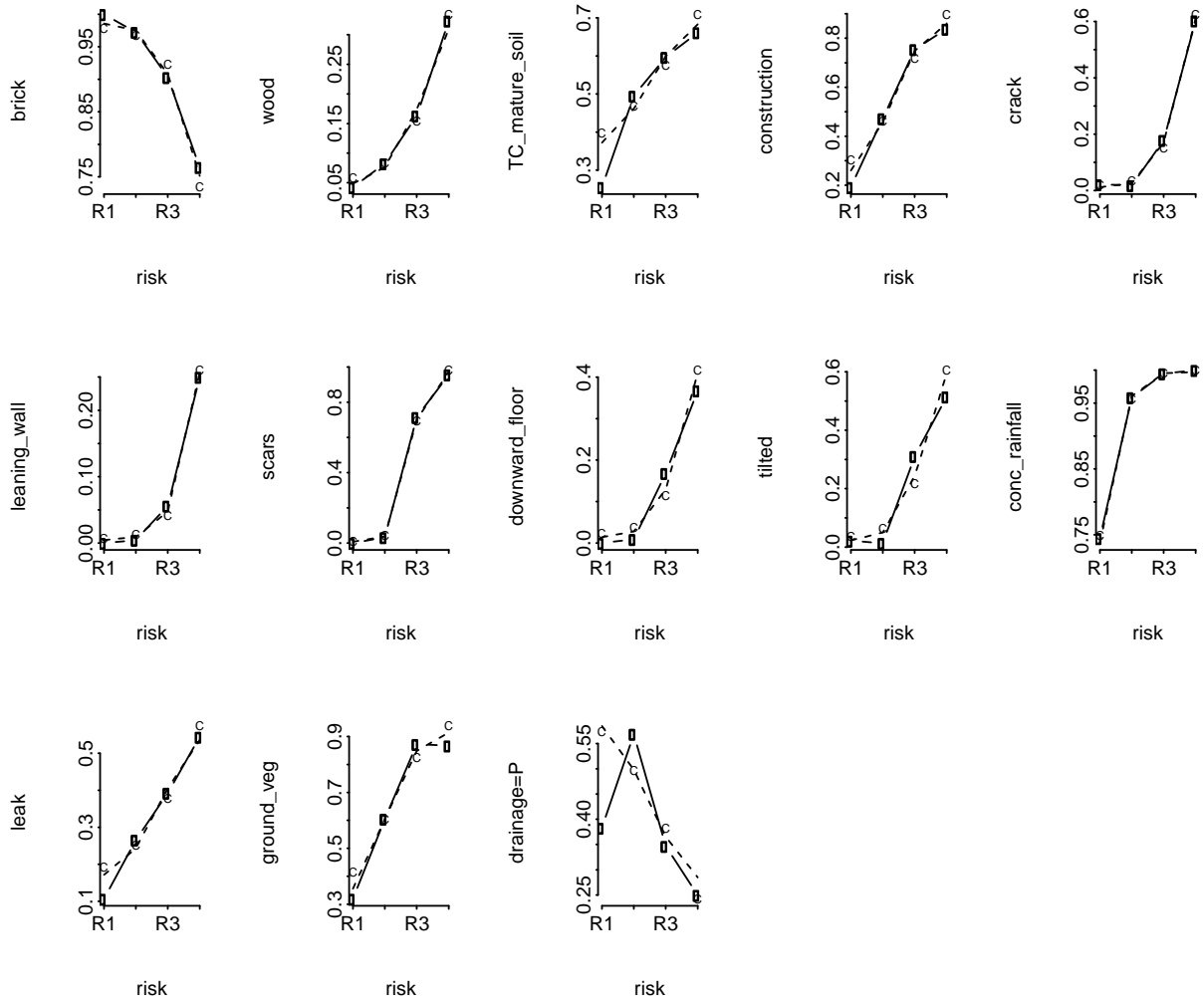
Model 5: Table with coefficient value, stander error, t-value and p-value

```
========================================================
                       Value Std. Error t value p value
--------------------------------------------------------
angleD                 0.24      0.49     0.49    0.31
angleE                 0.32      0.56     0.57    0.29
brickTRUE             -1.70      0.53    -3.22    0
woodTRUE               1.02      0.34     3.01    0
mixedTRUE              0.09      0.51     0.18    0.43
ENTRUE                 0.70      0.39     1.82    0.03
TC_mature_soilTRUE     0.58      0.23     2.53    0.01
TC_saprolite_soilTRUE  0.25      0.29     0.86    0.20
springTRUE            -0.22      0.68    -0.33    0.37
landfillTRUE           0.10      0.33     0.29    0.39
constructionTRUE       0.46      0.37     1.25    0.11
garbageTRUE            0.03      0.31     0.11    0.46
crackTRUE              2.18      0.36     6.11    0
leaning_wallTRUE       2.03      0.57     3.55    0
scarsTRUE              4.25      0.38    11.22    0
downward_floorTRUE     1.28      0.40     3.23    0
tiltedTRUE             0.85      0.34     2.47    0.01
conc_rainfallTRUE      1.63      0.49     3.32    0
wastewaterTRUE         0.60      0.24     2.46    0.01
leakTRUE              -0.41      0.25    -1.65    0.05
bananaTRUE             0.39      0.25     1.55    0.06
R1| R2                -0.72      0.91    -0.78    0.22
R2| R3                 3.56      0.94     3.78    0
R3| R4                 9.02      1.05     8.60    0
--------------------------------------------------------
```

Model 5: Test to check for ordinal fashion of the classifiers
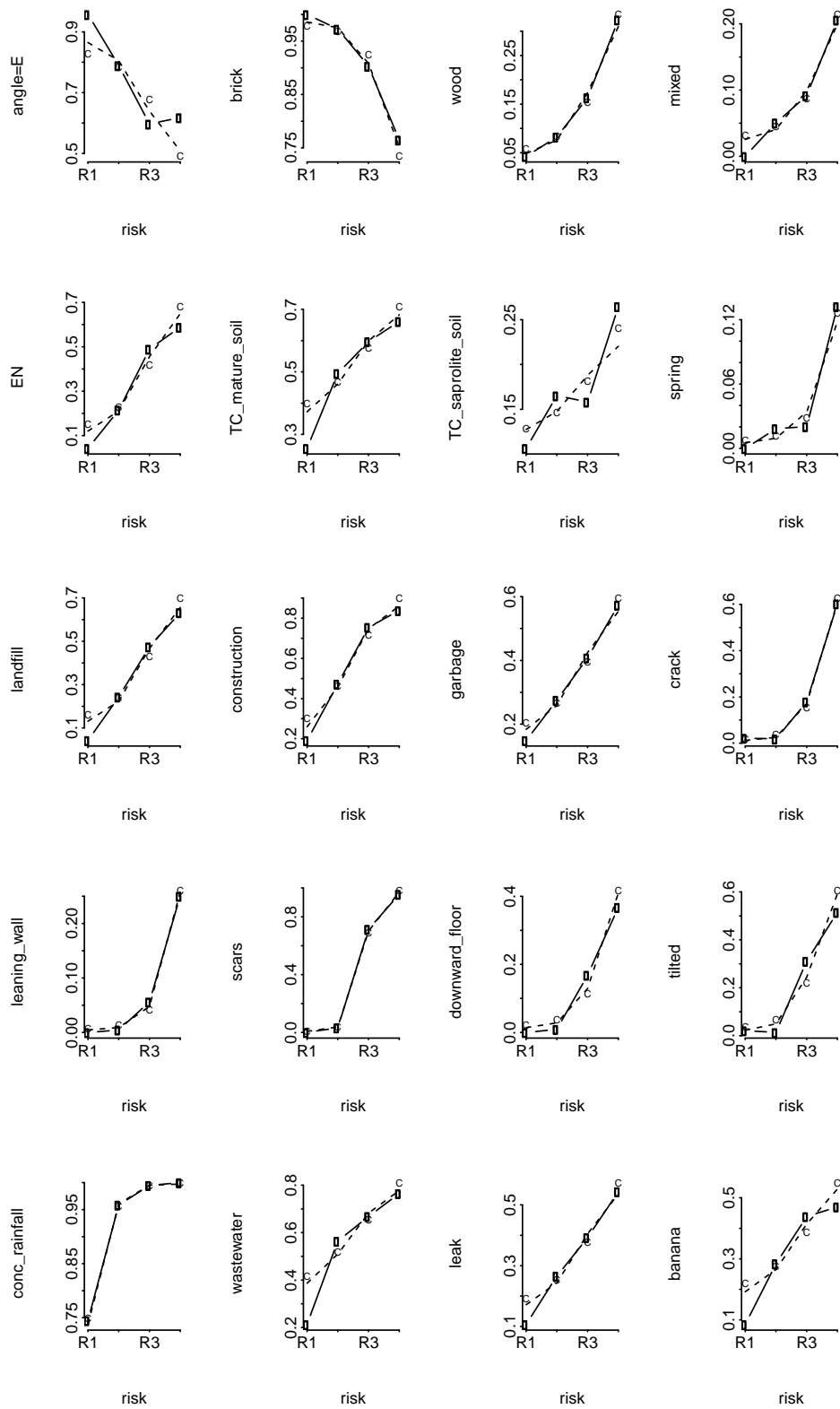
Model 6: Table with coefficient value, stander error, t-value and p-value

```
==================================================
                 Value Std. Error t value p value
--------------------------------------------------
brickTRUE         -1.77   0.43       -4.15    0
woodTRUE           1.04   0.33        3.15    0
ENTRUE             0.65   0.26        2.55    0.01
TC_mature_soilTRUE 0.65   0.22        2.90    0
crackTRUE          2.23   0.35        6.41    0
leaning_wallTRUE   2.06   0.56        3.66    0
scarsTRUE          4.31   0.38       11.43    0
downward_floorTRUE 1.26   0.40        3.17    0
tiltedTRUE         0.87   0.34        2.59    0
conc_rainfallTRUE  1.75   0.49        3.60    0
wastewaterTRUE     0.64   0.23        2.78    0
leakTRUE          -0.39   0.24       -1.61    0.05
bananaTRUE         0.48   0.24        1.98    0.02
R1| R2            -1.12   0.62       -1.80    0.04
R2| R3             3.08   0.66        4.67    0
R3| R4             8.50   0.78       10.93    0
--------------------------------------------------
```

Model 6: Test to check for ordinal fashion of the classifiers

178

Model 7: Table with coefficient value, stander error, t-value and p-value

```
============================================================
                          Value Std. Error t value p value
------------------------------------------------------------
angleD                     0.40    0.49     0.82    0.21
angleE                     0.54    0.56     0.96    0.17
brickTRUE                 -1.65    0.43    -3.82    0
woodTRUE                   1.04    0.33     3.12    0
ENTRUE                     0.69    0.39     1.77    0.04
TC_mature_soilTRUE         0.78    0.23     3.41    0
TC_saprolite_soilTRUE      0.13    0.30     0.43    0.33
TC_unstable_structureTRUE -0.70    0.78    -0.90    0.18
landfillTRUE               0.40    0.26     1.55    0.06
garbageTRUE                0.30    0.25     1.22    0.11
crackTRUE                  2.14    0.35     6.14    0
leaning_wallTRUE           2.14    0.57     3.73    0
tiltedTRUE                 1.05    0.33     3.18    0
scarsTRUE                  4.29    0.38    11.19    0
conc_rainfallTRUE          1.66    0.50     3.34    0
leakTRUE                  -0.38    0.24    -1.56    0.06
wastewaterTRUE             0.57    0.24     2.36    0.01
bananaTRUE                 0.27    0.26     1.02    0.15
treeTRUE                  -0.28    0.25    -1.14    0.13
ground_vegTRUE             1.13    0.28     4.08    0
R1| R2                    -0.06    0.86    -0.07    0.47
R2| R3                     4.36    0.91     4.79    0
R3| R4                     9.78    1.03     9.53    0
------------------------------------------------------------
```

Model 7: Test to check for ordinal fashion of the classifiers
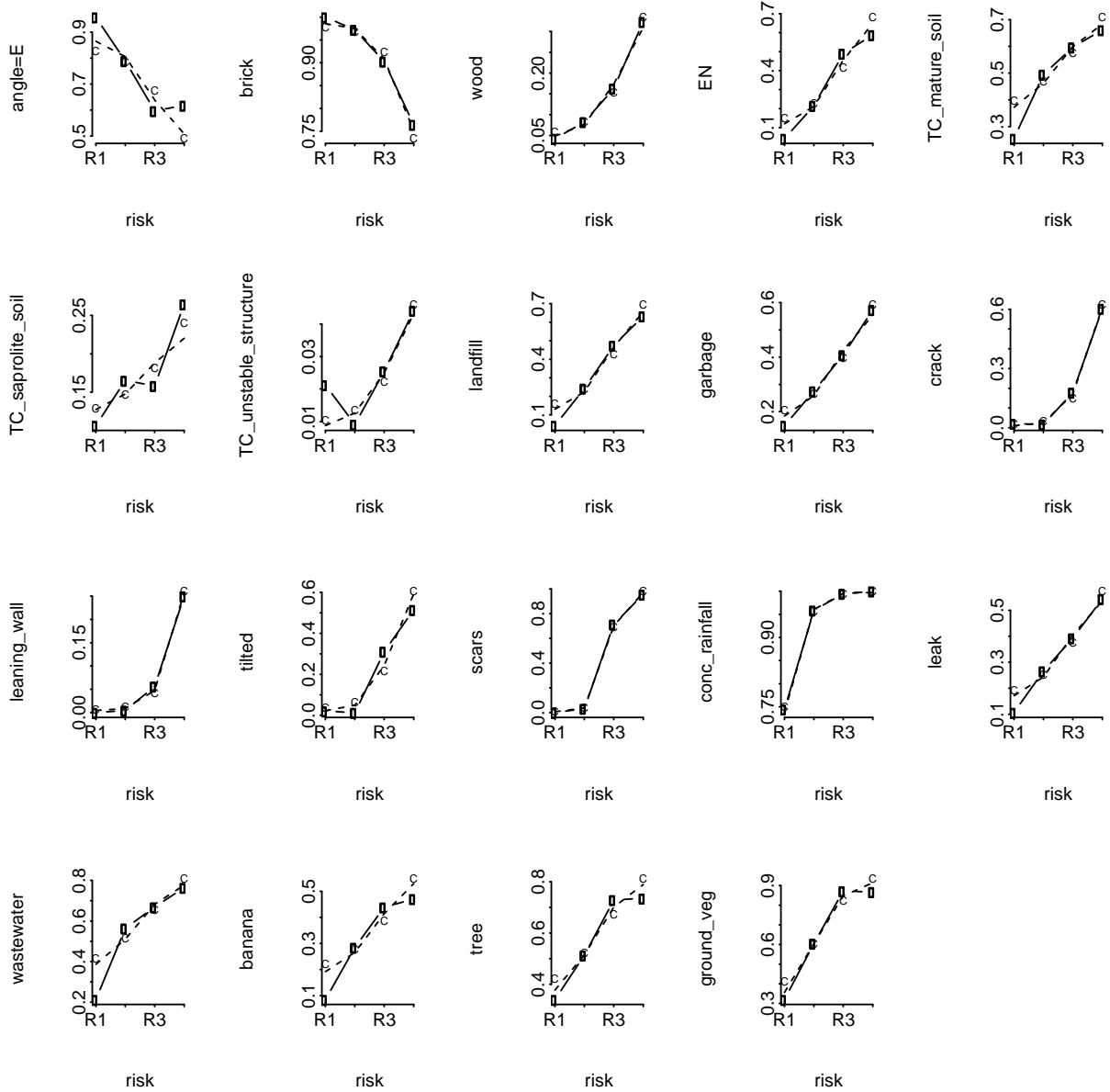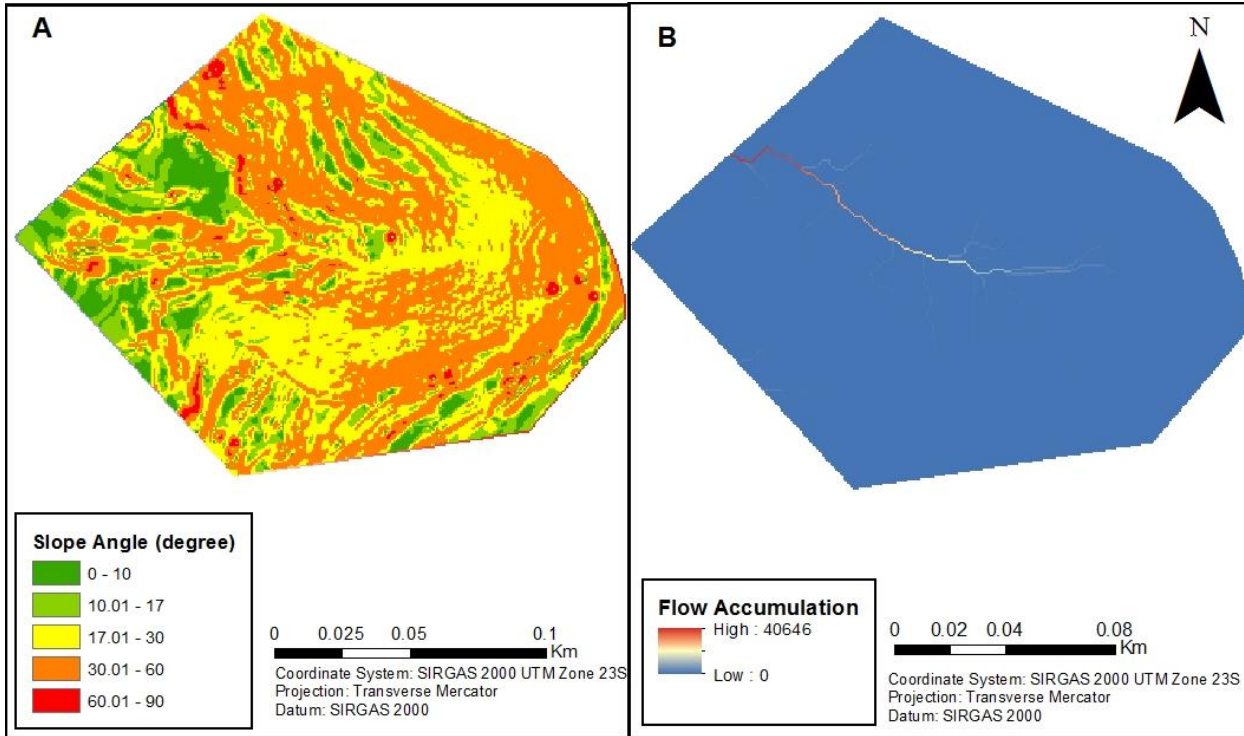
Figure 4.27. 4.27A and 4.27B - Raster from the disturbed site. Fig. 4.27A - Slope Angle in degrees. Part of the map has high slope angle (check orange and red). Fig. 4.27B – Higher flow accumulation values illustrate locations in which water would flow and accumulate. These rasters were used to compute slope stability using SHALSTAB.
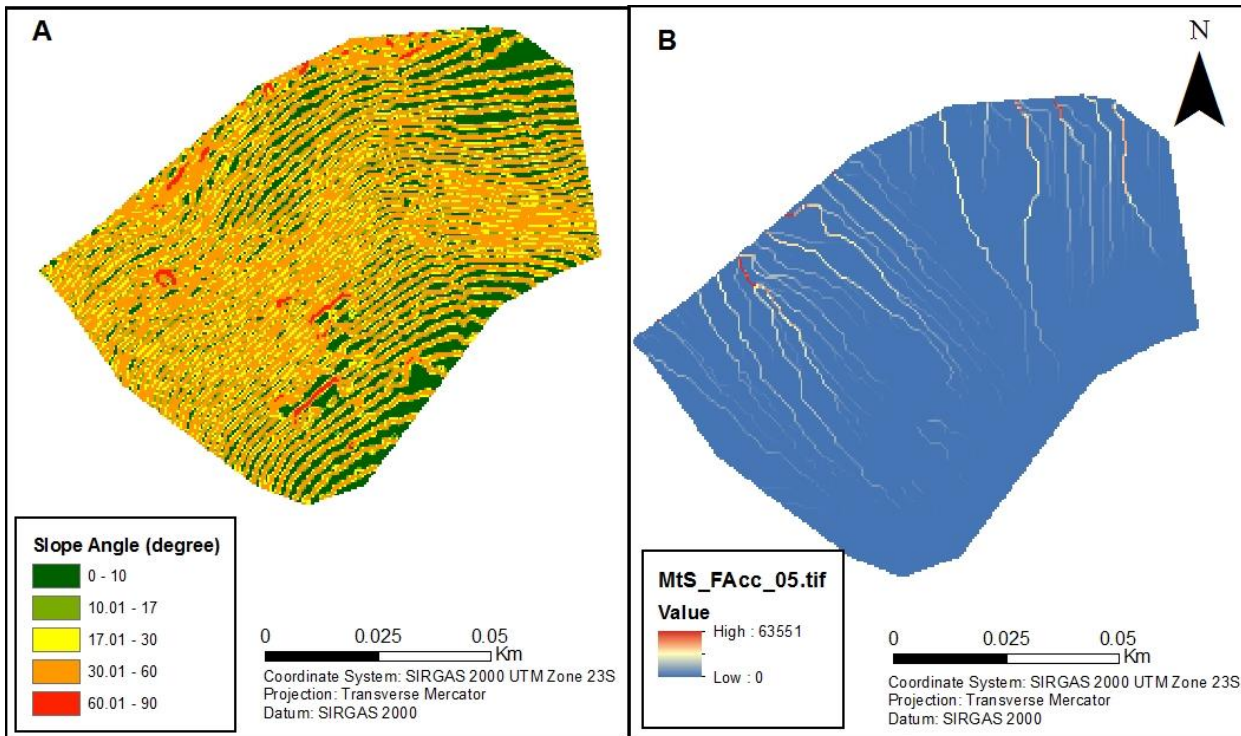
Figure 4.28. 4.28A and 4.28B - Raster from the undisturbed site. Fig. 4.28A Slope Angle in degrees. Part of the map has high slope angle (check orange and red). Fig. 4.28B – Higher flow accumulation values illustrate locations in which water would flow and accumulate. These rasters were used to compute slope stability using SHALSTAB.

APPENDEX 4.2

We used Eq. 4.1 and 4.2 to compute the field-saturated hydraulic conductivity. Therefore, we took

measurements of height (h) and diameters of the bottom (d1) and top (d2) of the bottomless bucket.

The bottomless bucket h=23.5 cm, d1=23cm, and d2=25cm.

Table 4.9 shows values measured in the field and necessary to compute K_{sat} (see Eq. 4.1 and

4.2) in the disturbed site and Table 4.10 for the undisturbed site.

Table 4.9. Values from the disturbed site necessary to compute K_{sat}. Height is the water height in the bottomless bucket when the infiltration rate is measured, area base is computed with d1, volume is the possible volume of the bucket, Depth is the depth of the bottomless bucket inside the soil, and L_G measured and computed with Eq. 03.

Location	Height (m)	Area base (cm)	Volume (cm³)	Depth (cm)	L_G(cm)
1	20	418.88	8377.68	3.5	10.15
2	18.25	418.88	7644.63	5.25	11.89
3	22	418.88	9215.44	1.5	8.17
4	21.98	418.88	9207.07	1.52	8.19
5	22.8	418.88	9550.55	0.7	7.37
6	21	418.88	8796.56	2.5	9.16

Table 4.10. Values from the undisturbed site necessary to compute K_{sat}. Height is the water height in the bottomless bucket when the infiltration rate is measured, area base is computed with d1, volume is the possible volume of the bucket, Depth is the depth of the bottomless bucket inside the soil, and LG measured and computed with Eq. 03.

Site	Height (cm)	Area base (cm)	Volume (cm³)	Depth (cm)	L_G (cm)
1	21.25	418.88	8901.28	2.25	8.91
2	21	418.88	8796.56	2.5	9.16
3	22.25	418.88	9320.17	1.25	7.92
4	21	418.88	8796.56	2.5	9.16
5	21.13	418.88	8851.02	2.37	9.03

APPENDIX 4.03

Site Disturbed A1
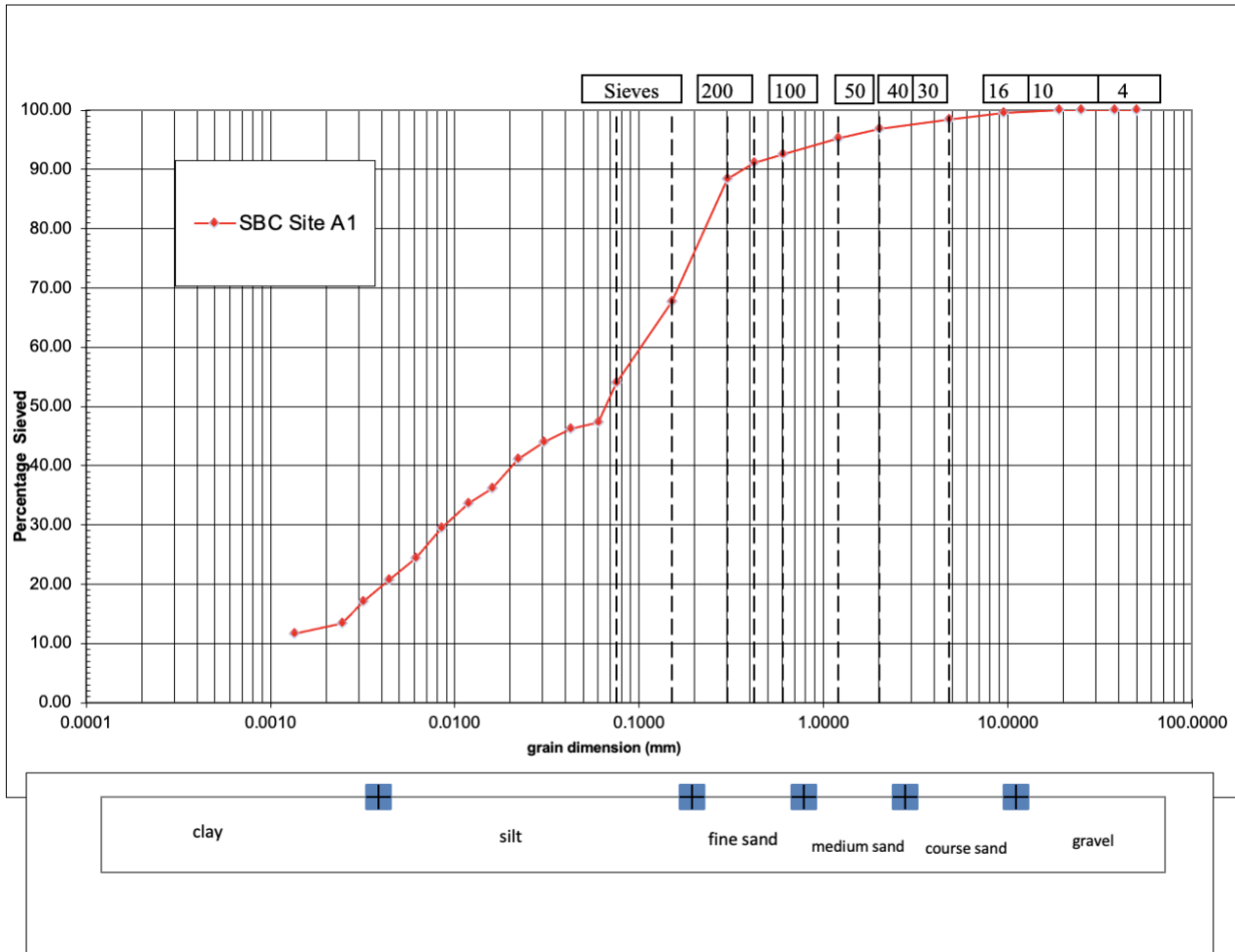
Grain Size	Percentage
Clay	14.36
Silt	55.59
Fine Sand	24.36
Medium Sand	1.68
Coarse Sand	3.74

Site Disturbed A2
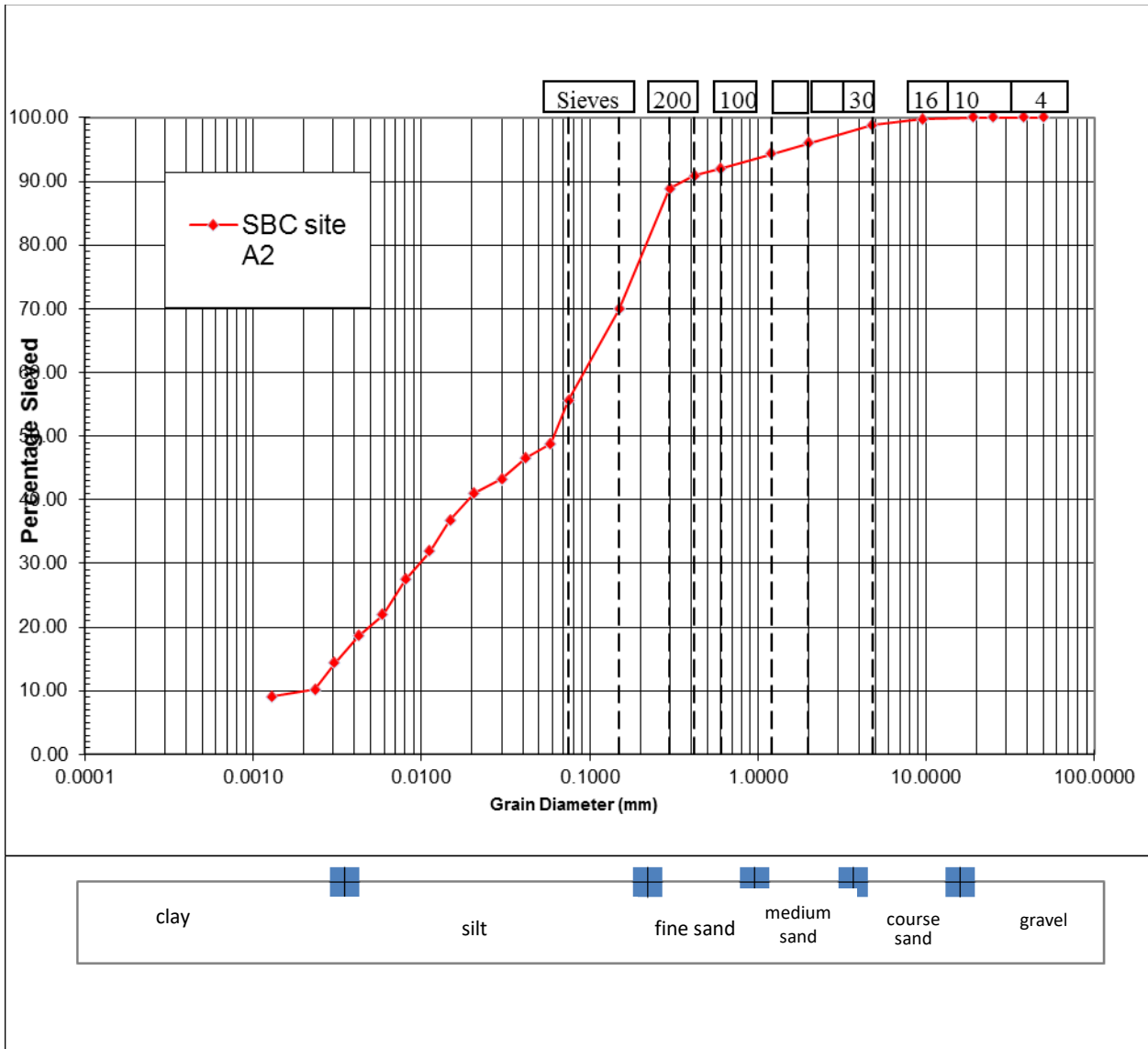
Grain Size	Percentage
Clay	14.36
Silt	55.59
Fine Sand	24.36
Medium Sand	1.68
Coarse Sand	3.74

Site Disturbed A3
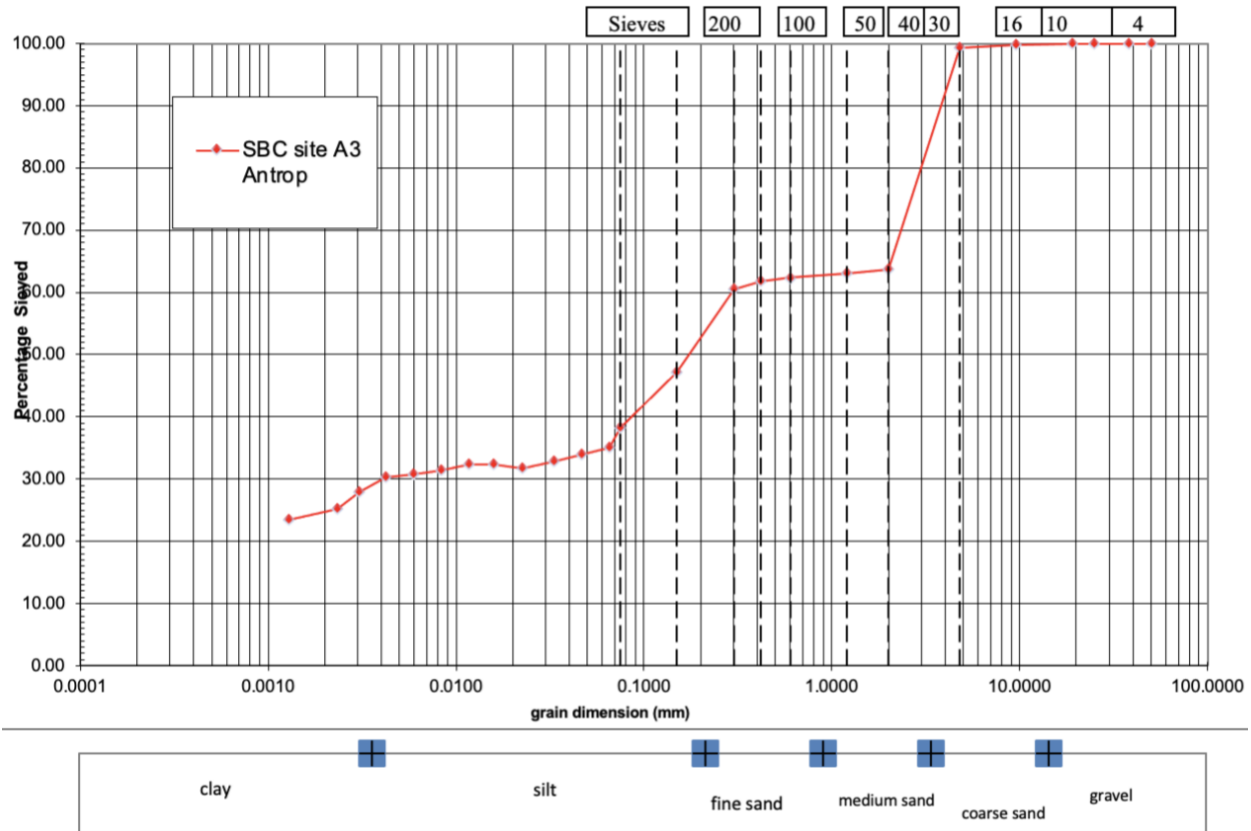
Grain Size	Percentage
Clay	35.53
Silt	11.59
Fine Sand	15.91
Medium Sand	0.60

| Coarse Sand | 36.12 |

Site Disturbed A4
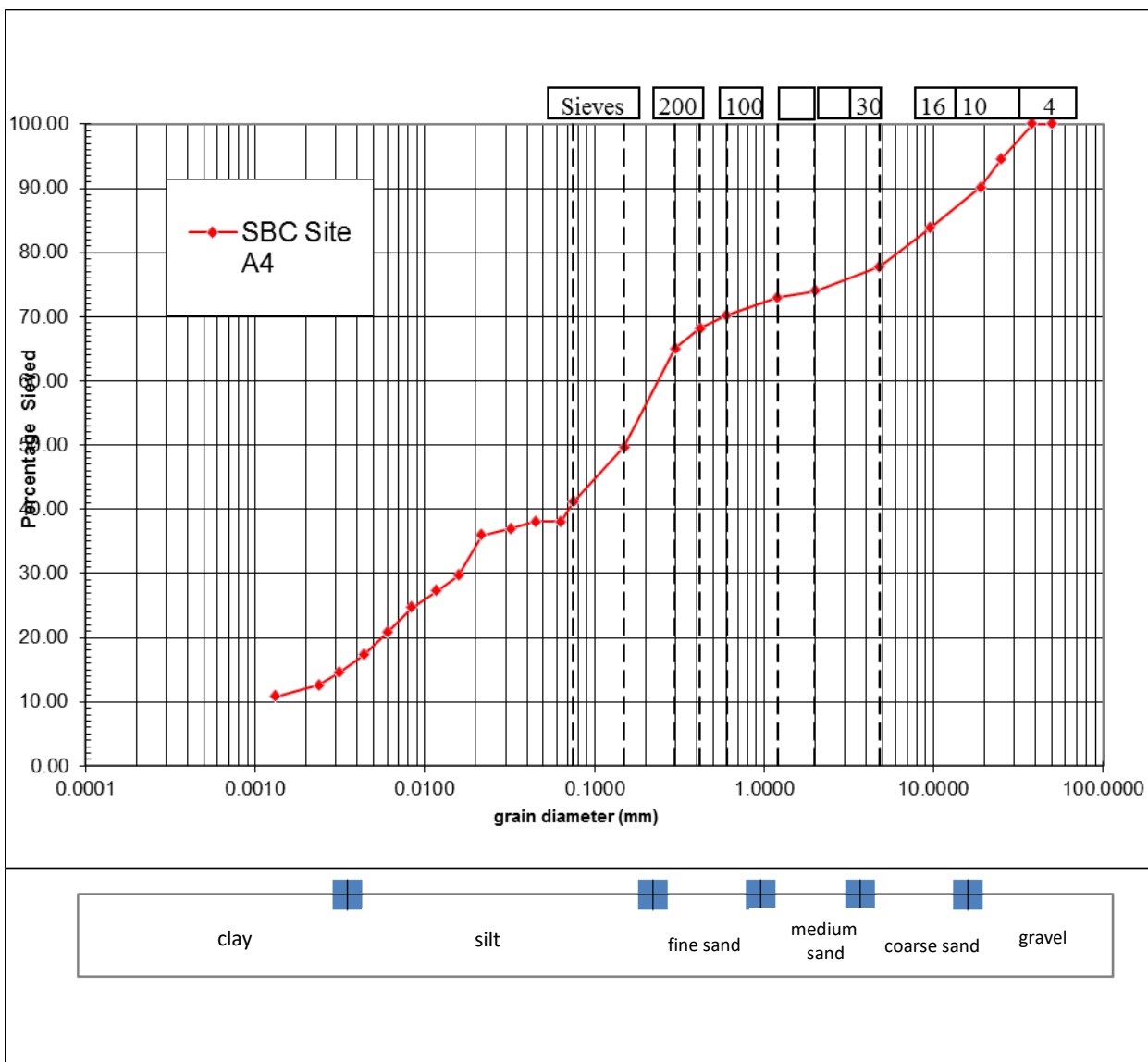
Grain Size	Percentage
Clay	13.60
Silt	36.12
Fine Sand	23.29
Medium Sand	0.08
Coarse Sand	10.67

187

Site Disturbed A5
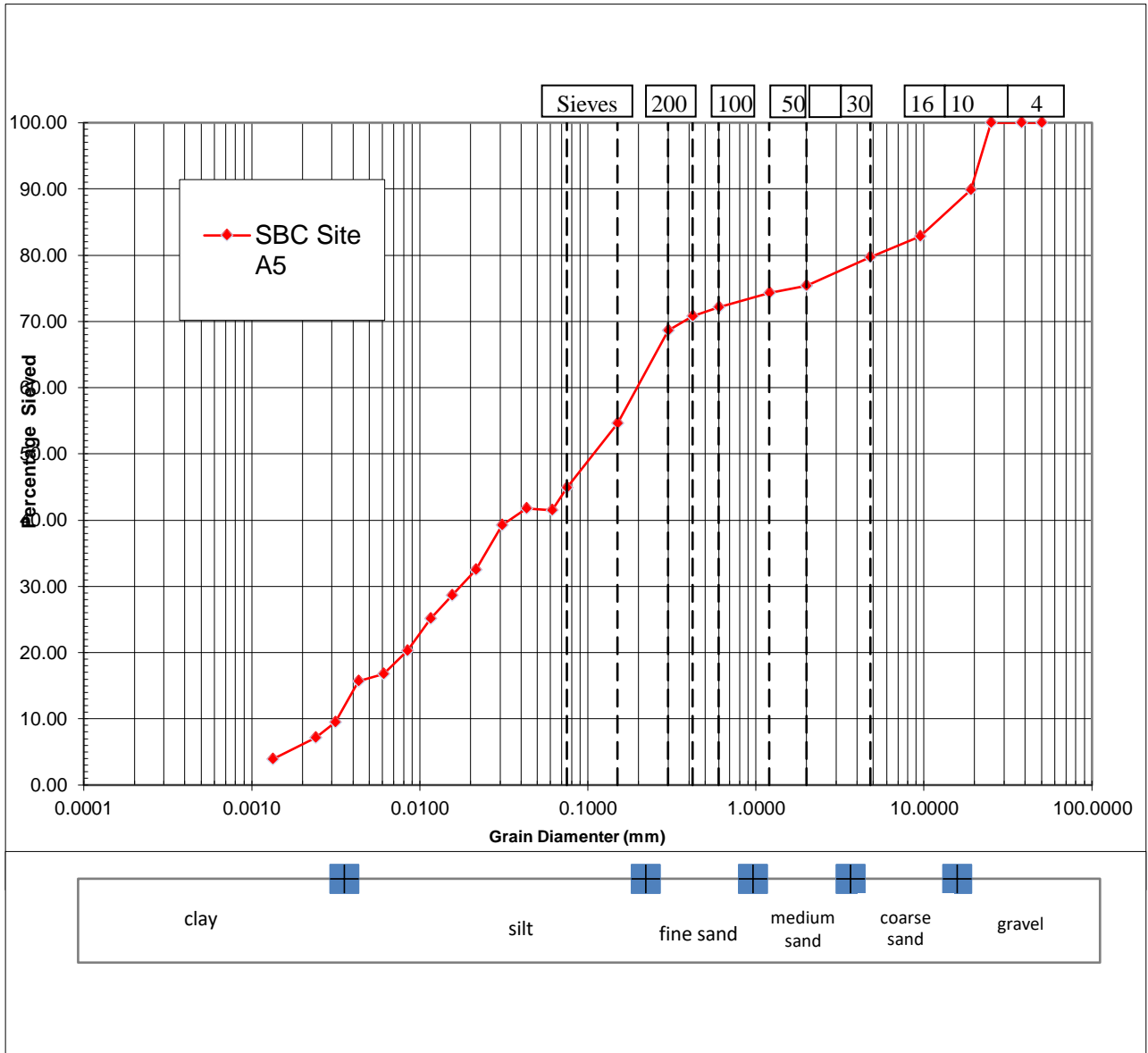
Grain Size	Percentage

Clay	7.15
Silt	47.47
Fine Sand	19.71
Medium Sand	1.05
Coarse Sand	7.50

Site Disturbed A6
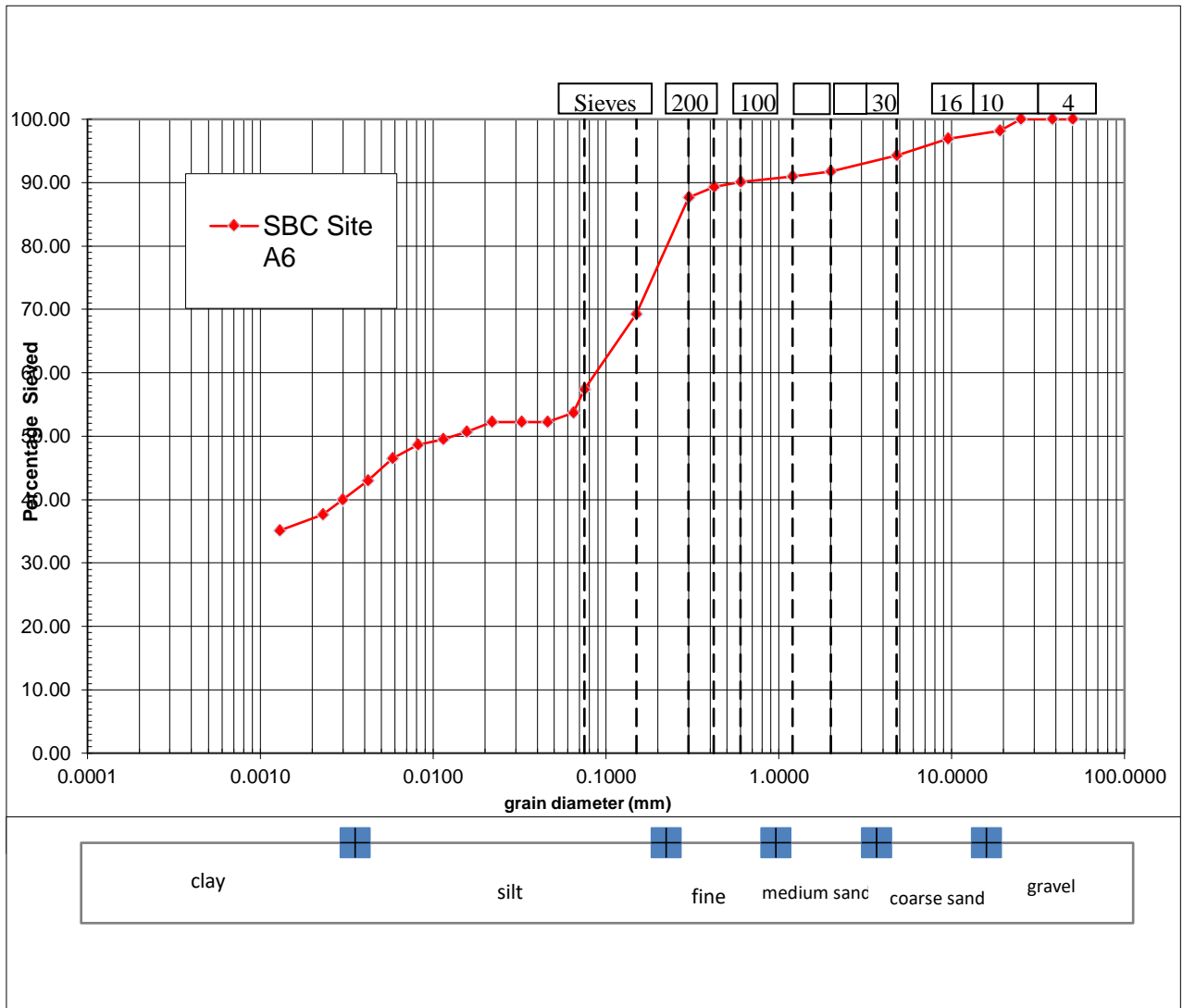
Grain Size	Percentage
Clay	37.60
Silt	31.70
Fine Sand	21.72

Medium Sand	0.75
Coarse Sand	5.13

Site Undisturbed N1
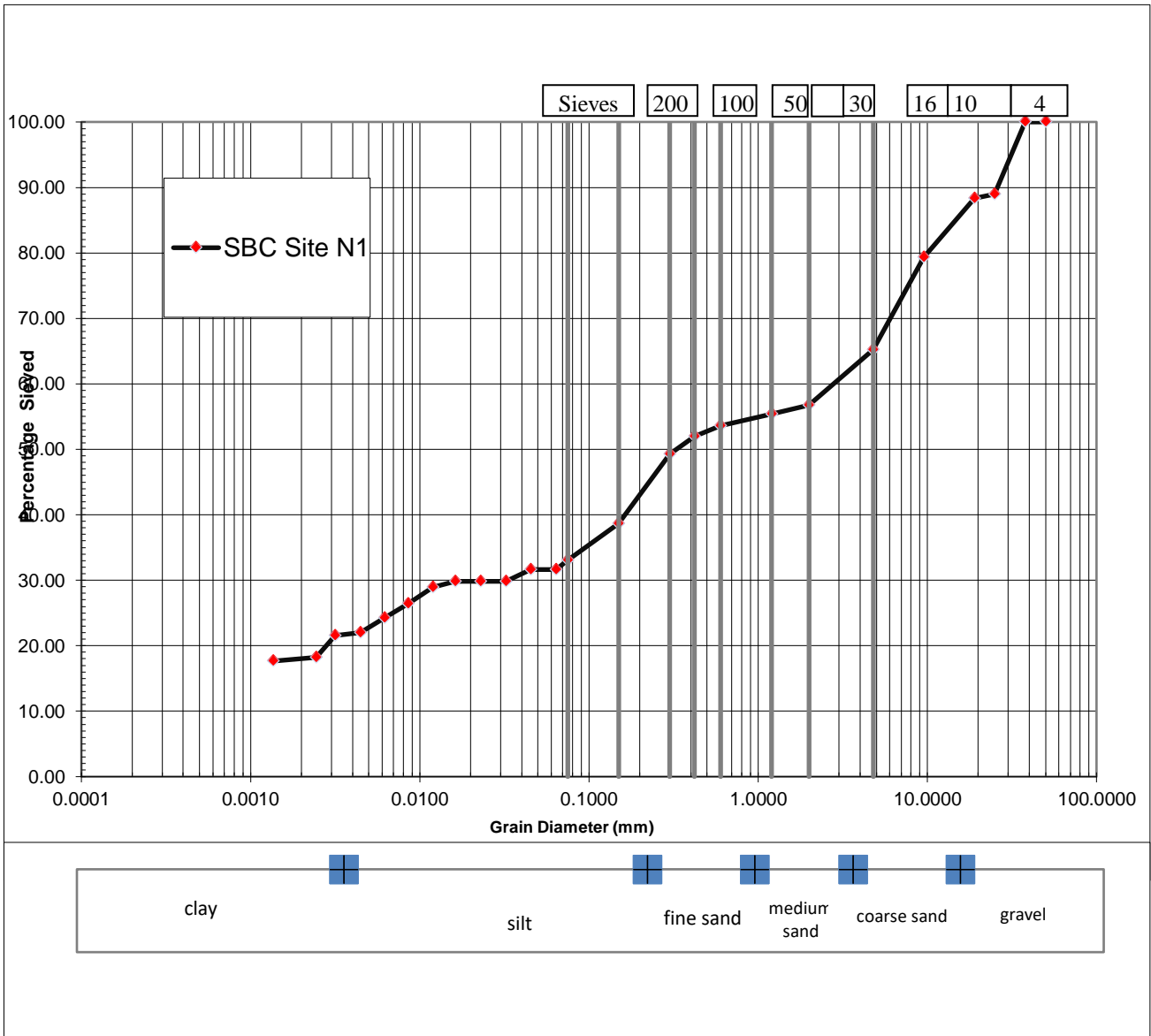
Grain Size	Percentage
Clay	18.26
Silt	20.35
Fine Sand	16.75
Medium Sand	1.40
Coarse Sand	22.57

Site Undisturbed N2
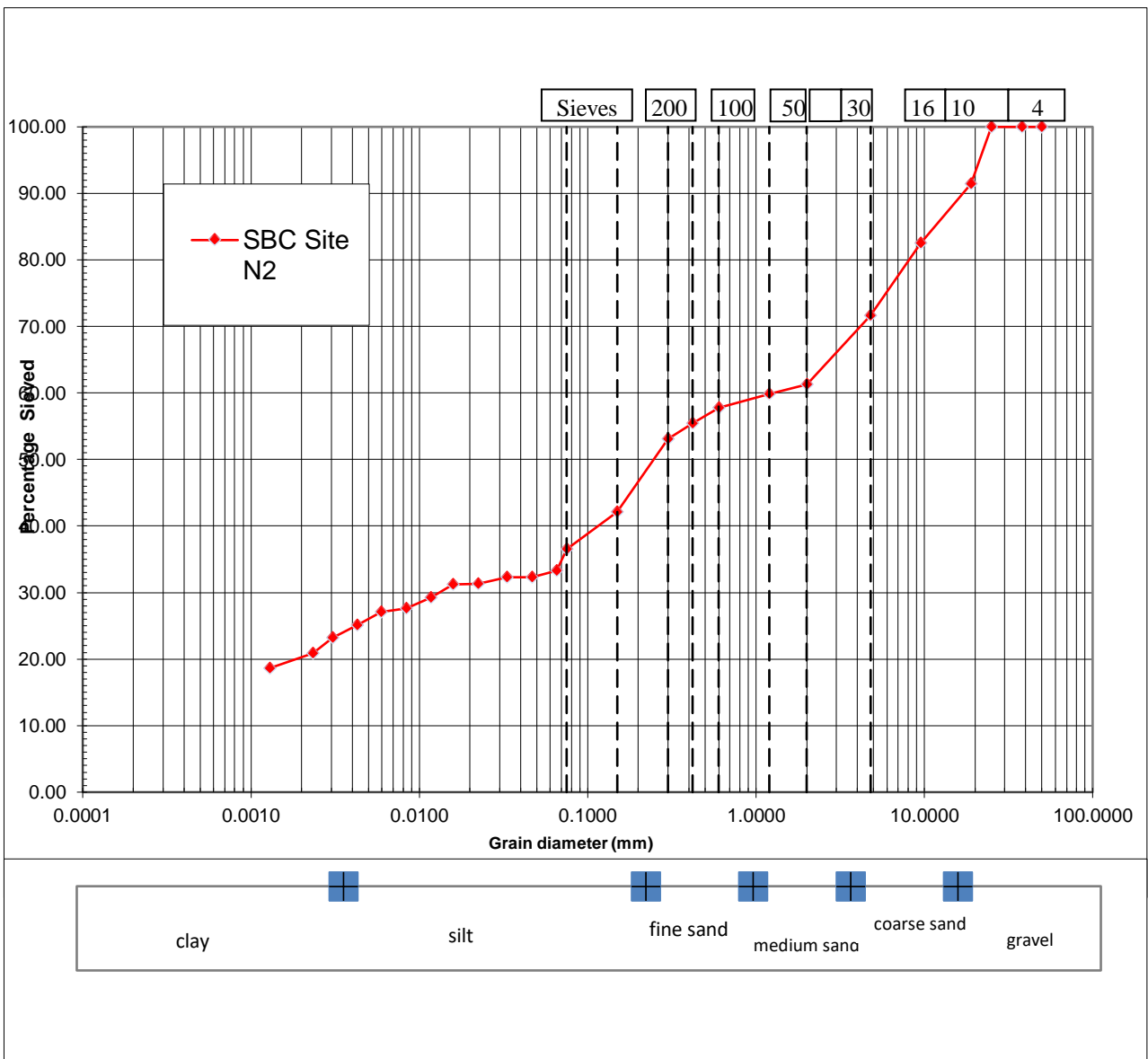
Grain Size	Percentage
Clay	23.25
Silt	18.87
Fine Sand	17.68
Medium Sand	1.51
Coarse Sand	21.18

Site Undisturbed N3
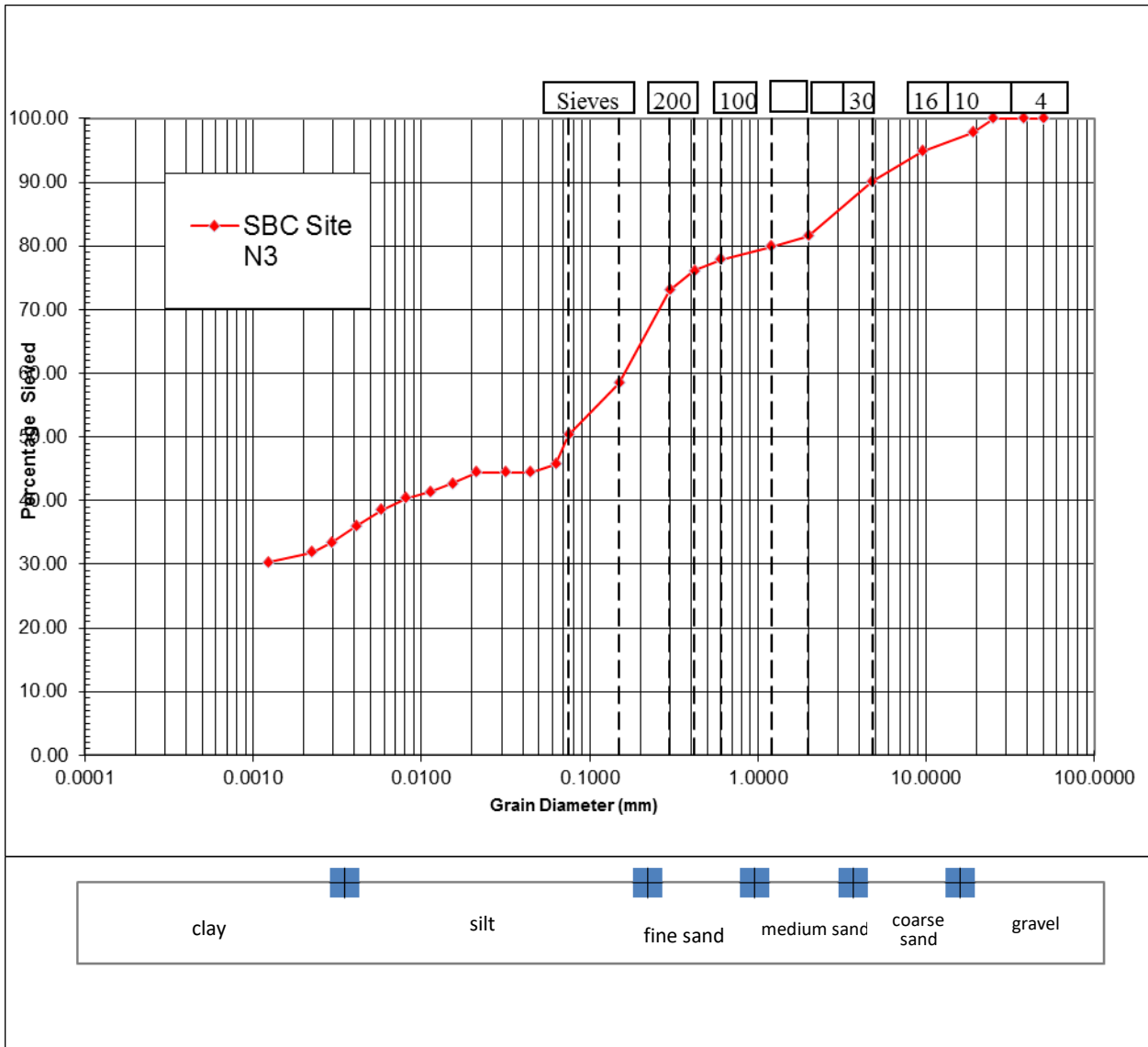
Grain Size	Percentage
Clay	33.45

Silt	25.03
Fine Sand	21.46
Medium Sand	1.59
Coarse Sand	13.33

Site Undisturbed N4
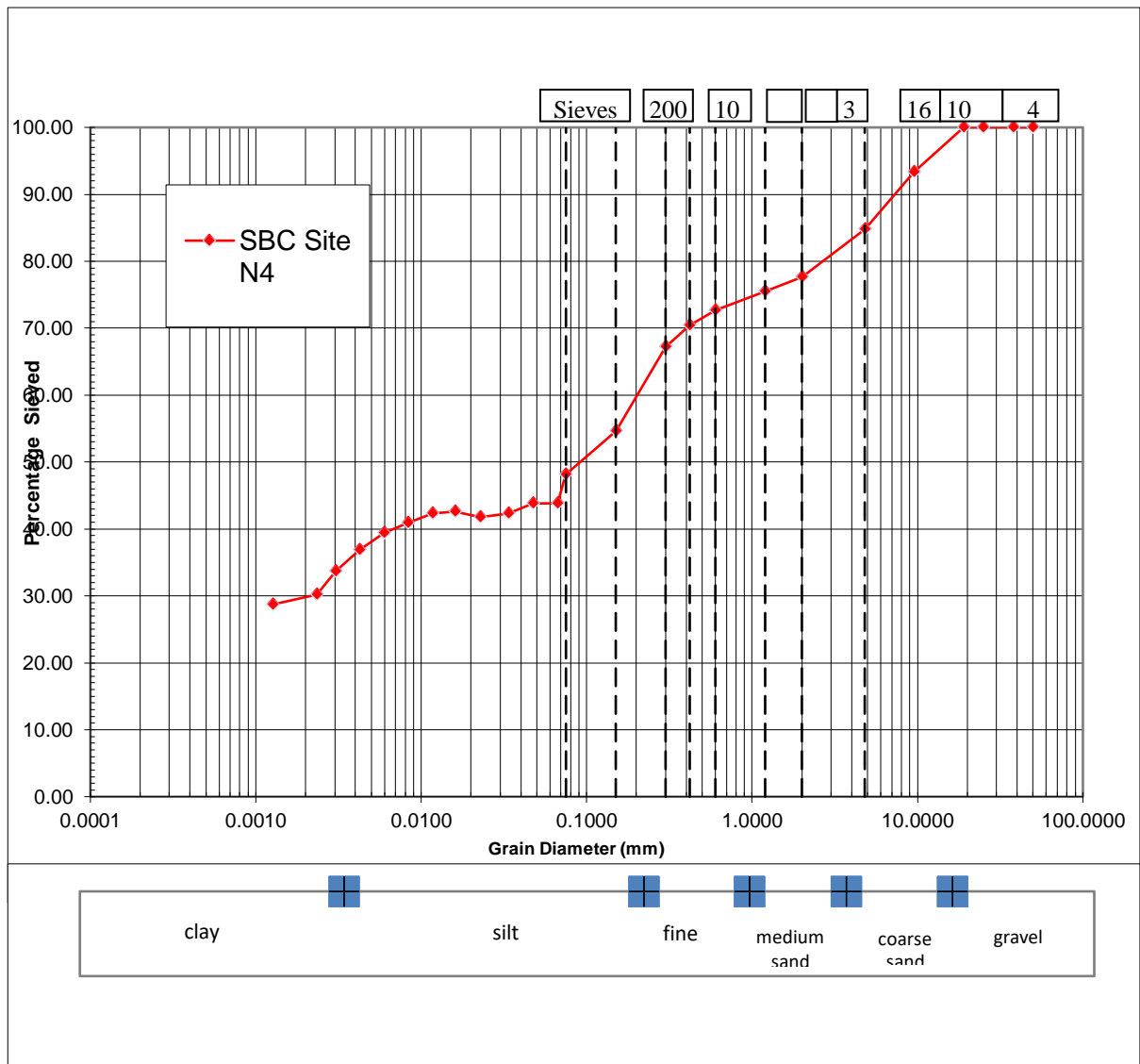
Grain Size	Percentage
Clay	33.65
Silt	14.52
Fine Sand	24.45
Medium Sand	5.05
Coarse Sand	15.63

Site Undisturbed N5
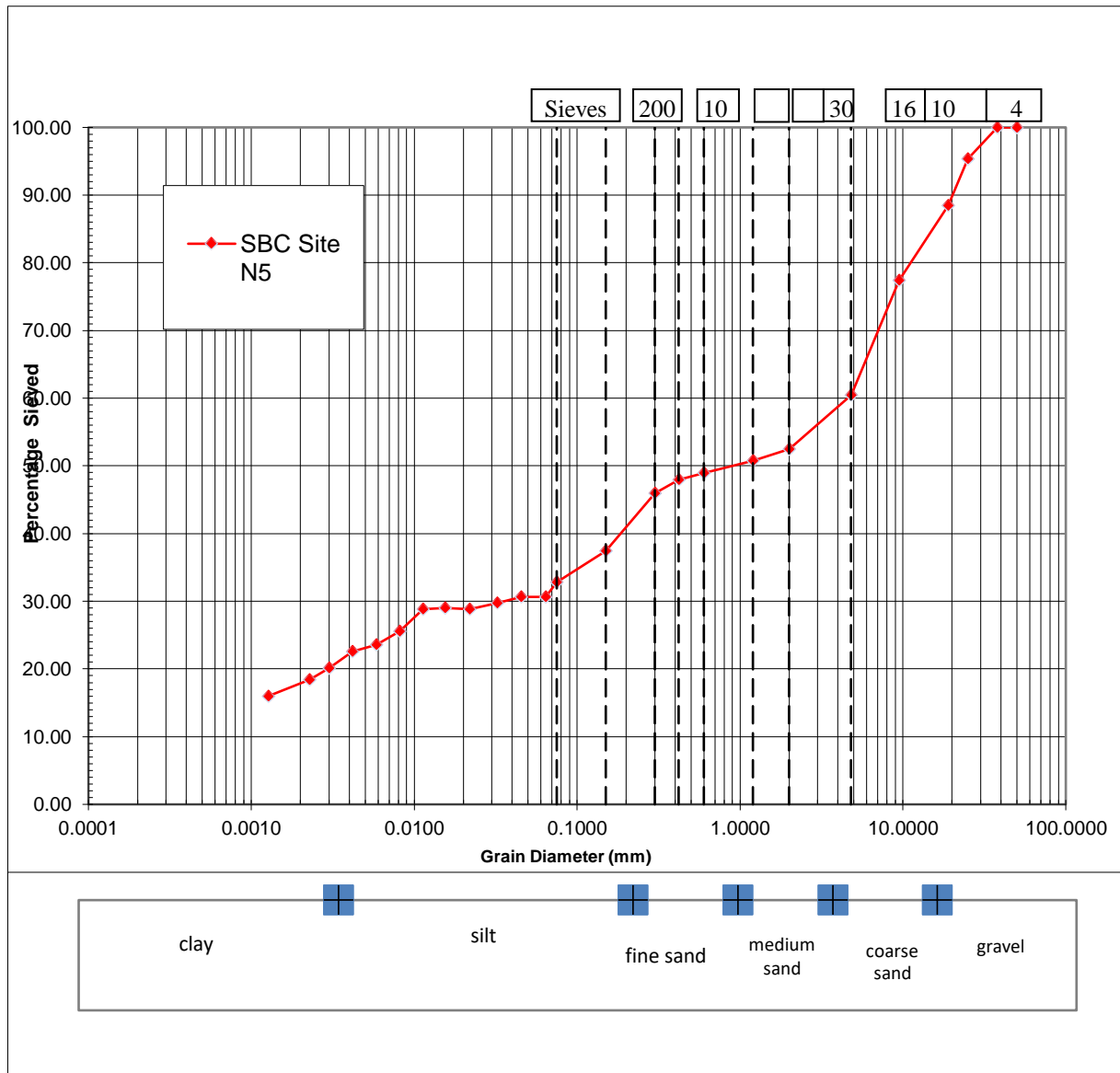
Grain Size	Percentage
Clay	24.32
Silt	13.10
Fine Sand	13.35
Medium Sand	1.72
Coarse Sand	24.90

APPENDIX 4.4

Site A03 (Normal Stress - 50 kPa)

Site A03 (Normal Stress 100 kPa)

Site A03 (Normal Stress 200 kPa)

Site A06 (Normal Stress 50 kPa)
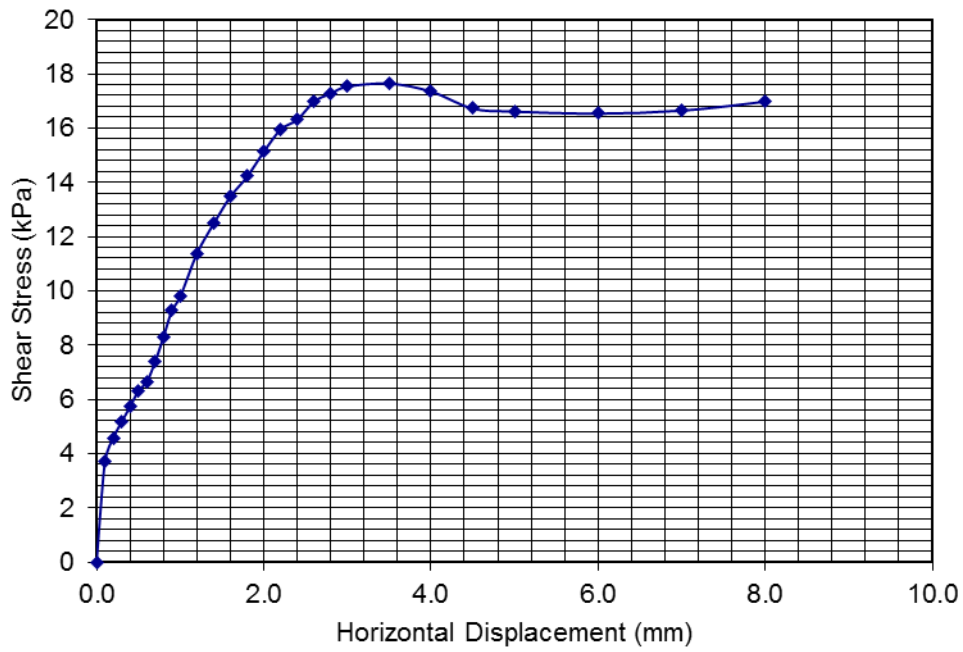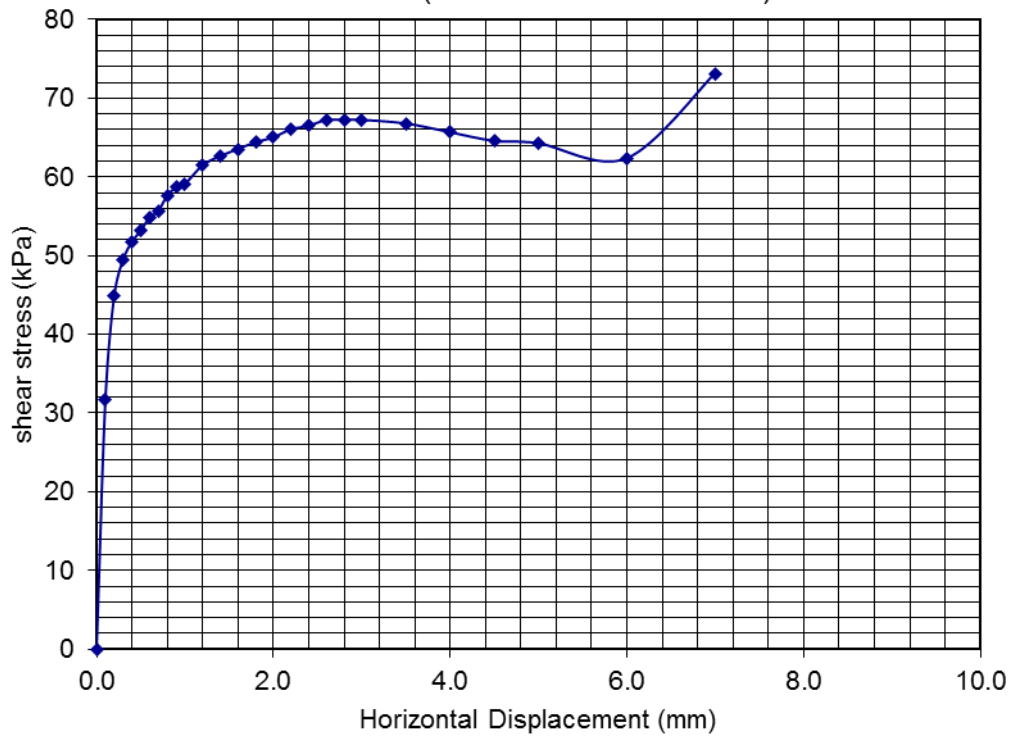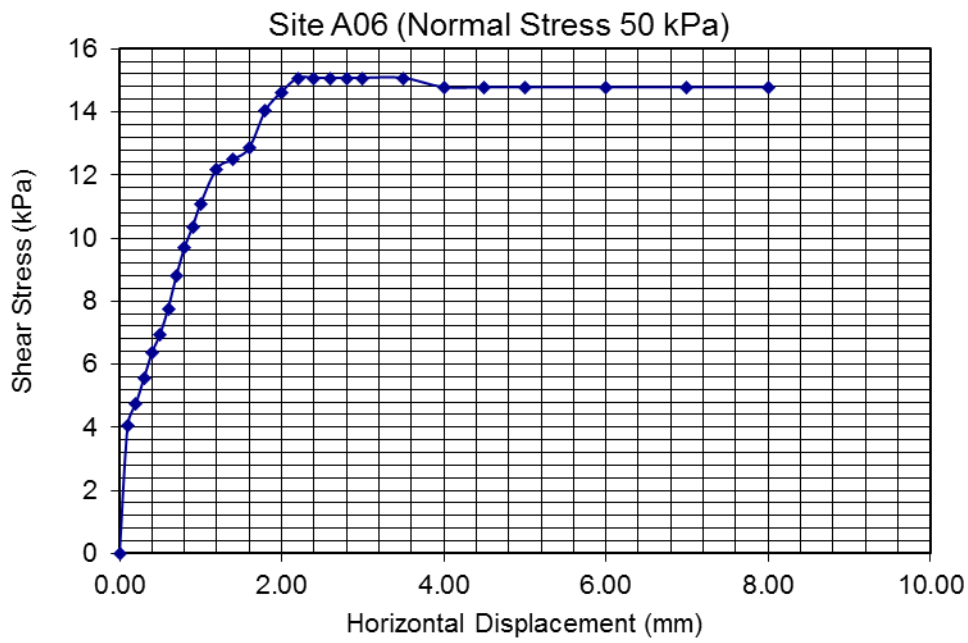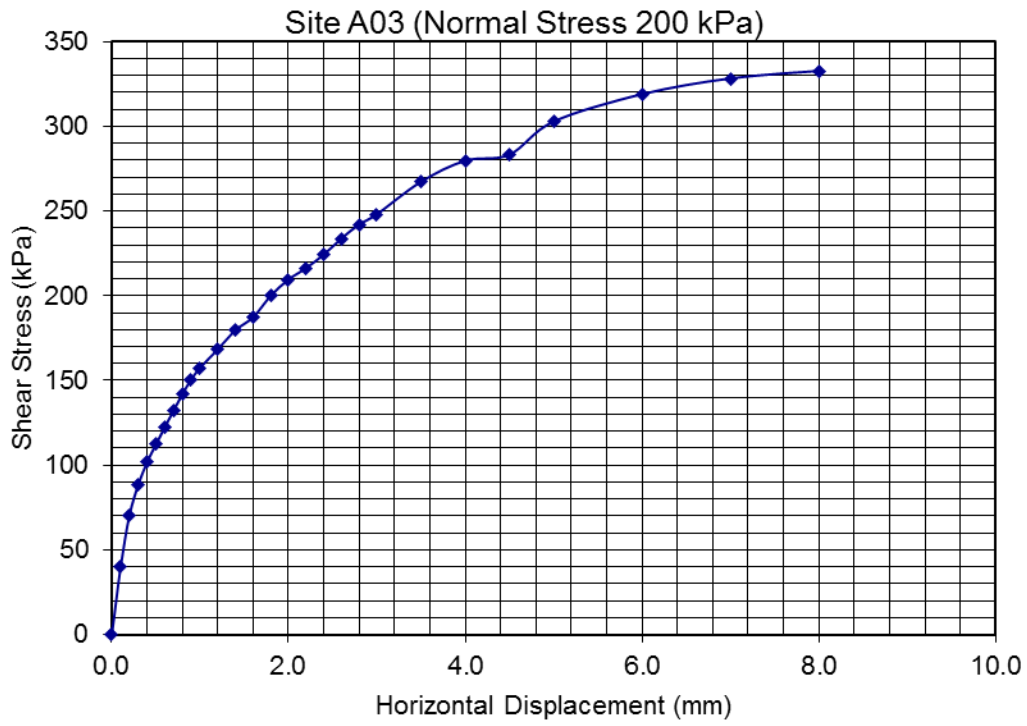
Site A06 (Normal Stress 100 kPa)
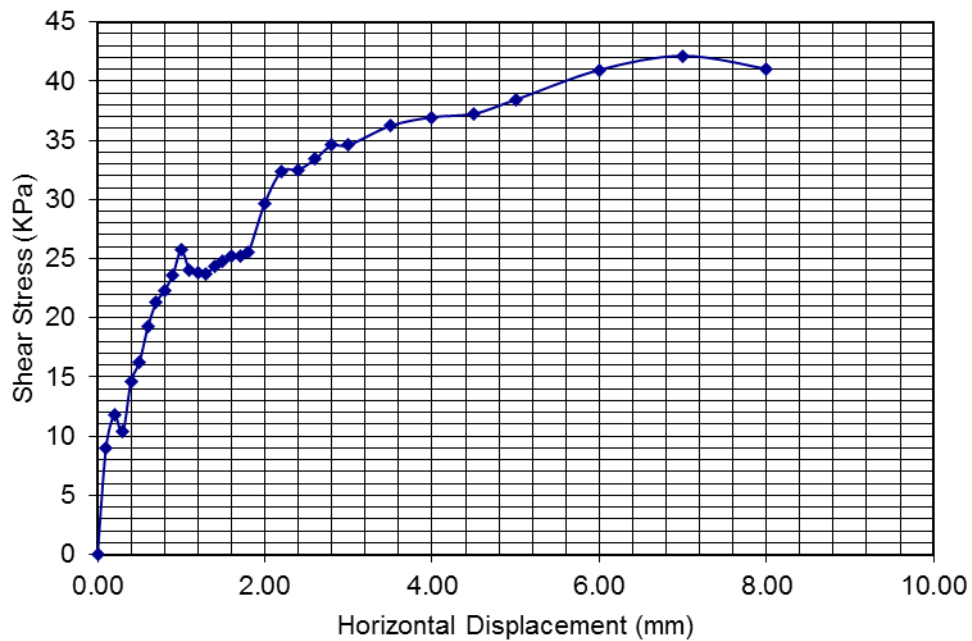
Site A06 (Normal Stress 200 kPa)
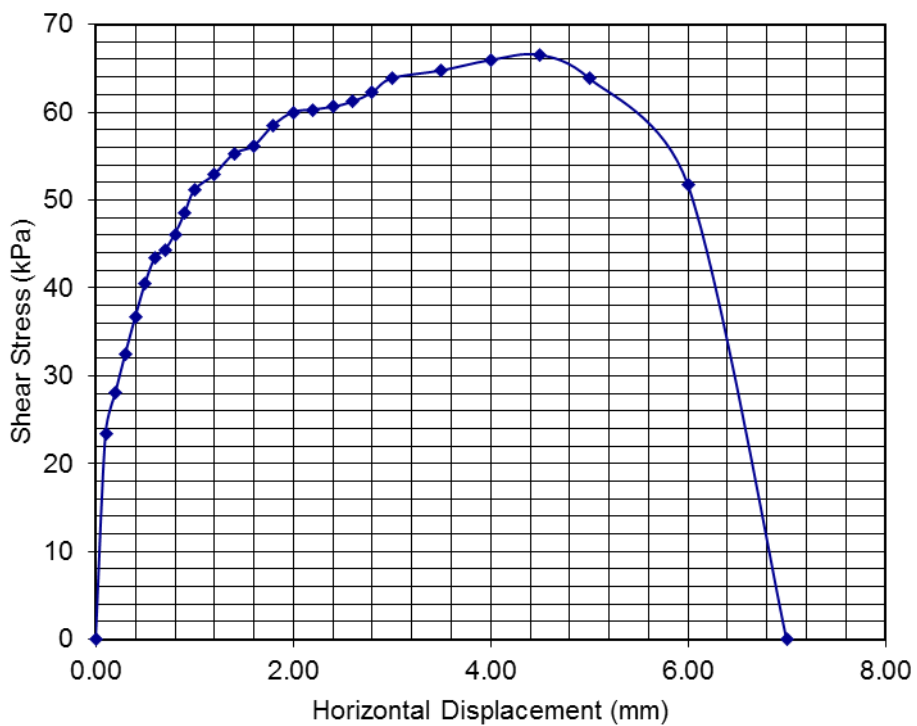
Site N1 - Normal Stress 50 kPa
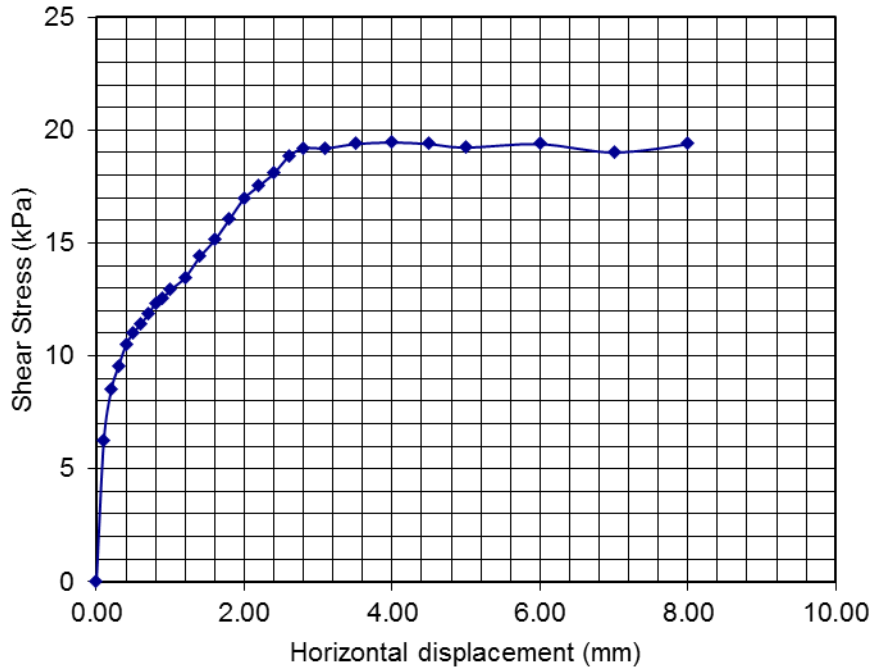
Site N1 - Normal Stress 100 kPa
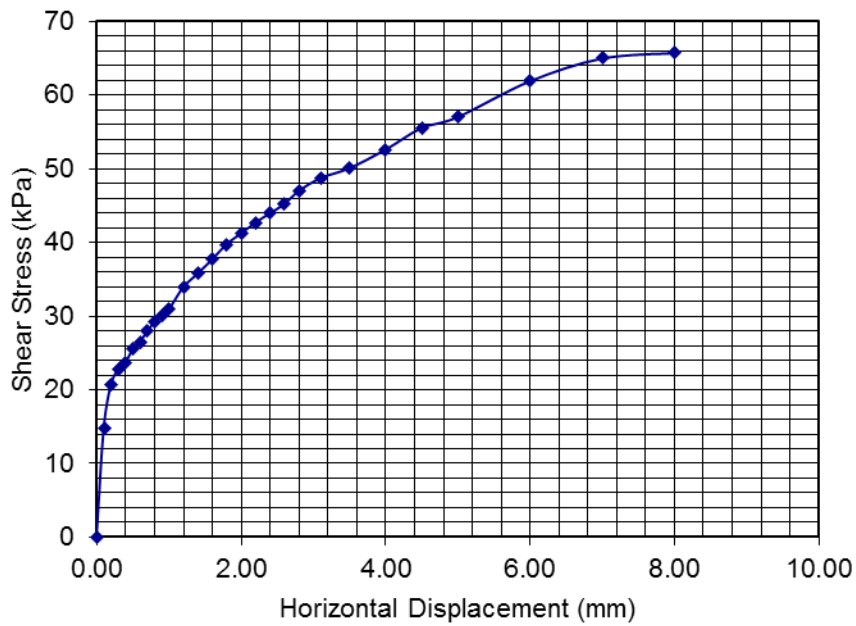
Site N1 - Normal Stress 200 kPa

Site N2 - Normal Stress 50 kPa

200

Site N2 - Normal Stress 100 kPa
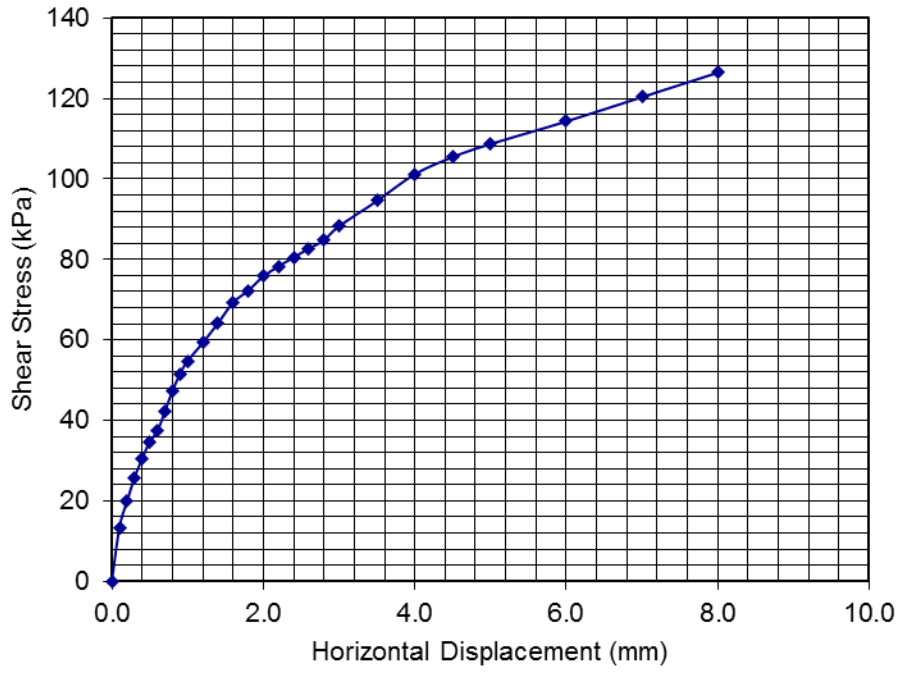
150PKa
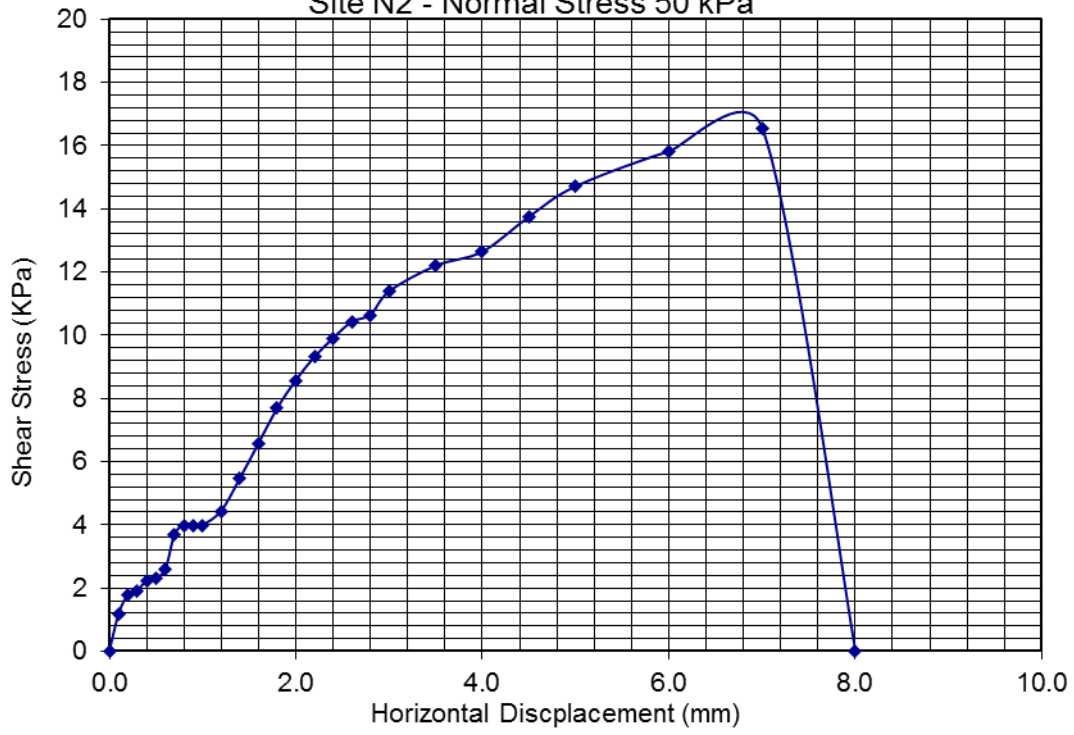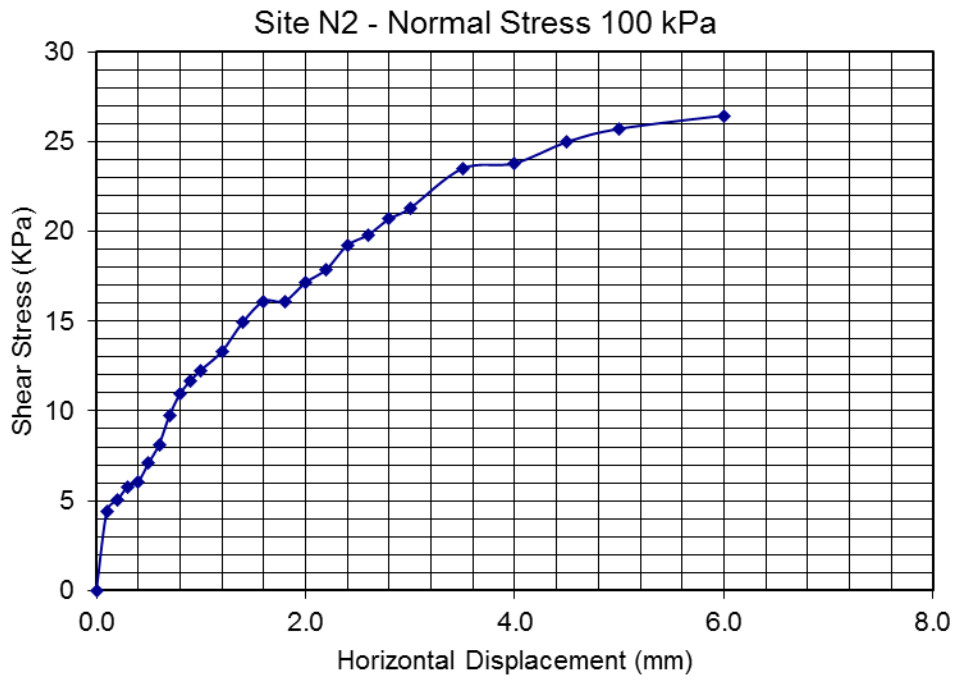
Site N2 - Normal Stress 150 kPa
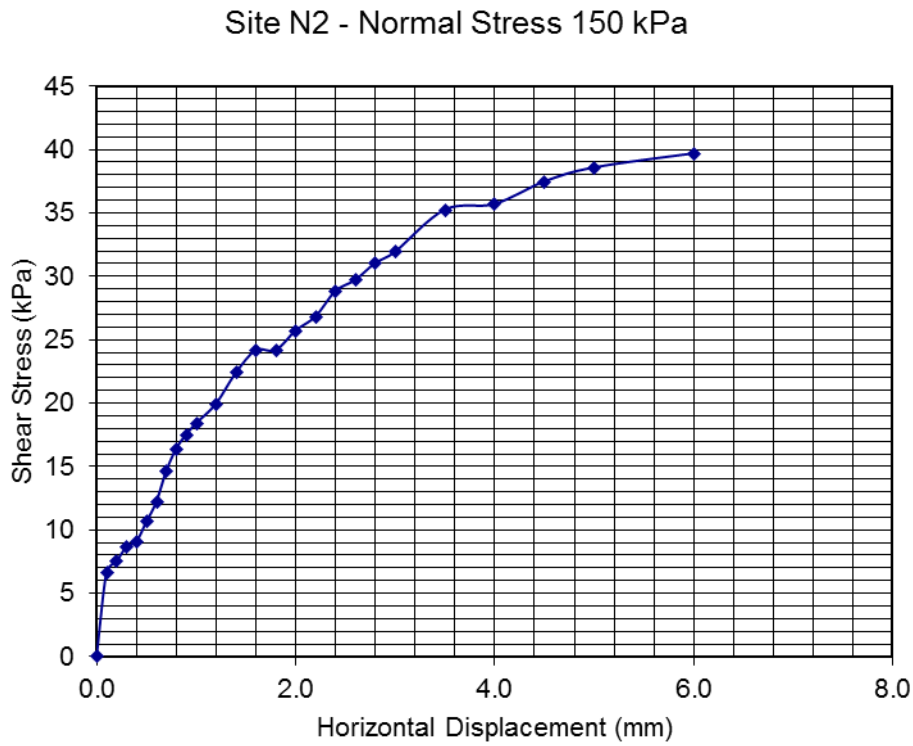
200 KPa

Site N2 - Normal Stress 200 kPa
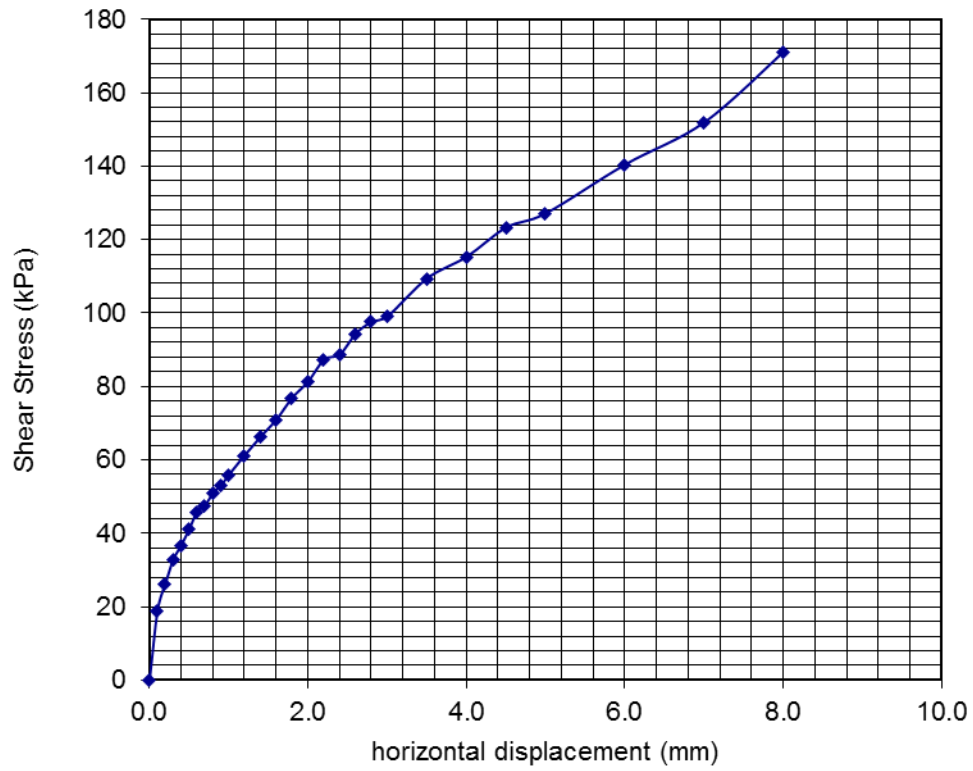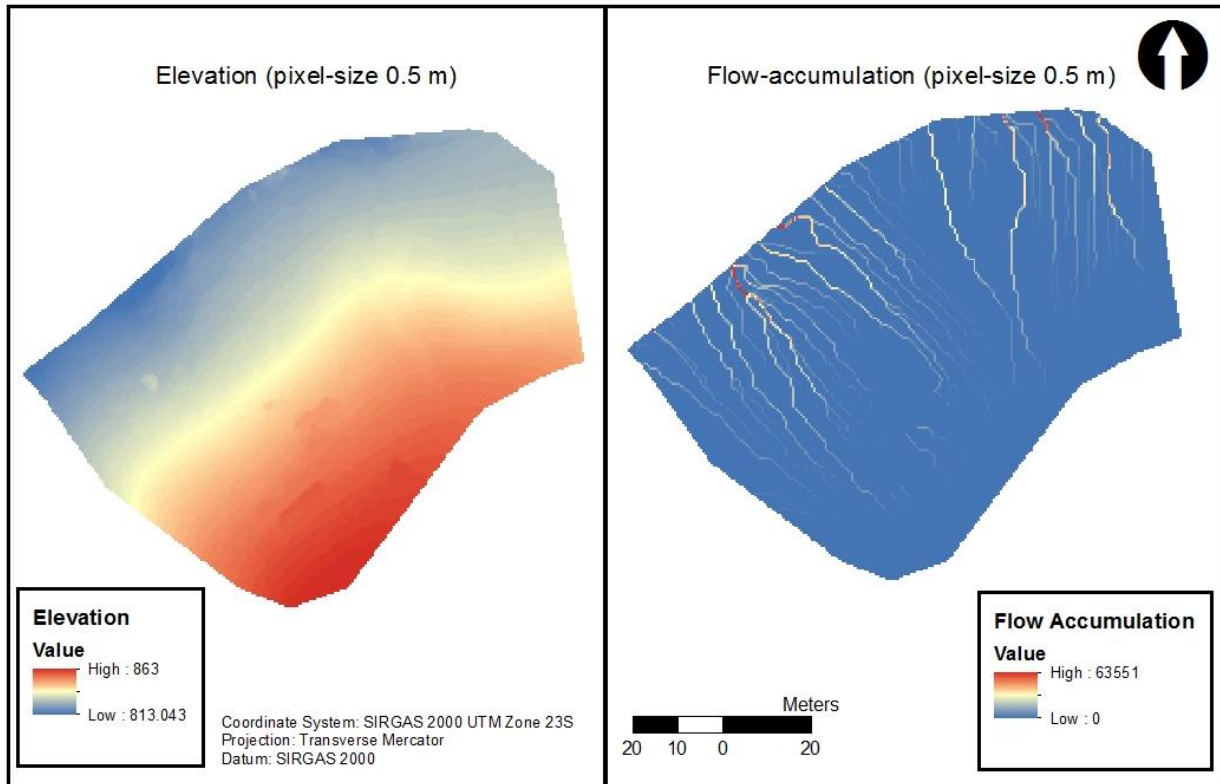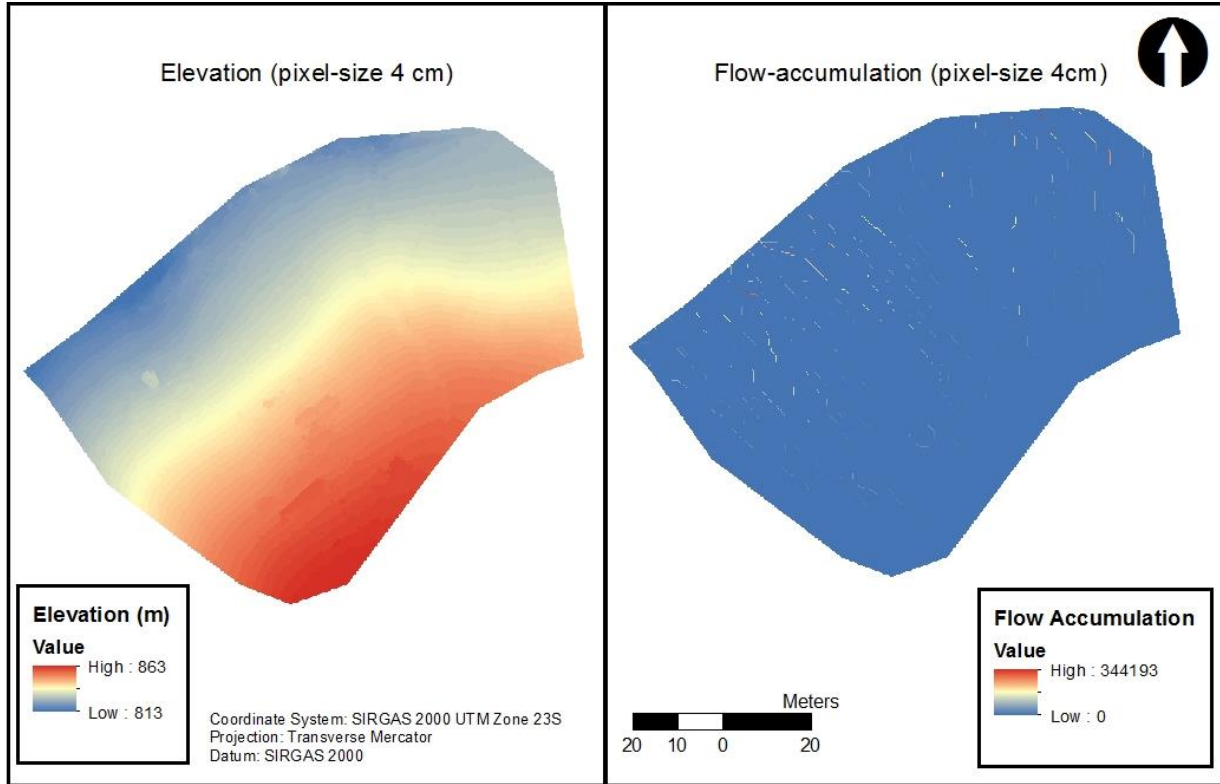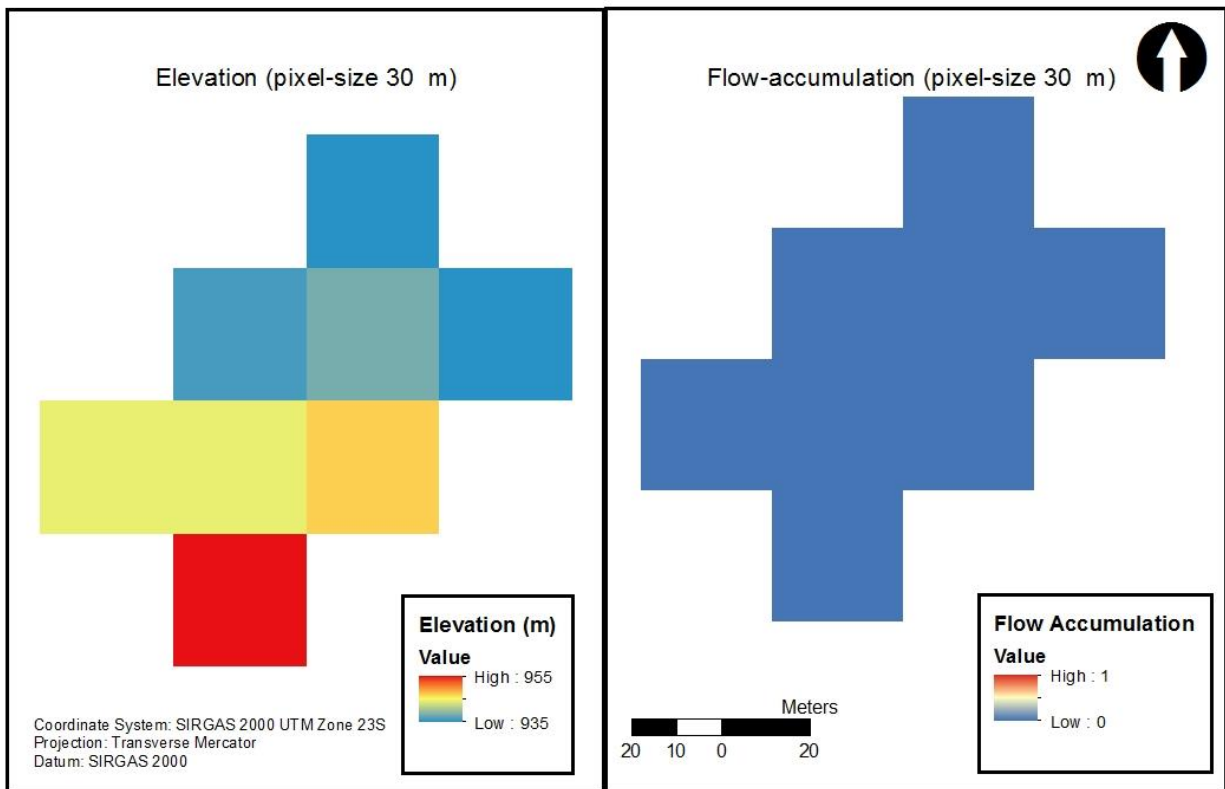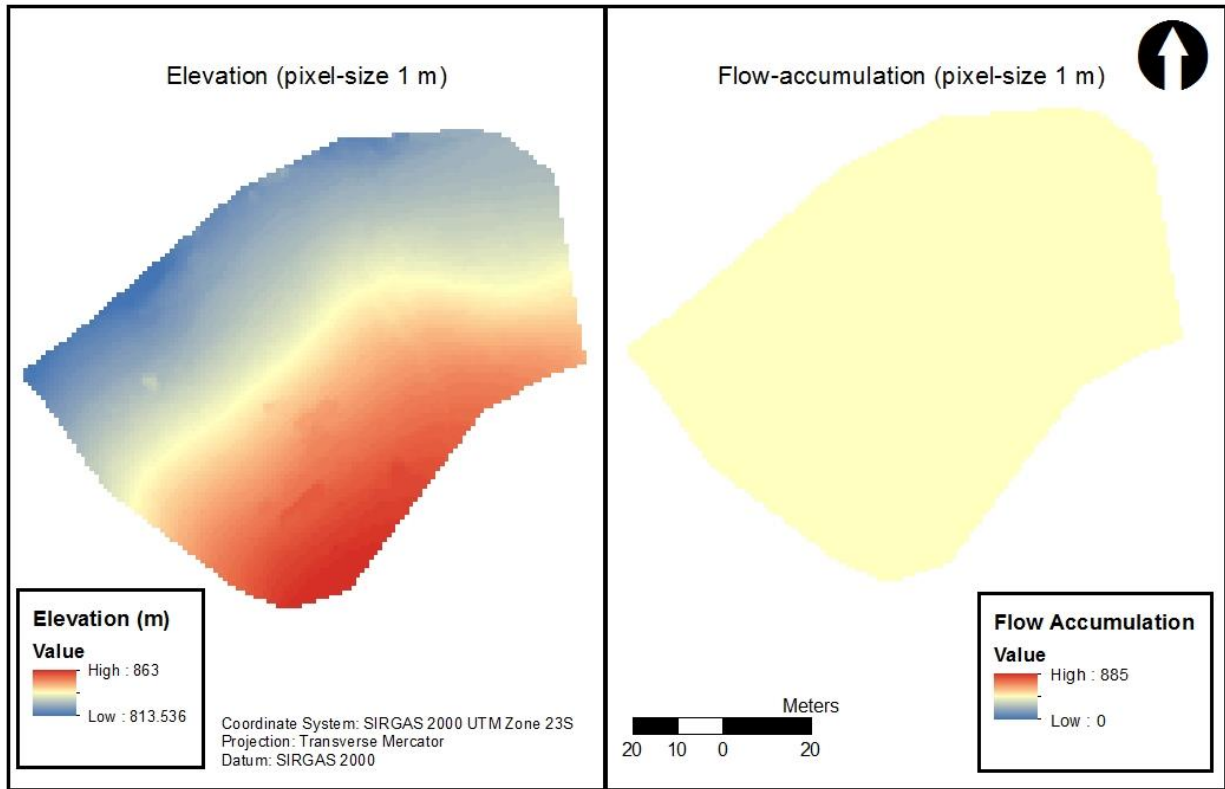
Appendix 5.1

Evacuation January

1. Information about evacuation was clear (yes, no)
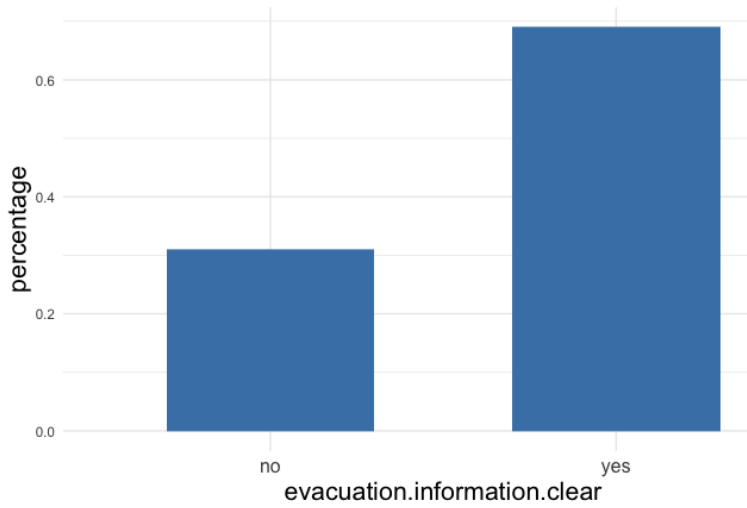
	Value	Perc[15]
Yes	311	0.69
No	141	0.31

2. Evacuation maps were easy to read? (yes, no)
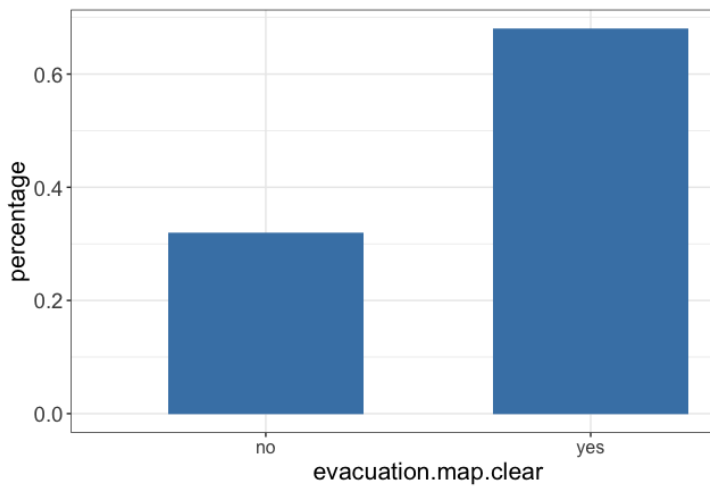
	Value	Perc[16]
Yes	302	0.68
No	145	0.32

---

[15] Value percentage computed excluding NA values.
[16] Value percentage computed excluding NA values.

3. Please check all that apply. Considering the **January 2018** evacuation order, I heard about the evacuation order from:
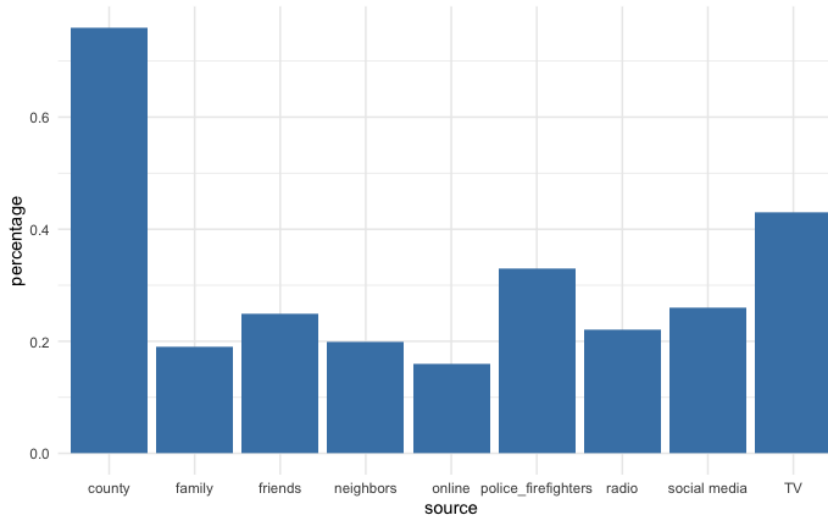
Source	Value	Per[17]
county	361	0.76
TV	205	0.43
radio	105	0.22
online	74	0.16
social media	121	0.26
friends	120	0.25
neighbors	94	0.20
family	90	0.19
police/ firefighters	157	0.33

4. Evacuated in January? (yes, no)
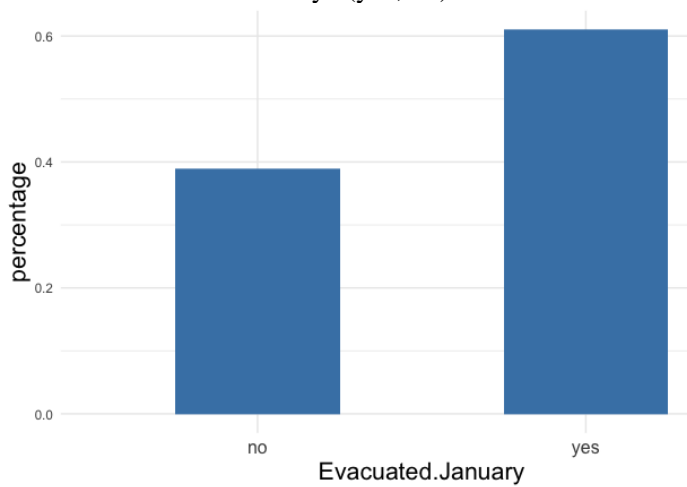
	Value	Perc[18]
Yes	307	0.61
No	193	0.39

---

[17] Value percentage computed excluding NA values.
[18] Value percentage computed excluding NA values.

5. Reasons to not evacuate
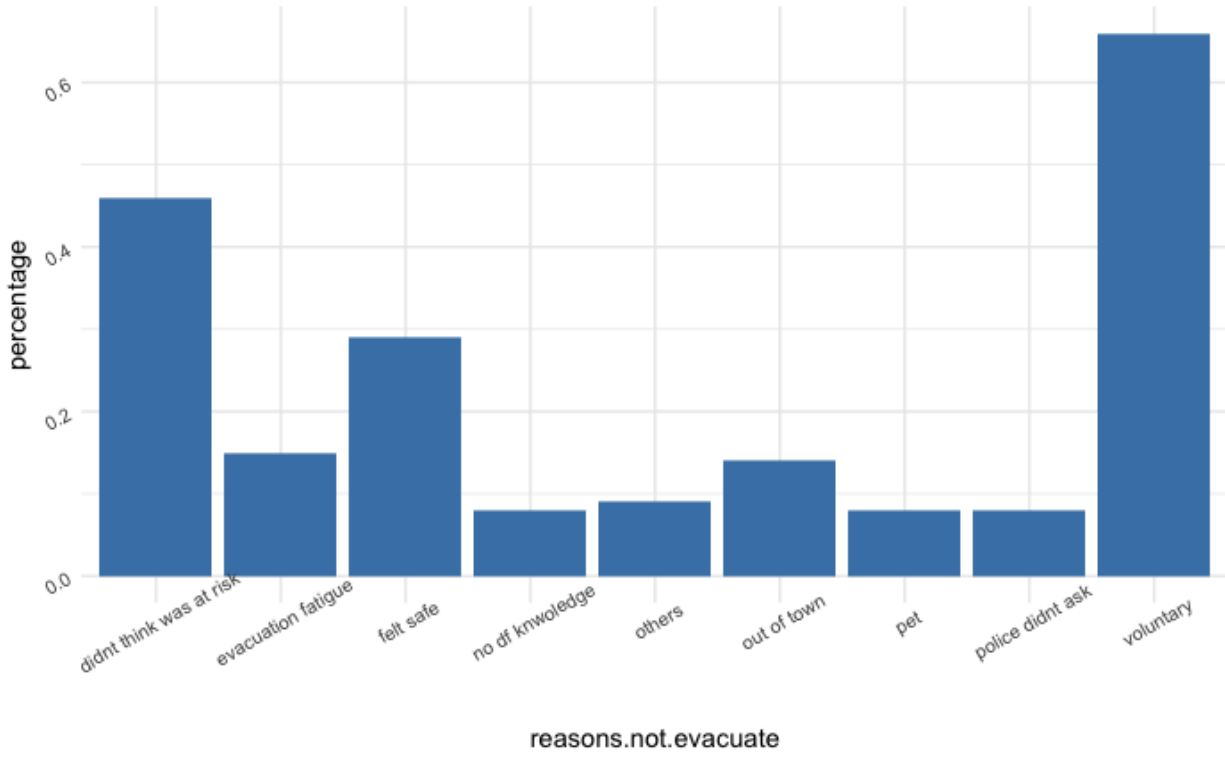
reasons not to evacuate	value	perc
voluntary	132	0.66
did not think was at risk	92	0.46
evacuation fatigue	30	0.15
out of town	28	0.14
felt safe	57	0.29
pet	16	0.08
police did not ask	16	0.08
no debris flow knowledge	15	0.08
others	18	0.09

6. When you evacuated, where did you go?
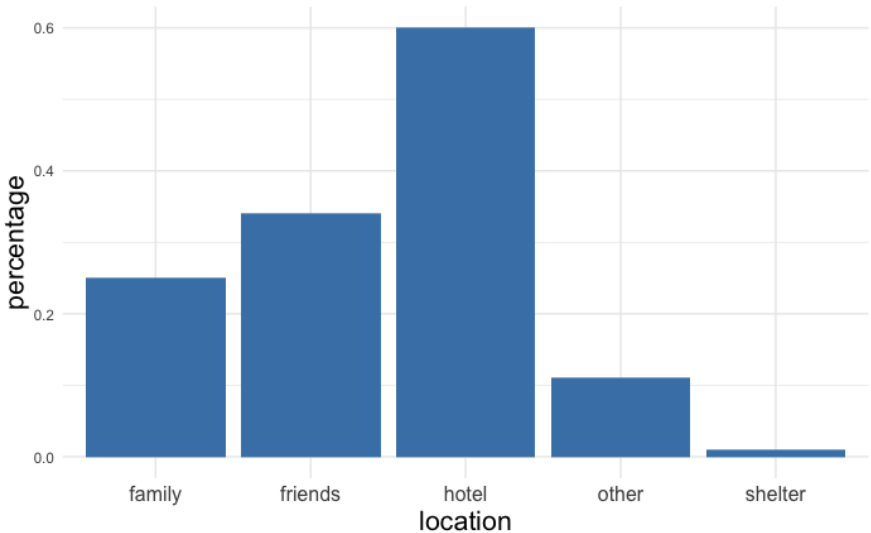
location	value	perc
hotel	198	0.60
friends	113	0.34
family	82	0.25
shelter	4	0.01
other	37	0.11

Evacuation March

1. Information about evacuation was clear (yes, no)
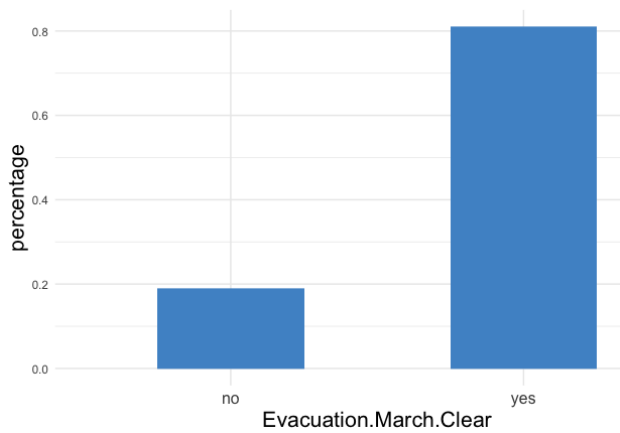
	Value	Perc[19]
Yes	355	0.81
No	83	0.19

2. Evacuation maps were easy to read? (yes, no)
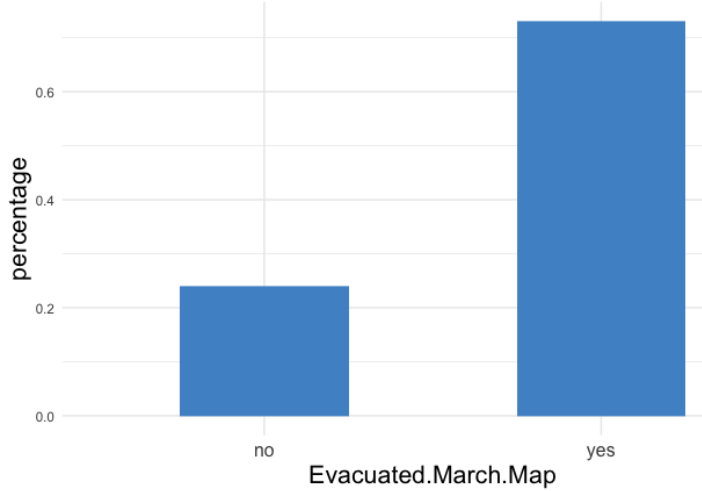
	Value	Perc[20]
Yes	330	0.73
No	109	0.24

---

[19] Value percentage computed excluding NA values.
[20] Value percentage computed excluding NA values.

3. Please check all that apply. Considering the **March 2018** evacuation order, I heard about the evacuation order from:
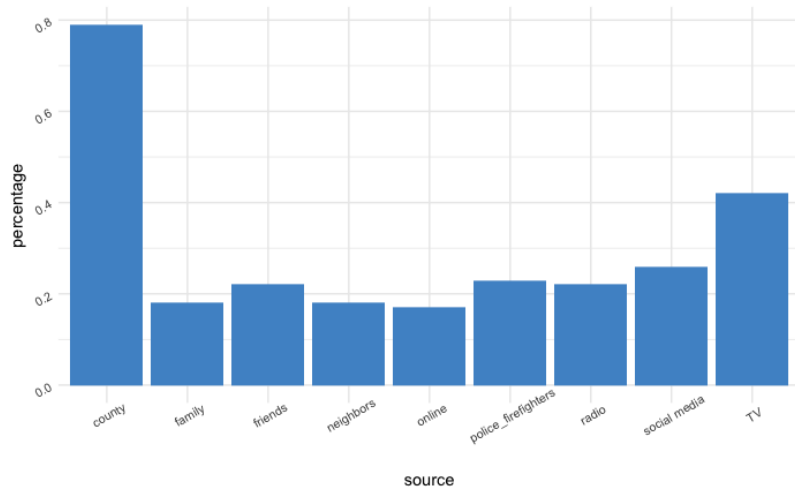
Source	Value	Per[21]
county	381	0.79
TV	200	0.42
radio	108	0.22
online	81	0.17
social media	124	0.26
friends	107	0.22
neighbors	85	0.18
family	87	0.18
police/ firefighters	113	0.23

4. Evacuated in March? (yes, no)
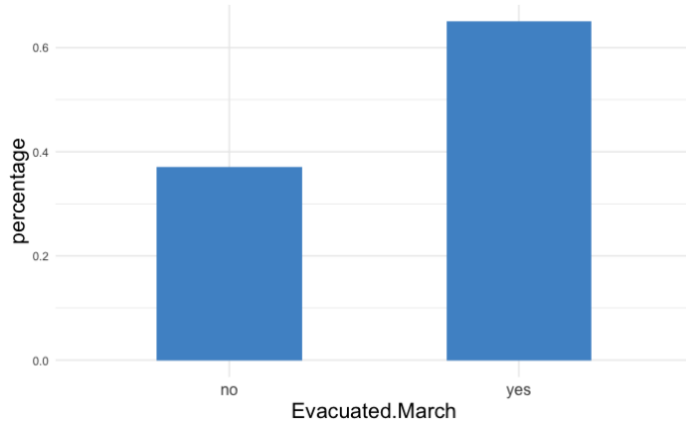
	Value	Perc[22]
Yes	298	0.65
No	168	0.37

---

[21] Value percentage computed excluding NA values.
[22] Value percentage computed excluding NA values.
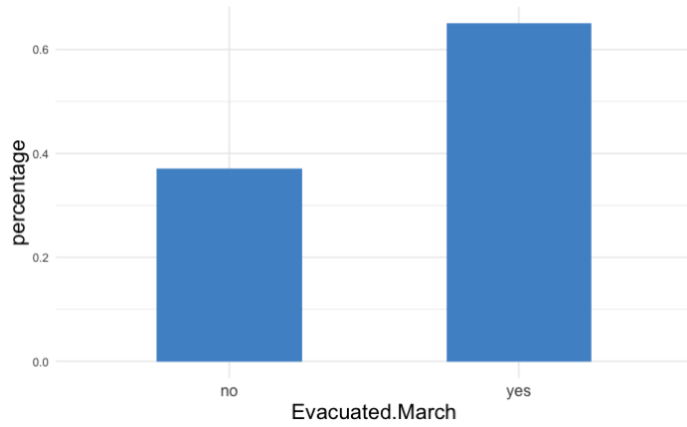
5. Reasons to not evacuate
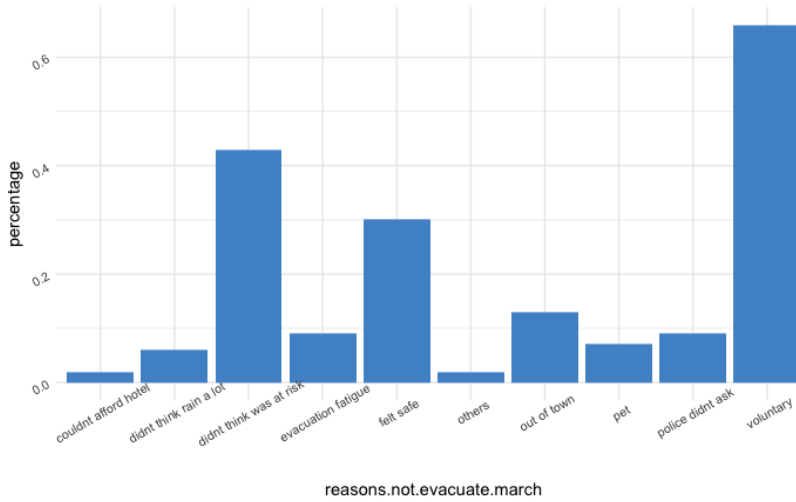
reasons not to evacuate	#	perc
voluntary	114	0.66
did not think was at risk	74	0.43
evacuation fatigue	16	0.09
out of town	23	0.13
felt safe	53	0.30
pet	12	0.07
police did not ask	16	0.09
did not think was going to rain a lot	11	0.06
could not afford hotel	4	0.02
others	4	0.02

6. When you evacuated, where did you go?
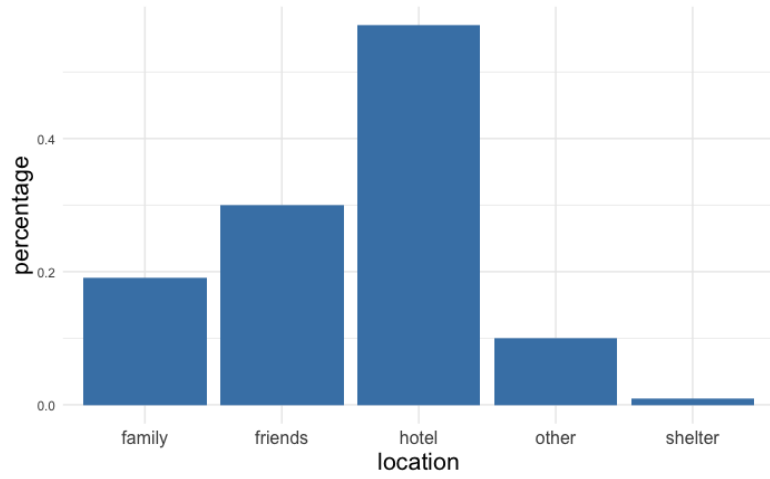
location	value	perc
hotel	181	0.57
friends	96	0.30
family	62	0.19
shelter	3	0.01
other	32	0.10